GEOLOGICAL SURVEY OF CANADA
COMMISSION GÉOLOGIQUE DU CANADA

CURRENT RESEARCH 1996-D
EASTERN CANADA AND NATIONAL AND GENERAL PROGRAMS

RECHERCHES EN COURS 1996-D
EST DU CANADA ET PROGRAMMES NATIONAUX ET GÉNÉRAUX

1996

Natural Resources Canada Ressources naturelles Canada

Canada

NOTICE TO LIBRARIANS AND INDEXERS

The Geological Survey's Current Research series contains many reports comparable in scope and subject matter to those appearing in scientific journals and other serials. Most contributions to Current Research include an abstract and bibliographic citation. It is hoped that these will assist you in cataloguing and indexing these reports and that this will result in a still wider dissemination of the results of the Geological Survey's research activities.

AVIS AUX BIBLIOTHÉCAIRES ET PRÉPARATEURS D'INDEX

La série Recherches en cours de la Commission géologique contient plusieurs rapports dont la portée et la nature sont comparables à ceux qui paraissent dans les revues scientifiques et autres périodiques. La plupart des articles publiés dans Recherches en cours sont accompagnés d'un résumé et d'une bibliographie, ce qui vous permettra, on l'espère, de cataloguer et d'indexer ces rapports, d'où une meilleure diffusion des résultats de recherche de la Commission géologique.

GEOLOGICAL SURVEY OF CANADA
COMMISSION GÉOLOGIQUE DU CANADA

CURRENT RESEARCH 1996-D

EASTERN CANADA AND NATIONAL AND GENERAL PROGRAMS

RECHERCHES EN COURS 1996-D

EST DU CANADA ET PROGRAMMES NATIONAUX ET GÉNÉRAUX

1996

Available in Canada from

Geological Survey of Canada offices:

601 Booth Street
Ottawa, Canada K1A 0E8

3303-33rd Street N.W.
Calgary, Alberta T2L 2A7

100 West Pender Street
Vancouver, B.C. V6B 1R8

or from

Canada Communication Group – Publishing
Ottawa, Canada K1A 0S9

and through authorized bookstore agents
and other bookstores

A deposit copy of this publication is also available for reference
in public libraries across Canada

Cat. No. M44-1996/4E
ISBN 0-660-16286-5

Price subject to change without notice

Cover description

Outcrop showing mingling of felsic and mafic magma, Birchtown Quarry, Shelburne, Nova Scotia. See paper by Currie et al. in this volume. Photo by K. Currie. GSC 1995-331

Affleurement montrant un mélange de roches magmatiques felsiques et mafiques, carrière Birchtown, Shelburne, Nouvelle-Écosse. Voir l'article de Currie et al. du présent volume de «Recherches en cours». (GSC 1995-331)

Separates

A limited number of separates of the papers that appear in this volume are available by direct request to the individual authors. The addresses of the Geological Survey of Canada offices follow:

Geological Survey of Canada
601 Booth Street
OTTAWA, Ontario
K1A 0E8
(FAX: 613-996-9990)

Geological Survey of Canada (Calgary)
3303-33rd Street N.W.
CALGARY, Alberta
T2L 2A7
(FAX: 403-292-5377)

Geological Survey of Canada (Victoria)
100 West Pender Street
VANCOUVER, B.C.
V6B 1R8
(FAX: 604-666-1124)

Geological Survey of Canada (Victoria)
P.O. Box 6000
9860 Saanich Road
SIDNEY, B.C.
V8L 4B2
(Fax: 604-363-6565)

Geological Survey of Canada (Atlantic)
Bedford Institute of Oceanography
P.O. Box 1006
DARTMOUTH, N.S.
B2Y 4A2
(FAX: 902-426-2256)

Quebec Geoscience Centre/INRS
2535, boulevard Laurier
C.P. 7500
Sainte-Foy (Québec)
G1V 4C7
(FAX: 418-654-2615)

Tirés à part

On peut obtenir un nombre limité de «tirés à part» des articles qui paraissent dans cette publication en s'adressant directement à chaque auteur. Les adresses des différents bureaux de la Commission géologique du Canada sont les suivantes :

Commission géologique du Canada
601, rue Booth
OTTAWA, Ontario
K1A 0E8
(facsimilé : 613-996-9990)

Commission géologique du Canada (Calgary)
3303-33rd St. N.W.,
CALGARY, Alberta
T2L 2A7
(facsimilé : 403-292-5377)

Commission géologique du Canada (Victoria)
100 West Pender Street
VANCOUVER, British Columbia
V6B 1R8
(facsimilé : 604-666-1124)

Commission géologique du Canada (Victoria)
P.O. Box 6000
9860 Saanich Road
SIDNEY, British Columbia
V8L 4B2
(facsimilé : 604-363-6565)

Commission géologique du Canada (Atlantique)
Institut océanographique Bedford
P.O. Box 1006
DARTMOUTH, Nova Scotia
B2Y 4A2
(facsimilé : 418-654-2615)

Centre géoscientifique de Québec/INRS
2535, boulevard Laurier
C.P. 7500
Sainte-Foy (Québec)
G1V 4C7

CONTENTS

Petrological data for southern Nova Scotia plutons relevant to beryl mineralization[1]

K.L. Currie, J.B. Whalen, and F.J. Longstaffe[2]
Continental Geoscience Division, Ottawa

Currie, K.L., Whalen, J.B., and Longstaffe, F.J., 1996: Petrological data for southern Nova Scotia plutons relevant to beryl mineralization; in Current Research 1996-D; Geological Survey of Canada, p. 1-10.

Abstract: Field, chemical, and O isotopic data indicate that southern Nova Scotia plutons crystallized from magma containing both mantle and crustal components. Although evolved portions of the plutons compositionally resemble plutons parental to rare-metal pegmatite fields, pegmatites are rare around southern Nova Scotia plutons. Beryl-bearing pegmatites, which crystallized at ~620°C, 4 kilobars under water-saturated conditions, occur only where host rocks were not subjected to previous sillimanite-grade metamorphism. Pegmatites of any kind are scarce in host rocks of high metamorphic grade. Absence of a pegmatite field can be ascribed to some combination of insufficient amounts of F, Cl, and B, and dehydration and plasticity of high-grade metamorphic host rocks. Significant loss of pegmatites to erosion is considered unlikely. These factors suggest that the potential for commercially exploitable beryl mineralization is low.

Résumé : Des données de terrain et des données sur la composition chimique et les isotopes de l'oxygène indiquent que les plutons du sud de la Nouvelle-Écosse ont cristallisé à partir d'un magma dont les composantes provenaient à la fois du manteau et de la croûte. Aux environs des plutons du sud de la Nouvelle-Écosse, les pegmatites sont peu nombreuses, même si des portions évoluées des plutons s'apparentent par la composition aux plutons originels des champs de pegmatites à métaux rares. Les pegmatites à béryl, qui ont cristallisé à une température d'env. 620 °C et une pression de 4 kilobars dans des conditions saturées en eau, ne sont présentes que là où les encaissants n'ont pas été métamorphisées au faciès des sillimanites. Les pegmatites de tout type sont rares dans les encaissants très métamorphisés. L'absence d'un champ de pegmatites peut être attribuée à une combinaison de facteurs dont notamment l'insuffisance de F, Cl et B, ainsi que la déshydratation et la plasticité des encaissants très métamorphisées. La perte importante de pegmatites par érosion est considérée improbable. Ces observations incitent à supposer que les chances de trouver une minéralisation en béryl commercialement exploitable sont faibles.

[1] Contribution to the Canada-Nova Scotia Cooperation Agreement on Mineral Development (1992-1995), a subsidiary agreement under the Canada-Nova Scotia Economic and Regional Development Agreement
[2] Department of Earth Sciences, The University of Western Ontario, London, Ontario N6A 5B7

INTRODUCTION

The Port Mouton, Shelburne, and Barrington Passage plutons of southern Nova Scotia form a group of peraluminous bodies which differ markedly from the much larger and better known Southern Nova Scotia Batholith to the north. In general these southern plutons contain more mafic material than the batholith (de Albuquerque, 1977; Tate, 1995) and were emplaced into metasedimentary rocks (Meguma Group) which had been metamorphosed at high temperatures and low pressures (Raeside and Jamieson, 1992). The Port Mouton and Shelburne plutons have an associated muscovite (±garnet ±tourmaline)-bearing pegmatite phase which contains a low tenor of beryl. We have conducted field and petrological investigations of all three plutons to determine the source of this mineralization and the conditions under which it developed.

GEOLOGICAL SETTING

The geological setting of the plutons (Fig.1) has been described recently in some detail (de Albuquerque, 1977; Rogers, 1985; Douma, 1988; Raeside and Jamieson, 1992; Currie and Whalen, 1994, 1995; Keppie and Dallmeyer, 1995). Only relevant points are outlined here.

The Port Mouton Pluton outcrops in a roughly elliptical area about 25 by 10 km with its major axis trending east-northeast. The pluton consists mainly of near-massive biotite-muscovite granodiorite to granite (~80 per cent) with subordinate biotite tonalite (~20 per cent), and negligible amounts of metasomatized mafic rocks. There is no obvious systematic distribution of these phases, and complex examples of mutual intrusion, boudinage and hybridization occur on a small scale (Douma, 1988; Currie and Whalen, 1994). Igneous layering on a scale of a few centimetres can be observed at scattered localities throughout the pluton. Pegmatites occur sparsely within the pluton as nebulous patches, and

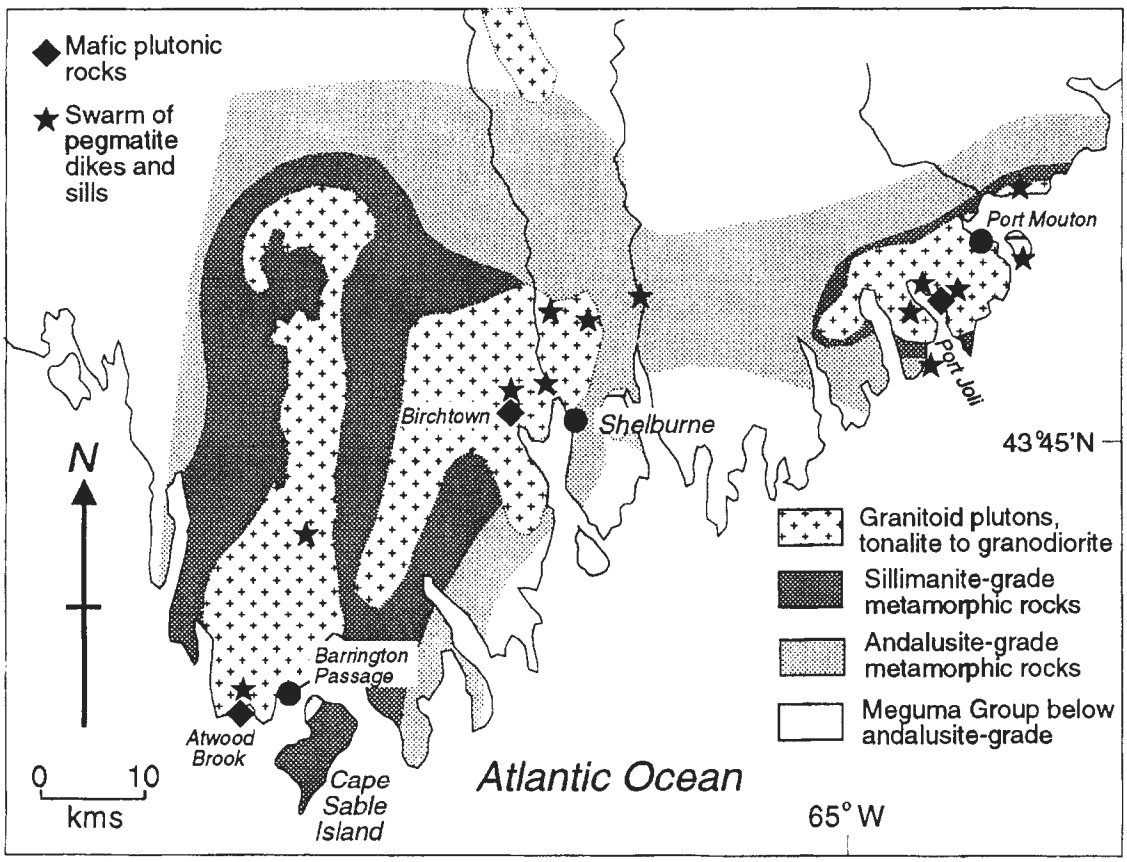

Figure 1. *Geological sketch of the southern Nova Scotia plutons (modified after Raeside and Jamieson, 1992)*

more commonly near the margins as composite sills or dykes interlayered with normal biotite-muscovite granodiorite or granite. Pegmatite is rare or absent in the host rock at distances of more than 100 m from the pluton. Pegmatites tend to show the same division as the rest of the pluton, that is into biotite-plagioclase pegmatites lacking potash feldspar, and muscovite-potash feldspar pegmatites, commonly containing garnet and tourmaline. However transitional cases with the assemblage biotite-muscovite-garnet-potash feldspar also occur. The maximum grain size in the pegmatites is about 3-5 cm. The Port Mouton Pluton intrudes andalusite-grade turbiditic greywacke of the Cambro-Ordovician Meguma Group. A narrow contact halo of sillimanite-grade rocks, no more than a few tens of metres wide, surrounds the pluton (Douma, 1988). A small area of migmatitic rocks outcrops on the northeast side of the pluton, but most of the aureole is fractured and intimately dyked rather than migmatitic.

The Shelburne Pluton forms an irregular body elongated toward the south-southwest. The maximum length is almost 30 km, and the width over the main portion about 20 km. Felsic rock types within the Shelburne Pluton are essentially identical to those in the Port Mouton Pluton. Well-developed layering is not present, but weak tectonic foliation occurs locally. One of the most interesting features of the Shelburne Pluton is an isolated mass of diorite exposed in quarries (Birchtown diorite). This material reacted extensively with surrounding felsic rocks producing a spectacular series of hybrids described last year (Currie and Whalen, 1995). Pegmatite patches, lenses and dykes of the same types as those in the Port Mouton Pluton occur within the eastern part of the Shelburne Pluton and in a region along the Jordan River, about 3 km east of the pluton. The western part of the Shelburne Pluton lies within a broad region of sillimanite-facies metamorphic rocks of the Meguma Group, whereas the eastern part is in lower-grade rocks typified by the assemblage staurolite+andalusite. The sillimanite isograd is cut almost at right angles by the pluton. Pegmatite bodies are rare in the sillimanite-grade portion, and no muscovite-bearing types are present.

The Barrington Passage Pluton forms an elongate, north-trending mass about 50 km long and 6-12 km wide. Much of the pluton consists of biotite tonalite with moderate to strong foliation, but more massive tonalite to granodiorite occurs in the northern part. A kilometre-scale lens of norite occurs near the southern margin of the body (Atwood Brook norite), and small, variably hybridized inclusions of this material are strewn through much of the south part of the pluton. Pegmatites are rare within and around the pluton, and no muscovite-bearing types occur. The pluton is surrounded by sillimanite-grade rocks with extensive development of migmatite which form part of a regional metamorphic culmination which includes the western part of the Shelburne Pluton (Fig.1).

MAJOR AND TRACE ELEMENT COMPOSITION OF THE PLUTONS

Representative major and trace element data for the three plutons are presented in Table 1, and shown graphically in Figures 2 and 3. Southern Nova Scotia plutons range in composition from quartz gabbro to monzogranite (Fig. 2A), and include both high-K (Port Mouton) and medium-K (Barrington Passage, Shelburne) varieties (Fig. 2B). With the exception of the included mafic bodies (Birchtown, Atwood Brook), all analyses are slightly to moderately peraluminous (Fig. 2C). The tonalite phase of the Port Mouton Pluton is enriched in light rare earth elements (LREEs) relative to the granodiorite phase, and lacks the negative Eu and Sr anomalies which characterize the granodiorite (Fig. 3A, C). Both the tonalite and granodiorite exhibit a marked negative Nb anomaly. Chondrite-normalized rare earth plots and primitive-mantle-normalized extended element plots for the Shelburne Pluton closely resemble those for granodiorite of the Port Mouton Pluton (Fig. 3A, C). The Barrington Passage tonalite is markedly depleted of heavy rare earth elements (HREEs) relative to the Port Mouton tonalite, and shows no marked Nb or Sr anomaly (Fig. 3B, D). One sample from the Atwood Brook norite and a xenolith from the Barrington Passage tonalite, possibly cognate to the Atwood Brook norite, are enriched in high field strength elements compared to the surrounding tonalite (Fig. 3B, D). The primitive mantle normalized extended element and chondrite-normalized rare earth element plots for the xenolith resemble those for metagreywacke of the Meguma Group, whereas one sample of the norite is more enriched than the Meguma Group. Another sample of the norite gives much less enriched and flatter patterns, more consistent with mantle derivation.

OXYGEN ISOTOPIC DATA FOR THE PLUTONS

For many samples, oxygen isotope data for minerals from the plutons and their contained pegmatites (Table 2) reflect a pattern of ^{18}O-enrichment typical of granitoid rocks (quartz> potassium feldspar>muscovite>biotite>garnet; Taylor, 1968, 1978). Longstaffe et al. (1980) obtained similar results in their study of southern Nova Scotia granitic rocks. Isotopic "temperatures" calculated from these data by the method of Bottinga and Javoy (1975) are scattered, but generally subsolidus and indicate that retrograde isotopic exchange has occurred. Such behaviour is typical of granitic rocks (Taylor, 1978; Longstaffe, 1982). Significant modification of rock or mineral $\delta^{18}O$ values during low temperature (<250°C) alteration is apparent for one Port Mouton pegmatite ($\delta^{18}O$ muscovite>potassium feldspar>quartz), one Port Mouton muscovite granodiorite ($\delta^{18}O$ potassium feldspar>quartz), and one Shelburne pegmatite ($\delta^{18}O$ muscovite>potassium feldspar). These findings coincide with thermobarometric data (see below) indicating formation or re-equilibration of muscovite and potassium feldspar at sub-solidus temperatures.

The $\delta^{18}O$ values vary positively with respect to SiO_2. Phases of the Port Mouton and Shelburne plutons with SiO_2>72 weight per cent exhibit values between +9.4 and +11.0‰, whereas tonalitic and more mafic phases (SiO_2=51-65 weight per cent) from all plutons generally have lower values, between +7.0 and +8.5‰. Longstaffe et al. (1980) reported a similar range of values for granitic rocks in this region, including samples from the Port Mouton Pluton (+8.9 to +11.7‰), the Shelburne Pluton (+8.4 to +10.4‰) and the Barrington Passage Pluton (+8.3 to +9.0‰). These values lie in the 'high' (> +10‰) and 'high-normal' (+8 to +10‰) granite $\delta^{18}O$ categories of Taylor (1968, 1978), interpreted as reflecting extensive (high) and some (high-normal) interaction with $\delta^{18}O$-rich supracrustal rocks.

In the Port Mouton Pluton, pegmatite quartz has high $\delta^{18}O$ values, similar to other felsic phases of the pluton, regardless of the host rock, although the one major pegmatite which lies outside the the pluton exhibits a particularly high value suggestive of interaction with its Meguma Group host. Pegmatite quartz from the Shelburne Pluton has high $\delta^{18}O$ values (+8.9 to +11.7‰) regardless of the setting of the pegmatite (early segregation, late veins, veins cutting the Birchtown diorite). These values are comparable to those reported by Longstaffe et al. (1980) for quartz from granodiorite of this pluton (+10.8‰). Pegmatites cutting the Birchtown diorite give $\delta^{18}O$ values 1-3‰ higher than those obtained from the diorite (see also Longstaffe et al., 1980). The Barrington Passage Pluton gives the lowest $\delta^{18}O$ values, increasing from +7.6‰ in the mafic rocks through +8.1‰ in the tonalite to +9.3‰ in the rare pegmatites. These lower values indicate that interaction with the metasedimentary host, which has a much higher value of +12.4‰ (+10.1 to +12.9‰ according to Longstaffe et al., 1980), has not been extensive.

Table 1. Representative chemical data for southern Nova Scotia plutons.

	1	2	3	4	5	6	7	8
SiO_2	73.97	64.95	73.85	64.50	56.75	51.40	70.27	72.90
TiO_2	0.16	0.62	0.18	0.75	0.84	0.83	0.48	0.09
Al_2O_3	13.93	16.60	14.70	16.65	12.55	14.65	14.10	14.60
Fe_2O_3	0.50	1.00	0.31	0.83	1.81	1.41	0.56	-
FeO	0.70	3.10	1.05	3.55	5.25	6.70	2.87	0.90*
MnO	0.07	0.10	0.05	0.08	0.14	0.16	0.06	0.01
MgO	0.37	1.71	0.42	2.34	8.74	10.40	1.42	0.17
CaO	0.84	4.02	1.64	4.07	6.89	8.78	2.03	0.98
Na_2O	3.70	3.72	4.91	3.93	2.03	2.57	2.41	3.78
K_2O	4.22	2.39	2.10	2.09	2.76	0.47	3.96	4.68
P_2O_5	0.23	0.19	0.21	0.29	0.39	0.13	0.15	0.15
LOI	0.81	0.57	0.47	0.47	0.82	0.63	-	-
* Total iron as FeO - no data								
Cr	12	35	12	66	515	494	-	21
Ni	0	0	0	14	11	26	13	5
Sc	0	13	3	15	37	33	12	3
V	0	69	13	77	176	159	56	-
Cu	0	0	0	8	4	8	11	9
Pb	16	11	15	9	6	3	5	27
Zn	34	43	24	47	49	54	62	44
Rb	181	68	90	87	119	11	217	160
Ba	311	687	271	417	764	189	468	360
Sr	53	476	97	290	265	525	120	86
Ga	19	21	16	22	13	14	17	19
Ta	0.65	0.56	1.85	1.22	1.00	0.38	-	0.53
Nb	9.0	10.5	8.9	13.5	13.5	6.3	12.0	7.7
Hf	2.00	4.90	2.43	5.45	5.43	1.82	-	2.7
Zr	68	176	103	204	183	62	165	89
Y	10	13	10	13	20	14	32	10
Th	5.29	8.05	5.36	2.22	8.59	1.34	27	20.7
U	4.55	0.00	5.68	0.00	3.77	0.00	4	5.3
La	9.96	26.93	12.53	18.28	14.47	11.57	-	22.3
Ce	22.35	54.44	25.32	38.69	37.36	25.82	64	44.6
F	275	565	308	521	1175	225	-	-
Cl	40	14	0	486	218	285	-	-

1. Muscovite granodiorite, Port Mouton Pluton; 2. Biotite tonalite, Port Mouton Pluton; 3. Muscovite granodiorite, Shelburne Pluton; 4. Biotite tonalite, Barrington Passage Pluton; 5. Diorite, Birchtown quarry; 6. norite, Atwood Brook; 7. Average of 568 S-type granites (Whalen et al., 1987); 8. Average Harney Peak Pluton biotite granite (Duke et al., 1992)

General congruence of $\delta^{18}O$ for pegmatites and associated felsic phases suggests that the observed major phases of the plutons are the main progenitors of the pegmatites. The consistently high values of $\delta^{18}O$ indicate massive involvement of supracrustal rocks similar to the Meguma Group in the genesis of the plutons. Local extreme values, particularly in pegmatites contacting the Meguma Group, may indicate more or less direct local input from the host rocks.

PETROGENETIC IMPLICATIONS

On Pearce et al. (1984) granitoid discrimination diagrams (not shown), all but the two mafic samples plot in the volcanic-arc granite field. The plutons may be subdivided in Figures 3C and D into "arc-like" with pronounced negative Nb anomalies (Port Mouton, Shelburne) and "non-arc-like" with no Nb anomaly (Barrington Passage). "Arc-like" patterns can be produced from "non-arc" magmas by crustal assimilation. If this is the case in southern Nova Scotia, then the Barrington Passage Pluton has assimilated less crustal material than the Shelburne and Port Mouton plutons, a hypothesis also compatible with the O isotope data. The anomalously high rare earth element and high field strength element content of mafic rocks in the Barrington Passage Pluton may reflect either assimilation of Meguma-like crustal material, or a primary alkaline, within-plate character.

Peraluminous mineralogy and chemistry plus elevated $\delta^{18}O$ values in the southern Nova Scotia plutons indicate derivation mainly from supracrustal sources (Longstaffe et al., 1980), that is S-type granites in the broad sense, although not strictly S-type under the narrow definition of Chappell and White (1992). Compared to the average of 568 S-type granite analyses from Australia (Table 1), analyses of southern Nova Scotia plutons are markedly richer in Na_2O and poorer in K_2O, and generally more evolved, that is richer in SiO_2 and poorer in FeO, MgO and related trace elements. Hybridization and mingling of peraluminous supracrustally

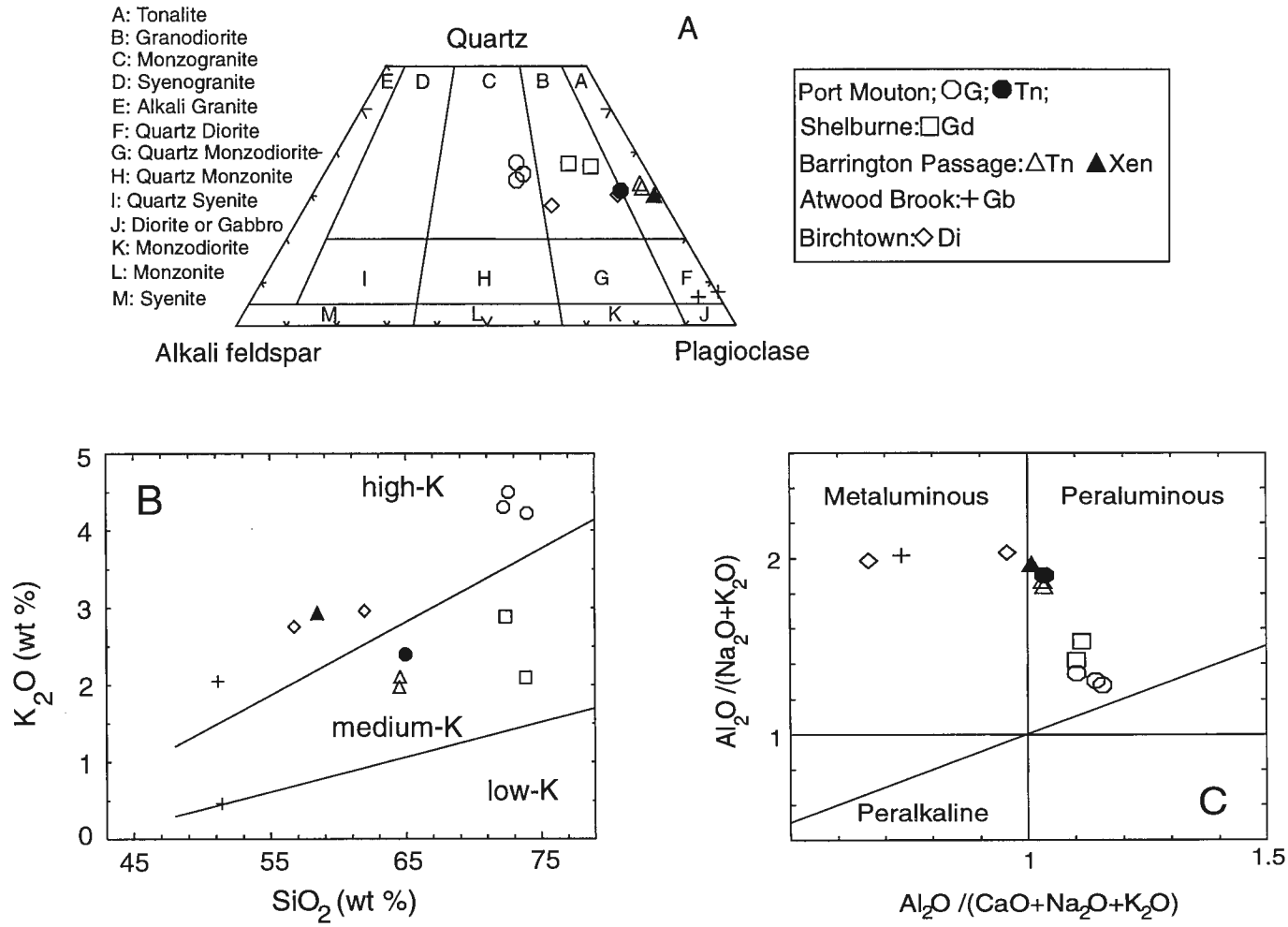

Figure 2. *Compositions of southern Nova Scotia plutons plotted on* ***(A)*** *mesonorm quartz-alkali feldspar-plagioclase classification (LeMaitre, 1989),* ***(B)*** *K_2O-SiO_2 plot;* ***(C)*** *Al index (molecular $Al_2O_3/(CaO+Na_2O+K_2O)$) vs. agpaitic index (molecular $Al_2O_3/(Na2O+K2O)$) (Maniar and Piccoli, 1989). Abbreviations for symbols are as follows; G=biotite-muscovite granodiorite and granite, Tn=biotite tonalite, Gd=granodiorite Xen=mafic xenolith, Gb=gabbro-norite, Di=diorite.*

derived granitoid rocks with contemporary metaluminous gabbroic to dioritic phases (Currie and Whalen, 1995) suggest that mantle-derived magma played a significant role in the origin and emplacement of these plutons, either directly by bulk assimilation processes (Huppert and Sparks, 1985, 1988) or indirectly as a source of heat. Spatial and apparent genetic relationships of beryl-bearing pegmatites to the biotite-muscovite granodiorite of the southern Nova Scotia plutons suggest that the sources of the pegmatites lie in relatively water-rich, supracrustally-derived material. Evolved parts of the southern Nova Scotia plutons (biotite-muscovite granodiorite to granite) resemble in composition the Harney Peak Pluton of South Dakota (Table 1) which is the source of a major rare element pegmatite field. However southern Nova Scotia plutons lack significant volumes of the strongly fractionated or evolved granites considered to be the immediate source of the pegmatite field around the Harney Peak Pluton (Duke et al., 1992).

PRESSURE-TEMPERATURE CONDITIONS OF EMPLACEMENT

Beryl-bearing pegmatites in this region commonly contain garnet, biotite, muscovite, potassium feldspar, and plagioclase. The pressure and temperature of formation of this assemblage can be determined with considerable accuracy using the methods outlined by Berman (1991) and compositions of coexisting minerals determined using an electron microprobe. Representative mineral composition data are given in Table 3. Garnet is manganese rich (MnO 12 to 15 weight per cent) with slight zoning from Mn-rich cores to Fe-rich rims. Biotite is iron rich. Micas contain low to negligible amounts of F and Cl (<0.4 weight per cent). Feldspars in contact with garnet, which is erratically distributed, approach pure albite and microcline, but plagioclase compositions as calcic as An_{30} occur remote from garnet (>10 cm).

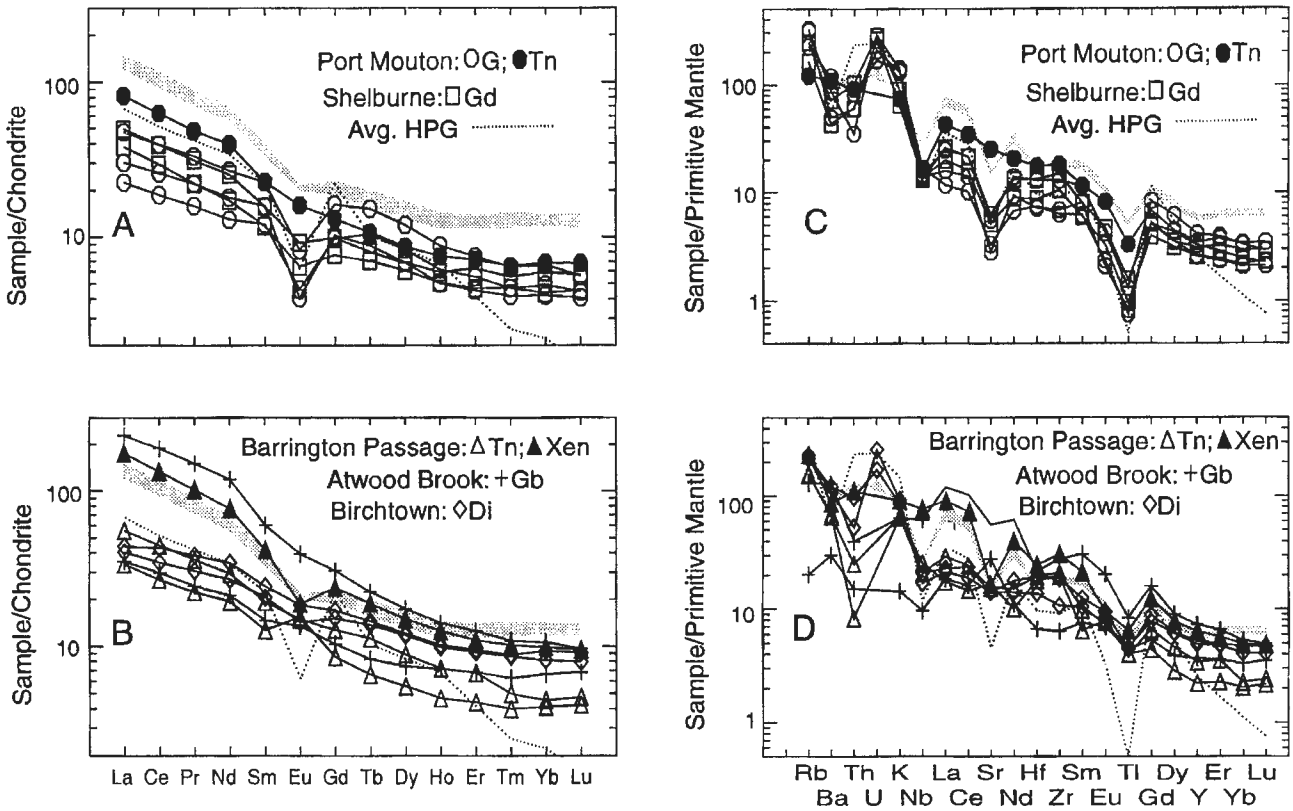

Figure 3. A, B) Chondrite-normalized rare earth element plots for southern Nova Scotia plutons. C, D) Extended element plots for southern Nova Scotia plutons. The field for two meta-greywackes of the Meguma Group (shaded area) is included for comparison, as well as the average biotite granite from the Harney Peak Pluton (dashed line, data from Duke et al., 1992). Normalizing values for chondrite and primitive mantle are from Sun (1982) and Taylor and McLennan (1985), respectively.

Figure 4 depicts results of P-T determination for a garnetiferous pegmatite from the Port Mouton Pluton (A) and one from the Shelburne Pluton (B). Assuming saturation with water, equilibria not involving muscovite give very consistent results with temperatures of 615-620°C (1σ errors of 5-20°C) and pressures of 3.8-4.5 kilobars (1σ errors of 0.3-0.7 kilobars). These conditions are consistent with solidus crystallisation of a water-saturated leucogranitic melt. Under these conditions, peraluminous melts should crystallize muscovite on the solidus. Introduction of muscovite into the P-T determinations gave scattered results in the subsolidus range with temperatures around 450°C and poorly determined pressures (Figure 4A, B). These data imply that no primary magmatic muscovite was analyzed. Either the muscovite grew entirely at subsolidus conditions, or magmatic muscovite has re-equilibrated under sub-solidus conditions. Support for the latter alternative is offered by the feldspars which are clearly too close to end-member compositions to be primary igneous compositions. Recalculation of P-T assuming a lower activity for water showed that muscovite would not be stable under any reasonable conditions (T>400°C) for activities of water less than 0.9.

In order to examine possible influence of host rocks on emplacement of pegmatites, P-T conditions were calculated for a migmatite in the aureole of the Barrington Passage Pluton and for an andalusite+staurolite-bearing metasedimentary rock east of the Shelburne Pluton. The former, with the assemblage sillimanite-muscovite-biotite-garnet-plagioclase (no potassium feldspar), gave P-T conditions of 620°C, 4.6 kilobars (Fig. 4C), whereas the latter, with the assemblage muscovite-biotite-garnet-staurolite-plagioclase, gave a well-constrained determination of 520°C, 4.5 kilobars. The first determination is independent of assumed water activity, but coexistence of muscovite with biotite and garnet at these temperatures requires activities near 1.0. The latter determination assumed a water activity of 1.0, and the consistency of the determination is lost if significantly lower values are assumed. These values are generally congruent with earlier estimates (Raeside and Jamieson, 1992) although estimated pressures are significantly higher.

Table 2. Average $\delta^{18}O$ values for phases of southern Nova Scotia plutons.

	Whole Rock	quartz	kfs	musc	bio	gar
Port Mouton Pluton						
tonalite	9.33	-	11.08	8.56	5.10	x
granodiorite	10.49	11.16	11.88	9.56	5.76	x
pegmatite	-	10.55	9.36	8.52	7.51	7.13
pegmatite[1]	-	11.77	11.92	12.98	x	7.56
country rocks	-	13.44	x	11.18	7.51	x
Shelburne Pluton						
diorite	8.89	-	-	x	-	x
granodiorite	9.67	-	-	-	-	x
pegmatite	-	11.46	10.27	11.09	9.48	7.74
pegmatite[2]	-	11.32	10.02	9.28	x	8.23
country rocks	11.49	-	x	-	-	-
Barrington Passage Pluton						
norite	7.61	-	-	x	-	x
tonalite	8.05	-	-	x	-	x
pegmatite	-	9.28	-	x	7.90	-
country rocks	12.39	-	x	-	-	x

[1] Sheet hosted by Meguma Group metasedimentary rocks.
[2] Dyke hosted by Birchtown diorite.
- no data. x mineral not present. Abbreviations; kfs - potassium feldspar, musc - muscovite, bio - biotite, gar - garnet

DISCUSSION

The data presented in this report, together with earlier data, suggest that southern Nova Scotia plutons originated from a magma which contained both mantle-derived and crust-derived components. The mantle-derived component is prominent in the case of the Birchtown diorite and Atwood Brook norite, but chemical and isotopic analyses indicate that even the most mafic rocks have assimilated crustal material. Differentiation of the plutons led eventually to formation of pegmatites, whose P-T conditions suggest crystallization at the water-saturated solidus. There is little or no evidence for a free aqueous phase under magmatic conditions (such as miarolitic cavities), or for extensive hydrothermal activity (for example hydrothermally altered wall rocks or swarms of quartz veins). Most isotopic data suggest modest re-equilibration at subsolidus temperatures, consistent with small scale circulation of fluids. Our data therefore generally support the model of London (1992) whereby pegmatites form by closed-system fractionation of water-rich magma, but a free aqueous phase appears very late in the process, if at all.

The composition of evolved (muscovite-bearing) phases of the plutons resembles that of plutons associated with rare-metal pegmatite fields, but no such field occurs around the southern Nova Scotia plutons. Absence of such a field could result from interplay of three factors. (1) The plutons contained insufficient or inappropriate volatiles. (2) The host rocks into which the plutons were emplaced were unfavourable. (3) The present exposure level is too deep for occurrence of abundant pegmatite.

The pegmatites crystallized under water-saturated, or near-saturated, conditions, but there is little evidence for a free aqueous phase at the magmatic stage. According to older models of pegmatite genesis, lack of a free aqueous phase would inhibit or prevent pegmatite formation (Jahns and Burnham, 1969). Currently popular models do not require a free aqueous phase for pegmatite formation (London, 1992),

Table 3. Representative electron microprobe data for pegmatites and host rocks of southern Nova Scotia plutons.

	1	2	3	4	5	6	7	8	9	10
SiO_2	33.98	46.27	35.96	67.60	63.50	35.17	47.06	36.94	27.56	61.99
TiO_2	1.09	0.00	0.05	-	-	1.58	0.28	0.03	0.66	-
Al_2O_3	18.54	35.58	20.59	19.63	18,49	19.29	35.84	20.87	54.01	23.69
FeO*	24.28	1.85	29.04	0.00	0.02	19.25	1.84	33.08	14.23	0.10
MnO	0.68	0.05	13.82	-	-	0.09	0.00	6.03	0.28	-
MgO	5.64	0.60	1.27	-	-	9.93	0.65	2.32	1.65	-
CaO	0.04	0.00	0.43	0.19	0.01	0.01	0.00	2.28	0.00	4.74
Na_2O	0.02	0.42	0.01	11.83	0.69	0.24	1.22	0.01	0.01	8.87
K_2O	8.51	11.03	0.00	0.05	16.39	9.13	9.46	0.01	0.02	0.34
F	0.37	0.00	-	-	-	0.01	0.00	-	-	-
Cl	0.03	0.00	-	-	-	0.01	0.00	-	-	-
Si	2.719	3.059	2.916	2.977	2.974	2.684	3.070	2.947	3.897	2.757
Ti	0.066	0.000	0.003	-	-	0.090	0.014	0.002	0.070	-
Al	1.749	2.772	1.968	1.019	1.020	1.735	2.756	1.962	9.002	1.242
Fe3	0.000	0.102	0.194	0.000	0.001	0.000	0.101	0.141	0.000	0.003
Fe2	1.625	0.000	1.772	0.000	0.000	1.228	0.000	2.066	1.676	0.000
Mn	0.046	0.003	0.950	-	-	0.006	0.001	0.408	0.033	-
Mg	0.673	0.059	0.154	-	-	1.130	0.064	0.275	0.347	-
Ca	0.004	0.000	0.037	0.009	0.001	0.001	0.000	0.195	0.000	0.226
Na	0.003	0.054	0.001	1.010	0.061	0.036	0.154	0.000	0.002	0.765
K	0.869	0.931	0.000	0.003	0.979	0.889	0.787	0.001	0.003	0.019
O	11	11	12	8	8	11	1	12	23.5	8
F	0.093	0.000	-	-	-	0.081	0.000	-	-	-
Cl	0.004	0.000	-	-	-	0.002	0.000	-	-	-

* Total iron as FeO. - not analysed
Ferric iron calculated in standard cells by reducing analysis to the stated number of oxygens, and then reducing the total number of cations to stoichiometric by oxidizing iron.
1-5. Biotite (1), muscovite (2), garnet (3), plagioclase (4) and potassium feldspar (5) from pegmatite, Shelburne Pluton.
6-10. Biotite (1), muscovite (2), garnet (3), staurolite (4) and plagioclase (5) from an andalusite-staurolite-garnet granofels east of the Shelburne Pluton.

but high contents of F, Cl, and B are ubiquitous in rare-metal pegmatites and granites associated with them. All of these elements have low abundances in southern Nova Scotia plutons (Table 1). The plutons probably contained insufficient amounts of these elements to generate an extensive pegmatite field.

Emplacement of dykes requires creation of a low pressure zones into which dykes can be emplaced. As host rocks become more plastic, brittle fracture requires progressively more rapid deformation, and dyke emplacement becomes progressively less probable. Plastically deformed migmatites and wrapping of foliation around plutons suggest that sillimanite-grade country rocks of the southern Nova Scotia plutons, possibly at temperatures over 600°C (Fig. 4C; Raeside and Jamieson, 1992), flowed readily in response to intrusion, and hence were an unfavourable host for dykes. A pegmatite on the margin of the Port Mouton pluton may have exchanged O isotopes with its Meguma Group host, presumably via an aqueous medium. The significance of such processes in generating rare-metal pegmatites is uncertain, but they would not occur in sillimanite and higher-grade rocks which were effectively dehydrated by anatexis. The high-grade rocks around the southern Nova Scotia plutons form an unfavourable host for pegmatites and possibly for processes within pegmatites.

Pressures obtained from new thermobarometry for pegmatites from southern Nova Scotia plutons are higher than older estimates. Any pegmatite field which once existed around these plutons could therefore have been lost to erosion. However, pressures around the Barrington Passage Pluton are identical to those around the Port Mouton Pluton. Therefore the presence of beryl-bearing pegmatites around the latter cannot be be due to less erosion, but must be ascribed to some combination of differing source, degree of interaction with crust and physical conditions not involving pressure. We do not consider erosional loss to be a major explanation of the scarcity of pegmatites around southern Nova Scotia plutons.

We find that factors relevant to beryl mineralization are generally unfavourable around the southern Nova Scotia plutons. We therefore conclude that the potential for commercially exploitable beryl mineralization is low.

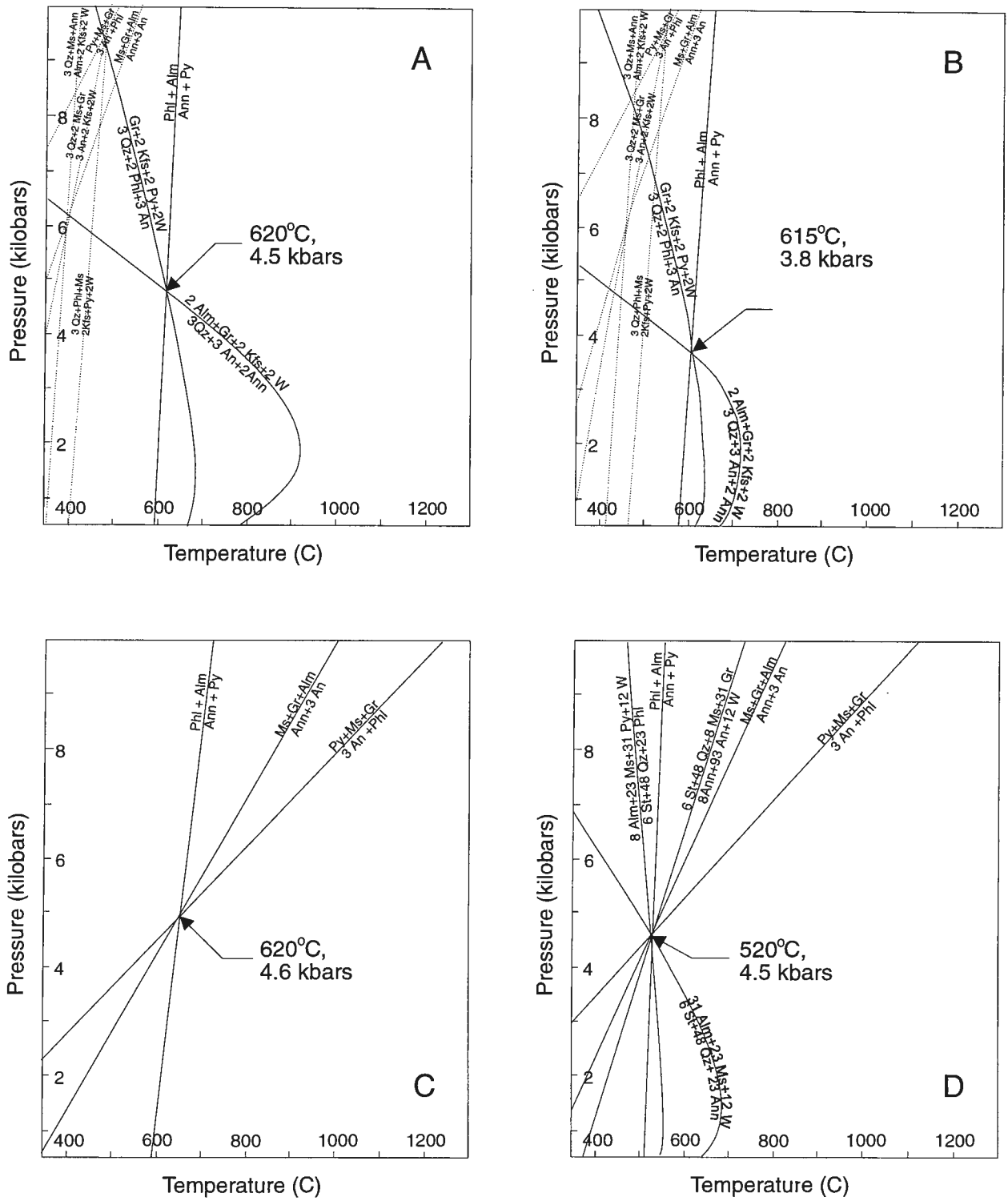

Figure 4. *Pressure-temperature determinations for emplacement of pegmatites of southern Nova Scotia plutons and for their host rocks.* ***A)*** *Pegmatite, Port Mouton Pluton,* ***B)*** *Pegmatite, Shelburne Pluton,* ***C)*** *Migmatite, aureole of Barrington Passage Pluton, and* ***D)*** *Andalusite-staurolite-garnet granofels, aureole of Shelburne Pluton. Pressure-temperature determinations made by the method of Berman (1991) using the following solutions models; garnet (Berman and Koziol, 1991), biotite (McMullin et al., 1991), plagioclase (Fuhrman and Lindsley, 1988). For other phases, ideal ionic solution was assumed. Abbreviations for components are as follows; An – anorthite, Ann – annite, Alm – almandine, Gr – grossular, Kfs – potassium feldspar, Ms – muscovite, Phl – phlogopite, Py – pyrope, Qz – quartz, St – staurolite, W – water. In A and B, muscovite-bearing reactions, believed to be subsolidus (see text), are shown as dotted lines and labelled in smaller type.*

REFERENCES

Berman, R.G.
1991: Thermobarometry using multiequilibrium calculations: a new technique with petrological applications; Canadian Mineralogist v. 29, p. 833-855.

Berman, R.G. and Koziol, A.M.
1991: Ternary excess properties of grossular-pyrope-almandine garnets and their influence in geothermobarometry; American Mineralogist, v. 76, p. 1223-1231.

Bottinga, Y. and Javoy, M.
1975: Oxygen isotope partitioning among the minerals in igneous and metamorphic rocks; Reviews of Geophysics and Space Physics v. 13, p. 401-418.

Chappell, B.W. and White, A.J.R.
1992: I- and S-type granites in the Lachlan Fold Belt; Transactions of the Royal Society of Edinburgh, Earth Sciences v. 83, p. 1-26.

Currie, K.L. and Whalen, J.B.
1994: A note on the occurrence of beryl in the Port Mouton pluton, southern Nova Scotia in Current Research 1994-D; Geological Survey of Canada, p. 73-77.
1995: A further note on the occurrence of beryl associated with southern Nova Scotia plutons in Current Research 1995-D; Geological Survey of Canada, p. 59-64.

de Albuquerque, C.A.R.
1977: Geochemistry of the tonalitic and granitic rocks of the southern Nova Scotia plutons; Geochimica et Cosmochimica Acta, v. 41, p. 1-13.

Douma, S.L.
1988: The mineralogy, petrology and geochemistry of the Port Mouton Pluton, Nova Scotia Canada; M.Sc. thesis, Dalhousie University, Halifax, Nova Scotia, 324 p.

Duke, E.F., Papike, J.J., and Laul, J.C.
1992: Geochemistry of a boron-rich peraluminous granite pluton: the Calamity Peak layered granite-pegmatite complex, Black Hills, South Dakota; Canadian Mineralogist, v. 30, p. 811-833.

Fuhrman, M.I. and Lindsley, D.H.
1988: Ternary feldspar modelling and thermometry; American Mineralogist v. 73, p. 201-216.

Huppert, H. and Sparks, R.S.J.
1985: Cooling and contamination of mafic and ultramafic magmas during ascent through continental crust; Earth and Planetary Science Letters, v. 74, p. 371-386.
1988: The generation of granitic magmas by intrusion of basalt into continental crust; Journal of Petrology, v. 29, p. 599-624.

Keppie, J.D. and Dallmeyer, R.D.
1995: Late-Paleozoic collision, delamination, short-lived magmatism and rapid denudation in the Meguma Terrane (Nova Scotia, Canada): constraints from $^{40}Ar/^{39}Ar$ isotopic data; Canadian Journal of Earth Sciences v. 32, p. 644-650.

Jahns, R.H. and Burnham, C.W.
1969: Experimental studies of pegmatite genesis: I. A model for the derivation and crystallisation of granitic pegmatites; Economic Geology, v. 84, p. 843-864.

LeMaitre, R.W.
1989: A classification of igneous rocks and glossary of terms; Blackwell, Oxford, 193 p.

London, D.
1992: The application of experimental petrology to the genesis and crystallization of granitic pegmatites; Canadian Mineralogist, v. 30, p. 499-540.

Longstaffe, F.J.
1982: Stable isotopes in the study of granitic pegmatites and related rocks; Mineralogical Association of Canada, Short Course Handbook 8, p. 373-404.

Longstaffe, F.J., Smith, T.E., and Muehlenbachs, K.
1980: Oxygen isotope evidence for the genesis of Upper Paleozoic granitoids from southwestern Nova Scotia; Canadian Journal of Earth Sciences, v. 17, p. 132-141.

Maniar, P.D. and Piccoli, P.M.
1989: Tectonic discrimination of granitoids; Geological Society of America Bulletin, v. 101, p. 635-643.

McMullin, D., Berman, R.G., and Greenwood, H.J.
1991: Calibration of the SGAM thermobarometer for pelitic rocks using data from phase equilibrium experiments and natural assemblages; Canadian Mineralogist, v. 29, p. 889-908.

Pearce, J.A., Harris, N.B.W., and Tindle, A.G.
1984: Trace element discrimination diagrams for the tectonic interpretation of granitic rocks; Journal of Petrology, v. 25, p. 956-983.

Raeside, R.P. and Jamieson, R.A.
1992: Low pressure metamorphism of the Meguma Terrane, Nova Scotia; Geological Association of Canada, Wolfville '92 Field Excursion C-5, Guidebook, 25 p.

Rogers, H.D.
1985: Field relations, petrography and geochemistry of granitoid plutons in the Shelburne area, southern Nova Scotia; Geological Survey of Canada, Open File 1835, 128 p.

Sun, S.S.
1982: Chemical composition and origin of the Earth's primitive mantle; Geochimica et Cosmochimica Acta, v. 46, p. 179-192.

Tate, M.C.
1995: The relationship between Late Devonian mafic intrusions and peraluminous granitoid generation in the Meguma lithotectonic zone, Nova Scotia, Canada; PhD. thesis, Dalhousie University, Halifax, Nova Scotia, 528 p.

Taylor, H.P., Jr.
1968: The oxygen isotope geochemistry of igneous rocks; Contributions to Mineralogy and Petrology, v. 19, p. 1-71.
1978: Oxygen- and hydrogen-isotope studies of plutonic granitic rocks; Earth and Planetary Science Letters, v. 38, p. 177-210.

Taylor, S.R. and McLennan, S.M.
1985: The Continental Crust: Its Composition and Evolution; Blackwell, Oxford, 312 p.

Whalen, J.B., Currie, K.L., and Chappell, B.W.
1987: A-type granites: geochemical characteristics, discrimination and petrogenesis, Contributions to Mineralogy and Petrology, v. 95, p. 407-419.

Geological Survey of Canada Project 730044

The Smithfield base metal (Pb-Zn) deposit in the Carboniferous Windsor Group, Nova Scotia: a case of mineralized synsedimentary breccia[1]

Denis Lavoie
Quebec Geoscience Centre, Sainte-Foy

Lavoie, D., 1996: The Smithfield base metal (Pb-Zn) deposit in the Carboniferous Windsor Group, Nova Scotia: a case of mineralized synsedimentary breccia; in Current Research 1996-D; Geological Survey of Canada, p. 11-16.

Abstract: Base metal occurrences in the Carboniferous Macumber Formation (Nova Scotia) are associated with carbonate breccias. Based on various evidence, three types of breccias have been recognized at the top of the Macumber Formation in the vicinity of the Walton and Jubilee deposits: an early (synsedimentary) and two late (tectonic and post-burial karstic).

The Smithfield Pb-Zn deposit in central Nova Scotia is hosted in the Macumber Formation. A detailed survey of nine drill cores intersecting the mineralized section not only documents the previously reported breccia types but also indicates that the synsedimentary breccia is widely distributed in the deep-water lithofacies of the Macumber Formation and that this breccia commonly hosts base metal deposits (major or minor) in the Carboniferous section.

Résumé : Les indices de métaux de base identifiés dans la Formation de Macumber du Carbonifère (Nouvelle-Écosse) sont associés à des brèches carbonatées. Divers éléments d'information ont permis de dégager trois types de brèches au sommet de la Formation de Macumber, dans les régions des gîtes de Walton et de Jubilee. L'un est précoce (synsédimentaire) et les deux autres sont tardifs (tectonique et karstique, postérieurs à l'enfouissement).

Le gisement de Pb-Zn de Smithfield, en Nouvelle-Écosse centrale, est encaissé dans la Formation de Macumber. Un examen détaillé de neuf carottes de forage interceptant la zone minéralisée permet non seulement de reconnaître les trois types de brèches, mais indique également que la brèche synsédimentaire est presque omniprésente dans les lithofaciès d'eau profonde de la Formation de Macumber et qu'elle est souvent l'encaissant de gisements (majeurs ou mineurs) de métaux de base dans l'intervalle carbonifère.

[1] Contribution to the Madgalen Basin NATMAP Project

INTRODUCTION

The middle Viséan (Early Carboniferous) Macumber Formation (Weeks, 1948) with the laterally equivalent and coeval Gays River Formation at the base of the Windsor Group (Bell, 1929), represents the first significant carbonate units in the post-Acadian successor Maritimes Basin (Fig. 1).

The Macumber Formation is locally characterized by mineralized carbonate breccias. The intimate association between base metal (Pb-Zn-Cu-Ba) mineralization and breccia has long been known for this part of the Windsor Group. However, the origin of these breccias has been the subject of much debate (for a recent review see Lavoie and Sangster, 1995; Lavoie et al., in press). A long lasting period (middle Viséan to latest Westphalian) of breccia events occurred during sedimentation, burial and after uplift of the succession (Lavoie and Sangster, 1995; Lavoie et al., in press). Based on sedimentological, diagenetic and geochemical characteristics of these breccias, three major types have been recognized: syn-sedimentary, late tectonic, and late solution collapse karstic breccias (Lavoie and Sangster, 1995; Lavoie et al., in press) These conclusions were reached through the study of two significant ore deposits (Walton and Jubilee, Fig. 1) and various base metal barren field sections. This contribution outlines the relationships between breccias and mineralization for a minor ore deposit in the central part of Nova Scotia, the Smithfield Pb-Zn deposit in the Shubenacadie structural sub-basin (Fig. 1).

GEOLOGICAL AND STRATIGRAPHIC SETTINGS

The Lower Carboniferous Windsor Group outcrops in many structural sub-basins of the Maritimes Basin (Fig. 1); a successor basin formed by extensional collapse of the Acadian orogen in Late Devonian time (Lynch and Tremblay, 1994). A thick Hadrynian-Middle Devonian succession constitutes the basement of this successor basin. At the base of the Windsor Group (Fig. 2), the Macumber Formation conformably overlies the Upper Devonian-lowermost Carboniferous continental siliciclastics of the Horton Group (Hamblin and Rust, 1989). Conversely, the coeval Gays River Formation unconformably overlies the metawacke of the Cambrian-Ordovician Meguma Group and other pre-Carboniferous

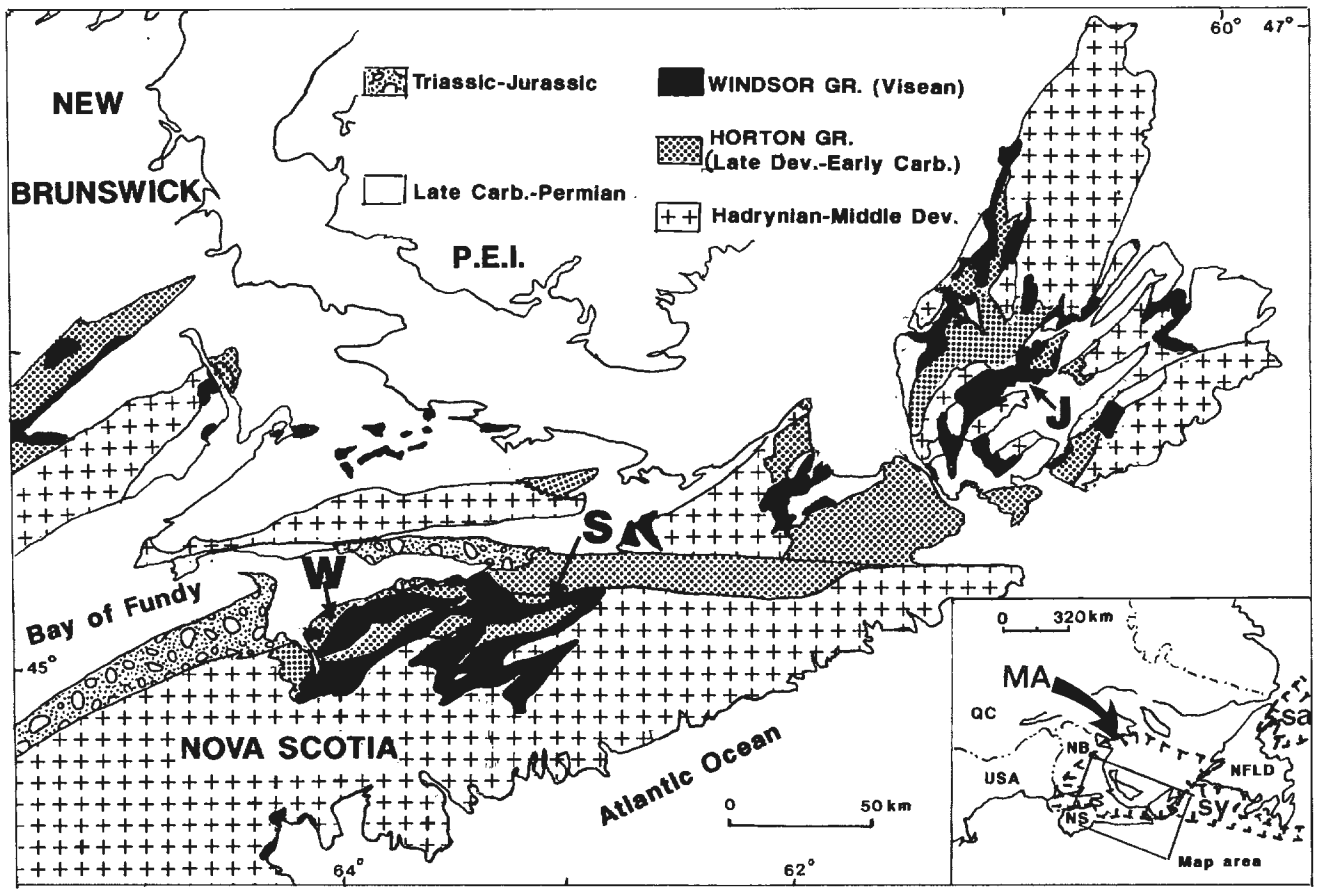

Figure 1. Geological and location map of Carboniferous structural sub-basins and various localities discussed in text. The W, J and S refer to Walton, Jubilee and Smithfield deposits, respectively. The inset locates the Maritimes Basin (MA), sa is for Saint-Anthony basin and sy is for Sydney basin. Modified from Boehner et al. (1989)

basement rocks. Both the Macumber and Gays River formations are overlain by a thick massive anhydrite unit (Carolls Corner Formation; Fig. 2). Base metal mineralizations are found in the Gays River and Macumber formations, however, breccia-hosted deposits are exclusive to the latter.

The Shubenacadie sub-basin is one of the numerous post-acadian structural basins in Nova Scotia (Fig. 1). It is predominantly a large syncline transected by abundant and variously oriented faults (Giles and Boehner, 1982). In the Shubenacadie sub-basin, the Devono-Carboniferous succession consists, in ascending order, of the Horton, Windsor, Canso and Pictou groups (Fig. 2); several major disconformities are present between and within units (Giles and Boehner, 1982). The stratigraphic section is overwhelmingly dominated by siliciclastic and locally by evaporite deposits. Carbonate rocks are concentrated in the Windsor Group where they only form a minor part of the unit except at its base. Here the coeval Gays River and Macumber formations constitute a regional significant marker unit.

REGIONAL DEPOSITIONAL SETTING AND EVOLUTION OF THE MACUMBER FORMATION

Over all Nova Scotia, the Macumber Formation consists of two major lithostromes (Schenk, 1967; Schenk et al., 1994; Lavoie and Sangster, 1995; Lavoie et al., in press): a lower, thin succession of interbedded lime mudstone, oolitic and intramicritic wackestone and packstone overlain by a thicker succession of interbedded laminar pelmicrite and sulphate. Locally, a brecciated interval caps the Macumber Formation (Lavoie and Sangster, 1995; Lavoie et al., in press). Recently, the two major sedimentary lithostromes have been interpreted as representing a lower interval of outer shelf storm-driven sedimentation overlain by deep-water microbial mats (Lavoie and Sangster, 1995; Lavoie et al., in press). Locally, a tectonofacies (calcmylonite) is developed in the microbial mat facies (Lynch and Tremblay, 1994). As a whole, the Macumber succession results from a rapid and major transgressive event that culminated in the deposition of regionally extensive deep-water anhydrite (Lavoie, 1995; Lavoie et al., in press).

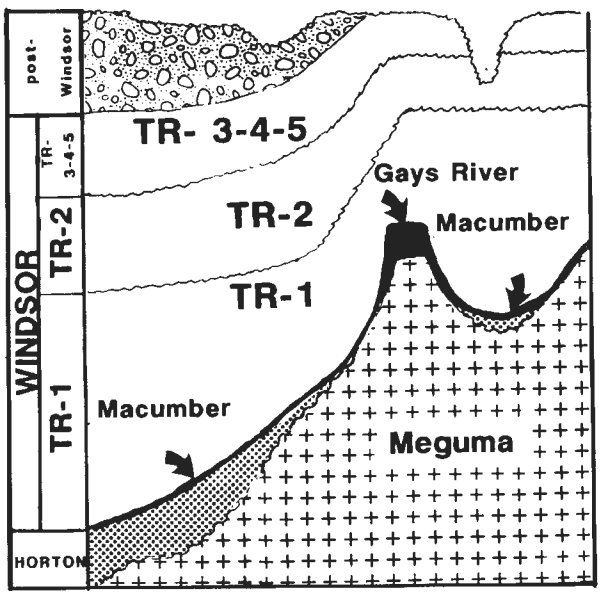

Figure 2. Major transgressive-regressive (T-R) cycles in the Windsor Group and stratigraphic position of the Macumber Formation. Modified from Giles (1981).

The recent research dealing with the breccias found in the upper part of the Macumber Formation has resulted in the recognition of three temporally distinct breccia events; syn-sedimentary slump breccia, late extensional detachment breccia and late solution collapse karstic breccia have been proposed (Lavoie and Sangster, 1995; Lavoie et al., in press). It is not the scope of this contribution to present an other detailed account of these breccias, readers interested are referred to the above cited literature. However, both the synsedimentary and tectonic breccias are mineralized (Walton and Jubilee deposits, respectively; Burtt, 1995; Fallara, 1995), conversely, the late karstic breccia is barren.

THE SMITHFIELD Pb-Zn DEPOSIT

Nine drill cores from the Smithfield deposit were described in detail. The carbonate at the base of the Windsor Group (the Macumber Formation) overlies various siliciclastic facies of the Horton Group. In all these cores, a systematic pattern in facies and mineralization can be easily recognized.

Lithofacies

Lime mudstone and wackestone

This facies, when present, is invariably at the base of the Macumber Formation where it forms a 5 to 20 cm-thick succession. These carbonate rocks, locally dolomitized, consist of lime mud and fine-grained pelmicrite with a wackestone depositional texture, both in centimetre-thick beds. They are commonly interlayered with minor (10-20%) shaly laminae, bioturbation is common but skeletal remains are lacking. This facies is fairly similar to a facies of the lower lithostrome of Lavoie and Sangster (1995). It most likely represents below fairweather wave base storm-driven sedimentation on an outer shelf.

Laminar micrite

This facies represents the dominant and typical rock unit of the Macumber Formation. The transition with the previous lithofacies is gradual over a decimetric interval. The locally dolomitized laminated facies forms a succession ranging from 5 cm up to 10 m in thickness. This facies consists of millimetre-thick micrite laminae interlayered with organic-rich black mudstone laminae. This facies is similar to the deep-water microbial mat facies of the upper lithostrome of Lavoie and Sangster (1995), the same interpretation is applied for this case.

Synsedimentary slump breccia

This facies, even if abundant, is sporadically developed in the Macumber Formation (Lavoie and Sangster, 1995), however, it is significant in that, in many areas, it hosts base metal mineralization (Lavoie and Sangster, 1995; Lavoie et al., in press). The transition with the previous laminar micrite facies is somewhat irregular. As described and illustrated by Lavoie and Sangster (1995; their figure 5), the synsedimentary slump breccia (see Lavoie and Sangster, 1995 for a detailed description) occurs in a cyclic and somewhat repetitive succession showing, over decimetric to metric intervals, an upward increase in soft-sediment deformations recorded in the deep-water microbial mats, culminating in a slump breccia. For the entire succession, the relative abundance of the breccia compared to undeformed and slumped microbial mats increases within the uppermost part of this facies. Locally, fragments of the breccia are coated with a millimetre-thick peloidal crust of likely microbial origin (Fig. 3a), this is a new argument for the synsedimentary origin of the breccia.

For the Smithfield deposit, this breccia is mineralized in barite, pyrite, galena, and sphalerite. The sulphide mineralization is invariably concentrated in the matrix of the breccia encasing the microbial mat fragments. This supports the claim that the synsedimentary brecciation created some microporosity in the matrix of the breccia that was later used by mineralizing fluids (Burtt, 1995; Lavoie and Sangster, 1995; Lavoie et al., in press).

Late karstic breccia: first event

A late karstic breccia occurs even more irregularly than the previous breccia; it is known as the Pembroke breccia as recently redefined by Lavoie and Sangster (1995). This breccia overlies the previously described synsedimentary breccia (Fig. 3b) but also occurs in centimetre-thick intervals within sections of the latter. The late karstic breccia is easily differentiated from the synsedimentary one by the polymictic nature of fragments (microbial mat, synsedimentary breccia, red mudstone and siltstone and sulphide fragments) and from

***Figure 3. a)** Fragment of recrystallized microbial mat coated by a crust of peloidal material (pen tip) of likely microbial origin indicating a sea floor brecciation process. **b)** Contact (arrow) between the greyish, monocompositional synsedimentary breccia and the overlying reddish, polycompositional late karstic breccia. Tape length is 30 cm. **c)** Late solution collapse karstic breccia of the second type, note the greyish colour; all visible clasts are siliciclastic.*

its reddish matrix. This breccia is generally barren and rare fragments of sulphide within the matrix support a post-ore event.

Late karstic breccia: second event

A second type of late karstic breccia is recognized in the Smithfield cores and at the Brookfield barite prospect. In most cases, this breccia overlies the first karstic breccia but it can be found anywhere in the Macumber section and even at the contact with the Horton Group. This matrix-supported breccia significantly differs from the first karstic type, it is polymictic with dominant siliciclastic fragments, carbonate clasts are rare, very small and part of the greyish, poorly unconsolidated matrix (Fig. 3c).

Evolution of the Macumber Formation at the Smithfield deposit

As for almost all sections of the Macumber Formation in the Maritimes Basin, the former sharply overlies continental siliciclastic facies of the Horton Group. A rapid and major transgressive event resulted in the sedimentation of outer shelf, below fairweather-wave base fine-grained wackestone and lime mudstone. Gradually, the sea level rise resulted in the establishment of below storm-wave base biosedimentation (e.g. microbial mats) on an upper slope setting. This slope interpretation is supported by the multiple unequivocal evidence for synsedimentary slumping and brecciation. The microbial mat facies is progressively interbedded with an increasing amount of sulphate nodules and laminae, now either leached or replaced by barite. The continuation of the sea level rise resulted in the precipitation of the basin-extensive deep-water massive anhydrite unit overlying the Macumber Formation (Lavoie, 1995).

The slump brecciation likely created some microporosity in the matrix of the resulting breccia that was used by sulphide-loaded brines leading to sulphide and barite precipitation. Following the mineralization event, uplift of the Macumber succession occurred and the mixed carbonate-evaporite interval was subjected to meteoric diagenesis, that is leaching the evaporite and to some extent, limestone, leading to the collapse of various parts of the Macumber. The resulting voids were filled by the karst breccia elements. Then either a second or a more mature stage of the first meteoric event led to the accumulation of the siliciclastic-rich matrix-supported breccia with only minute fragments of limestone. Because this last breccia can be found anywhere in the Macumber section, this suggests an irregular infiltration/dissolution pattern by meteoric fluids.

Comparison with the Walton deposit

The Walton deposit (Fig. 1) has been shown to occur in a thick synsedimentary breccia interval at the top of the Macumber Formation (Burtt, 1995; Lavoie and Sangster, 1995; Lavoie et al., in press). However, the sulphide mineralization occurs as a massive replacement of the entire carbonate breccia interval, both the matrix and clasts of microbial mats are mineralized. Therefore, even if the synsedimentary breccia is the host rock for both deposits, the mineralization event is more important at Walton. The main lithological difference between the two deposits, besides a somewhat thicker synsedimentary breccia interval at Walton, is the mineralogy of the carbonates rocks; at Walton it is siderite whereas at Smithfield it is limestone that is locally dolomitized. This difference is in accord with the hypothesis that the microporosity and permeability generated through slumping and brecciation could only be preserved efficiently if the resulting voids were rapidly filled by a calcite cement-inhibiting phase (Lavoie et al., in press). The stable isotope signatures of carbonate from Walton show that the sideritization occurred in the presence of a hydrocarbon-rich fluid (Sangster et al., 1994); hydrocarbons are known to be an efficient cement-inhibiting phase (Feazel and Schatzinger, 1985). The smaller and low-grade limestone deposit at Smithfield likely suggests poor preservation of the plumbing system.

CONCLUSIONS

The study of the small Smithfield deposit allows us to shed light on its origin and help clarify previous findings pertinent to larger deposits such as Walton (Lavoie and Sangster, 1995; Lavoie et al., in press). As for the sideritized Walton deposit and for barren limestone sections of the Macumber Formation, a similar succession of facies is recorded with the presence of a fairly thick mineralized synsedimentary breccia section. Interestingly, the base metal mineralization is concentrated in the matrix of the breccia as supported by the preferred concentration of sulphides; fragments are not mineralized. However, for the Walton deposit, sulphides occur as massive replacement of both matrix and clasts. The origin for this discrepancy is likely recorded in the early sideritization event that occurred in the presence of hydrocarbon-rich interstitial fluids at Walton, preserving a significantly larger volume of porosity and a more efficient plumbing system for the late ore event. Therefore, it is significant that not only the presence of an interval of synsedimentary slump breccia is critical for some base metal occurrences in the Lower Carboniferous carbonate section in Nova Scotia, but that the porosity generated through the brecciation has to be preserved from calcite cementation. This preservation is recorded in the extensive sideritization at Walton that occurred in the presence of hydrocarbon-rich phase in the surrounding fluids. The poor preservation of porosity at Smithfield could be related to the absence of a calcite-inhibiting phase in the pores, which resulted in a low-grade and low-tonnage deposit.

ACKNOWLEDGMENTS

I wish to express my deepest gratitude to the staff of the Nova Scotia Department of Natural Resources Core Facility in Stellarton. Thanks are extended to D.F. Sangster who recognized the need for a good understanding of the breccia problem in the Carboniferous section in Nova Scotia in relation with base metal occurrences. F.J. Hein is thanked for allowing

access to some of her data on the Smithfield deposit. Finally, M.M. Savard suggested many fine and pertinent points in her critical reading of the manuscript.

REFERENCES

Bell, W.A.
1929: Horton-Windsor district Nova Scotia; Geological Survey of Canada, Memoir 155, 268 p.

Boehner, R.C., Giles, P.S., Murray, D.A., and Ryan, R.J.
1989: Carbonate buildups of the Gays River Formation, Lower Carboniferous Windsor Group, Nova Scotia; in Reefs, Canada and adjacent areas, (ed.) H.H.J. Geldsetzer, N.P. James, and G.E. Tebbutt; Canadian Society of Petroleum Geologists, Memoir 13, p. 609-621.

Burtt, M.D.
1995: Geology of the B-baseline zone, Walton Ba-Cu-Pb-Zn-Ag deposit, Nova Scotia; MSc. thesis, Ottawa-Carleton Geoscience Centre, Ottawa, Ontario, 117 p.

Fallara, F.
1995: Pétrographie, géochimie et métallogénie de l'indice de Pb-Zn de Jubilee à l'île du Cap Breton en Nouvelle-Écosse; MSc. thesis, INRS-Géoressources, Ste-Foy, Québec.

Feazel, C.T., and Schatzinger, R.A.
1985: Prevention of carbonate cementation in petroleum reservoirs; in Carbonate Cements, (ed.) N. Schneiderman and P.M. Harris; Society of Economic Paleontologists and Mineralogists, Special Publication 36, p. 97-106.

Giles, P.S.
1981: Major transgressive-regressive cycles in Middle to Late Visean rocks of Nova Scotia; Nova Scotia Department of Mines and Energy, Paper 81-2.

Giles, P.S. and Boehner, R.C.
1982: Geological map of the Shubenacadie and Musquodoboit basins, central Nova Scotia; Nova Scotia Department of Mines and Energy, Map 82-4, scale 1:50 000.

Hamblin, A.P. and Rust, B.R.
1989: Tectono-sedimentary analysis of alternate-polarity half-graben basin-fill successions: Late Devonian - Early Carboniferous Horton Group, Cape Breton Island, Nova Scotia; Basin Research, v. 2, p. 239-255.

Lavoie, D.
1995: Circum-Euramerica Early Carboniferous (Viséan) basins: evidence for a salinity stratified ocean [abs.]: Geological Society of America, Abstracts with program, v. 27, p. A-451.

Lavoie, D. and Sangster, D.F.
1995: Origins and timing of basal Windsor carbonate breccias, Nova Scotia; in Current Research 1995-D: Geological Survey of Canada, p. 1-10.

Lavoie, D., Sangster, D.F., Savard, M.M., and Fallara, F.
in press: Multiple breccia events in the lower part of the Carboniferous Windsor Group, Nova Scotia; Atlantic Geology, v. 31, no. 3.

Lynch, G. and Tremblay, C.
1994: Late Devonian-Carboniferous detachment faulting and extensional tectonics in western Cape Breton Island, Nova Scotia, Canada; Tectonophysics. v. 238, p. 55-69.

Sangster, D.F., Savard, M.M., and Burtt, M.D.
1994: Isotope geochemistry of the Macumber Formation and altered equivalents, Walton deposit area, Kennetcook sub-basin; in Program and summaries, Eighteenth annual review of activities, (ed.) D.R. MacDonald; Nova Scotia Department of Natural Resources, Report 94-2, p. 49.

Schenk, P.E.
1967: The Macumber Formation of the Maritimes Provinces - a Mississippian analogue to recent strand-line carbonates of the Persian Gulf; Journal of Sedimentary Petrology, v. 37, p. 365-376.

Schenk, P.E., von Bitter, P.H., and Matsumoto, R.
1994: Deep-basin/deep-water carbonate-evaporite deposition of a saline giant: Loch Macumber, Atlantic Canada; Carbonates and Evaporites, v. 9, p. 187-210.

Weeks, L.J.
1948: Londonderry and Bass River map-areas, Colchester and Hants Counties, Nova Scotia; Geological Survey of Canada, Memoir 245.

Geological Survey of Canada Project 860018MB

Pore structure evolution of compacting muds from the seafloor, offshore Nova Scotia

T.J. Katsube, G.N. Boitnott[1], P.J. Lindsay, and M. Williamson[2]
Mineral Resources Division, Ottawa

Katsube, T.J., Boitnott, G.N., Lindsay, P.J., and Williamson, M., 1996: Pore structure evolution of compacting muds from the seafloor, offshore Nova Scotia; in Current Research 1996-D; Geological Survey of Canada, p. 17-26.

Abstract: Permeability and pore-size distribution were determined for unconsolidated mud samples of different grain-size distributions, from the ocean floor (offshore Nova Scotia), at different effective pressures of up to 100 MPa. The purpose was to provide information on mud permeability and pore structure evolution as they are transformed into shale through compaction, a requirement for modelling of sedimentary basin development and hydrocarbon exploration.

Results indicate that permeabilities are 10^{-20}-10^{-18} m^2, and that samples with large fractions of fine grains (2-8 μm) show considerable decrease in permeability with pressure, whereas these with larger fractions of large grains (10-60 μm) show smaller decreases. A sample representing the former distribution shows smaller variation in pore-sizes, compared to one representing the latter. Both display unimodal pore-size distributions (modes of 25-160 nm), showing little change with increase in compacted pressures, although porosities decrease with pressure. Surface areas also show little changes with pressure.

Résumé : Des travaux ont permis de déterminer la perméabilité et la distribution du diamètre des pores d'échantillons de boue de différentes granulométries provenant du plancher océanique (au large de la Nouvelle-Écosse) et soumis à différentes pressions efficaces (atteignant 100 MPa). Il s'agissait d'obtenir des informations sur la perméabilité des boues et sur l'évolution de la structure des pores à mesure que les boues se transforment en shale par compaction. Ces données sont indispensables pour la modélisation de l'évolution des bassins sédimentaires et l'exploration des hydrocarbures.

Les données indiquent que les perméabilités s'élèvent à 10^{-20}-10^{-18} m^2, mais aussi que les échantillons aux fractions importantes à grain fin (2-8 μm) affichent une diminution considérable de la perméabilité avec la pression, tandis que ceux aux fractions plus importantes à grain grossier (10-60 μm) présentent une diminution plus faible. Un échantillon du premier groupe susmentionné montre une variation plus faible du diamètre des pores comparativement à un échantillon du deuxième groupe. Dans les deux cas, la distribution du diamètre des pores est unimodale (modes de 25-160 nm), révélant peu de changements avec l'augmentation des pressions de compaction, même si les valeurs de porosité diminuent avec la pression. Les aires superficielles varient également peu avec la pression.

[1] New England Research, Inc., 76 Olcott Drive, White River Junction, Vermont, 05001 U.S.A.
[2] GSC Atlantic, Dartmouth

INTRODUCTION

Information on permeability and pore structure evolution of muds as they are transformed into shale, through compaction and heat, is important for modelling of sedimentary basin development and hydrocarbon exploration (e.g., Mudford and Best, 1989; Williamson 1992; Williamson and Smyth, 1992). It is of particular importance for understanding the processes of abnormal pressure development (over and under pressures). Information on the petrophysical and pore structure characteristics of shales at various depths (e.g., Katsube and Williamson, 1994, 1995; Katsube et al., 1995) is starting to accumulate. This is contributing to the understanding of various physical processes during basin development. However, there has been little confirmation of these characteristics by measuring petrophysical parameters of muds as they are experimentally compacted into simulated shale conditions in the laboratory. For this reason, a series of laboratory petrophysical tests have been carried out on mud samples, from the seafloor offshore Nova Scotia, that were compacted to different pressures (10-100 MPa).

Table 1. Laboratory number, identification (I.D.) number, and depth information for the unconsolidated seafloor sediment samples, from offshore Nova Scotia.

Laboratory Sample No.	Sample I.D. No.	Depth from Sea Floor (m)
VSF-A	88010-002	1.895 -1.995
VSF-B	88010-017	5.43 - 5.49
VSF-C	88010-002	6.30 - 6.38
VSF-D	88010-017	5.43 - 5.49a
VSF-E	88010-002	3.43 - 3.51
VSF-F	Hudson-86.034-30	7.50 - 7.60

Table 2a. Permeability (k) as a function of confining pressure for an unconsolidated seafloor sample from offshore Nova Scotia (partially from Katsube and Coyner, 1994).

Sample/ (Mes. No.)	Pressures (Mpa) Confining	Pore	Effective	Permeability (10^{-21} m^2)
VSF-F	6.0	5.0	1.0	443
	7.0	5.0	2.0	325 ± 5
	8.0	5.0	3.0	223 ± 8
	9.0	5.0	4.0	157 ± 22
	10.0	5.0	5.0	97 ± 8
	11.0	5.0	6.0	60 ± 1
	12.0	5.0	7.0	63
	13.0	5.0	8.0	62.5 ± 5
	14.0	5.0	9.0	61.5 ± 5
	15.0	5.0	10.0	57 ± 2
	9.8	5.4	4.4	68
	14.7	5.1	9.6	46
	19.8	5.1	14.7	29
	24.3	5.0	19.3	25
	30.0	5.0	25.0	23
	34.8	5.0	29.8	19
	39.0	5.0	34.9	23
	45.1	5.0	40.1	14

The petrophysical tests consist of permeability, particle-size distribution, and pore-size distribution determinations. Permeability measurements were made at pressures in the range of 1-100 MPa for six seafloor samples. Particle-size data was obtained for each of these samples. Two of these samples were selected for fabrication of discs of about 2.5 cm in diameter and 0.5-1.0 cm in thickness at confining pressures of 10-100 MPa. Six such discs were fabricated from each of the two samples. Then, the pore-size distribution was measured for each of these discs by mercury porosimetry. Little interpretation of the data has been performed to date. However, the purpose of this paper is to document this data, since preliminary observations suggest that they have the potential of producing useful information for the understanding of sedimentary basin development processes.

Table 2b. Permeability (k) as a function of confining pressure (P_c) for unconsolidated seafloor samples from offshore Nova Scotia.

Sample/ (Mes. No.)	P (Mpa) P_c	P_p	P_e	k (10^{-21} m^2)	ℓ (mm)
VSF-A	0.0				12.0
	9.0	5.0	4.0	920 ± 30	8.28
	27	5.0	22	640 ± 80	7.70
	45	5.0	40	400 ± 90	7.29
	63	5.0	58	310 ± 70	7.09
	81	5.0	74	220 ± 80	7.07
	99	5.0	94	180 ± 50	7.06
VSF-B	0.0				12.0
	9.0	5.0	4.0	290 ± 30	6.63
	27	5.0	22		(5.77)
	45	5.0	40	45 ± 8	5.51
	63	5.0	58	20.9	5.34
	81	5.0	74	13.3	5.32
	99	4.0	95	10.0	5.31
VSF-C	0.0				12.0
	9.0	5.2	3.8	141 ± 20	7.51
	45	5.2	39.8	13.1 ± 3.5	6.50
	63	5.2	57.8	<10	-
VSF-D	0.0				12.0
	15.3	5.1	10.2	125 ± 32	5.77
	27	5.1	21.9	62 ± 16	5.44
	45	5.0	40	27 ± 16	5.06
	63	5.2	57.8	14 ± 7.2	4.93
	81	4.8	76.2	11.8 ± 3.1	4.92
	99	4.9	94.1	10.6 ± 1.0	4.90
VSF-E	0.0				12.0
	9.0	5.6	3.4	107 ± 7	6.48
	27	5.0	22	<10	-

P_c = Confining pressure
P_p = Pore pressure
P_e = Effective pressure
P = Pressure
k = Permeability
ℓ = Length of specimen

METHOD OF INVESTIGATION

Samples and sample preparation

Core samples of unconsolidated seafloor sediments (from offshore Nova Scotia), with a diameter of 7.5-9.5 cm and a length of 5-20 cm, were obtained. Sample identification numbers with information on their depth from the seafloor are listed in Table 1. Plug specimens of 2.54 cm in diameter and 1.1-1.3 cm were taken from these samples for permeability measurements. A specimen of 50-100 mL was taken from each sample for particle-size analysis. Two samples (VSF-D and VSF-E) were selected for compacted disc fabrication and pore-size distribution analysis. First, two plug specimens of 2.54 cm in diameter and 4-5 cm were taken from each of these two samples. These plugs were then sliced into 6-8 disc subspecimens of 1.1-1.4 cm for each sample. Subsequent to compaction by processes described later, about one half of each disc specimen was used for the pore-size distribution tests.

Permeability measurements

The permeabilities were measured by two different types of measuring techniques. Sample VSF-F was measured by the transient-pulse technique. Description of the technique, procedures, and part of the data has previously been published (Katsube and Coyner, 1994). The rest of the five samples were measured by the sinusoidal technique (Kranz et al., 1990; Fischer, 1992).

The plug specimens, from the five samples, were inserted into a stainless steel consolidometer which has internal and external diameters of 2.54 and 7.62 cm, respectively. The sample chamber of the consolidometer is outfitted with an up-stream pore pressure line, while the piston of the consolidometer contains a down-stream pore pressure line connected to a transducer for measuring pore fluid pressure at the opposing end of the specimen. High permeability porous ceramic filters covered by filter membranes were used to distribute the pore pressure at the ends of the specimen, therefore allowing fluid movement but preventing any extrusion of the specimen material. The stress exerted on the specimen by the consolidometer piston was hydraulically servo-controlled. A line volume displacement transducer (LVDT) spanning the two pieces of the consolidometer, at each end of the specimen, is used to measure the specimen length during compaction.

A 27 000 ppm NaCl brine was used as the pore fluid. The specimen was first loaded to a compaction stress of about 1 MPa and the specimen length recorded. At this point, the consolidometer was evacuated of trapped air by use of a vacuum, and then sealed with high pressure fittings. Subsequently, the specimen was loaded to 9 MPa compaction stress. Next, the pore pressure at the up-stream end of the specimen was increased to 5 MPa and the system allowed to equilibrate. Once the initial compaction of the specimen had occurred and the pore pressure in the down-stream end equilibrated with the applied pressure at the up-stream end, the specimen length was recorded (by the LVDT) and the first sequence of permeability measurements made.

Permeability was determined by controlling perturbations in the pore pressure at the up-stream end of the specimen and measuring the pressure response at the down-stream end by the transducer. At each compaction stress, up to five different pressure transients were used for these permeability measurements. They include 10, 25, and 67 second period sinusoids, a 0.7 MPa step increase, and a 0.7 MPa step decrease in pore pressures. Compaction stresses were varied between 9 and 99 MPa. At each compaction stress, the permeability measurements were initiated after the pressures at both ends of the specimen had equilibrated. Permeability was computed by fitting the measured response to analytical solutions which include the effect of specific storage of the specimen (Kranz et al., 1990; Fischer, 1992).

Particle-size distribution analysis

The particle-size distribution of the samples were determined using the Brinkman (laser) Particle Size Analyzer. This analyzer measures the diameter of a particle directly, using the "time of transition theory". Particle diameter (D) equals the time (t) required for the laser beam moving at a fixed, known velocity (v) to traverse the particle such that D = t x v. Measurements are made within a narrow plane and all particles outside the plane are out of focus and not seen by the

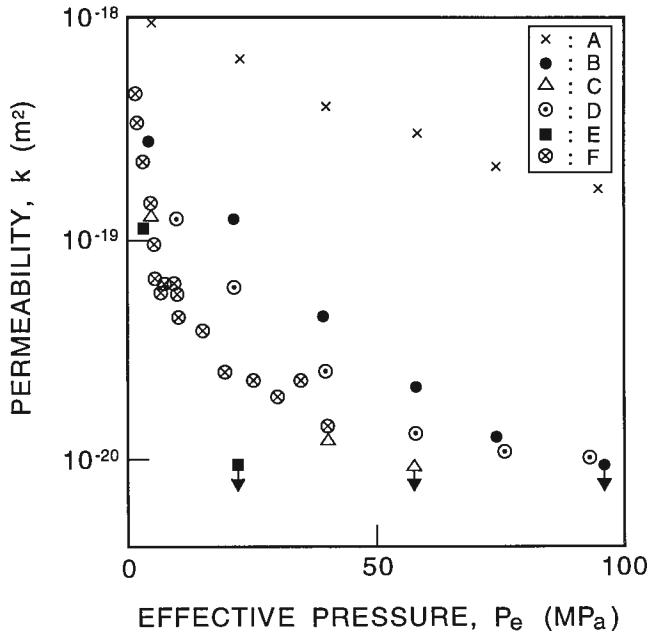

Figure 1. *Permeability-stress (k-P_e) relationship for six unconsolidated mud samples from the ocean floor, offshore Nova Scotia. These curves are placed in the following three groups, G-1, G-2, G-3: G-1 – VSF-A,G-2 – VSF-B, VSF-C, VSF-D, VSF-F, G-3 – VSF-E.*

instrument. When a particle interrupts the laser beam, it's shadow crosses a photodiode and it's diameter is calculated. Particle sphericity is assumed. Algorithms reject particles that are measured off-centre or out of focus.

Compacted disc fabrication

Solid disc specimens were fabricated by inserting the plug specimens into the stainless steel consolidometer, used for the permeability measurements, and then loading the specimens to specified pressures, ranging from 10 to 100 MPa. In this case, both up-stream and down-stream pore pressure lines were vented to atmosphere, allowing water to escape during compaction. At each specified pressure, the load was maintained for up to one hour, until the specimen was considered to be fully compacted. That is, the length of the specimen had stabilized. The specimen was then unloaded, removed from the consolidometer, and preserved for other analyses.

Pore-size distribution analysis

Pore-size distribution of these shale specimens was determined by mercury intrusion porosimetry, following the procedures described in previous publications (e.g. Katsube and Walsh, 1987; Katsube and Issler, 1993), using an equilibration time of 45 seconds for each of the high pressure steps, and 10 seconds for the low pressure (<0.7 MPa) steps. These measurements were made by ORTECH (Toronto, Ontario)

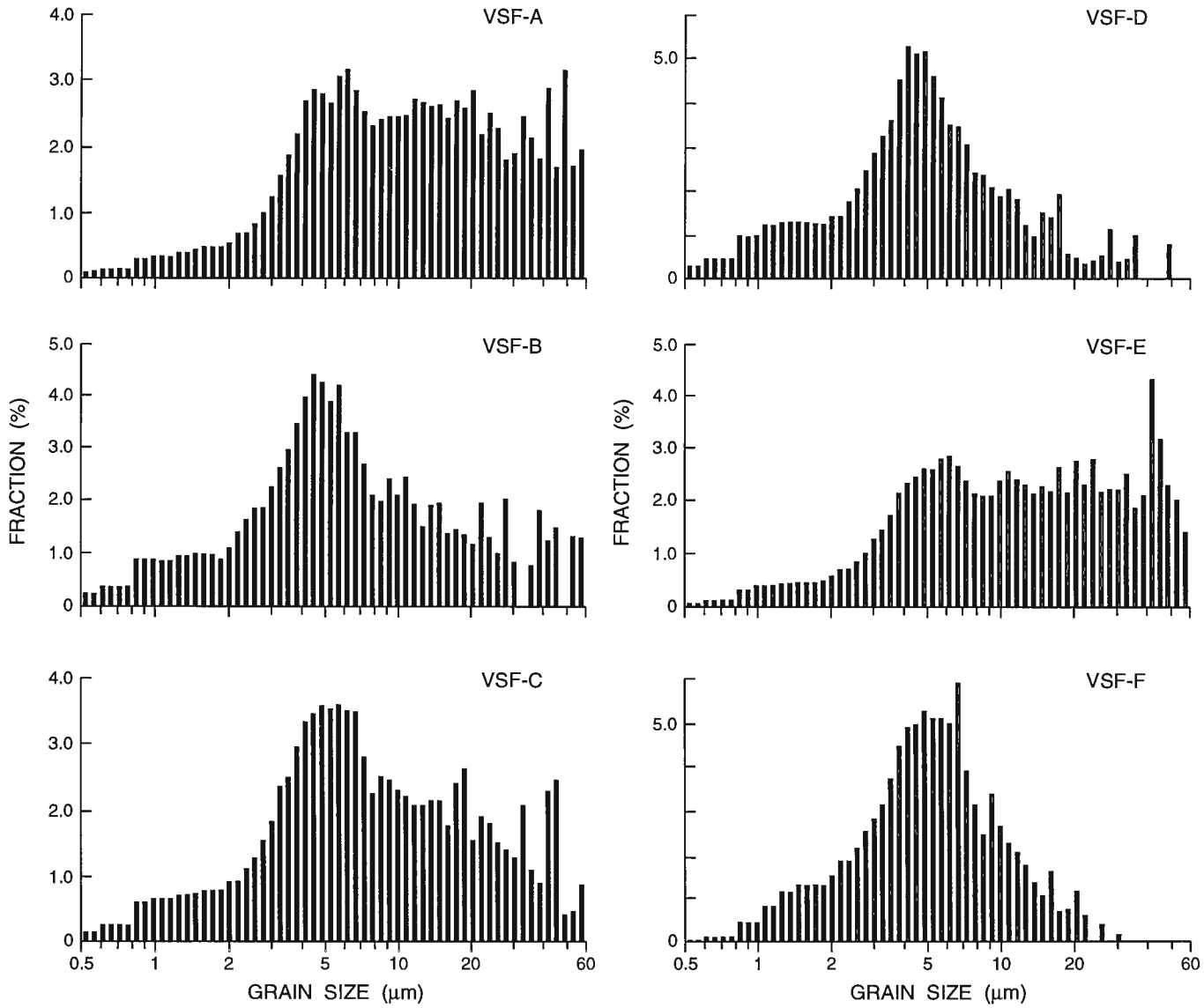

Figure 2. *Particle-size distribution for six unconsolidated mud samples from the ocean floor, offshore Nova Scotia. These distributions are placed in the following two groups, UDG and PDG: UDG: VSF-B, VSF-C, VSF-D and VSF-F, PDG: VSF-A and VSF-E.*

using a Micromeritics Autopore 9200 mercury porosimeter with an available pressure range of 0.14-420 MPa and an equivalent pore-size range of 10-0.003 μm. Further details of the measuring technique, procedures and data presentation methods are described in (Katsube and Issler, 1993). Methods for surface area (A) determination from the pore-size distribution are found in Rootare (1970).

EXPERIMENTAL RESULTS

The results of the permeability (k) as a function of pressure (P_c, P_e) measurements are listed in Tables 2a and 2b, and are displayed in Figure 1. The P_c and P_e are the confining and effective pressures, respectively. The k-P_e relationship can be divided into three groups: G-1, G-2, and G-3. Group G-1 is

Table 3a. Pore-size distribution data for different pore-size ranges (d) obtained by mercury porosimetry for compacted mud samples, from offshore Nova Scotia.

	VSF-D1	VSF-D2	VSF-D3	VSF-D4	VSF-D5	VSF-D6
d_a(nm)	ϕ_a (%)					
3.2	0.24	0.29	0.20	0.32	0.84	0.37
5.0	0.68	0.94	0.77	0.98	1.60	0.87
7.9	0.86	1.01	0.97	1.14	1.40	1.08
12.6	1.35	1.55	1.56	1.78	2.18	1.85
20.0	2.21	2.44	2.69	3.28	3.04	3.32
31.6	2.68	3.02	3.75	5.34	4.32	6.08
50.1	10.99	13.48	11.55	10.72	10.52	7.33
79.4	9.27	5.27	3.36	1.42	1.56	1.08
126	1.03	0.82	0.81	0.60	0.64	0.60
200	0.68	0.48	0.38	0.32	0.39	0.46
316	0.38	0.27	0.32	0.16	0.27	0.12
501	0.15	0.08	0.16	0.12	0.04	0.12
794	0.11	0.13	0.08	0.00	0.25	0.15
1259	0.04	0.00	0.12	0.04	0.00	0.04
1995	0.00	0.00	0.00	0.08	0.00	0.06
3162	0.02	0.00	0.04	0.02	0.10	0.06
5012	0.00	0.06	0.12	0.00	0.00	0.00
7943	0.00	0.00	0.02	0.00	0.00	0.02
ϕ_{Hg1}	30.7	29.8	26.9	26.3	27.2	23.6
ϕ_{Hg2}	31.2	30.4	28.0	26.7	28.4	24.1
d_{hg}	55.2	48.7	54.7	37.3	43.1	37.9
δ_{BD}	1.88	1.91	1.98	2.00	2.06	2.08
δ_{SD}	2.73	2.74	2.74	2.73	2.88	2.73
A	18.2	20.0	18.0	20.5	24.9	18.8
ϕ_s	10.8	9.6	9.5	8.1	8.5	7.7
ϕ_{rr}	0.351	0.323	0.352	0.308	0.312	0.328
P	10	20	40	60	80	100

d_a = Geometric mean pore-sizes for the different pore-size (d) ranges (nm).
d_{hg} = Geometric mean of the entire pore-size distribution (nm).
ϕ_a = Partial porosity (%).
ϕ_{Hg1} = Total porosity measured by mercury porosimetry for pore sizes up to 10 μm (%).
ϕ_{Hg2} = Total porosity measured by mercury porosimetry for pore sizes up to 250 μm (%).
δ_{BD} = Bulk density (g/mL).
δ_{SD} = Skeletal density (g/mL).
A = Surface area (m^2/g).
ϕ_s = Storage porosity (%).
ϕ_{rr} = ϕ_R/ϕ_{Hg1}.
P Compacted pressure (MPa).

Table 3b. Pore-size distribution data for different pore-size ranges (d) obtained by mercury porosimetry for compacted mud samples, from offshore Nova Scotia.

	VSF-E1	VSF-E2	VSF-E3	VSF-E4	VSF-E5	VSF-E6
d_a(nm)	ϕ_a (%)					
3.2	0.24	0.28	0.19	0.75	0.28	0.33
5.0	0.63	0.83	0.68	1.46	0.94	0.79
7.9	0.73	0.83	0.78	1.25	0.88	0.87
12.6	0.99	1.14	1.05	1.70	1.24	1.27
20.0	1.49	1.81	1.50	0.00	1.62	1.95
31.6	1.68	1.85	1.68	1.20	2.04	2.35
50.1	3.34	4.17	4.00	5.00	4.04	4.24
79.4	4.79	5.50	4.48	3.44	3.78	3.51
126	4.75	4.21	3.00	2.00	2.40	2.04
200	2.78	2.71	2.03	1.29	1.66	1.31
316	2.31	2.12	1.91	1.01	1.26	1.12
501	1.92	1.02	1.52	0.85	1.02	0.91
794	2.39	0.63	1.15	1.19	1.16	1.12
1259	1.23	0.43	0.82	0.89	1.00	0.69
1995	0.95	0.24	0.94	0.63	0.70	0.42
3162	0.45	0.20	0.64	0.42	0.32	0.23
5012	0.22	0.08	0.31	0.16	0.20	0.12
7943	0.00	0.00	0.04	0.04	0.02	0.02
ϕ_{Hg1}	30.9	28.0	26.7	23.3	24.6	23.3
ϕ_{Hg2}	31.7	28.5	27.6	24.1	25.6	24.2
d_{hg}	149	87.7	131	93.5	110	91.2
δ_{BD}	1.86	1.97	1.95	2.02	2.00	2.08
δ_{SD}	2.73	2.75	2.69	2.80	2.69	2.74
A	13.3	14.5	12.5	20.6	14.1	13.8
ϕ_s	18.3	14.4	14.8	10.4	12.8	12.0
ϕ_{rr}	0.592	0.516	0.554	0.448	0.523	0.515
P	10	20	26	32	40	50

d_a = Geometric mean pore-sizes for the different pore-size (d) ranges (nm).
d_{hg} = Geometric mean of the entire pore-size distribution (nm).
ϕ_a = Partial porosity (%).
ϕ_{Hg1} = Total porosity measured by mercury porosimetry for pore sizes up to 10 μm (%).
ϕ_{Hg2} = Total porosity measured by mercury porosimetry for pore sizes up to 250 μm (%).
δ_{BD} = Bulk density (g/mL).
δ_{SD} = Skeletal density (g/mL).
A = Surface area (m^2/g).
ϕ_s = Storage porosity (%).
ϕ_{rr} = ϕ_R/ϕ_{Hg1}.
P Compacted pressure (Mpa).

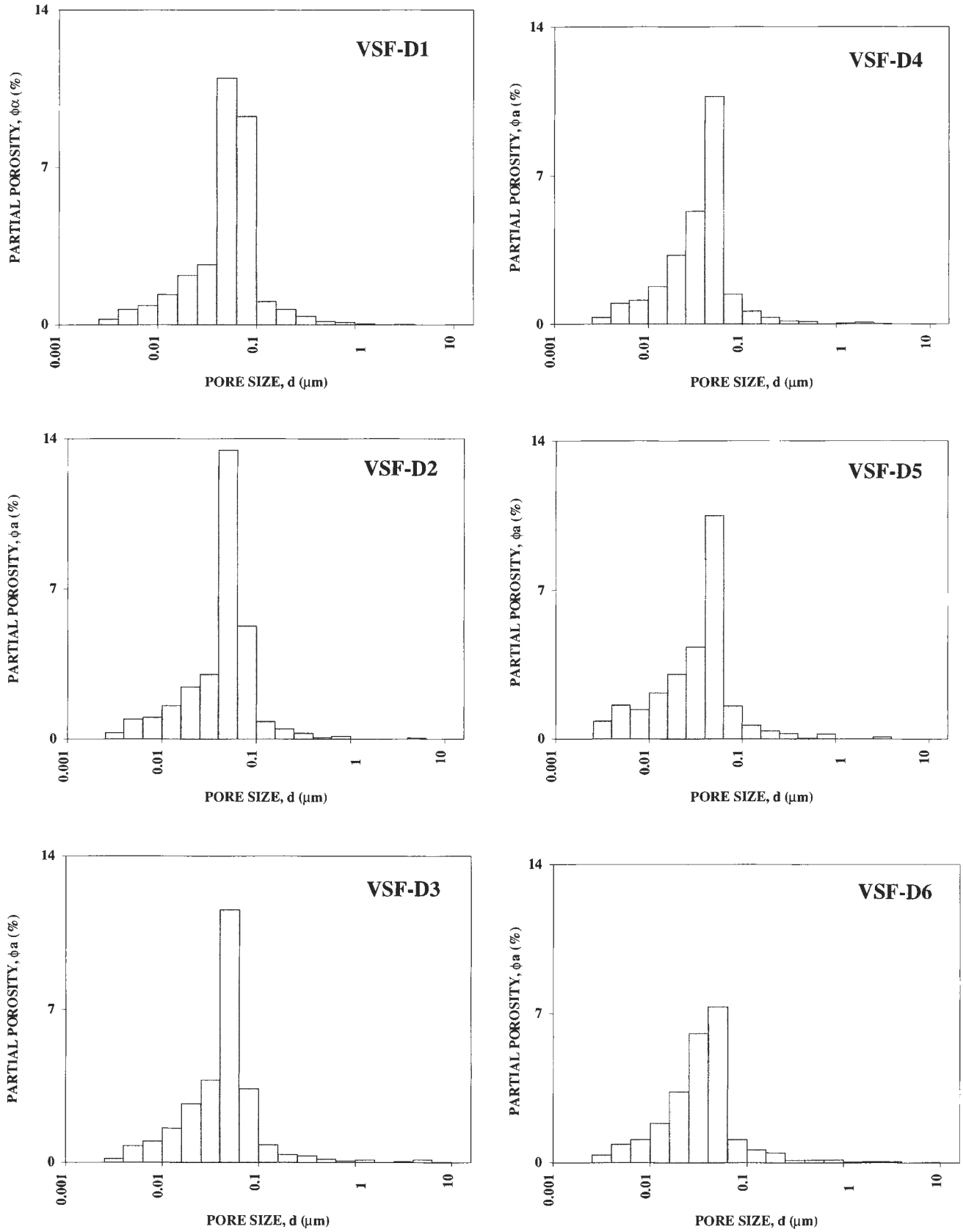

Figure 3a. Pore-size distributions for sample VSF-D at different compacted pressures. The digits of 1 to 6 after the sample number VSF-D represent the compacted pressures of 10, 20, 40, 60, 80, and 100 MPa, respectively.

represented by sample VSF-A which shows only a limited permeability (k) decrease with increased effective pressure (P_e), as shown in Figure 1. Group G-2 is represented by samples VSF-B, VSF-C, VSF-D, and VSF-F which show an initial rapid decrease followed by a gradual decrease of k with increased P_e. Group G-3 is represented by VSF-E showing an extremely rapid decrease of k with increased P_e, which reaches 10^{-20} m² at low P_e values (20 MPa).

The results of the particle-size distribution analysis are displayed in Figure 2 for all six samples. These data can be divided into two groups: a unimodal distribution group (UDG) and a pulse distribution group (PDG). Unimodal distribution group is represented by samples VSF-B, VSF-C, VSF-D, and VSF-F. Pulse distribution group in represented by samples VSF-A and VSF-E.

The results of the pore-size determinations for different compacted pressures are listed in Tables 3a and 3b, for the two samples VSF-D and VSF-E. These results are also displayed in Figures 3a, 3b, 4a, and 4b.

DISCUSSION AND CONCLUSIONS

Samples displaying relatively large decreases of permeability (k) with increasing effective pressure (P_e) (G-2 group, Fig. 1) have a larger fraction of small grains (unimodal distribution group, Fig. 2). Sample VSF-A, which shows less change in k (G-1), has a larger fraction of large grains (pulse distribution group). These trends are expected, since the larger fraction of large grains (pulse distribution group) are more likely to develop a framework-supported texture resulting in G-1

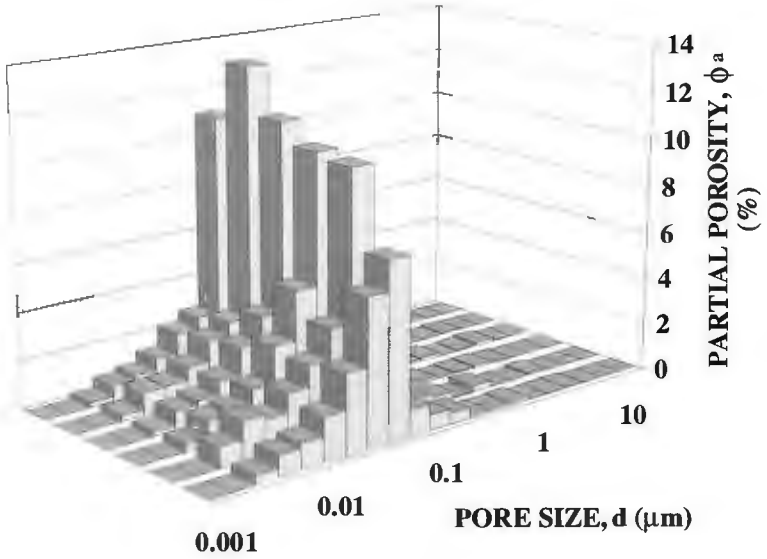

Figure 3b.

The pore-size distribution in Figure 3a (sample VSF-D) displayed in 3-dimensional mode.

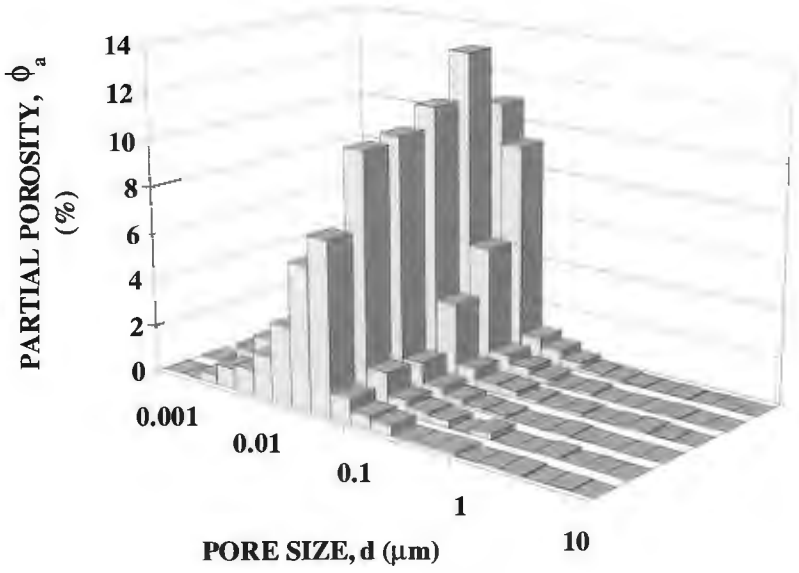

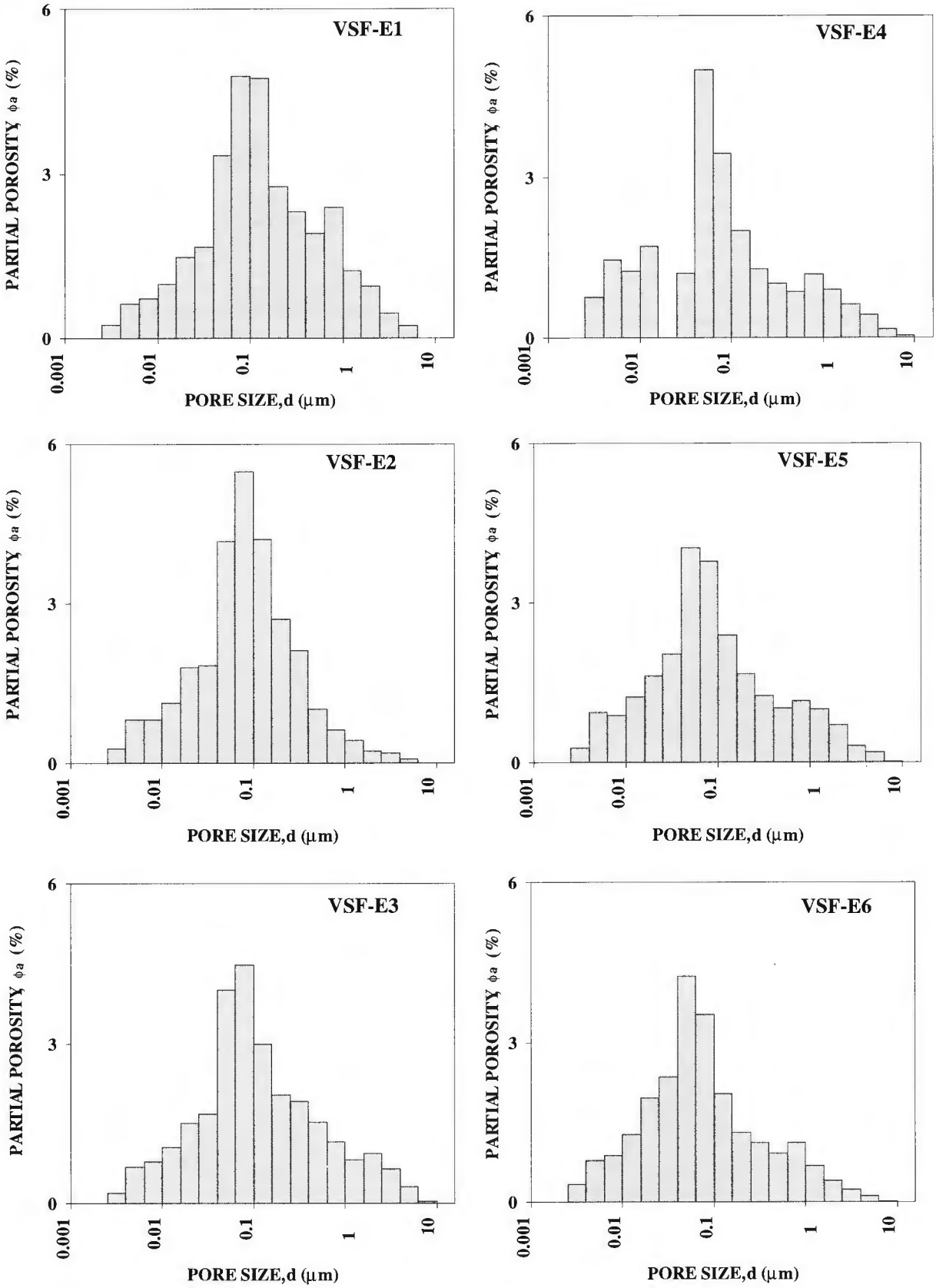

Figure 4a. *Pore-size distributions for sample VSF-E at different compacted pressures. The digits of 1 to 6 after the sample number VSF-E represent the compacted pressures of 10, 20, 26, 32, 40, and 50 MPa, respectively.*

group k-P_e curves. This is in contrasted to a larger fraction of small grains (unimodal distribution group), which are likely to develop a more matrix-supported type of framework, resulting in the G-2 type of k-P_e curves. According to these trends, sample VSF-E which belongs to the pulse distribution group particle-size distribution group, would be expected to show little change in k with P_e (G-2). On the contrary, it shows the largest decrease of k with P_e (G-3), a trend that is difficult to understand.

The pore-size distributions of samples VSF-D and VSF-E (Fig. 3a to 4b) show little changes with increasing compacted pressures, although the effective porosities (ϕ_{Hg1}) and the maximum values of the partial porosities (ϕ_a) decrease to some extent under these conditions. It is interesting that sample VSF-D which shows a smaller variation in pore-sizes belongs to the unimodal distribution group (UGD) of particle-sizes, and sample VSF-E which shows larger variation in pore-sizes belongs to the pulse distribution group (PDG) of the particle-sizes.

The surface area (A) values for both samples, VSF-D and VSF-E, show little changes with increasing compacted pressures (Tables 3a and 3b). However, the A value for sample VSF-D (18-25 m^2), which has a larger fraction of small particle-sizes (unimodal distribution group), is larger than that of sample VSF-E (13-15 m^2), which has a larger fraction of large particle-sizes (pulse distribution group). This is a result that is expected.

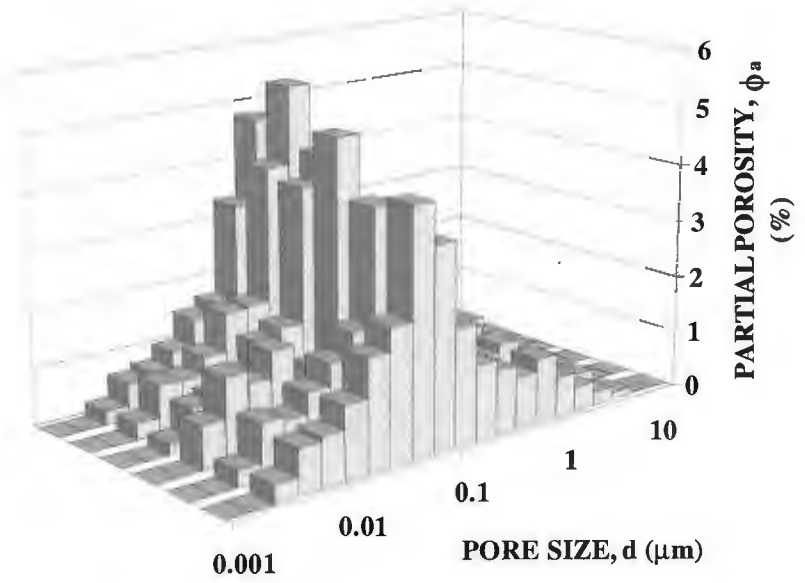

Figure 4b.

The pore-size distribution in Figure 4a (sample VSF-E) displayed in 3-dimensional mode.

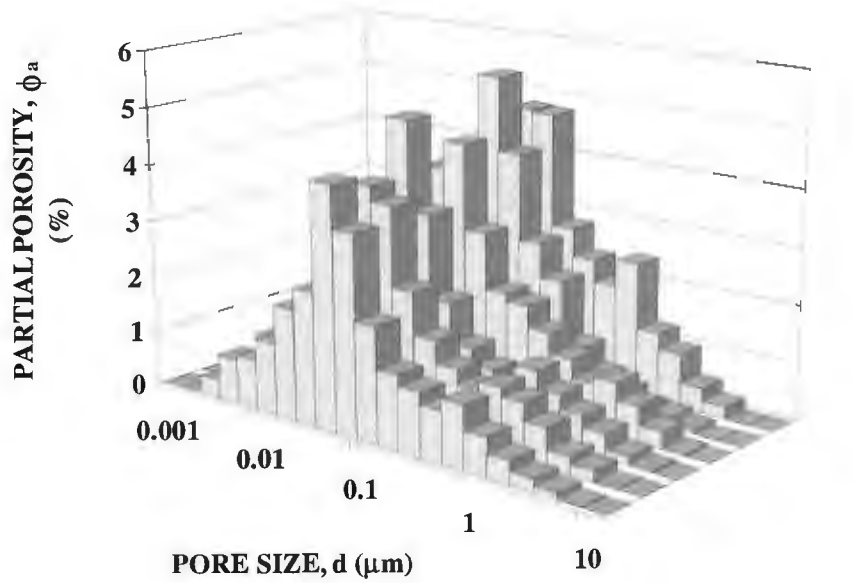

ACKNOWLEDGMENTS

The authors thank K.M. Moran (Geological Survey of Canada – Atlantic) for providing the six unconsolidated seafloor samples. The authors also acknowledge the efficient work of B. Smith (ORTECH International, Toronto, Ontario) who did the mercury porosimetry measurements, and that by M. Wygergangs (Geological Survey of Canada) who did the particle-size analysis. The authors thank P. Moir (Geological Survey of Canada, Atlantic) for critically reviewing this paper and making useful suggestions. The main part of the funding for this study was provided through the Office of Energy Research and Development (OERD).

REFERENCES

Fischer, G.J.
1992: The determination of permeability and storage capacity; pore pressure oscillation method; in Fault Mechanics and Transport Properties of Rock, Academic Press.

Katsube, T.J. and Coyner, K.
1994: Determination of permeability(k)-compaction relationship from interpretation of k-stress data for shales from Eastern and Northern Canada; in Current Research 1994-D, Geological Survey of Canada, p. 169-177.

Katsube, T.J. and Issler, D.R.
1993: Pore-size distribution of shales from the Beaufort-MacKenzie Basin, northern Canada; in Current Research, Part E; Geological Survey of Canada, Paper 93-1E, p. 123-132.

Katsube, T.J. and Walsh, J.B.
1987: Effective aperture for fluid flow in microcracks; International Journal of Rock Mechanics and Mining Sciences and Geomechanics Abstracts, v. 24, p. 175-183.

Katsube, T.J. and Williamson, M.A.
1994: Effects of diagenesis on shale nano-pore structure and implications for sealing capacity; Clay Minerals, v. 29, p. 451-461.
1995: Critical depth of burial of subsiding shales and its effect on abnormal pressure development; in Proceedings of the Oil and Gas Forum '95 ("Energy from Sediments"), Geological Survey of Canada, Open File 3058, p. 283-286.

Katsube, T.J., Bloch, J., and Issler, D.R.
1995: Shale pore structure evolution under variable sedimentation rates in the Beaufort-MacKenzie Basin; in Proceedings of the Oil and Gas Forum '95 ("Energy from Sediments"), Geological Survey of Canada, Open File 3058, p. 211-215.

Krantz, R.L., Saltzman, J.S., and Blacic, J.D.
1990: Hydraulic diffusivity measurements on laboratory rock samples using an oscillating pore pressure method; International Journal of Rock Mechanics and Mineral Sciences, v. 27, p. 345-352.

Mudford, B.S. and Best, M.E.
1989: Venture Gas Field, offshore Nova Scotia; case study of overpressuring in region of low sedimentation rate: American Association of Petroleum Geologists, Bulletin, v. 73, p. 1383-1396.

Rootare, H.M.
1970: A review of mercury porosimetry; Perspectives of Powder Metallurgy, v. 5, p. 225-252.

Williamson, M.A.
1992: The subsidence, compaction, thermal and maturation history of the Egret Member source rock, Jeanne D'Arc Basin, offshore Newfoundland; Bulletin of Canadian Petroleum Geology, v. 40, no. 2, p. 136-150.

Williamson, M.A. and Smyth, C.
1992: Timing of gas and overpressure generation in the Sable Basin offshore Nova Scotia; Bulletin of Canadian Petroleum Geology, v. 40, no. 2, p. 151-169.

Geological Survey of Canada Project 870057

Magmatic significance of the relationships between the mafic and felsic phases of the Folly Lake pluton, Cobequid Highlands, Nova Scotia[1]

G. Pe-Piper[2], M. Zeeman[2], and D.J.W. Piper
GSC Atlantic, Dartmouth

Pe-Piper, G., Zeeman, M., and Piper, D.J.W., 1996: Magmatic significance of the relationships between the mafic and felsic phases of the Folly Lake pluton, Cobequid Highlands, Nova Scotia; in Current Research 1996-D; Geological Survey of Canada, p. 27-33.

Abstract: The principally gabbroic Folly Lake pluton includes minor granite phases. Some predate the main gabbro intrusion, others cut the gabbro pluton. Granite-gabbro contacts are commonly lobate, with chilling of gabbro towards dykes of granite, suggesting the presence of two immiscible magmas. This interpretation is supported by evidence for a gradual change in amphibole and biotite mineral chemistry across lobate contacts. Syn-magmatic deformation features suggest that there was relative movement between gabbro blocks during granite intrusion. All the granite phases are of similar geochemical composition, suggesting multiple magma batches from a single source.

Résumé : Le pluton principalement gabbroïque de Folly Lake inclut des phases granitiques mineures. Certaines précèdent la principale intrusion de gabbro, d'autres recoupent le pluton de gabbro. Les contacts entre le granite et le gabbro sont habituellement lobés, la bordure de solidification du gabbro étant orientée vers les dykes de granite, ce qui suggère la présence de magmas immiscibles. Cette interprétation est corroboré par des indices de transformation graduelle dans la composition chimique des amphiboles et de la biotite au passage des contacts lobés. Les éléments de déformation synmagmatique font supposer un mouvement relatif des blocs de gabbro les uns par rapport aux autres, au moment de l'intrusion des granites. Comme toutes les phases granitiques sont de composition géochimique semblable, les multiples poches de magma pourraient provenir d'une source unique.

[1] Contribution to Canada-Nova Scotia Cooperation Agreement on Mineral Development (1992-1995), a subsidiary agreement under the Canada-Nova Scotia Economic and Regional Development Agreement.
[2] Department of Geology, Saint Mary's University, Halifax, Nova Scotia B3H 3C3

INTRODUCTION

The Folly Lake gabbro is a latest Devonian-earliest Carboniferous pluton of mainly gabbro with minor granite bodies. It is part of the Avalon terrane of northern Nova Scotia and lies immediately north of the Rockland Brook fault, a major splay of the Cobequid fault zone (Fig. 1). To the north and east of the Folly Lake gabbro, the Hart Lake-Byers Lake granite both cuts and is cut by the gabbro.

This paper describes field relationships of gabbro to intermediate and felsic rocks in the broad (≈1 km wide) contact zone of the Folly Lake gabbro and the Hart Lake-Byers Lake granite and examines their significance in the magmatic evolution of the plutonic rocks. It is based on detailed mapping that started a few years ago and was completed in the summer of 1995. The question addressed in this paper is what is the nature of the mafic and felsic magmas in the contact zone? Were there two co-existing immiscible magmas, mafic and felsic, with some mingling and/or mixing or was there a sequential intrusion of alternating mafic and felsic magmas? A preliminary study of these issues was made by Zeeman (1992).

REGIONAL GEOLOGY

Nomenclature of plutonic rocks in the Cobequid Highlands was established by Donohoe and Wallace (1982, 1985). In the north-central Cobequid Highlands, they recognized the predominantly granitic Gilbert Hills and Hart Lake-Byers Lake plutons and the predominantly gabbroic Wyvern and Folly Lake plutons. (In previous publications, the hornblende gabbro of these plutons has been generally termed diorite). New mapping (Piper et al., 1993 and unpublished data) has shown that these igneous rocks form an essentially continuous plutonic complex (the Hart Lake-Byers Lake-Folly Lake pluton, or HLBL-FL pluton) extending over 65 km from east to west and 10 km from north to south. The southeastern margin of the Hart Lake-Byers Lake-Folly Lake pluton is marked by the syn-magmatic Rockland Brook fault (Miller et al., 1995) that appears to have been an important magma pathway (Koukouvelas and Pe-Piper, 1995). Granite is a minor component of the Folly Lake gabbro near the Rockland Brook fault. Granite, gabbro, and intermediate rocks (tonalite, granodiorite) are common within a 1 to 2 km wide contact zone of the Folly Lake gabbro and the Hart Lake-Byers Lake granite. Megascopic relationships from the quarry north of Folly Lake have been described by Koukouvelas and Pe-Piper (1995). In this paper, small scale relationships are described from two representative areas: Higgins Mountain and Rory's Pond road (Fig. 1).

DESCRIPTION OF FIELD GEOLOGY OF THE CONTACT ZONE

Rory's Pond road

The eastern contact of Folly Lake gabbro with Hart Lake-Byers Lake granite has been investigated along Rory's Pond road. The Hart Lake-Byers Lake pluton is mainly granite with some diabase dykes; the Folly Lake pluton consists of gabbro with <40% granite and rare late diabase.

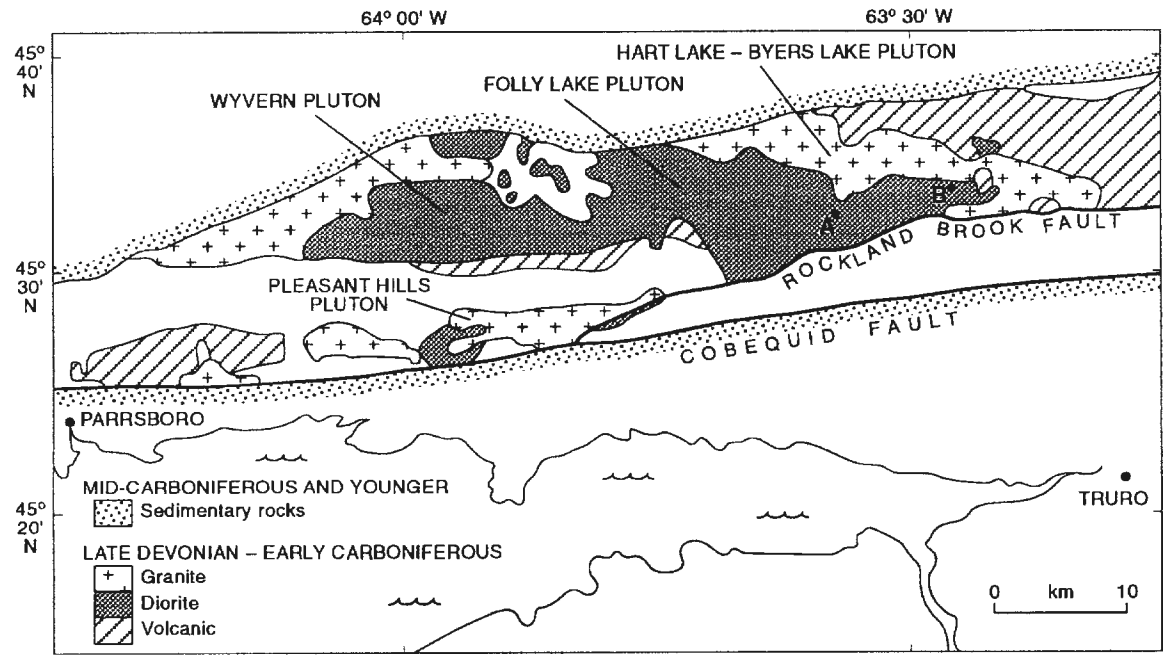

Figure 1. *Map showing the plutonic rocks of the north-central Cobequid Highlands, using nomenclature of Donohoe and Wallace (1982, 1985). A=Higgins Mountain section; B=Rory's Pond road section.*

The granite bodies in the Folly Lake pluton vary from coarse- to fine-grained with porphyritic, pegmatitic, aplitic, and equigranular textures. The gabbro units are medium- to fine-grained with 10-20% granitic dykes near the regional contact with granite and 2-5% granitic dykes farther away from the Hart Lake-Byers Lake pluton. Hybrid rocks of granodiorite composition are rare.

Most of the late diabase dykes intrude the granite, with minor assimilation but in two instances an aplitic granite intrudes a diabase and a diabase inclusion with irregular margins occurs in a granite (Fig. 2A).

Many of the gabbro-granite contacts are very irregular with lobate contacts (Fig. 2A, B, C) in which the gabbro is chilled against the granite (Fig. 2A, 3B), or less commonly granite chilled against gabbro. Gabbro enclaves in the granite are rounded and many have irregular contacts (Fig. 2B). A few contacts show some mixing between the granite and gabbro phases. The granodiorite is inhomogeneous, exhibiting more felsic and more mafic areas typical of a mixed rock. Some gabbro bodies have net-like dyking by granite with both irregular lobate (Fig. 2C) and straight contacts (Fig. 2D). More voluminous granite intrusion results in the formation of mafic enclaves (Koukouvelas and Pe-Piper, 1996). All these meso-scale textural relationships are similar to those described by Wiebe (1993) as representing injection of mafic magma into a silicic magma chamber.

Multiple intrusive events can commonly be recognized. In one case, a hybrid granodiorite contains a gabbro xenolith, is in contact with gabbro that has a chilled margin, and the gabbro is cut by granite veins. Inclusions of a distinctive porphyritic gabbro occur in both a fine grained gabbro and a nearby granite. A coarse granite dyke has a chilled margin against a gabbro that itself shows a chilled margin against hybrid granodiorite (Fig. 3A). One pegmatitic granite is intruded by a porphyritic gabbro that has a chilled margin.

In places, evidence exists for syn-magmatic deformation of the plutonic rocks. Pre-full crystallization fabrics, generally recognizable from aligned feldspars, are present in some granodiorite near contacts with both gabbro and granite. One outcrop (Fig. 3B) of irregular granite veins against which gabbro shows chilled lobate margins shows strong orientation of feldspars in the granite veins, suggesting deformation while the granite was more plastic than the gabbro. In many

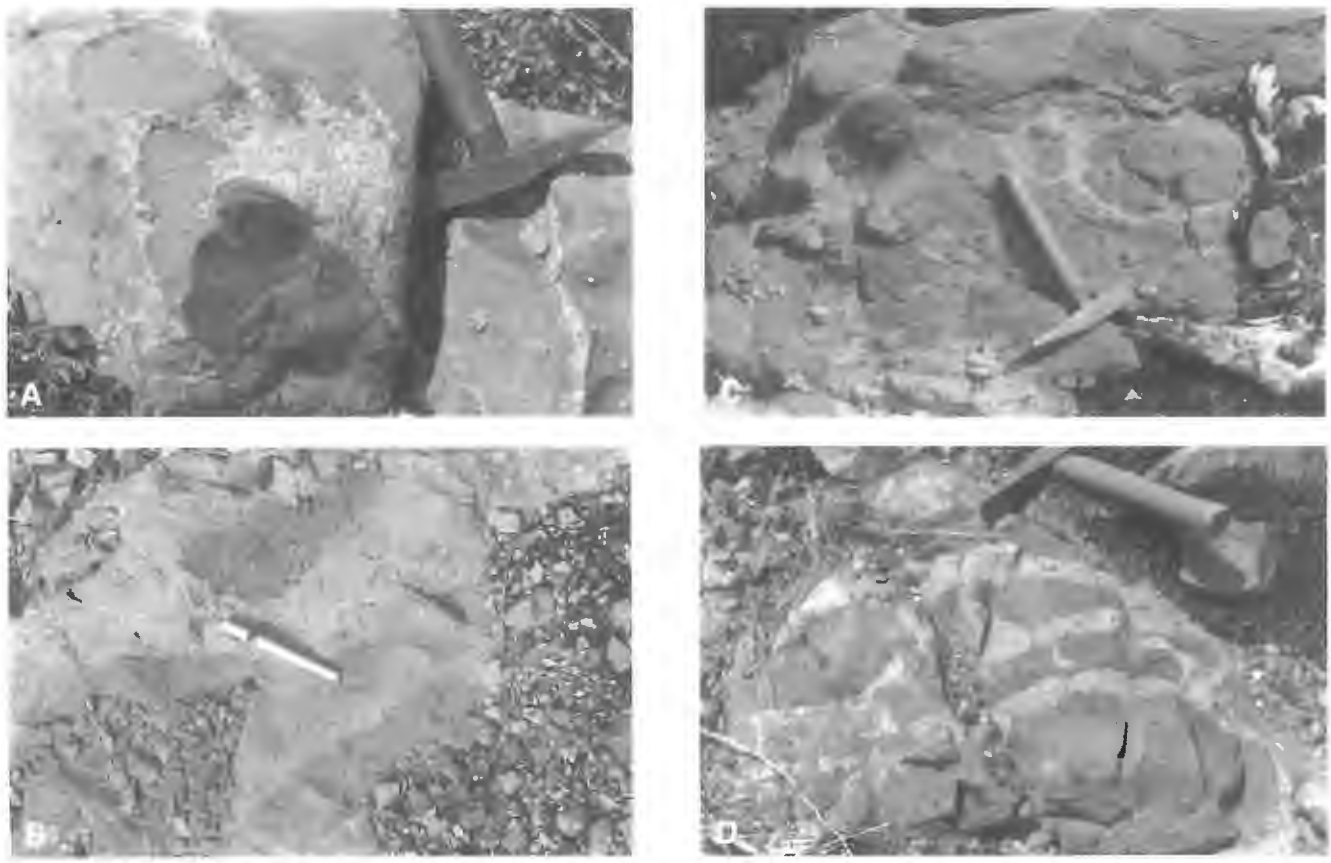

A) Lobate contact between granite and gabbro.

B) Irregular contact of gabbro and granite, with the gabbro showing chilling, and a gabbro xenolith in granite.

C) Irregular veins of granite in gabbro.

D) Net veining of granite in gabbro (chocolate bar structure of Koukouvelas and Pe-Piper, 1996).

***Figure 2.** Photographs showing relationships between gabbro and granite, Rory's Pond road.*

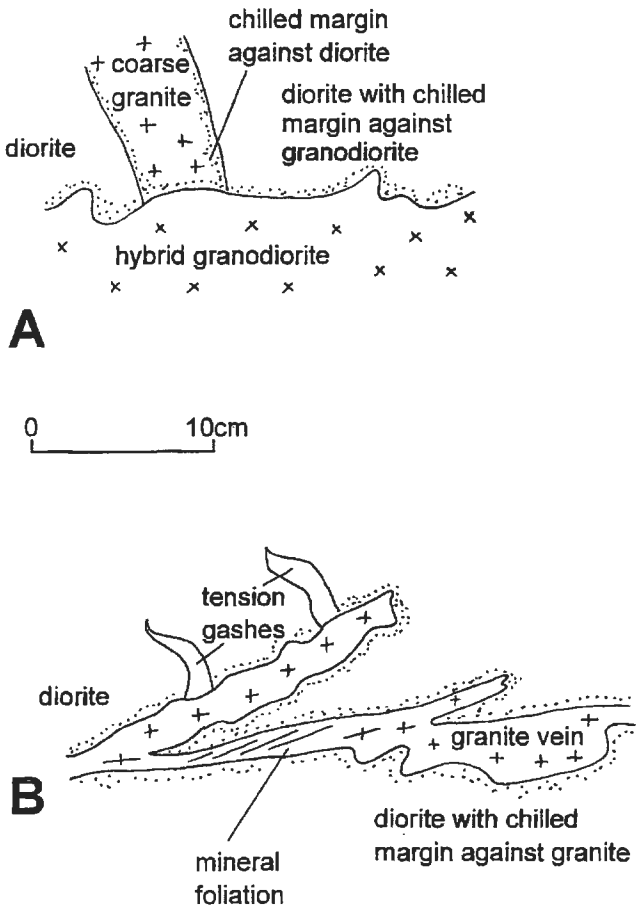

Figure 3. Field sketches of relationships between gabbro and granite, Rory's Pond road. A) Gabbro with chilled margin against slightly foliated granodiorite, cut by discontinuous coarse granite dykes. B) Gabbro with chilled margin against granitic veins. Granite veins show a strong mineral fabric. Gabbro cut by tension gashes filled with felsic minerals.

outcrops, some granite dykes are offset along other dykes, suggesting relative movement of host gabbro blocks during granite intrusion.

Higgins Mountain

Plutonic rocks are well exposed along a woods road from the Trans-Canada Highway to the transmission line along Higgins Mountain (A in Fig. 1), immediately east of Rockland Brook. Along this section the pluton consists of fine grained gabbro with hybrid and granite phases locally making up to 10-30% of the outcrop in the form of dykes and irregular pods. Several granitic stocks occur along this section, the largest (400 m across) being in the northern part of the section. Minor diabase and gabbro intrusions cutting the granite were also found in this area. This section is located 0.5 to 3 km from the mapped contact zone between the Folly Lake gabbro and the Hart Lake-Byers Lake granite.

The granitic dykes and pods vary greatly in composition, texture, and grain size. The granite suite includes fine- to coarse-grained K-feldspar granite and hybrid rocks (quartz monzodiorite, tonalite and quartz diorite) with equigranular, inequigranular, porphyritic, and pegmatitic textures. Some granitoid dykes contain gabbroic enclaves that are finer grained than the surrounding gabbro. Gabbro near contacts with large granite bodies may exhibit an increase in K-feldspar crystals toward the granite. Some dykes of granite are straight sided with chilled margins in the granite. Dykes of hybrid intermediate lithologies are also found. There are a few lobate contacts between the granite and diorite, in some cases with chilled margins to gabbro bodies against granite. In most places contacts were gradational between the gabbro and larger granite bodies, with the gradational sections being of tonalitic composition. Many small granitic dykes have a mafic reaction rim near the contact.

The southern contact of the large granite stock in the north of the section exhibits lobate sinuous contacts between the granite and gabbro. Near the contact the gabbro has plagioclase phenocrysts and the granite has K-feldspar phenocrysts. The granite is of quartz monzodiorite composition near the contact, becoming more felsic away from the contact. Areas of reddened granite within the granite stock generally have more mafic minerals; there is also reddening along fractures.

The last coarse plutonic phase is a brecciated very coarse hornblende gabbro in dykes centimetres to decimetres in width. Diabase dykes crosscut both gabbro and granite dykes. Aplite veins also crosscut gabbro and granite dykes, having sharp contacts with the gabbro but are locally gradational with the granitoids. Secondary alteration is found only locally and consists of minor epidote alteration in the gabbro and granite and rare silicification along north-south fractures.

DISCUSSION OF FIELD RELATIONSHIPS

On Rory's Pond road, the oldest rocks appear to be altered and fractured granite. These are cut by large gabbro bodies and smaller gabbro dykes and veinlets. Faulting in the granite may have provided a conduit for the diorite to surface and in doing so the hot mafic magma have remelted some granite and formed irregular contacts. On the other hand, much granite occurs as dykes that clearly crosscut gabbro and contain gabbroic enclaves. These granite dykes are geochemically similar to the oldest granite. Their emplacement is thus more easily explained as a later magma pulse from the same source, rather than as local high-level anatectic melts of older granite intruded by hot mafic magmas. More probably, the hybrid rocks and granodiorite record such anatexis. Syn-magmatic deformation in granite and granodiorite provides evidence of relative movement between blocks of gabbro during intrusion.

On Higgins Mountain, the granite-gabbro relationship is less clear. Evidence that some granite may be older than the gabbro is: a) assimilation of granite in gabbro as evidenced by increase in K-feldspar in the gabbro towards the contact, b) chilling of gabbro against granite, and c) the introduction

Table 1. Examples of analyses of amphibole and biotite across lobate contacts between granite and gabbro.

HORNBLENDE								
distance from contact	gabbro				granite			
	-14mm		-8mm		1mm		12mm	
	c	r	c	r	c	r	c	r
SiO_2	47.72	46.38	46.10	46.81	45.30	46.32	48.93	49.37
TiO_2	1.22	1.57	1.08	0.90	1.43	1.14	0.41	0.43
Al_2O_3	6.37	7.44	6.81	6.57	6.24	6.04	3.94	3.89
FeO_t	16.20	16.43	19.18	19.31	19.11	18.90	20.53	19.96
MgO	13.12	12.53	10.56	10.57	10.52	10.41	10.74	10.84
CaO	11.55	11.77	12.35	11.80	11.64	10.90	11.85	11.98
Na_2O	1.77	1.87	1.49	1.46	1.75	1.56	1.22	1.26
K_2O	0.48	0.55	0.70	0.62	0.81	0.67	0.56	0.41
Total	98.66	98.77	98.71	98.38	97.16	96.63	98.73	98.65
Atomic formula on the basis of 23 oxygen								
Si	7.025	6.853	6.921	7.024	6.926	7.076	7.340	7.380
Ti	0.135	0.174	0.122	0.102	0.164	0.131	0.046	0.048
Al	1.106	1.296	1.205	1.162	1.125	1.088	0.697	0.686
Fe"	1.995	2.030	2.408	2.423	2.443	2.415	2.576	2.495
Mg	2.879	2.759	2.363	2.364	2.397	2.370	2.401	2.415
Ca	1.822	1.863	1.987	1.897	1.907	1.784	1.905	1.919
Na	0.505	0.536	0.434	0.425	0.519	0.462	0.355	0.365
K	0.090	0.104	0.134	0.119	0.158	0.131	0.107	0.078

BIOTITE							
distance from contact	gabbro		granite				
	-14mm		1mm		8mm		12mm
	c	r	c	r	c	r	c
SiO_2	36.82	35.69	37.28	37.06	36.77	36.17	31.59
TiO_2	2.82	2.68	3.81	3.83	3.83	3.61	2.61
Al_2O_3	13.14	13.88	12.13	12.16	12.32	12.77	11.93
FeO_t	23.34	23.58	23.28	23.50	24.67	25.64	32.04
MgO	10.38	10.15	10.28	9.65	8.65	8.07	7.93
CaO	0.00	0.15	0.00	0.05	0.00	0.00	0.00
Na_2O	0.31	0.32	0.25	0.27	0.26	0.33	0.37
K_2O	9.03	8.34	9.33	9.33	9.00	8.30	7.18
Total	95.92	94.79	96.64	96.01	95.71	95.15	93.83
Atomic formula on the basis of 22 oxygen							
Si	5.695	5.585	5.737	5.749	5.746	5.698	5.269
Ti	0.328	0.315	0.441	0.447	0.450	0.428	0.327
Al	2.396	2.561	2.201	2.224	2.270	2.372	2.346
Fe"	3.019	3.086	2.996	3.049	3.224	3.378	4.469
Mg	2.393	2.367	2.358	2.231	2.015	1.895	1.971
Na	0.093	0.075	0.097	0.081	0.079	0.101	0.120
K	1.782	1.665	1.832	1.846	1.794	1.668	1.528
All analyses by electron microprobe using geological standards							

of some mafic material into granite near the contact. As on Rory's Pond road, there is common crosscutting evidence for granite intruding gabbro.

Rocks of intermediate composition in the Folly Lake pluton, commonly showing hybrid textures, are interpreted to have formed by the mixing of felsic and mafic magmas. Such rocks may form on a large scale if a hot mafic magma intrudes a cooler granite or felsic magma. Evidence of this process is the lobate granite-gabbro contacts with chilling of the gabbro, the introduction of diffuse mafic material into the granite and of xenocrysts of K-feldspar into the gabbro. Where granite is a minor phase, there is textural evidence that mingling of felsic and mafic magmas may have taken place. In both areas, the chilling of gabbro and gabbroic enclaves against granite with lobate contacts suggests that felsic and mafic magmas may have co-existed as immiscible magmas or crystal mushes. Where intermediate or granitic dykes cut gabbro, it is not possible to distinguish whether the more felsic lithology is essentially synchronous or considerably later, because gabbro crystallized at higher temperatures.

Aplite and pegmatitic dykes are late features, cutting the plutonic rocks. Diabase-gabbro bodies cut all other igneous lithologies.

Table 2. Geochemical whole rock analyses.

	Rory's Pond road				TCH at Folly Lake			
	early granite	main gabbro	later granite	late db	main gabbro	later granite	aplite dyke	late db
sample	4660	5061	4656	4653	4620	4614	4621	4611
SiO_2	75.38	47.26	76.34	44.53	49.83	74.87	73.85	47.54
TiO_2	0.20	2.93	0.15	3.06	2.16	0.24	0.07	2.23
Al_2O_3	12.34	14.63	11.88	14.36	14.87	12.55	13.85	14.94
Fe_2O_{3t}	2.25	15.15	1.77	13.78	11.33	2.25	1.26	12.23
MnO	0.04	0.25	0.03	0.30	0.18	0.04	0.02	0.19
MgO	0.68	5.88	0.69	6.61	6.23	0.82	0.69	6.49
CaO	0.18	8.73	0.16	9.50	9.50	0.77	1.75	10.09
Na_2O	3.99	3.00	3.31	3.11	3.36	3.66	4.06	3.26
K_2O	5.06	1.21	5.32	1.08	1.05	5.32	4.72	0.66
P_2O_5	0.02	0.48	0.01	0.82	0.37	0.03	0.02	0.37
L.O.I	0.20	0.40	0.00	1.80	0.20	0.20	0.40	1.40
Total	100.34	99.92	99.66	98.95	99.08	100.75	100.69	99.40
Ba	113	384	57	394	285	147	74	245
Rb	178	52	206	114	36	242	307	35
Sr	9	369	11	282	349	47	138	330
Y	60	50	78	43	34	93	84	31
Zr	369	239	276	273	226	710	169	192
Nb	44	18	46	24	16	57	71	15
Th	12	<5	19	4	<5	25	26	4
Pb	<5	82	11	15	<5	<5	9	<5
Ga	24	24	25	22	19	25	28	19
Zn	90	256	40	249	117	49	13	128
Cu	<5	64	<5	40	44	<5	<5	60
Ni	6	52	7	85	68	10	4	93
V	<5	324	<5	316	255	1	20	287
Cr	21	64	34	110	166	33	25	16

All analyses by X-ray fluorescence analysis. Major elements in wt %, trace elements in ppm.
L.O.I. = loss on ignition.

^{39}Ar-^{40}Ar dating by Nearing (1995) and U-Pb dating by Doig et al. (in press) shows that the igneous activity that produced the Folly Lake pluton may have lasted more than 10 Ma. Dating of specific phases is consistent with the geological evidence for age sequence. The observed mingling and mixing and sequential intrusive activity may have taken place over several million years.

CHEMICAL MINERALOGY AND GEOCHEMISTRY

Mineral analyses of amphibole, feldspar and biotite were conducted across felsic-mafic contacts on five samples (Table 1). The types of contacts examined were two embayed gabbro-granite contacts, a gabbro with a sharp-sided granitic vein, a gabbro enclave in a granite porphyry and a gabbro enclave in granite. An attempt was made to determine compositional variation from core to rim of each mineral on both the felsic and mafic side, at the contact and at several centimetres from the contact.

Samples from enclaves show no systematic trends in mineral chemistry. All other samples show a progressive increase in Fe/Fe+Mg in the amphibole and biotite from within the mafic side, across the contact and into the felsic rock (Table 1). Similarly the An content of the plagioclase progressively decreases from the interior of the mafic rock, across the contact and into the interior of the felsic rock. These trends suggest the granite and gabbro were still crystallizing and therefore in a fluid state when they came into contact with each other. There may have been some magmatic mingling across the contact. In contrast, no such gradual change is seen in the enclaves, which were probably emplaced as solid xenoliths. Most of the mafic rocks have some reverse zoned crystals and one granite sample in contact with diorite has a number of reversed zoned crystals suggesting these rocks experienced some disequilibrium during crystallization.

Chemical analyses are available from representative samples from both the gabbroic and granitic phases of all ages. In Table 2, we present selected data from Rory's Pond road and from the transition zone between the Folly Lake and Hart Lake-Byers Lake plutons exposed on the Trans-Canada Highway near the north end of Folly Lake. Both the early and the late granitoid lithologies have similar chemical composition and show fractionation trends similar to those inferred for other Devonian-Carboniferous granites of the Cobequid Highlands (Pe-Piper et al., 1991). This suggests that they were all derived by a similar process from a common source and are not the product of high-level anatectic melting.

CONCLUSIONS

1. The Folly Lake "pluton" is predominantly gabbro, but granite and hybrid phases locally make up 10 to 40% of the outcrop.
2. A sequence of intrusion can be recognized from crosscutting phases. Contact relationships indicate mingling and mixing of two immiscible magmas, mixing of magma with previously solidified rocks, and normal intrusive relationships. Near the Rockland Brook fault, the oldest igneous phase appears to be granite.
3. Where there are embayed contacts between mafic and felsic phase, mineralogical data indicate that the rocks in both sides were in a fluid state when they came into contact.
4. The early granite, later granite, and aplite are similar geochemically supporting the hypothesis that they were all derived by a similar process from a common source.

REFERENCES

Doig, R., Murphy, J.B., Pe-Piper, G., and Piper, D.J.W.
in press: U-Pb geochronology of late Paleozoic plutons, Cobequid Highlands, Nova Scotia, Canada: evidence for late Devonian emplacement adjacent to the Meguma-Avalon terrane boundary in the Canadian Appalachians; Geological Journal.

Donohoe, H.V. and Wallace, P.I.
1982: Geological map of the Cobequid Highlands, Nova Scotia; Nova Scotia Department of Mines and Energy, Map 82-09, scale 1:50 000, 4 sheets.

Donohoe, H.V., Jr. and Wallace, P.I.
1985: Repeated orogeny, faulting and stratigraphy of the Cobequid Highlands, Avalon Terrane of northern Nova Scotia; Geological Association of Canada-Mineralogical Association of Canada Joint Annual Meeting, Fredericton, New Brunswick, Guidebook 3, 77 p.

Koukouvelas, I. and Pe-Piper, G.
1995: The role of granites in the evolution of the Folly Lake diorite, Cobequid Highlands, Nova Scotia; in Current Research 1995-D; Geological Survey of Canada, p. 33-38.
1996: The Hart Lake-Byers Lake and Folly Lake plutons, Cobequid Highlands, Nova Scotia: deformation history inferred from mafic enclaves; in Current Research 1996-D; Geological Survey of Canada Paper.

Miller, B.V., Nance, R.D., and Murphy, J.B.
1995: Kinematics of the Rockland Brook fault, Nova Scotia: implications for the interaction of the Meguma and Avalon terranes; Journal of Geodynamics, v. 19, p. 253-270.

Nearing, J.D.
1995: Thermochronologic evolution of the Cobequid Highlands, Nova Scotia. (Abstract); Atlantic Geoscience Society Annual Meeting, Antigonish, February 1995, p. 22.

Pe-Piper, G., Piper, D.J.W., and Clerk, S.B.
1991: Persistent mafic igneous activity in an A-type granite pluton, Cobequid Highlands, Nova Scotia; Canadian Journal of Earth Sciences, v. 28, p. 1058-1072.

Piper, D.J.W., Pe-Piper, G., and Loncarevic, B.D.
1993: Devonian-Carboniferous deformation and igneous intrusion in the Cobequid Highlands; Atlantic Geology, v. 29, p. 219-232.

Wiebe, R.A.
1993: Basaltic injections into floored silicic magma chambers; Eos, 74, p. 1-3.

Zeeman, M.M.
1992: The petrology and geochemistry of the Folly Lake pluton and the contact relationships between mafic and felsic phases, Cumberland and Colchester counties, Nova Scotia; B.Sc. (hons) thesis, Saint Mary's University, Halifax, Nova Scotia, 105 p.

Geological Survey of Canada Project 920062

The Hart Lake-Byers Lake-Folly Lake pluton, Cobequid Highlands, Nova Scotia: deformation history inferred from mafic enclaves[1]

I. Koukouvelas[2] and Georgia Pe-Piper[2]
GSC Atlantic

Koukouvelas, I. and Pe-Piper, G., 1996: The Hart Lake-Byers Lake-Folly Lake pluton, Cobequid Highlands, Nova Scotia: deformation history inferred from mafic enclaves; in Current Research 1996-D; Geological Survey of Canada, p. 35-40.

Abstract: The Hart Lake-Byers Lake granite and Folly Lake gabbro make up a composite pluton emplaced along the Rockland Brook fault in latest Devonian time. Mafic enclaves are common in granite veins cutting gabbro near the contact of the major granite and gabbro bodies. Three types of enclaves are distinguished: (I) "chocolate-bar" enclaves with angular margins resulting from extensional disruption; (II) ellipsoidal enclaves forming from type I by shear deformation in granitic dykes; and (III) large plastically deformed stoped rafts of gabbro. Deformation of ellipsoidal enclaves decreases northward from the Rockland Brook fault.

Résumé : Le granite de Hart Lake-Byers Lake et le gabbro de Folly forment un pluton composite mis en place le long de la faille de Rockland Brook au Dévonien terminal. Les enclaves mafiques sont nombreuses dans les filons de granite recoupant le gabbro près du contact entre les principaux massifs de granite et de gabbro. On distingue les trois types d'enclaves suivants : I) les enclaves en forme de «barres de chocolat» aux bords anguleux par rupture d'expansion; II) les enclaves ellipsoïdales se formant à partir des enclaves du type I par cisaillement dans des dykes granitiques; III) les gros blocs de gabbro assimilés par le magma et déformés de façon plastique. La déformation des enclaves ellipsoïdales diminue vers le nord à partir de la faille de Rockland Brook.

[1] Contribution to Canada-Nova Scotia Cooperation Agreement on Mineral Development (1992-1995), a subsidiary agreement under the Canada-Nova Scotia Economic and Regional Development Agreement.
[2] Department of Geology, Saint Mary's University, Halifax, Nova Scotia B3H 3C3

INTRODUCTION

The Hart Lake-Byers Lake granite and Folly Lake gabbro (Donohoe and Wallace, 1982, 1985) together form the largest pluton of the Cobequid Highlands. The Folly Lake gabbro occupies most of the southern and western part of the pluton and the Hart Lake-Byers Lake granite the northern and eastern part of the pluton (Fig. 1). In the contact zone between these two lithologies, outcrop-scale and map-scale crosscutting relationships and hybrid igneous phases are observed. Mafic enclaves in granite provide markers for inferring strain during magma emplacement and cooling. In the present paper, we present new results of detailed observations of contact relations between mafic and felsic magmas with special emphasis on the mafic enclaves that are concentrated close to this contact.

GEOLOGICAL SETTING

The Cobequid-Chedabucto fault zone is a 300-km-long, 5- to 15-km-wide, zone which is interpreted to mark the suture between the Avalon and Meguma terranes (Eisbacher, 1969, 1970; Keppie, 1989; Keen et al., 1991). The zone cuts greenschist facies rocks and is characterized by complex magmatic activity represented by a series of plutonic bodies along its trace.

The Hart Lake-Byers Lake-Folly Lake pluton is characterized by two compositionally distinct magmas that intruded Silurian metasediment and syn-plutonic volcanic rocks of the late Devonian – early Carboniferous Fountain Lake Group. It is bounded to the south by the Rockland Brook fault, a major dextral strike slip fault, that was active during the emplacement of the pluton and appears to have been the principal magma pathway (Koukouvelas and Pe-Piper, 1995). Radiometric dating of zircon by the U-Pb method suggests that the granite is latest Devonian (362 Ma) (Doig et al., in press). During detailed mapping of the pluton, abundant mafic enclaves were observed in the granite phases and in granitic dykes that cut the gabbroic phases. These enclaves indicate mingling between the two magmas and thus we can use these as indicators for the conditions under which intrusion took place.

Detailed mapping of the pluton along the regional contact of gabbro (to the southwest) with granite (to the northeast) shows that the granite dykes with mafic enclaves have intruded older gabbro. In places, however, this gabbro clearly intrudes older granite. In many cases, gabbro-granite contacts are lobate and show chilling of gabbro against granite. Contact relationships have been described in more detail by Pe-Piper and Koukouvelas (1995) and Pe-Piper et al. (1996). Regionally, the contact between the granite and gabbro strikes northwest and dips southwest and is well exposed in streams flowing north or south.

In several places the zone between the two lithologies is defined by petrologically transitional phases such as tonalite and granodiorite, some of which are homogenous (derived from intermediate magma) and others of which show complex mingling of lithologies resulting from mixing of crystal mushes. Homogenous intermediate rocks commonly form dykes, both parallel to and sub-orthogonal to the mapped contact. In these dykes and close to the contact abundant mafic enclaves are observed.

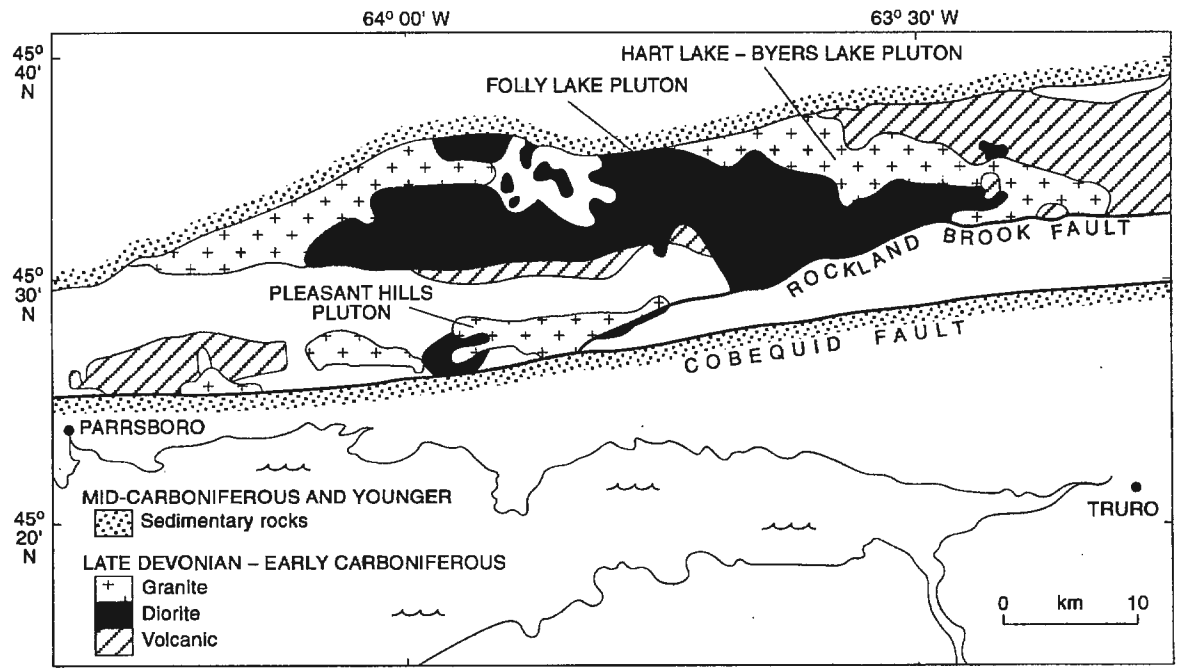

Figure 1. *Map showing regional location of the Folly Lake-Hart Lake-Byers Lake pluton and relationship to the Rockland Brook fault.*

MAFIC ENCLAVES

Introduction

The presence of enclaves in plutonic rocks that are deformed into ellipsoidal shapes (Vernon et al., 1988; Hutton, 1982, 1988) has been traditionally used for the description of pluton deformation. The application of drop-deformation theory, which treats emulsions of two liquids (Hinch and Acrivos, 1980; Rallison, 1984), provides a method of modelling the deformation and stability of enclaves (Williams and Tobisch, 1994). The method shows that flow velocity and temperature of the host intrusion and the composition of the enclaves are important in determining enclave morphology.

Detailed observations at several sites across the diorite-granite contact in the Hart Lake-Byers Lake-Folly Lake pluton show that there are three different types of enclave swarms, separated on the basis of their shape, aspect ratio, and the percentage of mafic and felsic lithologies at outcrop scale. The aspect ratio is an index of the final deformation and is measured as the ratio of the long axis to the short axis dimensions of each enclave.

Description of types I-III

Type I consists of decimetre-scale angular diorite enclaves surrounded by a dense network of granite dykelets or dykes up to 10 cm wide (Fig. 2A). These are here called "chocolate-bar" enclaves, a term used previously for boudins (Ramsay and Hubert, 1983), and implying extension in two dimensions. Typical outcrops of this type have been mapped in East Branch Great Village river (station A, Fig. 3). In the same outcrop we mapped progressive deformation of angular enclaves to elliptical shapes in shear zones. In other sites that lack any structural deformation the shapes of the enclaves remain angular and suggest that chocolate-bar enclaves represent the initial shape of the enclaves in the pluton. This observation removes the uncertainty when elipticity of enclaves is used to define the amount of deformation. The proportion of mafic to felsic lithologies is typically 95%.

Type II consists of swarms of ellipsoidal enclaves, reaching maximum size of 25 cm by 10 cm. The enclaves are mainly rounded (95%) with a few angular (5%), with aspect ratios ranging from 2.1 to 4.6 (Fig. 2B). These enclave swarms are observed mainly in shear zones or close to major granite-diorite contacts. Typical outcrops of enclaves in shear zones

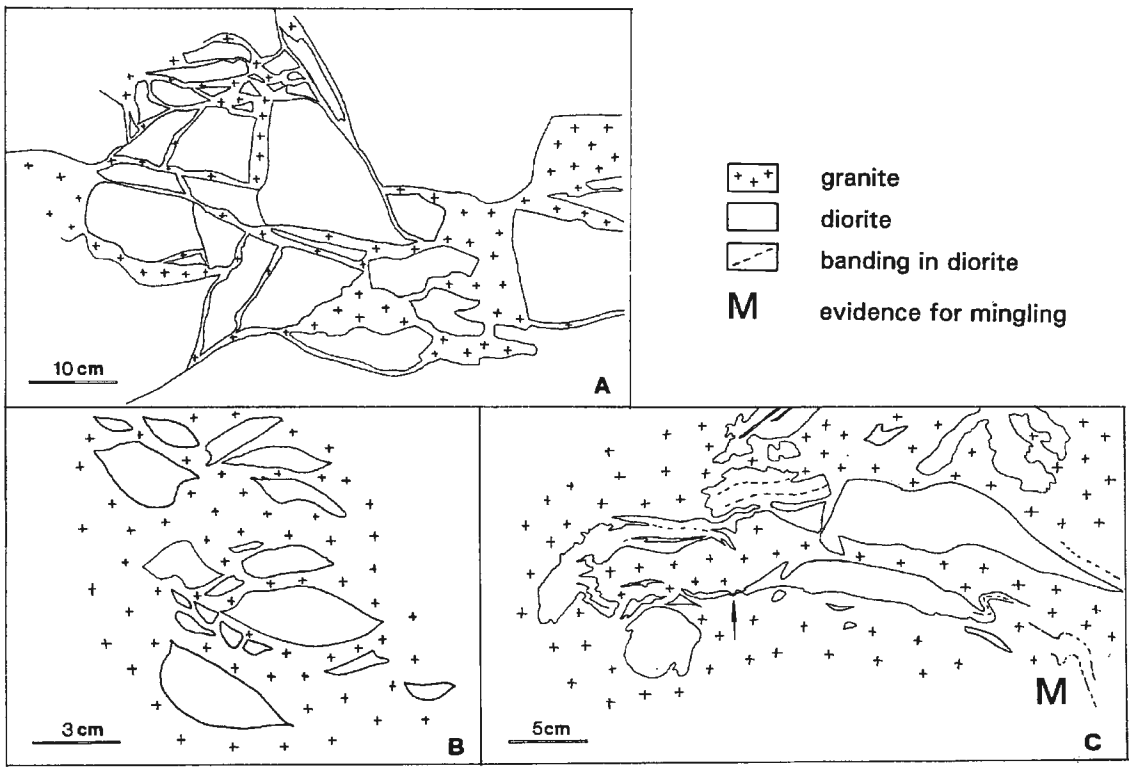

Figure 2. *Sketches showing the three types of enclave swarms.* ***A)*** *Type I chocolate-bar enclaves and granitic dykelets or dykes.* ***B)*** *Type II ellipsoidal enclaves with aspect ratios ranging from 2.1 to 4.6.* ***C)*** *Type III enclaves. The long body of the enclave is partially disrupted by wedging and the tips of the enclaves are strongly folded; some physical mixing of the enclave with the felsic magma is also visible (for details see text).*

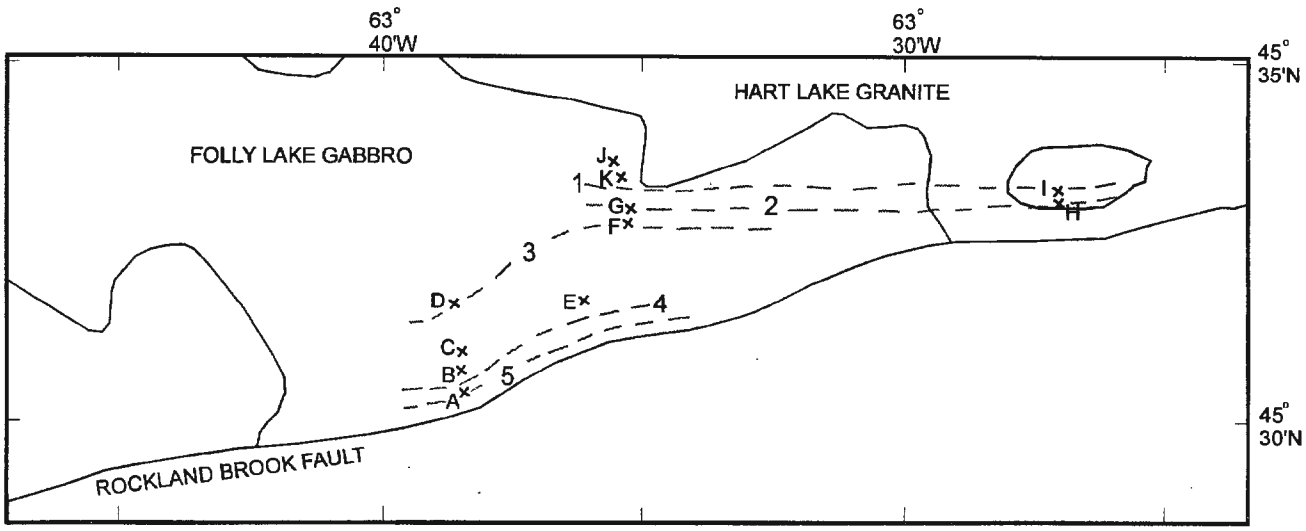

Figure 3. *Simplified geological map of the Folly Lake-Hart Lake-Byers Lake pluton showing structural contours based on the aspect ratios of enclaves at eight localities in the pluton. Note that the contours trend subparallel to the Rockland Brook fault. A-K are locations of detailed observations of enclaves (Table 1).*

have been mapped in the East Branch Great Village river (stations B and D, Fig. 3). In plan these shear zones are exposed over several square metres in a continuous outcrop, deforming initially angular enclaves (Fig. 4). The percentage of mafic to felsic lithologies is typically about 20%. All enclaves are observed to follow the contact in a parallelism that is induced by the mechanical response of the enclave during the flow of the host rock (sensu Williams and Tobisch, 1994). As the long axis of an enclave was rotated into near-parallelism with the shear zone boundaries, the enclave was deformed under shear deformation. During this deformation, the length is reduced and the enclave is broken up into smaller pieces. The shear zones with flattened enclaves are characterized by wider granitic dykes than those of type I. This means that the increase in width of the granitic dykes is combined with an increase in the shear deformation. A plot of enclave aspect ratio on a geological map shows progressive deformation of the enclaves towards the Rockland Brook fault (Fig. 3), ranging from >4 near the fault to <1.5 in the northern part of the pluton. Quartzite xenoliths from gabbro/diorite in the Rockland Brook fault zone exposed in the Portapique River west of the study area have a mean aspect ratio of 5.5.

Type III enclaves are plastically deformed, up to 50 cm in length by 5 cm wide (Fig. 2C). These enclaves are rarer than the other two types and are best seen at station C (Fig. 3). These enclaves show progressive plastic deformation of the enclave tips while the main body remains rectangular and granite appears to have penetrated along compositional planes in the diorite (Fig. 2C). The plastic deformation, in some cases, has lead to physical mixing or mingling of the two rock types.

Table 1. Aspect ratio of gabbroic enclaves.

Station (Fig. 1)	Map reference		Aspect ratio	Standard deviation	Number of observations
Great Village River and tributaries					
A	449961	5039562	4.6	1.6	15
B	449964	5039827	3.7	2.0	10
C	449953	5039959	[Type III enclaves]		
D	450344	5041498	3.0	1.1	15
E	453110	5040781	3.7	1.0	7
F	454224	5043769	3.0	1.3	11
G	454200	5044108	2.2	0.5	22
Debert River					
H	464742	5044249	2.2	0.5	14
I	464702	5044488	2.1	0.3	14
Higgins Mountain					
J	453522	5045106	1.9	0.7	12
K	453763	5044636	1.4	0.2	11
Portapique River (quartzite in gabbro/diorite)					
L	444110	5036613	5.5	2.7	24

Interpretation of enclaves

Type I and II enclave swarms are characterized by chocolate-tablet enclaves (type I) and ellipsoidal enclaves (type II). The ellipsoidal shape is directly correlated with the width of the host granitic dyke. The preservation of chocolate-bar enclaves would require relatively cool diorite (below 900°C according to Williams and Tobisch, 1994) and low flow velocity in the granite. Zones with both undeformed and deformed enclaves show that the deformation of the enclaves was concentrated at sites of strong shear deformation.

The plastic deformation of type III enclave swarms suggests a higher temperature of the gabbro, probably resulting from a deeper magmatic level than the other two types. Magmatic stoping may have been an important process for deriving large enclaves of diorite.

The degree of deformation of type II enclaves shows a progressive decrease northward away from the Rockland Brook fault (Fig 3). Shear zones with deformed enclaves are separated by zones with undeformed enclaves. These shear zones are subparallel to the Rockland Brook fault. Evidence of major shear zones is found at least 4 km north of the trace of the Rockland Brook fault (Fig. 3). Type III enclaves have been found only within 1 km of the Rockland Brook fault.

These relationships, combined with the observation that granite becomes progressively more abundant towards the Rockland Brook fault (Koukouvelas and Pe-Piper, 1995), indicate that a set of dextral strike-slip faults parallel with the Rockland Brook fault as well as the Rockland Brook fault itself were the most important structural elements for the evolution of the felsic magmatism of the Hart Lake-Byers Lake-Folly Lake pluton.

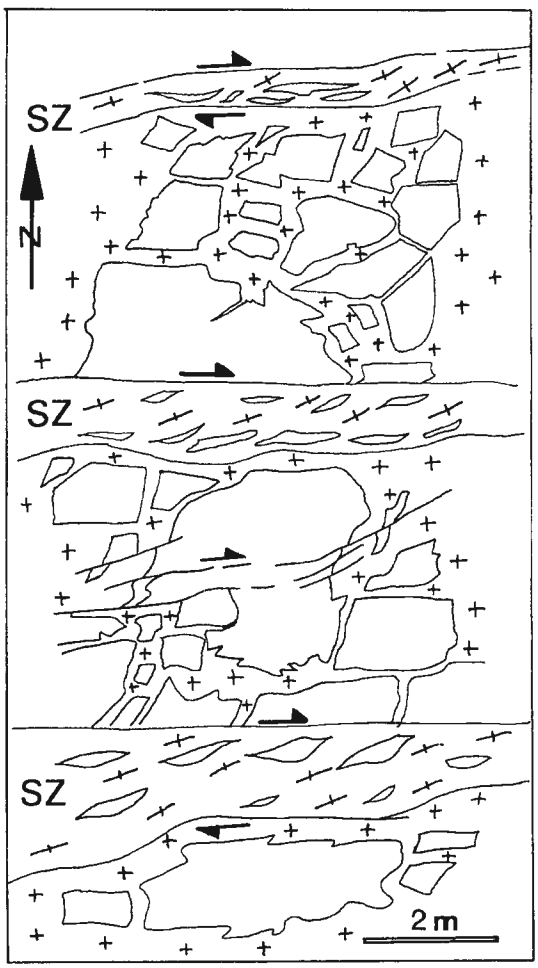

Figure 4. Map view of a 14-m-wide zone with chocolate-bar enclaves crossed by four shear zones. Shear zones are centimetre-scale to 1 m wide, spaced at 4 m. In the shear zones the enclaves are deformed to an ellipsoidal shape with an aspect ratio of 2.5 to 4.7. Note the parallelism of the enclaves with the shear zone boundaries. (Located at station A, East Branch Great Village River, Fig. 3).

CONCLUSIONS

Three types of mafic enclave in granitic dykes are distinguished: (I) "chocolate-bar" enclaves with angular margins resulting from extensional disruption; (II) ellipsoidal enclaves forming from type I by shear deformation in granitic dykes; and (III) large, plastically deformed, stoped rafts of gabbro. Type I enclaves show a progressive change to type II as a result of shear deformation in granite dykes. Synmagmatic shear deformation has taken place in shear zones subparallel to the Rockland Brook fault and overall the deformation of ellipsoidal enclaves decreases northward from the Rockland Brook fault. Type III enclaves developed under higher temperature conditions and show plastic deformation and partial mingling with felsic magma.

REFERENCES

Doig, R., Murphy, J.B., Pe-Piper, G., and Piper, D.J.W.
in press: U-Pb geochronology of late Paleozoic plutons, Cobequid Highlands, Nova Scotia, Canada: evidence for late Devonian emplacement adjacent to the Meguma-Avalon terrane boundary in the Canadian Appalachians; Geological Journal.

Donohoe, H.V. and Wallace, P.I.
1982: Geological map of the Cobequid Highlands, Nova Scotia; Nova Scotia Department of Mines and Energy, Map 82-09, scale 1:50 000, 4 sheets.

Donohoe, H.V., Jr. and Wallace, P.I.
1985: Repeated orogeny, faulting and stratigraphy of the Cobequid Highlands, Avalon Terrane of northern Nova Scotia; Geological Association of Canada - Mineralogical Association of Canada Joint Annual Meeting, Fredericton, New Brunswick, Guidebook 3, 77 p.

Eisbacher, G.H.
1969: Displacement and stress field along part of the Cobequid Fault, Nova Scotia; Canadian Journal of Earth Sciences, v. 6, p. 1095-1104.
1970: Deformation mechanisms of mylonitic rocks and fractured granites in the Cobequid Mountains, Nova Scotia, Canada; Geological Society of America Bulletin, v. 81, p. 2009-2020.

Hinch, E.J. and Acrivos, A.
1980: Long slender drops in a simple shear flow; Journal Fluid Mechanics, v. 98, p. 305-328.

Hutton, D.H.W.
1982: A method for the determination of the initial shapes of deformed xenoliths in granitoids; Tectonophysics, v. 85, p. 45-50.
1988: Igneous emplacement in a shear zone termination: the biotite granite at Strontian, Scotland; Bulletin of the Geological Society of America, v. 100, p. 1392-1399.

Keen, C.E., Kay, W.A., Keppie, J.D., Marillier, F.J.Y., Pe-Piper, G., and Waldron, J.G.F.
1991: Crustal characteristics of the Canadian Appalachians southwest of Nova Scotia, from deep marine reflection profiling; Canadian Journal of Earth Sciences, v. 28, p. 1096-1111.

Keppie, J.D.
1989: Northern Appalachian terranes and their accretionary history; Geological Society of America, Special Paper 230, p. 159-192.

Koukouvelas, I. and Pe-Piper G.
1995: The role of granites in the evolution of the Folly Lake diorite, Cobequid Highlands, Nova Scotia; in Current Research 1995-D; Geological Survey of Canada, p. 33-38.

Pe-Piper, G., Zeeman, M., and Piper, D.J.W.
1996: Magmatic significance of the relationships between the mafic and felsic phases of the Folly Lake pluton, Cobequid Highlands, Nova Scotia; in Current Research 1996-C; Geological Survey of Canada.

Rallison, J.M.
1984: The deformation of small viscous drops and bubbles in shear flows; Annual Review Fluid Mechanics, v. 98, p. 625-633.

Ramsay, J.G. and Hubert, M.I.
1983: The techniques of modern structural geology; Academic Press.

Vernon, R.H., Etheridge, M.A., and Wall, V.J.
1988: Shape and microstructure of microgranitoid enclaves: indicators of magma mingling and flow; Lithos, v. 22, p. 1-11.

Williams, Q. and Tobisch, O.T.
1994: Microgranitic enclave shapes and magmatic strain histories: constraints from drop deformation theory; Journal of Geophysical Research, v. 99, p. 24359-24368.

Geological Survey of Canada Project 920062

Field evidence for the extent and style of overthrusting along the northeastern margin of the Cobequid Highlands, Nova Scotia[1]

David J.W. Piper, Paul Durling[2], and Georgia Pe-Piper[3]
GSC Atlantic, Dartmouth

Piper, D.J.W., Durling, P., and Pe-Piper, G., 1996: Field evidence for the extent and style of overthrusting along the northeastern margin of the Cobequid Highlands, Nova Scotia; in Current Research 1996-D; Geological Survey of Canada, p. 41-46.

Abstract: Seismic evidence for thrusting of Precambrian and Silurian rocks over the late Devonian – early Carboniferous Fountain Lake Group of the Scotsburn Anticline is confirmed by field evidence. A belt of variably foliated Precambrian, Silurian and probably lower Carboniferous rocks form the hanging wall of the thrust fault and are onlapped by the molasse-like Falls Formation. The age of thrusting is stratigraphically confined to the late Tournaisian.

Résumé : Des données de terrain corroborent les résultats de levés sismiques selon lesquels des roches précambriennes et siluriennes chevauchent celles du Groupe de Fountain Lake (Dévonien tardif-Carbonifère précoce) associées à l'anticlinal de Scotsburn. Une zone de roches du Précambrien, du Silurien et probablement du Carbonifère inférieur à foliation variable forme le compartiment supérieur de la faille de chevauchement et est recouverte en biseau d'aggradation par la Formation de Falls de type molassique. Selon la stratigraphie, l'âge du chevauchement est confiné au Tournaisien tardif.

[1] Contribution to Canada-Nova Scotia Cooperation Agreement on Mineral Development (1992-1995), a subsidiary agreement under the Caanda-Nova Scotia Economic and Regional Development Agreement.
[2] Durling Geophysics, 36 Beaufort Drive, Dartmouth, Nova Scotia B2W 5V4
[3] Department of Geology, Saint Mary's University, Halifax, Nova Scotia B3H 3C3

INTRODUCTION

Seismic data described by Durling (1996) show evidence of significant thrusting in the northeast Cobequid Highlands. Thick volcanic and overlying sedimentary rocks of the Fountain Lake Group that were drilled in the Irving-Chevron Scotsburn No. 2 well can be traced in seismic reflection profiles beneath an area of Precambrian and Silurian rocks in the northeastern Cobequid Highlands. In this paper, we describe the field evidence for thrusting of older rocks over the Fountain Lake Group of the Scotsburn anticline.

SEISMIC DATA

During the 1970s and 1980s, petroleum industry seismic reflection data were collected over the Scotsburn anticline and the northeastern Cobequid Highlands. These data provide a dense grid of seismic profiles permitting subsurface examination of the boundary between the Cobequid Highlands and Cumberland Basin. This boundary was overstepped by Late Carboniferous sedimentation, and can be studied only using geophysical techniques, such as seismic reflection methods. Seismic investigations (Durling, 1996) show that over-thrusting occurred along parts of this boundary, providing important constraints for the interpretation of outcrop data in the eastern Cobequid Highlands.

The seismic data were interpreted in concert with geological map data and borehole data. The Irving-Chevron Scotsburn No. 2 well (hereafter, the Scotsburn well) was used to identify key seismic horizons within the Fountain Lake Group, an Upper Devonian to Lower Carboniferous volcanic and clastic sediment unit. It comprises three distinct lithological units: 1) a lower felsic volcanic unit, 2) a middle mafic volcanic unit (both contain minor interbedded clastic rocks), and 3) an upper unit consisting of red, fine grained sandstone and siltstone with interbedded mafic volcanic rocks.

The most distinct and laterally continuous reflection within the Fountain Lake Group correlates with the contact between the mafic volcanic and the overlying clastic rocks (Durling, 1996). This seismic marker was mapped in the sub-surface in an east-west direction for about 55 km and up to 17 km in a north-south direction. It was recognized in the subsurface as far south as the surface trace of the Waugh River Fault and the northeastern part of the Rockland Brook fault (Fig. 1).

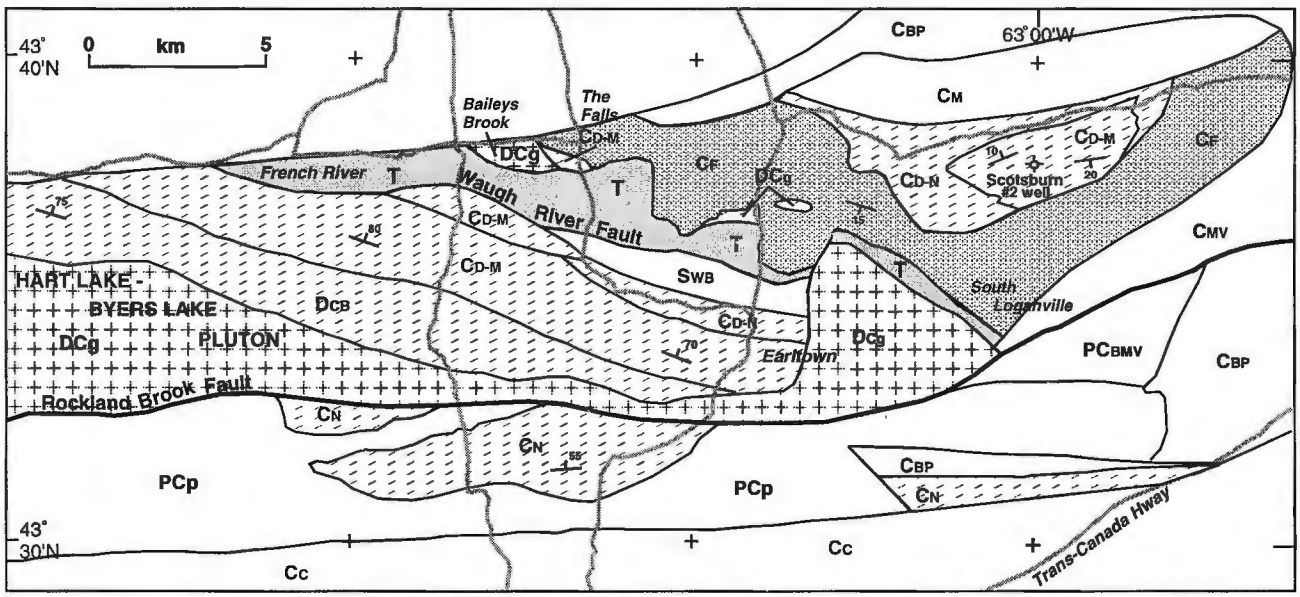

CBP Boss Point Fm
Cc Canso Group
CMV Millsville Fm
CM Middleborough Fm
CF Falls Fm
CN Nuttby Fm
Diamond Brook Fm
CD-N Nabiscumb Brook Mbr
CD-M McKay Brook Mbr
DCB Byers Brook Fm
DCg Granite and porphyritic rhyolite
SWB Wilson Brook Fm
PCDMV Dalhousie Mountain Volcanics
PCp Late Precambrian plutonic rocks
T Thrust tectonic unit includes Warwick Mountain Fm, Wilson Brook Fm and Fountain Lake Gp

Figure 1. *Summary geological map of the northeastern Cobequid Highlands. Post-Horton rocks based in part on Donohoe and Wallace (1982) and Chandler et al. (1994).*

A comparison between the sub-surface distribution of the seismically determined top of Fountain Lake Group volcanic rocks, and the distribution of surface mapped rocks, demonstrates overthrust relationships (Durling, 1996, his fig. 6). East of Warwick Mountain, both Precambrian and Silurian rocks occur up to 5 km north of the Waugh River fault (Donohoe and Wallace, 1982). In this area, the seismic data show that the Fountain Lake Group occurs in the sub-surface at 3-5 km depth (Durling, 1996), placing older rocks over younger rocks. Seismic profiles in the area are void of reflections in their upper parts, south of the known distribution of Upper Carboniferous rocks. The reflection-poor areas are interpreted to be caused by steeply dipping or highly deformed rocks within the hanging wall of a thrust fault.

NEW FIELD DATA IN THE NORTHEASTERN COBEQUID HIGHLANDS

Introduction

New mapping in the northeastern Cobequid Highlands has shown an east-northeast-striking zone of variably foliated rocks with a diverse protolith. Many of these foliated rocks were previously mapped as the late Precambrian Warwick Mountain Formation and the Silurian Earltown Formation (Donohoe and Wallace, 1982). We show below that these rocks represent the hanging wall of the thrust fault interpreted from seismic data and refer to them as the "thrust tectonite unit". We describe below the regional distribution of rock units in the northeastern Cobequid Highlands from northeast to southwest, i.e. from footwall to hanging wall.

Fountain Lake Group northeast of the thrust zone

In the Scotsburn anticline, the Scotsburn well penetrated a thick sequence of rhyolitic volcanic rocks (Byers Brook Formation) overlain principally by basalt (McKay Brook member of the Diamond Brook Formation), the highest flows of which are exposed at the surface. The McKay Brook member is overlain in surface outcrop by the Nabiscumb Brook member, comprising a sequence of fluvial conglomerate, sandstone, and siltstone, with finer facies in the north and paleocurrents generally to the northwest or north. The rapid southward coarsening of the member suggests a proximal source, with the basin margin probably marked by the eastern part of the Rockland Brook fault. The conglomeratic Falls Formation overlies the Nabiscumb Brook member. The upper part of the McKay Brook member in the well has mid Tournaisian palynomorphs (Utting et al., 1989).

Southwest of the Scotsburn anticline, immediately north of the "thrust tectonite unit" are several small bodies of relatively undeformed porphyritic rhyolite (north of Earltown) and basalt (at The Falls). The basalt is steeply dipping and youngs to the north.

Falls Formation

Onlapping the porphyritic rhyolite and northeast of the "thrust tectonite unit" are thick conglomerate and coarse sandstone of the Falls Formation. Seismic reflection profiles on the southeast limb of the Scotsburn anticline show that the contact of this formation with the Millsville Formation can be traced into Windsor Group reflections beneath the Gulf of St Lawrence. Clasts include Fountain Lake volcanic rocks, fossiliferous Silurian sandstone, and deformed siliciclastic rocks of the "thrust tectonite unit" (Donohoe and Wallace, 1985). The Falls Formation is older than the late Viséan Middleborough Formation (Ryan and Boehner, 1990; Chandler et al., 1994).

Thrust zone

Along the northeastern rim of the Cobequid Highlands, northeast of the Waugh River fault and southwest of the Falls Formation, are some areas of little deformed lower Paleozoic and Neoproterozoic rocks. These rocks were assigned to the Silurian Earltown and Precambrian Warwick Mountain formations by Donohoe and Wallace (1982). They include fossiliferous Silurian shelf clastic rocks and thick-bedded sandstone turbidites correlated with the Neoproterozoic Jeffers Group. In places, apparent thrust faults between slices of these rocks are occupied by porphyritic rhyolite or gabbro. Seismic profiles show that these older rocks are located above Fountain Lake Group volcanic rocks continuous with those at the Scotsburn well.

In the same area, deformed rocks with a flat-lying foliation, in places mylonitic, are widespread. Locally, the deformed rocks show gradational contacts with less deformed rocks; elsewhere, contacts with other rock types are faulted. The identification and correlation of the protolith of the deformed rocks are not yet complete, but probably include: (a) Precambrian volcaniclastic turbidites and/or tuffs in the Loganville area, similar to the Keppoch Formation of the Antigonish Highlands and the Dalhousie Mountain volcanic unit of the extreme eastern Cobequid Highlands; (b) Precambrian siliciclastic turbidites similar to nearby undeformed lithologies; (c) porphyritic rhyolite and gabbro; (d) mafic volcanic rocks (e.g. lower French River) that resemble the Diamond Brook Formation; and (e) some grey sericitic phyllites of unknown protolith. Kinematic indicators in the foliated rocks are quite variable, but the principal mylonite zones show south-dipping mineral lineation.

This assemblage of highly deformed rocks, together with less deformed Precambrian and Silurian rocks, is referred to as the "thrust tectonite unit". Geochemical analyses show that the foliated porphyritic rhyolite and gabbro in (c) above are geochemically similar to the porphyritic rhyolite and gabbro bodies between thrust slices of the Jeffers Group (Table 1). Gabbro units have TiO_2>1.2%, Y>20 ppm and rhyolite units have Y>300 ppm and Pb>10 ppm, which Pe-Piper et al. (1991, 1994) showed was characteristic of late Devonian – earliest Carboniferous igneous activity.

Fountain Lake Group southwest of the thrust zone

The Fountain Lake Group volcanic unit to the southwest of the "thrust tectonite unit" consists of steeply dipping interbedded volcanic rocks and sediments, commonly with quite brittle deformation. Younging directions are variable, but are most commonly to the north. The stratigraphic section consists of several kilometres of Byers Brook Formation apparently overlain by Diamond Brook Formation. The Byers Brook Formation consists principally of felsic pyroclastic rocks, flows, and domes, with minor basalt and sediments (lacustrine silt and conglomerate). Sediments contain Tournaisian and Emsian/Eifelian (presumably reworked) palynomorphs (Donohoe and Wallace, 1982). The Diamond Brook Formation consists of many basalt flows, some with feldspar megacrysts (McKay Brook member), that pass up into red mudstone and sandstone (Nabiscumb Brook member).

The southwestern margin of the Fountain Lake Group is marked by a gradual increase in abundance of intrusive porphyritic rhyolite, which is in contact with fine grained granite of the Hart Lake-Byers Lake pluton to the south. The southern boundary of the pluton is the Rockland Brook fault, a major fault with a 100-m-wide mylonite zone that shows a south-dipping foliation and mineral lineations that suggest both dip-slip and dextral strike-slip motion. It is interpreted as the main magma pathway for the Folly Lake gabbro, the Hart Lake-Byers Lake granite, and intrusive rhyolite in the Nuttby Mountain area.

Synthesis

We interpret the rocks of the northeastern Cobequid Highlands as forming a thrust sheet rooted in the Rockland Brook fault. The Rockland Brook fault dips southward and shows steeply dipping mineral foliation. The principal plutons immediately north of the fault show evidence for north-vergent thrusting (Pe-Piper and Koukouvelas, 1994). The steeply dipping Fountain Lake Group between the Rockland Brook and Waugh River faults is interpreted as a complex thrust sheet with tight folds. Such a structure would account for the variable facing directions. The less deformed Precambrian and Silurian rocks of the "thrust tectonite unit" are intruded by porphyritic rhyolite and gabbro along north-vergent thrust faults: a similar relationship in country rock north of the Pleasant Hills pluton is described below. These minor igneous bodies may be analogous to the early stages of pluton emplacement in larger plutons such as the Pleasant Hills and Hart Lake-Byers Lake plutons (Pe-Piper and Koukouvelas, 1994).

The mylonite of the "thrust tectonite unit" represents the principal deformation zone in the hanging wall of the major thrust fault. The Falls Formation represents a molasse deposit derived from the advancing thrust front to the south.

We cannot exclude the possibility that the geometric relationship revealed by the seismic reflection profiles of the thrust tectonite unit over the Fountain Lake Group is the result of predominantly west-northwest strike-slip motion along the Waugh River fault, rather than north-northeast-vergent thrusting. The thrust tectonite unit extends 30 km along strike, implying that major strike-slip motion would be required. This interpretation poses questions about the eastward extension of the Waugh River fault and the lack of mylonitic or cataclastic deformation along the fault itself. It less elegantly explains the apparent continuity of north-vergent thrusting though Horton times. If this hypothesis is correct, it would imply that the steeply dipping Fountain Lake Group was tightly folded within a shear zone.

THE NORTHERN MARGIN OF THE PLEASANT HILLS PLUTON: A LESS-DEFORMED ANALOGUE OF THE THRUST TECTONITE UNIT

Mapping of the area north of the Pleasant Hills pluton in the central Cobequid Highlands (Fig. 2) shows a geological setting similar to that inferred for the older rocks of the "thrust tectonite unit", except that highly deformed and mylonitic

Table 1. Selected geochemical analyses of small intrusions in the "thrust tectonite unit".

	fol. gabbro	fol. gabbro	fol. gabbro	porph. rhyolite
sample	103	7748	7789	7804
SiO_2	46.70	47.17	47.06	67.56
TiO_2	3.06	1.76	3.02	0.47
$Al2O_3$	13.30	15.38	13.04	15.86
$Fe2O_3$	15.20	12.27	15.34	2.51
MnO	0.33	0.17	0.21	0.14
MgO	5.55	6.37	3.84	0.44
CaO	8.31	8.76	7.26	2.57
Na_2O	2.85	3.07	3.52	4.35
K_2O	0.91	1.05	0.72	3.15
P_2O_5	0.40	0.21	0.38	0.10
L.O.I	2.62	4.53	6.43	3.16
Total	99.23	100.74	100.82	100.31
Ba	328	507	439	619
Rb	33	33	20	115
Sr	277	378	306	104
Y	43	20	43	40
Zr	259	105	259	261
Nb	16	15	20	14
Th	4	<1	<1	1
Pb	19	<1	3	25
Ga	25	21	21	20
Zn	145	135	115	93
Cu	57	103	138	29
Ni	51	78	15	<3
V	396	202	347	26
Cr	102	175	27	<14

Locations: 103 – Miller Brook; 7748 – Bailey's Brook; 7789,7804 – French River.

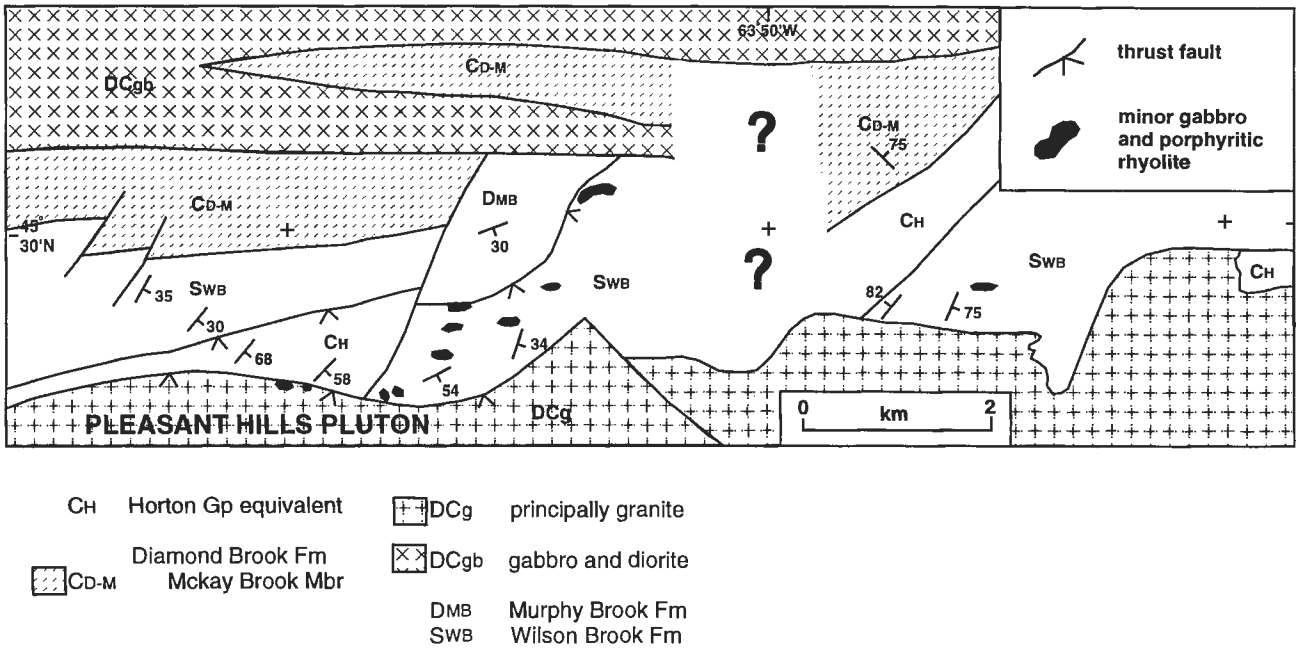

Figure 2. Summary geological map of the area north of the Pleasant Hills pluton, showing the observed distribution of minor intrusions.

rocks are absent. The Pleasant Hills pluton intrudes Silurian Wilson Brook Formation, with the northern margin of the pluton generally being a south-dipping thrust contact with local overturning of bedding in country rock (Fig. 2). East- or northeast-striking outcrop zones of Fountain Lake Group basalt (Diamond Brook Formation), Horton Group equivalent clastic sediments (Piper, 1994), and middle Devonian Murphy Brook Formation have fault contacts with the Wilson Brook Formation (Fig. 2). Several of these fault contacts are demonstrably thrust faults, and thrust faults also occur within the Wilson Brook Formation. In places, faults are occupied by gabbro and/or porphyritic rhyolite sheets, typically 5-20 m thick. These intrusive sheets have geochemical signatures (Table 2) similar to late Devonian – early Carboniferous intrusive rocks elsewhere in the Cobequid Highlands and are similar to the minor intrusions described above from the "thrust tectonite unit" of the northeastern Cobequid Highlands. We suggest that this outcrop pattern would have been similar to that in the "thrust tectonite unit" of the northeastern Cobequid Highlands prior to intense thrust deformation of that unit.

REGIONAL SYNTHESIS

Seismic data show at least 5 km of overthrusting of Precambrian and Silurian rocks of the "thrust tectonite unit" over relatively flat-lying Fountain Lake Group. Such thrusting accounts for the steep dips and inconsistent facing directions in the several kilometre thick Fountain Lake Group of the eastern Cobequid Highlands. It is consistent with the regional evidence for north-vergent thrusting associated with

Table 2. Selected geochemical analyses of small intrusions north of the Pleasant Hills pluton.

	GABBRO			RHYOLITE		
	Murphy Brook	E B Economy River		Murphy Brook	Black Brook	
sample	6551	6649	7269	7267	7330	7339
SiO_2	46.26	45.73	51.15	69.92	71.11	75.68
TiO_2	1.49	2.48	2.64	0.61	0.69	0.27
Al_2O_3	15.95	15.18	13.91	12.37	11.92	11.95
Fe_2O_3	11.67	13.27	13.90	5.21	5.30	2.76
MnO	0.21	0.21	0.25	0.07	0.06	0.04
MgO	8.20	6.42	4.93	2.20	1.31	0.52
CaO	10.10	10.67	7.57	4.22	2.11	0.61
Na_2O	2.29	2.29	3.61	3.45	3.94	3.19
K_2O	0.67	0.48	0.17	0.29	3.01	4.22
P_2O_5	0.16	0.30	0.44	0.08	0.08	0.02
L.O.I	1.80	2.40	1.96	1.56	0.44	0.66
Total	98.80	99.43	100.53	99.98	99.97	99.92
Ba	236	176	299	97	98	561
Rb	31	22	5	5	97	70
Sr	320	313	377	243	74	146
Y	23	33	52	65	104	96
Zr	94	175	272	420	734	681
Nb	7	11	15	27	61	44
Th	<5	<5	<5	13	15	15
Pb	<5	<5	11	15	<5	14
Ga	18	20	19	21	20	14
Zn	85	104	121	46	65	30
Cu	65	49	28	0	7	7
Ni	123	76	55	28	14	<5
V	232	257	321	89	70	23
Cr	143	89	92	76	39	17

pluton emplacement along the Rockland Brook fault. There may have been a component of strike slip motion along the Waugh River fault, but positive evidence for this is lacking.

The age of the main thrusting event is constrained by the age of youngest deformed rocks and the overlying Falls Formation. Thrusting is younger than the mid-Tournaisian Diamond Brook Formation. The undeformed Falls Formation, containing foliated detritus, can be traced on seismic profiles to be of Windsor age or older and is older than the late Viséan Middleborough Formation. The Falls Formation thus probably corresponds to the upper part of the Horton Group, implying that the thrusting is of Late Tournaisian to Early Viséan age. It may represent a late phase of a continual process of north-vergent thrusting throughout Horton time.

ACKNOWLEDGMENTS

Field tapes of Anschutz (Canada) Exploration Ltd. seismic data were donated to the GSC by Pembina Resources Ltd. Chevron Canada Resources made migration copies of the seismic data available. Jason Goulden and Craig Doucette assisted with field work. We thank Peter Giles and François Marillier and participants of the NATMAP field trip for discussion.

REFERENCES

Chandler, F.W., Gall, Q., Gillis, K., Naylor, R., and Waldron, J.
1994: A progress report on the geology of the Stellarton Gap, Nova Scotia, including the Stellarton Coal Basin; in Current Research 1994-D; Geological Survey of Canada, p. 113-122.

Donohoe, H.V. and Wallace, P.I.
1982: Geological map of the Cobequid Highlands, Nova Scotia; Nova Scotia Department of Mines and Energy, Map 82-09, Scale 1:50 000, 4 sheets.

Donohoe, H.V., Jr. and Wallace, P.I.
1985: Repeated orogeny, faulting and stratigraphy of the Cobequid Highlands, Avalon Terrane of northern Nova Scotia; Geological Association of Canada - Mineralogical Association of Canada Joint Annual Meeting, Fredericton, New Brunswick, Guidebook 3, 77 p.

Durling, P.
1996: A seismic reflection study of the Fountain Lake Group in the Scotsburn anticline area, northern Nova Scotia; in Current Research 1996-D; Geological Survey of Canada.

Pe-Piper, G. and Koukouvelas, I.
1994: Earliest Carboniferous plutonism, western Cobequid Highlands, Nova Scotia; in Current Research 1994-D; Geological Survey of Canada, p. 103-107.

Pe-Piper, G., Piper, D.J.W., and Clerk, S.B.
1991: Persistent mafic igneous activity in an A-type granite pluton, Cobequid Highlands, Nova Scotia; Canadian Journal of Earth Sciences, v. 28, p. 1058-1072.

Pe-Piper, G., Piper, D.J.W., Parlee, K., and Turner, D.S.
1994: Geology of the headwaters of the River Philip, Cobequid Highlands; Geological Survey of Canada Open File 2887.

Piper, D.J.W.
1994: Late Devonian - earliest Carboniferous basin formation and relationship to plutonism, Cobequid Highlands, Nova Scotia; in Current Research 1994-D; Geological Survey of Canada, p. 109-112.

Ryan, R.J. and Boehner, R.C.
1990: Cumberland basin geology map, Tatamagouche and Malagash, Cumberland, Colchester and Pictou counties; Nova Scotia Department of Mines and Energy, Map 90-14, 1: 50 000 scale.

Utting, J., Keppie, J.D., and Giles, P.S.
1989: Palynology and stratigraphy of the Lower Carboniferous Horton Group, Nova Scotia; Geological Survey of Canada, Bulletin 396, p. 117-143.

Geological Survey of Canada Project 920062

A seismic reflection study of the Fountain Lake Group in the Scotsburn anticline area, northern Nova Scotia[1]

P. Durling[2]
GSC Atlantic

Durling, P., 1996: A seismic reflection study of the Fountain Lake Group in the Scotsburn anticline area, northern Nova Scotia; in Current Research 1996-D; Geological Survey of Canada, p. 47-53.

Abstract: Petroleum industry seismic reflection profiles were interpreted, in conjunction with published geological maps and the Irving-Chevron No. 2 well, to study the structure, stratigraphy, and distribution of the Fountain Lake Group in the Scotsburn anticline area. Two seismic facies were recognized: 1) a low amplitude and 2) a high amplitude seismic facies. They correlate with red sandstone and siltstone, and interbedded sedimentary and volcanic rocks of the Fountain Lake Group, respectively. Several south-dipping faults were mapped that affect the Fountain Lake Group. Most of these show apparent, reverse, dip separation on the seismic profiles.

The top of the high amplitude facies was mapped through the Scotsburn anticline area, and a two-way time map was made. The reflections extend for 55 km in an east-west direction and up to 17 km north to south. Published surface maps show that Precambrian and lower Paleozoic rocks overlie the Fountain Lake Group reflections, demonstrating overthrust relationships.

Résumé : L'interprétation de profils de sismique réflexion obtenus par l'industrie pétrolière s'est faite en tenant compte de cartes géologiques publiées et des données provenant du puits Irving-Chevron n° 2; le but consistait à étudier le style structural, la stratigraphie et la répartition du Groupe de Fountain Lake dans la région de l'anticlinal de Scotsburn. Deux faciès sismiques ont été identifiés, l'un de faible amplitude et l'autre de forte amplitude. Le premier est corrélatif des grès et des siltstones rouges du Groupe de Fountain Lake et le second l'est des interstratifications de roches sédimentaires et volcaniques du même groupe. Plusieurs failles à pendage sud découpant le Groupe de Fountain Lake ont été cartographiées. La plupart de ces failles présentent une séparation inclinée inverse sur les profils sismiques.

Le sommet du faciès de forte amplitude a été cartographié dans toute la région de l'anticlinal de Scotsburn et une carte des temps aller-retour a été établie. Les réflexions de ce sommet ont permis de le suivre sur 55 km dans une direction est-ouest et sur 17 km du nord au sud. Les cartes des unités en surface montrent que des roches du Précambrien et du Paléozoïque inférieur reposent sur le Groupe de Fountain Lake, indiquant des liens de charriage.

[1] Contribution to Canada-Nova Scotia Cooperation Agreement on Mineral Development (1992-1995), a subsidiary agreement under the Canada-Nova Scotia Economic and Regional Development Agreement.
[2] Durling Geophysics, 36 Beaufort Drive, Dartmouth, Nova Scotia B2W 5V4

INTRODUCTION

The Cobequid Highlands is an elongate east-west upland area in northern mainland Nova Scotia (Fig. 1). At the eastern end of the Cobequid Highlands, the structural trend changes from east to northeast. The Scotsburn anticline is a broad, doubly plunging, northeast-striking anticline. It is onlapped by Carboniferous sediments on its north, east, and west sides. On its southern and southwestern sides, the rocks of the anticline are in faulted and unconformable contact with Precambrian and lower Paleozoic rocks (Donohoe and Wallace, 1982).

The oldest rocks exposed in the core of the Scotsburn anticline (Fig. 2) are volcanic and clastic rocks of the Fountain Lake Group (FLG). The Fountain Lake Group was subdivided by Donohoe and Wallace (1982) into two formations; the older Byers Brook Formation and the younger Diamond Brook Formation (Fig. 3). The former comprises mainly felsic rhyolite and tuff, whereas the latter consists of mostly mafic volcanic rocks (McKay Brook Member) and continental, red to grey sandstone, siltstone, and conglomerate (Nabiscumb Brook Member). These sedimentary rocks contain (possibly reworked?) Middle Devonian (Donohoe and Wallace, 1982) and Tournaisian spores (Utting et al., 1989). In the core of the Scotsburn anticline, mainly red sandstone and siltstone outcrop (Boehner et al., 1986), with minor mafic volcanic rocks south of the Scotsburn No. 2 well. These rocks were mapped as the McKay Brook Member. Rocks in the Scotsburn anticline, previously assigned to the Nabiscumb Brook Member, were dated as Viséan and were re-assigned to the Middleborough Formation of the Windsor Group (Ryan and Boehner, 1990). The total thickness of the Fountain Lake Group is estimated to be in excess of 5000 m (Donohoe and Wallace, 1985).

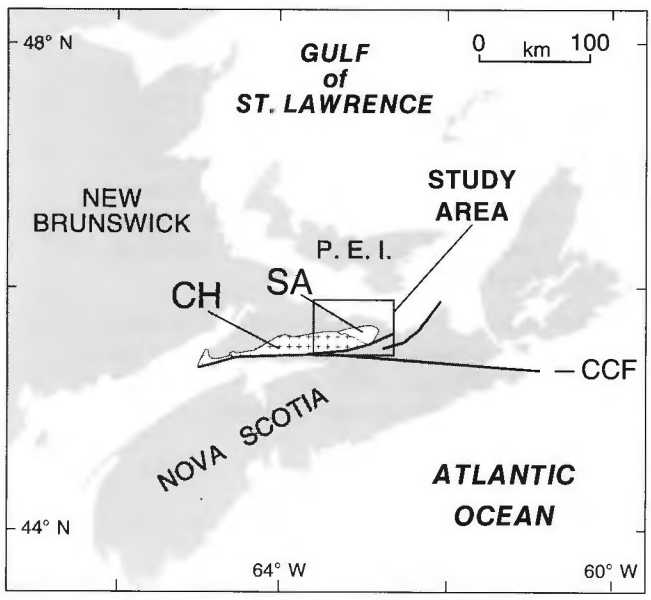

Figure 1. Map of the Maritime Provinces showing the location of the Cobequid Highlands (CH), the Scotsburn anticline (SA), the Cobequid-Chedabucto Fault (CCF) and the study area.

The most recent mapping of the uppermost contact of the Fountain Lake Group was completed by Ryan and Boehner (1990) and Chandler et al. (1994). The Fountain Lake Group is overlain by conglomeratic rocks of the Falls and Claremont formations (Fig. 2). They are distinguished on the basis of clast composition, with the former comprising dominantly basaltic clasts and the latter granitic clasts (Chandler et al., 1994). Yeo (1987) interpreted the Falls Formation to be Horton Group equivalent (Fig. 3). Seismic data on the east flank of the anticline show a bright reflection near the mapped base of the Claremont Formation. The reflection was correlated with Windsor Group reflections in Northumberland Strait (Durling, unpublished data). On the west side of the Scotsburn anticline, Donohoe and Wallace (1982) mapped all the conglomerate rocks as Falls Formation. Later, Ryan and Boehner (1990) mapped the same rocks as Claremont Formation. For this study, the Falls and Claremont formations were considered together as one unit.

SEISMIC REFLECTION DATA

Petroleum industry seismic reflection data were collected in the study area by Anschutz (Canada) Exploration in 1972 and by Chevron Canada Resources in 1980-81 (Fig. 2). All data are multi-channel, with the fold varying from 12 (Anschutz) to 24 (Chevron). Stack and migration copies of the data were available for the interpretation. The structural interpretation of the area was greatly improved through the use of migrated data, as the bedding dip in the area generally ranges from 20° to 50°, and locally many faults are present.

The entire Anschutz database was donated to the Geological Survey of Canada for research purposes. Most of the seismic lines were subsequently reprocessed (Marillier and Durling, 1995). The reprocessed sections, available in digital form, were interpreted using seismic interpretation software on a computer workstation. The Chevron data exist only in paper form. These were interpreted on paper, and the horizons were digitized and integrated with the digital data.

SEISMIC CHARACTER OF THE FOUNTAIN LAKE GROUP

Two Fountain Lake Group horizons were mapped within the study area; 1) the top of the Fountain Lake Group and 2) the top of the Fountain Lake Group volcanic rocks. These horizons correspond to the top of low amplitude and high amplitude seismic facies, respectively, on the seismic reflection profiles. Subsurface control on these horizons was provided by surface geological maps and reports, and the Irving-Chevron Scotsburn No. 2 well (Irving-Chevron, 1981).

Top of the Fountain Lake Group

The Falls and Claremont formations, being mostly conglomeratic rocks, are generally seismically transparent (Fig. 4). The contact between the Fountain Lake Group and the overlying rocks, where extrapolated from outcrop onto the seismic

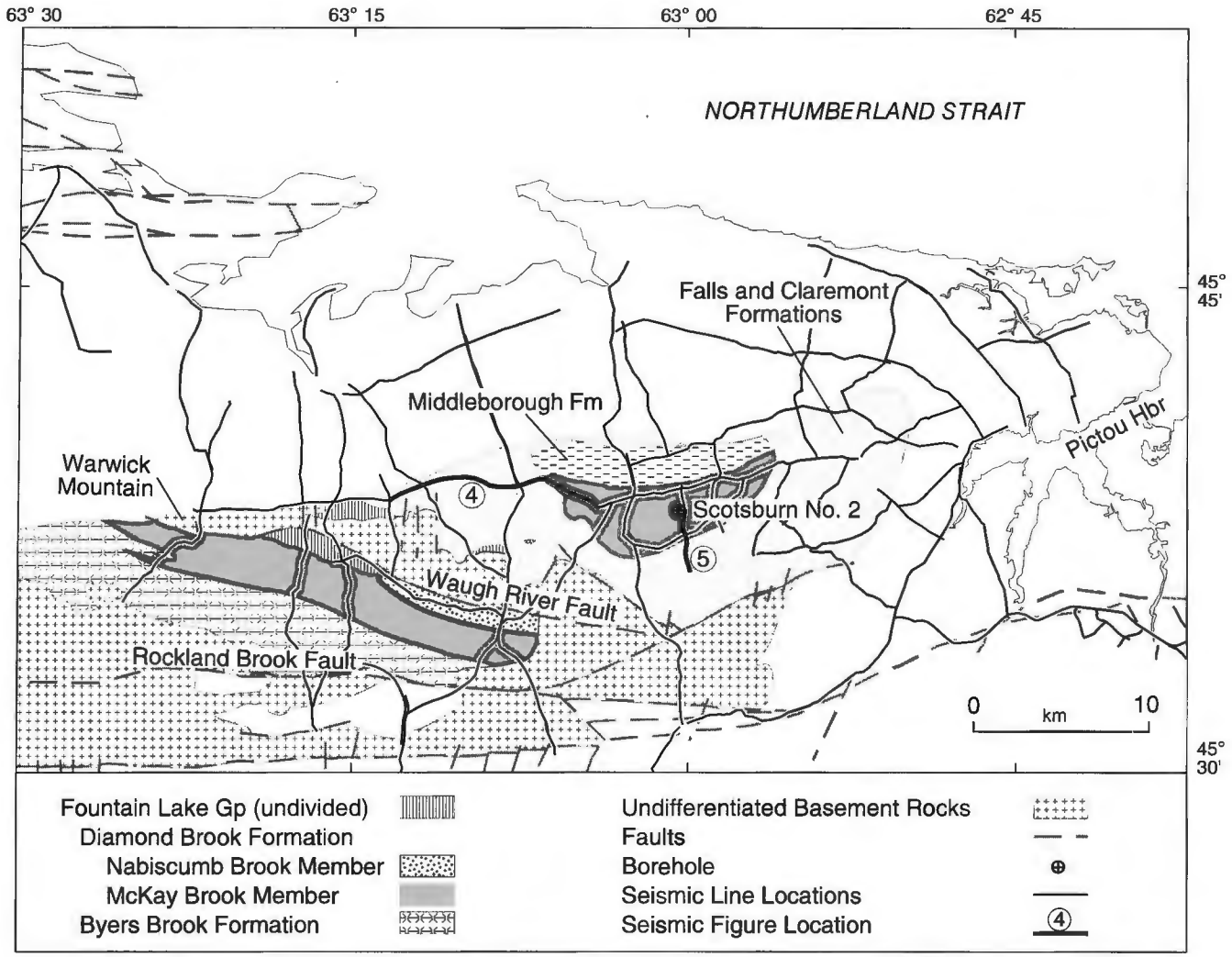

Figure 2. *Simplified geological map of the study area with the distribution of seismic reflection data superimposed. Geology compiled from Donohoe and Wallace (1982), Miller et al. (1989), Ryan and Boehner (1990), and Chandler et al. (1994).*

data, corresponds to a change in reflection character from a transparent zone (conglomerate) to low amplitude, discontinuous reflections (Fountain Lake Group). Due to their subdued seismic response, these rocks are referred to as the low amplitude seismic facies. They correspond to mapped outcrop of red sandstone and siltstone of the McKay Brook Member (Donohoe and Wallace, 1982).

The top of the Fountain Lake Group can only be identified on a few seismic profiles. Locally there is very little difference in seismic response between the low amplitude, Fountain Lake Group, seismic facies and the reflection free Falls and Claremont Formations. Consequently, a map of the top of Fountain Lake Group horizon was not made. Some qualitative observations were made on the thickness of the low amplitude seismic facies, from a combined interpretation using both the outcrop and seismic data. These data indicate that the low amplitude seismic facies is twice as thick to the west of the anticline than to the east. It is not clear whether these differences are due to erosion or non-deposition.

GROUP	FORMATION	MEMBER
Cumberland	Claremont	
Mabou	Middleborough	
?Horton	Falls	
Fountain Lake	Diamond Brook	Nabiscumb Brook
		McKay Brook
	Byers Brook	

Figure 3. *Simplified stratigraphy from the study area. No contact relationships implied. Compiled from Donohoe and Wallace (1982), Yeo (1987), Ryan and Boehner (1990), and Chandler et al. (1994).*

Top of Fountain Lake Group volcanic rocks

In the Scotsburn No. 2 well, mafic volcanic rocks, interbedded with minor red sandstone and siltstone, were encountered in the upper 625 m of the well (Fig. 5). These are underlain by felsic pyroclastic rocks, mafic volcanic rocks, and rhyolite, interbedded with minor clastic rocks. A synthetic seismogram from the well shows that these rocks give rise to numerous high amplitude reflections, which correlate favourably with the adjacent seismic profile (Fig. 5). These reflections comprise the high amplitude seismic facies of the Fountain Lake Group. The low amplitude seismic facies is imaged in the extreme upper left of Figure 5.

The high amplitude seismic facies of the Fountain Lake Group is made up of numerous, discontinuous reflections, among more continuous reflections. The continuous reflections may represent clastic units. Locally, stratigraphic discontinuities, such as downlap (Fig. 4), occur within the high amplitude seismic facies. The discontinuities occur at several stratigraphic levels, and an attempt was made to map them. Unfortunately, they could only be mapped for very short distances. For the most part, the high amplitude seismic facies is a monotonous sequence of discontinuous reflections, in which the regional correlation of individual seismic events is not possible.

The top of the high amplitude seismic facies can be traced with confidence throughout the study area (Fig. 6), mainly due to the dramatic difference in seismic response between it and the overlying rocks. This seismic marker was mapped in the sub-surface in an east-west direction for about 55 km and up to 17 km in a north-south direction. It was recognized in the subsurface as far south as the surface trace of the Waugh River Fault and the northeast extension of the Rockland Brook Fault.

STRUCTURE OF THE SCOTSBURN ANTICLINE

The "top of volcanics" horizon is defined by concentric, circular contours (Fig. 6). The contours emphasize that the Scotsburn anticline is a doubly plunging structure. The highest point on the anticline occurs near the Scotsburn No. 2 well, whereas the deepest point occurs in the extreme northeast of the study area. In this area, the "top of volcanics" horizon is about 2.9 s or 5800 m (based on an average seismic velocity of 4000 m/s).

The northern margin of the Scotsburn anticline is affected by numerous faults. Figure 6 shows a simplified interpretation of the distribution and orientation of the most significant faults. The correlation of specific faults from line to line is uncertain, but the interpreted northeasterly trend of the faults appears reasonable. Most of the faults appear to dip southerly, at moderate to steep angles, although some low angle faults were recognized. Many of the faults show an apparent reverse

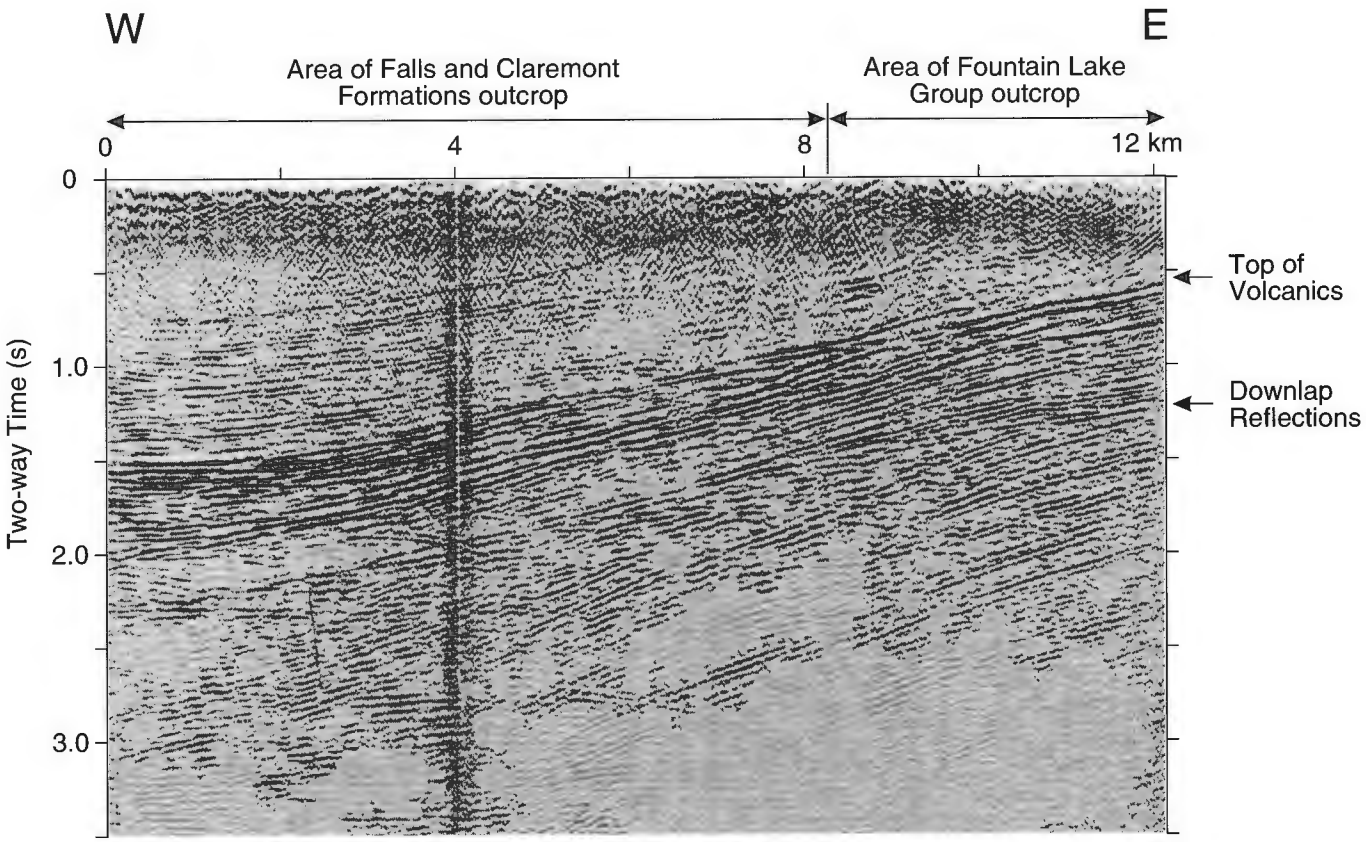

Figure 4. *Chevron seismic reflection profile 22. See Figure 2 for location.*

separation, based on the correlation of the "top of volcanics" horizon across individual faults. An upper limit on the age of the faulting is established by the Malagash Formation (Westphalian C-D; Ryan and Boehner, 1990), which is not affected by the faulting. The Malagash Formation is, however, folded. The youngest unit affected by the faulting is the Boss Point Formation (Late Namurian to Middle Westphalian A; Ryan and Boehner, 1990). This relationship was seen on only one seismic profile.

In the western part of the study area, the trend of the contours on the "top of volcanics" horizon changes from northeast to east. The shape of the structure also changes from that of an anticline to a monocline. The southern limb of the anticline appears to be faulted off along the surface trace of the Waugh River Fault. North of the Waugh River Fault, Precambrian and lower Paleozoic rocks belonging to the Warwick Mountain and Earltown formations, respectively, were mapped at the surface (Donohoe and Wallace, 1982). The distribution of these rocks with respect to contours on the "top of volcanics" seismic horizon is shown in Figure 6 (in light shading). These data show that older rocks overlie younger rocks, demonstrating the presence of previously unknown thrust faults. An Early Carboniferous age is suggested for this thrust faulting by syn-emplacement deformation of plutons (ca. 360 Ma; Pe-Piper and Koukouvelas, 1994) and the distribution of course clastic rocks (Falls Formation; Piper et al., 1996).

The southeastern margin of the Scotsburn anticline is the northeast extension of the Rockland Brook Fault (Miller et al., 1989). This fault was interpreted as a Precambrian-Cambrian, southeast dipping, thrust fault, which was re-activated during the Late Paleozoic (Miller et al., 1989). The Rockland Brook Fault was mapped through the Cobequid Highlands, but its northeastern extension in the Carboniferous sediments was not recognized (Yeo, 1987; Chandler et al., 1994). The southeasterly termination of the "top of volcanics" horizon clearly marks the location of a fault, interpreted here as the Rockland Brook Fault. Seismic profiles in the vicinity of Pictou Harbour show disrupted reflections suggesting significant faulting. Outcrop data in the same area record erratic bedding attitudes from the Malagash Formation (Chandler et al., 1994). These

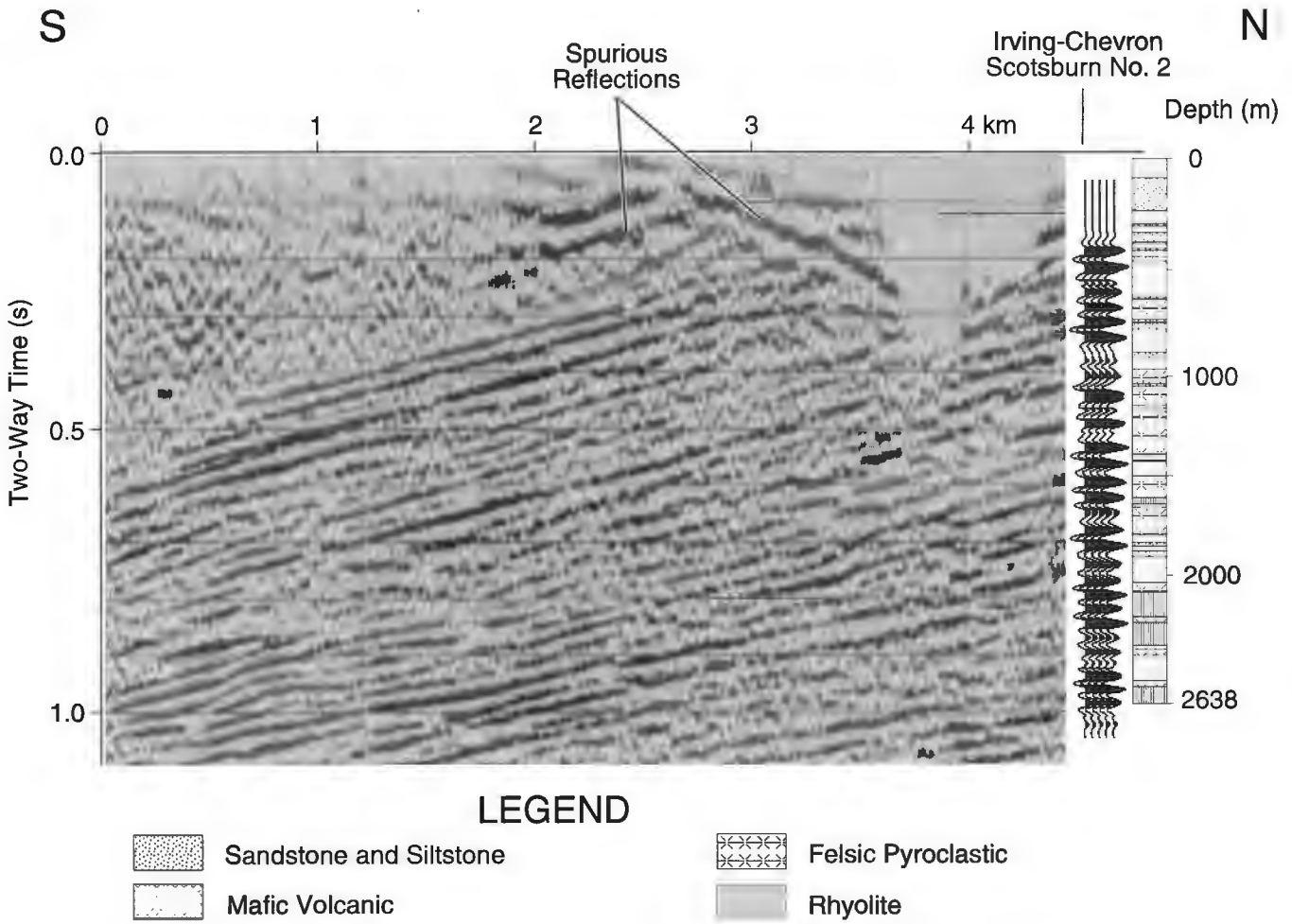

Figure 5. *Chevron seismic reflection profile 5, through the Irving-Chevron Scotsburn No. 2 well. The synthetic seismogram and the geology in the well were compiled from Irving-Chevron (1981). See figure 2 for location.*

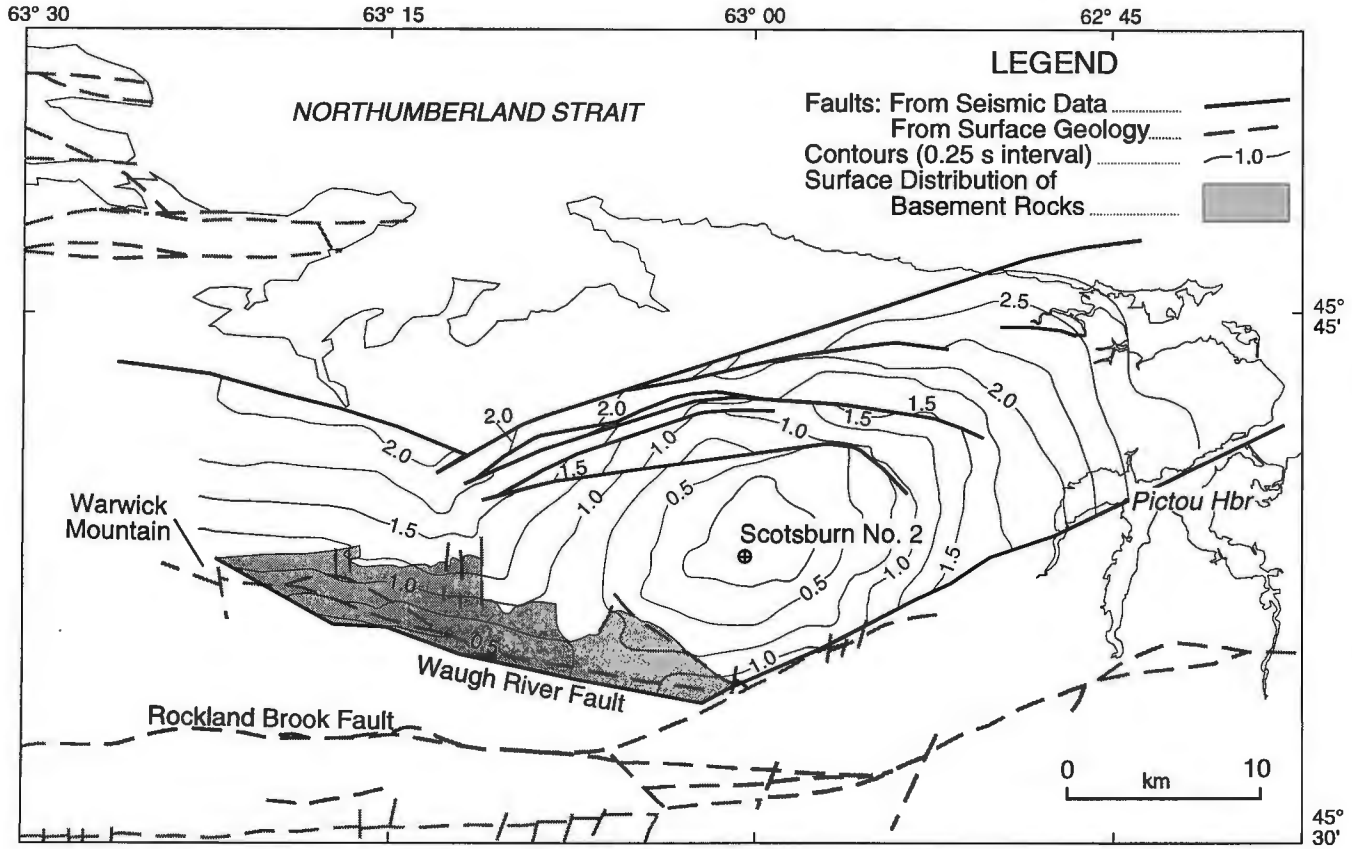

Figure 6. *Two-way time structure map of the top of the high amplitude seismic facies (top Fountain Lake Group volcanic rocks). Geology and scale as in Figure 2.*

data support the conclusions of Miller et al. (1989) that the northeast extension of the Rockland Brook Fault was active during the Late Carboniferous.

The east-striking, southerly dipping, thrust fault identified between the Fountain Lake Group and the Middleborough Formation (Donohoe and Wallace, 1982; Ryan and Boehner, 1990) was not recognized on the seismic reflection data. The fault was reported near the axis of the anticline, between the Middleborough Formation and the McKay Brook Member (Fig. 2). In this area, the "top of volcanics" horizon is near the surface (Fig. 6), and appears to be continuous through the location of the fault. If a fault is present between the Fountain Lake Group and the Middleborough Formation, as predicted by outcrop data, the fault involves minimal offset of the volcanic rocks.

CONCLUSIONS

A comparison of the seismic facies identified on the seismic reflection profiles with outcrop and well data in the Scotsburn anticline area suggests: 1) the low amplitude seismic facies corresponds to red sandstone and siltstone rocks presently mapped as part of the Diamond Brook Formation; 2) the high amplitude seismic facies corresponds to mafic and felsic volcanic rocks, assigned to the Diamond Brook and Byers Brook formations; and 3) seismic data cannot be used to subdivide the thick, Fountain Lake Group volcanic sequence.

The seismic reflection data were successfully used to map the distribution of the top of the Fountain Lake Group volcanic sequence in the Scotsburn anticline. The Fountain Lake Group reflections were mapped in the subsurface for 55 km in an east-west direction and up to 17 km in a north-south direction. In the vicinity of Warwick Mountain, Precambrian to Silurian rocks (Donohoe and Wallace, 1982) overlie Fountain Lake Group reflections, clearly demonstrating overthrust relationships. At present, the age of this overthrusting has not been deduced from the seismic data. Thrust faults on the northern margin of the Scotsburn anticline, which may or may not be related to the thrusting to the south, affects the Boss Point Formation but not the Malagash Formation.

ACKNOWLEDGMENTS

The quality of the seismic reflection database was greatly enhanced by the efforts of Pembina Resources Limited and Chevron Canada Resources, who provided digital field tapes and migrated stack sections, respectively, for this study.

Thanks are due to F. Marillier, D.J.W. Piper, G. Pe-Piper, J.W.F. Waldron, and P.S. Giles for stimulating discussions of the seismic interpretations.

REFERENCES

Boehner, R.C., Calder, J.H., Carter, D.C., Donohoe, H.V. Jr., Ferguson, L., Pickerill, R.K., and Ryan, R.J.
1986: Carboniferous-Jurassic sedimentation and tectonics: Minas, Cumberland and Moncton Basins, Nova Scotia and New Brunswick; Atlantic Geoscience Society, Special Publication Number 4, 122 p.

Chandler, F.W., Gall, Q., Gillis, K., Naylor, R., and Waldron, J.
1994: A progress report on the geology of the Stellarton Gap, Nova Scotia, including the Stellarton Coal Basin; in Current Research 1994-D; Geological Survey of Canada, p. 113-122.

Donohoe, H.V. and Wallace, P.I.
1982: Geological map of the Cobequid Highlands, Nova Scotia; Nova Scotia Department of Mines and Energy, scale 1:50 000.
1985: Repeated orogeny, faulting, and stratigraphy in the the Cobequid Highlands, Avalon Terrain of northern Nova Scotia; Geological Association of Canada/Mineralogical Association of Canada, Excursion 3, p. 77.

Irving Oil Limited and Chevron Standard Limited.
1981: Final well history, Scotsburn No. 2, Pictou County, Nova Scotia; Nova Scotia Department of Mines and Energy, Assessment Report 11E/10C 39-M-27(02), 26 p.

Marillier, F. and Durling, P.
1995: Preliminary results from reprocessing of seismic reflection data in the Cumberland Basin, Nova Scotia; in Current Research 1995-D; Geological Survey of Canada, p. 45-52.

Miller, B.V., Nance, R.D., and Murphy, J.B.
1989: Preliminary kinematic analysis of the Rockland Brook Fault, Cobequid Highlands, Nova Scotia; in Current Research, Part B; Geological Survey of Canada, Paper 89-1B, p. 7-14.

Pe-Piper, G. and Koukouvelas, I.
1994: Earliest Carboniferous plutonism, western Cobequid Highlands, Nova Scotia; in Current Research 1994-D; Geological Survey of Canada, p. 103-107.

Piper, D.J.W., Durling, P., and Pe-Piper, G.
1996: Field evidence for the extent and style of overthrusting along the northeastern margin of the Cobequid Highlands, Nova Scotia; in Current Research 1996-D; Geological Survey of Canada.

Ryan, R.J. and Boehner, R.C.
1990: Cumberland Basin geology map: Tatamagouche and Malagash; Nova Scotia Department of Mines and Energy, Map 90-14, scale 1:50 000.

Utting, J., Keppie, J.D., and Giles, P.S.
1989: Palynology and stratigraphy of the Lower Carboniferous Horton Group, Nova Scotia; in Contributions to Canadian Paleontology, Geological Survey of Canada, Bulletin 396, p. 117-143.

Yeo, G.M.
1987: Geological map of the New Glasgow-Tony River area (NTS 11E/10 and 11E/15s); Geological Survey of Canada, Open File Map 1656, scale 1:50 000.

Geological Survey of Canada Project 880032

Horton Group sedimentary rocks adjacent to the Cobequid Highlands, Nova Scotia[1]

David J.W. Piper
GSC Atlantic, Dartmouth

Piper, D.J.W., 1996: Horton Group sedimentary rocks adjacent to the Cobequid Highlands, Nova Scotia; in Current Research 1996-D; Geological Survey of Canada, p. 55-60.

Abstract: Sedimentary rocks coeval with the late Famennian-Tournaisian Horton Group occur in two basins, one on the northern and the other on the southern margin of the Cobequid Highlands. In both basins, Horton-equivalent rocks are steeply dipping and dismembered by later tectonism. In the northern Cobequid Highlands, the Fountain Lake Group consists of several kilometres of predominantly felsic volcanic rocks passing up into a thick sequence of mafic flows. Sediments interbedded with and overlying the mafic flows contain Tournaisian palynomorphs. This volcanism is younger than most other volcanic activity in the Magdalen basin. Sediments on the southern margin of the Cobequid Highlands contain Tournaisian palynomorphs only in the Nuttby Formation, but Horton-type sediment facies are widespread in units that commonly contain rhyolitic and granitic detritus and are cut by late granite veins and gabbro sheets. These sediments accumulated south of a basin margin defined by the Rockland Brook and Kirkhill faults.

Résumé : Des roches sédimentaires contemporaines du Groupe de Horton du Famennien tardif-Tournaisien s'observent dans deux bassins, dont l'un est situé sur la bordure nord et l'autre sur la bordure sud des hautes terres de Cobequid. Dans les deux bassins, les roches équivalentes au Groupe de Horton ont un pendage fort et sont morcelées par le tectonisme tardif. Sur la bordure nord des hautes terres de Cobequid, le Groupe de Fountain Lake se compose de plusieurs kilomètres de volcanites surtout felsiques, se transformant vers le haut en une séquence puissante de coulées mafiques. Les roches sédimentaires, interstratifiées avec les coulées mafiques et les surmontant, contiennent des palynomorphes tournaisiens. Ce volcanisme est plus récent que la plupart des autres épisodes volcaniques du bassin de la Madeleine. Sur la bordure sud des hautes terres de Cobequid, les roches sédimentaires ne contiennent des palynomorphes tournaisiens que dans la Formation de Nuttby; les faciès sédimentaires de type Horton sont cependant abondants dans les unités, qui renferment généralement des débris rhyolitiques et granitiques en plus d'être recoupées par des filons tardifs de granite et des feuillets de gabbro. Ces sédiments se sont accumulés au sud d'un bassin défini par les failles de Rockland Brook et de Kirkhill.

[1] Contribution to Canada-Nova Scotia Cooperation Agreement on Mineral Development (1992-1995), a subsidiary agreement under the Canada-Nova Scotia Economic and Regional Development Agreement.

INTRODUCTION

The Cobequid Highlands of northern Nova Scotia (Fig. 1) were the site of large igneous intrusions and associated volcanism at about the Devonian-Carboniferous boundary (Piper et al., 1993; Doig et al., in press). Magma was emplaced along faults of the Cobequid fault zone defining a flower structure and was emplaced coincident with rapid uplift and northward-directed thrusting (Pe-Piper and Koukouvelas, 1994). Several sedimentary rock units were associated with this igneous and deformational event, either being interbedded with volcanic rocks or containing igneous clasts and yet intruded by late igneous phases. The main plutonic igneous activity largely dates from 363 to 358 Ma (Doig et al., in press) but Nearing (1995) identified late igneous phases some 10 Ma younger.

Two main assemblages of Horton-age rocks are distinguished in the Cobequid Highlands. South of the Rockland Brook fault and its westward continuation in the Kirkhill fault, the rocks show facies similar to those in the type Horton Group of the Windsor sub-basin (e.g. Martel and Gibling, 1991). North of the Rockland Brook and Kirkhill faults, predominantly volcanic rocks of the Fountain Lake Group are widespread. They are geochemically similar to the main plutons of the Cobequid Highlands (Pe-Piper et al., 1991) and the upper part of the group (the Diamond Brook Formation) contains Tournaisian palynomorphs.

FACIES PRESENT

Several mappable sub-units characterized by particular sedimentary facies have been distinguished in probable Horton Group rocks of the Cobequid Highlands (Piper, 1994). These facies can be compared with those described by Martel and Gibling (1991) from the type Horton Group and Hamblin (1992) from Cape Breton Island. Brief descriptions and preliminary interpretations are presented, to provide a basis for the inventory of occurrences of Horton-age rocks presented below.

Terrestrial breccia

Terrestrial breccias are poorly sorted deposits of predominantly volcanic detritus in which original bedding is difficult to determine. The breccias in places pass up into sorted granule conglomerate and sandstone, red mudstone, thin limestone, and green siltstone. This facies is best known from the Fountain Lake Group of the northern Chignecto peninsula and is described in more detail by Piper et al. (in press).

Terrestrial conglomerate and sandstone

Thick bedded medium and coarse sandstone, in places cross-bedded, and conglomerate with scoured bases are interpreted as alluvial fan and fluvial sediments. They commonly interbed with minor red or grey mudstone and fine sandstone. These lithologies resemble the "Grey, medium grained sandstone to boulder conglomerate (fan delta)" facies assemblage of Hamblin (1992).

Lacustrine argillite and siltstone

This facies consists of grey to black mudstone containing variable numbers of siltstone laminae, ranging from <1 mm to several centimetres thick. In places, thin graded fine sandstone beds are found, which exceptionally show convolute lamination or Bouma sequences of turbidite structures. Locally, thin beds and nodules of dolomite are found. This facies resembles the "Dark grey mudstone (open lacustrine) facies" assemblage of Hamblin (1992) and the "Grey clayshale and claystone (Facies 1)" and in part the "Alternating sandstone, siltstone and claystone (Facies 2)" of Martel and Gibling (1991). This facies probably includes both deep and shallow water lacustrine sediments. Mudrocks tend to be much more indurated than in the type Horton area and palynomorphs are rarely well preserved, probably due to increasing thermal maturity towards the Cobequid fault zone (Utting and Hamblin, 1991).

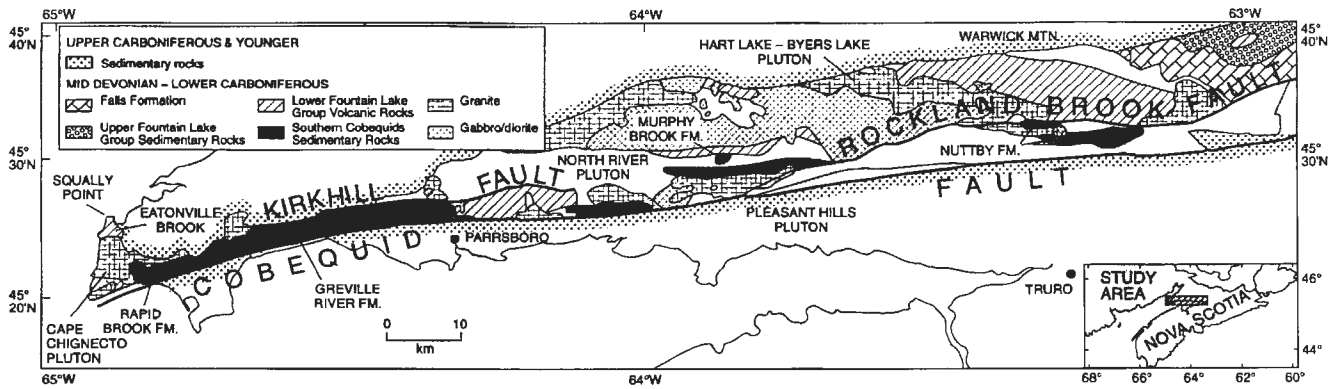

Figure 1. General geological map of the Cobequid Highlands showing distribution of probable Horton Group sedimentary rocks.

Lacustrine marginal sandstone

This facies consists of medium to thick bedded fine and medium sandstone, locally with thin beds of fine pebble conglomerate and pebbly sandstone. Coarsening- and thickening-up cycles are visible in places, with lacustrine argillite and siltstone underlying and purple-green terrestrial mudstone overlying this facies. The facies resembles the "Grey, very fine to fine-grained sandstone (nearshore/shoreline)" of Hamblin (1992).

Fluvial sandstone and grey siltstone

This facies consists of medium and fine sandstone, commonly crossbedded, interbedded with thick grey siltstone. Grey rip-up clasts occur in some sandstone units. These sediments are probably a subaerial delta plain facies. They differ from the lacustrine marginal sandstone in having channelled bases to thick beds and tending to have fining-up sandstone packets. This facies is less pebbly than the fan delta facies assemblage of Hamblin (1992).

Purple-green terrestrial mudstone

This facies includes mudstone and siltstone that range from purple to red to green, commonly interbedded with fine sandstone. Beds are commonly mottled, probably by rootlets or pedogenic concretions. This facies resembles the "Red siltstone to fine-grained sandstone (interdeltaic mudflat)" facies assemblage of Hamblin (1992). Parts of this facies resemble the "Green mudstone (Facies 3)" of Martel and Gibling (1991).

OCCURRENCES OF HORTON GROUP ROCKS

Introduction

A brief inventory of probable Horton Group rocks is presented below, describing facies present, style of deformation, evidence of age, and relationship to igneous phases.

South of Cape Chignecto pluton

Donohoe and Wallace (1982, 1985) mapped Rapid Brook Formation conglomerate and Greville River Formation sandstone south of the Cape Chignecto pluton, extending eastward to near Parrsboro. Piper (1994) showed that the two formations appeared to be lateral facies equivalents. The Rapid Brook Formation comprises principally terrestrial conglomerate including both undeformed and deformed plutonic clasts. The Greville River Formation comprises fluvial sandstone and grey siltstone and lacustrine black argillite with siltstone laminae. The rocks have been tightly folded and locally conglomerates are flattened. Conglomerate units contain granite and gabbro clasts derived from the Cape Chignecto pluton, which has yielded a U-Pb zircon age of 358 ± 2 Ma (Doig et al., in press). Minor pegmatitic granite veins cut lacustrine facies sediments northwest of Advocate. No palynomorphs have been recovered, but Donohoe and Wallace (1982) obtained indeterminate plant fossils.

North of Cape Chignecto pluton

Volcanic rocks of the Fountain Lake Group in the northern Chignecto peninsula are described in detail by Piper et al. (in press). Thin sedimentary rocks interbedded with the volcanic rocks include breccia, conglomerate, red and green siltstone, and limestone. Samples of sediment were barren of palynomorphs. Volcanic clast breccia and coarse sandstone unconformably overlie Fountain Lake Group east of Squally Point and is intruded by a gabbro dyke along a north-south wrench fault (Piper et al., in press). A small outcrop of conglomerate unconformably overlies Fountain Lake Group in Eatonville Brook (Piper, 1994).

South of North River pluton

Small fault slices of sedimentary rocks, mapped by Donohoe and Wallace (1982) as undivided Devonian-Carboniferous, outcrop in Harrington River and on Lynn Road, to the southwest of the North River pluton. Facies are lacustrine marginal sandstone and purple-green terrestrial mudstone. The sediments are cut by a microgranite dyke in Harrington River.

South of the North River pluton, in the East, Bass and North rivers area, rocks mapped by Donohoe and Wallace as undivided Devonian-Carboniferous and as Jeffers Group all show similar facies. They consist predominantly of lacustrine argillite and siltstone with some lacustrine marginal sandstones that are in places pebbly. Purple-green terrestrial mudstone is locally present. Just south of North River pluton in the Bass River area, granule conglomerate is interbedded with lacustrine argillite and siltstone. Clasts consist principally of quartz (<12 mm) with rare lithic fragments of volcanic rocks (<15 cm). A similar conglomerate along East River includes rare clasts of flow-banded rhyolite and granite. At the southern boundary of the unit in the Bass River area, lacustrine marginal sandstone facies is cut by granite veins. Along North River, lacustrine argillite and siltstone are cut by a fine granite phase at the southern contact with the North River pluton.

Murphy Brook Formation

The Murphy Brook Formation, north of the Pleasant Hills pluton, is in fault contact with Silurian Wilson Brook Formation and the Fountain Lake Group. Donohoe and Wallace (1982, 1985) obtained a mid-Devonian age from plant fossils. The facies in the Murphy Brook Formation, however, resemble those of the Horton equivalent rocks of the southern Cobequid Highlands and the abundant rhyolite clasts in conglomerate suggest that this formation is younger than the 363 Ma main igneous event of the Cobequid Highlands. The rocks dip gently to moderately southward and are locally cleaved. Two main facies are found. Angular pebble conglomerate consists largely of rhyolite clasts and is interbedded with minor coarse and medium sandstone. Grey shaly

siltstone and interbedded muddy sandstone are locally cut in the upper part of the formation by pebbly crossbedded medium sandstone, interpreted as a lacustrine delta plain sediment.

North of Pleasant Hills pluton

On the northern margin of the Pleasant Hills pluton is a cleaved, moderate to steeply dipping sediment unit comprising terrestrial conglomerate and sandstone and purple-green terrestrial mudstone (Piper, 1994). The sandstone contains common isolated pebbles of granite similar to the Pleasant Hills pluton. Conglomerate consists principally of rhyolite clasts. This unit is hornfelsed and intruded by fine grained granite dykes at the contact with the Pleasant Hills pluton.

An isolated area of outcrop north of Toad Lake (see Fig. 2 of Piper et al., 1996) consists of fissile grey siltstone, laminated fine sandstone, and macroscopic plant fragments that are of no biostratigraphic value (T. Taylor, pers. comm., 1994). This unit resembles sediments of the Murphy Brook Formation.

Nuttby Formation

The Nuttby Formation outcrops south of the Rockland Brook fault in North River, the Middle and West branches of North River, and in upper East Branch Chiganois River.

Donohoe and Wallace (1982) recorded Tournaisian palynomorphs from the North River area; a further Tournaisian sample has been found in the Middle Branch North River area (G. Dolby, pers. comm., 1995). All the sections of the Nuttby Formation are deformed, with steeply dipping rocks, common fold closures, and many faults. It is thus difficult to measure continuous stratigraphic sections. The deformed rocks are cut by large diabase-fine gabbro dykes that are metres to tens of metres thick and commonly have a moderate dip to the south.

Facies present in the Nuttby Formation include:

1. lacustrine argillite and siltstone, with rare graded fine sandstone beds. Locally, thickening and coarsening up sequences are present, passing up into lacustrine marginal sandstone. Some argillite and siltstone has calcareous nodules.
2. lacustrine marginal sandstone, in places in thickening- and coarsening-up sequences capped by red silty mudstone. The highest sandstone units are crossbedded and interbed with thin granule conglomerate.
3. purple-green terrestrial mudstone facies is rare, and includes red silty mudstone and interbedded medium sandstone. Caliche is locally found.
4. terrestrial sandstone and conglomerate, with thick bedded medium and coarse sandstone and locally fine pebble conglomerate in beds up to 2 m thick. Clasts are principally quartz, rhyolite, and foliated quartz sandstone. The conglomerate facies is coarsest and thickest in the northern part of the outcrop area.

In the North River area, cataclastically deformed Nuttby Formation is in apparent fault contact with late Precambrian granite (Pe-Piper et al., in press). The Nuttby Formation is cut by veins of very fine pink granite. This suggests minor fault-controlled igneous activity similar to that in the Bass River south of the North River pluton. In the West North River area, granite veins cut a gabbro that appears to intrude deformed Nuttby Formation.

Byers Brook Formation

Predominantly felsic volcanic rocks of the Byers Brook Formation in the northeastern Cobequid Highlands are interbedded with conglomerate, sandstone, and siltstone. Gower (1988) mapped a "marker" well-rounded pebble conglomerate interbedded with lacustrine siltstone in the area immediate east of Wentworth, stratigraphically in the middle of the Byers Brook Formation. Our mapping suggests that this unit can be traced eastward to near Earltown. Most sediments interbedded with pyroclastic rocks are poorly sorted conglomerate, pebbly coarse to medium sandstone and red mudstone.

The voluminous felsic rocks of the Byers Brook Formation probably correlate with the main emplacement of the geochemically similar granite plutons at 363-358 Ma (Doig et al., in press). On the basis of the 353 ± 4 Ma age for the Devonian-Carboniferous boundary (Claoué-Long et al., 1992), this correlates with the mid to late Famennian and immediately predates deposition of the type Horton Group. The lack of thick felsic ash deposits in the type Horton Group is consistent with this age for the Byers Brook Formation.

McKay Brook member of the Diamond Brook Formation

The McKay Brook member consists principally of basalt flows, with minor interbedded sediment. Donohoe and Wallace (1982) obtained both Tournaisian and middle Devonian palynomorphs from siltstone in Macdonald Brook west of Earltown, suggesting that the middle Devonian taxa were reworked. Utting et al. (1989) obtained Tournaisian palynomorphs from the upper part of the McKay Brook member in the Scotsburn #2 well.

The principal sediments interbedded with basalt flows are reddish poorly sorted siltstone and mudstone. Less commonly, red or grey medium and fine sandstone is interbedded with basalt. Pebble conglomerate, with principally rhyolite and some basalt clasts, is found locally. Along Macdonald Brook, a sedimentary unit >10 m thick interbeds with basalt. It consists of grey fine sandstone and silty mudstone, fine pebble conglomerate, red mudstone, and crossbedded medium and coarse litharenite. Facies are interpreted as fluvial and possibly lacustrine.

Nabiscumb Brook member of the Diamond Brook Formation

Sedimentary rocks interbed with and overlie basalt flows in the upper part of the Diamond Brook Formation in the Waugh River valley northwest of Earltown and in the Scotsburn anticline. In the southern part of the Scotsburn anticline, poorly sorted pebble conglomerate, medium and fine sandstone, and minor red mudstone are interbedded with rare basalt flows. Coarser sandstone and conglomerate have scoured bases to beds and are commonly crossbedded. In the axis of the anticline and on its northern limb, purple and grey silty mudstone units predominate, with interbedded fine and medium sandstone and rare basalt flows. Coarser sandstone beds have scoured bases and contain rare pebbles and caliche intraclasts. Paleocurrents were generally to the north. The Falls Formation, consisting of medium and coarse red conglomerate and minor interbedded sandstone, may overlie the Nabiscumb Brook member conformably; no field evidence for an unconformity was found.

In the Waugh River valley northwest of Earltown, the Nabiscumb Brook member consists of fining-up sequences of red fine pebble conglomerate and sandstone interbedded with red siltstone and mudstone. Caliche pebbles are present in the conglomerate.

DISCUSSION AND CONCLUSIONS

The Nuttby Formation contains Tournaisian palynomorphs. Other Horton-like sediment units in the southern Cobequid Highlands have not yielded useable palynomorphs. Nevertheless, all have sediment facies that resemble those of the Horton Group of the Windsor and Ainslie sub-basins. Conglomerate units all contain rhyolite clasts and in several units granite clasts are also present, suggesting an age younger than the main 363-358 Ma igneous event of the Cobequid Highlands. All the Horton-like units of the southern Cobequid Highlands are tightly folded and steeply dipping, and are commonly cleaved. This deformation style is typical of major strike-slip shear zones. Significant vertical motion on the major faults is indicated by the rapid unroofing of granite. Near major faults, minor fine granite intrusions cut the Horton-like sediments. In several areas, particularly the Nuttby Formation, sediments are cut by gabbro sheets. In the Nuttby Formation, these sheets appear to post-date folding. Regionally, mafic dykes cut Horton sediments in several localities in Nova Scotia, but dykes cutting Windsor or younger rocks are rare or absent. The coarsest conglomerate in the Horton Group of the southern Cobequid Highlands is found closest to the Rockland Brook and Kirkhill faults, suggesting that these faults may have formed the northern margin of the Windsor sub-basin.

In the northern Cobequid Highlands, the Fountain Lake Group volcanic rocks are partly older than and partly coeval with the type Horton Group. Sediments interbedded with the main volcanic sequence are principally alluvial or fluvial, although there is local evidence of lacustrine conditions. Except in the Scotsburn anticline, the Fountain Lake Group is steeply dipping and probably tightly folded. It is locally cut by diabase dykes and some larger mafic and intermediate intrusions. In the Scotsburn anticline, fluvial sediments overlying the main volcanic succession show a rapid facies change northward, suggesting derivation from a nearby basin margin (perhaps marked by the northeast continuation of the Rockland Brook fault). The Falls Formation, representing detritus from a thrust block in the northeastern Cobequid Highlands, is also probably of Horton age (Piper et al., 1996). The Tournaisian volcanism of the Diamond Brook Formation is significantly younger than the mid-to late-Devonian volcanism of the Antigonish area and western Cape Breton Island (Blanchard et al., 1984).

REFERENCES

Blanchard, M.-C., Jamieson, R.A., and More, E.B.
1984: Late Devonian-Early Carboniferous volcanism in western Cape Breton Island, Nova Scotia; Canadian Journal of Earth Sciences, v. 21, p. 762-774.

Claoué-Long, J.C., Jones, P.L., Roberts, J., and Maxwell, S.
1992: The numerical age of the Devonian-Carboniferous boundary; Geological Magazine, v. 129, p. 281-291.

Doig, R., Murphy, J.B., Pe-Piper, G., and Piper, D.J.W.
in press: U-Pb geochronology of late Paleozoic plutons, Cobequid Highlands, Nova Scotia, Canada: evidence for late Devonian emplacement adjacent to the Meguma-Avalon terrane boundary in the Canadian Appalachians; Geological Journal.

Donohoe, H.V. and Wallace, P.I.
1982: Geological map of the Cobequid Highlands, Nova Scotia; Nova Scotia Department of Mines and Energy, Map 82-09, scale 1:50 000, 4 sheets.

Donohoe, H.V., Jr. and Wallace, P.I.
1985: Repeated orogeny, faulting and stratigraphy of the Cobequid Highlands, Avalon Terrane of northern Nova Scotia. Geological Association of Canada - Mineralogical Association of Canada Joint Annual Meeting, Fredericton, New Brunswick, Guidebook 3, 77 p.

Gower, D.P.
1988: Geology and genesis of uranium mineralisation in subaerial felsic volcanic rocks of the Byers Brook Formation and the comagmatic Hart Lake granite, Wentworth area, Cobequid Highlands, Nova Scotia; MSc. thesis, Memorial University of Newfoundland, St. John's, Newfoundland, 357 p.

Hamblin, A.P.
1992: Half-graben lacustrine sedimentary rocks of the lower Carboniferous Strathlorne Formation, Horton Group, Cape Breton Island, Nova Scotia, Canada; Sedimentology, v. 39, p. 263-284.

Martel, A.T. and Gibling, M.R.
1991: Wave-dominated lacustrine facies and tectonically controlled cyclicity in the Lower Carboniferous Horton Bluff Formation, Nova Scotia, Canada; Special Publications of the International Association of Sedimentologists, no. 13, p. 223-243.

Martel, A.T., McGregor, D.C., and Utting, J.
1993: Stratigraphic significance of Upper Devonian and Lower Carboniferous miospores from the type area of the Horton Group, Nova Scotia; Canadian Journal of Earth Sciences, v. 30, p. 1091-1098.

Nearing, J.D.
1995: Thermochronologic evolution of the Cobequid Highlands, Nova Scotia (Abstract); Atlantic Geoscience Society Annual Meeting, Antigonish, February 1995, p. 22.

Pe-Piper, G., Piper, D.J.W., and Clerk, S.B.
1991: Persistent mafic igneous activity in an A-type granite pluton, Cobequid Highlands, Nova Scotia; Canadian Journal of Earth Sciences, v. 28, p. 1058-1072.

Pe-Piper, G. and Koukouvelas, I.
1994: Earliest Carboniferous plutonism, western Cobequid Highlands, Nova Scotia; in Current Research 1994-D; Geological Survey of Canada, p. 103-107.

Piper, D.J.W.
1994: Late Devonian-earliest Carboniferous basin formation and relationship to plutonism, Cobequid Highlands, Nova Scotia; in Current Research 1994-D; Geological Survey of Canada, p. 109-112.

Piper, D.J.W., Durling, P., and Pe-Piper, G.
1996: Field evidence for the extent and style of overthrusting along the northeastern margin of the Cobequid Highlands, Nova Scotia; in Current Research 1996-D; Geological Survey of Canada.

Piper, D.J.W., Pe-Piper, G., and Loncarevic, B.D.
1993: Devonian-Carboniferous deformation and igneous intrusion in the Cobequid Highlands; Atlantic Geology, v. 29, p. 219-232.

Piper, D.J.W., Pe-Piper, G., and Pass, D.J.
in press: The early Carboniferous volcanic rocks of the northern Chignecto peninsula, Cobequid Highlands, Nova Scotia; Atlantic Geology.

Utting, J. and Hamblin, A.P.
1991: Thermal maturity of the Lower Carboniferous Horton Group, Nova Scotia; International Journal of Coal Geology, v. 19, p. 439-456.

Utting, J., Keppie, J.D., and Giles, P.S.
1989: Palynology and stratigraphy of the Lower Carboniferous Horton Group, Nova Scotia; Geological Survey of Canada, Bulletin 396, p. 117-143.

Geological Survey of Canada Project 920062

The distribution and features of the Spruce Lake Formation, Tetagouche Group, New Brunswick[1]

Neil Rogers and Cees van Staal
Continental Geoscience Division, Ottawa

Rogers, N. and van Staal, C., 1996: The distribution and features of the Spruce Lake Formation, Tetagouche Group, New Brunswick; in Current Research 1996-D; Geological Survey of Canada, p. 61-69.

Abstract: Detailed geological and geochemical investigations of the bimodal felsic and mafic volcanic rocks that formed early in the Middle Ordovician Tetagouche Group extensional submarine basin have led to the recognition of the Spruce Lake Formation. The felsic volcanic rocks are predominantly feldspar-phyric, largely dacitic effusive flows and cryptodomes and co-eruptive pyroclastic deposits. These rocks are interbedded with lenses of pillow basalts of the Forty Mile tholeiite suite. As chemically similar basalts also occur in the younger Flat Landing Brook Formation, a further chemical discrimination is proposed based on the original feldspar composition.

Several massive sulphide deposits occur in the Orvan Brook porphyry member of the Spruce Lake Formation. These massive sulphide deposits are thought to have formed from synvolcanic hydrothermal systems, in reducing, relatively deep marine conditions. The current distribution of deposits is due to the interplay of intense deformation and erosion.

Résumé : Ce sont des analyses géologiques et géochimiques détaillées des volcanites felsiques et mafiques bimodales formées dès le début du bassin sous-marin d'expansion associé au Groupe de Tetagouche de l'Ordovicien moyen, qui ont permis de délimiter la Formation de Spruce Lake. Les volcanites felsiques sont surtout des coulées effusives et des cryptodômes essentiellement dacitiques à phénocristaux de feldspath et des dépôts pyroclastiques co-éruptifs. Ces roches sont interstratifiées avec des lentilles de basalte coussiné de la suite tholéiitique de Forty Mile. Étant donné que des basaltes de composition chimique semblable sont également présents dans la Formation de Flat Landing Brook plus récente, on propose une discrimination chimique plus poussée en se basant sur la composition originelle en feldspath.

Plusieurs gisements de sulfures massifs sont situés dans le membre porphyrique d'Orvan Brook de la Formation de Spruce Lake. Ils auraient été mis en place à partir de systèmes hydrothermaux synvolcaniques, dans des conditions marines réductrices d'eau relativement profonde. La répartition actuelle des gisements est due à l'interaction d'une déformation intense et de processus d'érosion accentués.

[1] Contribution to the Canada 1994-1999 Bathurst Mining Camp, Canada-Brunswick Exploration and Science and Technology (EXTECH II) Initiative.

INTRODUCTION

The Spruce Lake Formation (informally called the Caribou Mine Formation by Rogers, 1994, 1995) is one of several felsic volcanic dominated formations that occur within the Tetagouche Group of northern New Brunswick (Fig. 1). The Spruce Lake Formation hosts several massive sulphide deposits, including the economically important Caribou orebody. Herein we summarize and describe the lithologies present in the Spruce Lake Formation and document their relationships with the massive sulphide deposits. The structural/stratigraphic relationships between the Spruce Lake Formation and adjacent parts of the Tetagouche Group, particularly the Canoe Landing Lake Formation (van Staal and Fyffe, 1991) are also discussed.

The Spruce Lake Formation was first recognized following a study of the physical and chemical characteristics of the felsic volcanic rocks of the Tetagouche Group. Immobile element chemistry provided a "window" through the pervasive deformation, enabling the recognition of the distinctive features of each of the individual felsic volcanic units (Rogers, 1994). Chemically, the Spruce Lake Formation is primarily distinguished from the other felsic volcanic rocks in the Tetagouche Group by its relatively high Y/Zr ratio (Fig. 2).

GEOLOGICAL SETTING

The Tetagouche Group consists dominantly of mafic and felsic volcanic rocks which are interbedded with subordinate sedimentary rocks. Within the Spruce Lake Formation, the sediments are largely bluish-black shales, although red shale and chert layers are locally common. The Tetagouche Group lies disconformably upon the clastic sediments of the Lower Ordovician Miramichi Group (van Staal and Fyffe, 1991) and consists of several, generally northwardly younging, major imbricate thrust sheets (van Staal et al., 1991). In addition to the Spruce Lake Formation, eight other formations and a complex have been defined in the Tetagouche Group (van Staal and Fyffe, 1991; van Staal et al., 1992; Fyffe, 1994; Langton, 1994; Wilson, 1994). These are (i) the Patrick Brook Formation, which consists of dark grey sandstones, characterized by abundant volcanic quartz phenoclasts, interlayered with black shales; (ii) the Vallée Lourdes Formation, comprising greenish grey siltstone interbedded with calcareous sandstone and minor polymictic conglomerate; (iii) the Canoe Landing Lake Formation, which consists of two distinct basaltic suites (the Canoe Landing Lake alkali basalts and the structurally overlying Nine Mile Brook tholeiites); (iv) the Nepisiguit Falls Formation, that consisting of a dacitic to rhyolitic suite of largely pyroclastic quartz-feldspar porphyries; (v) the Clearwater Stream Formation, which is described

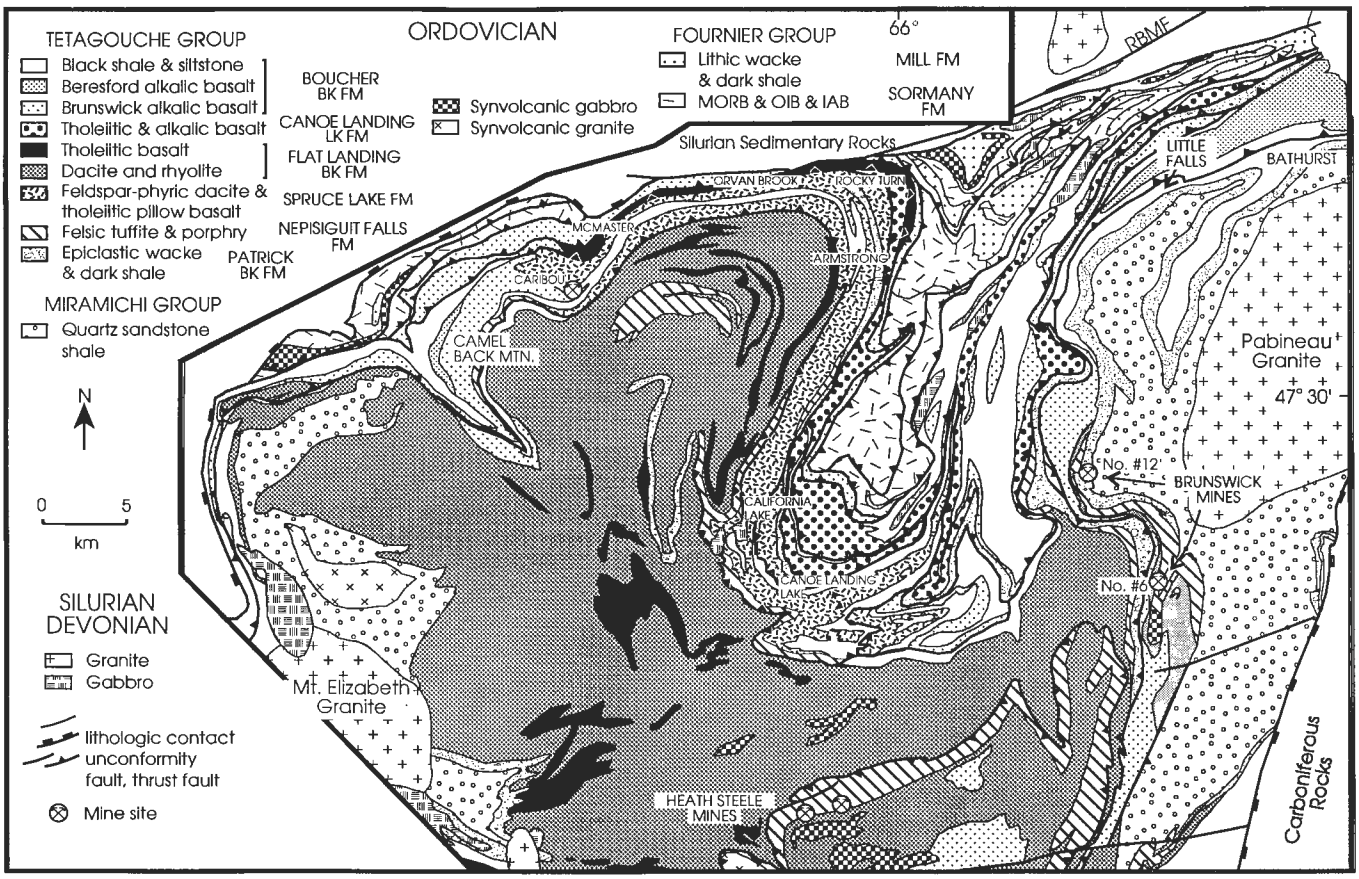

Figure 1. *General geology of the Bathurst camp, New Brunswick.*

as feldspar-phyric felsic pyroclastic rocks; (vi) the Flat Landing Brook Formation, a regionally extensive unit of very sparsely feldspar-phyric eruptive felsic volcanics (vii) the Boucher Brook Formation, thinly bedded, dark grey to black, feldspathic siltstone/shale rhythmites grading upward into a black shale and chert; (viii) the Tomogonops Formation, very low grade calcareous clastic sediments which have been interpeted to be a Late Ordovician flysch; and (ix) the Stony Brook Complex, a suite of feldspar-phyric felsic volcanic flows and subvolcanic intrusions. The age relationships of these formations are not completely understood at present. However the volcanic rocks of the Nepisiguit Falls, Stony Brook, Clearwater Stream, and Canoe Landing Lake formations are thought to have erupted contemporaneously with the Spruce Lake Formation at ca. 470 Ma (Sullivan and van Staal, 1993), whilst the Flat Landing Brook Formation is slightly younger (Sullivan and van Staal, 1990; Lentz and van Staal, 1995).

Deformation was polyphase and complex (van Staal and Williams, 1984). The D_1 and D_2 involved thrusting and tight to isoclinal folding, which produced a strong composite $S_{1/2}$ foliation parallel to bedding. Most of the large scale open folds are D_4 structures. The D_1 deformation was accompanied by low-grade regional metamorphism, dated at 447 ± 6 Ma (van Staal et al., 1990). The metamorphic grade increases towards the southwest of the Bathurst mining camp.

FELSIC VOLCANIC ROCKS

The felsic volcanic rocks of the Spruce Lake Formation have been divided into four members based on chemical and petrographic variations. Three of these members are dominated by feldspar-phyric porphyries that likely were emplaced as submarine extrusive flows and cryptodomes (Rogers, 1995) and subordinate pyroclastic units and rare epiclastic sandstones. The pyroclastic rocks are recognizable within all three of the feldspar-phyric members, and therefore, probably formed as co-eruptive deposits with the effusive flows. The majority of the pyroclastic rocks are coarse volcanic breccias containing up to boulder size clasts largely comprised of feldspar-phyric felsic volcanic rocks typical of the Spruce Lake Formation. However, rare aphyric felsic volcanic and basalt clasts are also present locally. Most of the aphyric felsic volcanic clasts are derived from contemporary ash deposits (described below); however some are clearly rhyolites. The source of these rhyolite clasts is not known as aphyric rhyolites are only recognized within the younger Flat Landing Brook Formation. Rare aphyric rhyolites have recently been identified in thrust sheets that otherwise wholly comprise Spruce Lake Formation, suggesting that these are indeed part of the Spruce Lake Formation. However, the chemical affinities of these rocks have not yet been determined. The ashes occur as a sequence of very fine grained, water lain, volcanically derived, light silvery green rocks, which typically occur towards the top of (and are possibly laterally equivalent to) the Spruce Lake Formation. Locally, such sediments occur as rip-up clasts in the effusive flows (Fig. 3), which provides evidence of contemporaneous deposition.

When the deformation state is low, the feldspar porphyries can be recognized by the distribution, shape, and abundance of the phenocrysts (Rogers, 1995). The potassium-feldspar phenocrysts are generally euhedral to subhedral, pseudomorphed to metamorphic microcline, and reach a maximum length of 10 mm (Fig. 4). These phenocrysts originally were sodium-rich sanidine, with simple twinning, and have been altered and transformed into chess-board albites and/or patch perthites. Feldspar microphenocrysts are anhedral and constitute up to 20% of the rock by volume. The Orvan Brook porphyry member is readily identified by its distinctive high concentration of opaque pseudomorphs after biotite (Fig. 5). The groundmass is a lower greenschist assemblage of feldspar, quartz, chlorite, muscovite, stilpnomelane, and/or biotite. Phengitic muscovite and stilpnomelane are the principal

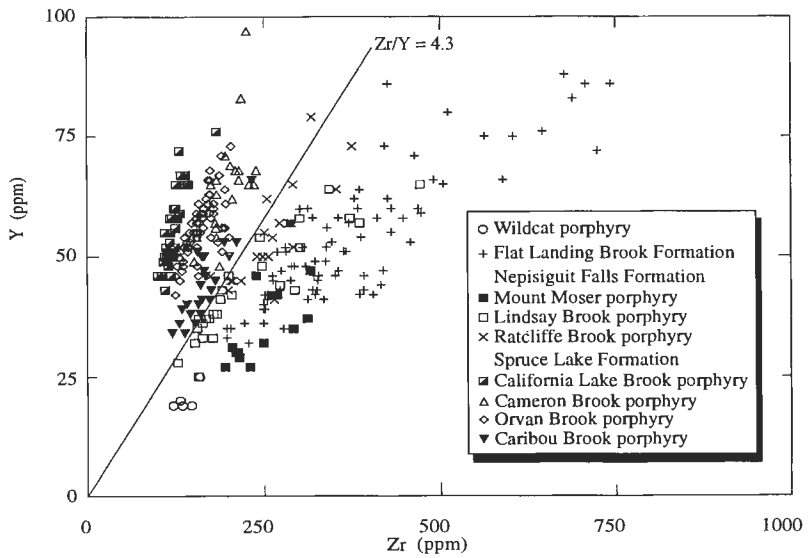

Figure 2.

Y-Zr discrimination plot for the Tetagouche Group felsic volcanic rocks.

phyllosilicates below the biotite isograd. The presence of phengite gives the rocks a very typically bright green colour and soapy lustre.

A quartz-feldspar porphyry informally referred to as the Caribou Brook porphyry has tentatively been included in the Spruce Lake Formation, as it occurs with the feldspar porphyries and has petrographic and chemical affinities with the Orvan Brook porphyry. It is petrographically very similar to the feldspar porphyries, except that it also has a quartz phenocryst phase. The quartz phenocryst content is highly variable, ranging from about 10% by volume to less than 1%; this variability is probably due to resorption, as abundant embayments in the quartz phenocrysts indicate that this process was common (Fig. 6). Tamura (1995) has shown that quartz can be resorbed during fractionation from dacite as a result of a liquidus boundary shift caused by the addition of H_2O. The volcanic rocks of the Spruce Lake Formation plot in the field of dacite and rhyodacite (Fig. 7). They have the highest Y/ZR ratios (>4.3, Fig. 2) of all the felsic volcanic rocks in the Tetagouche Group and are best discriminated on the TiO_2-Zr plot (Fig. 8).

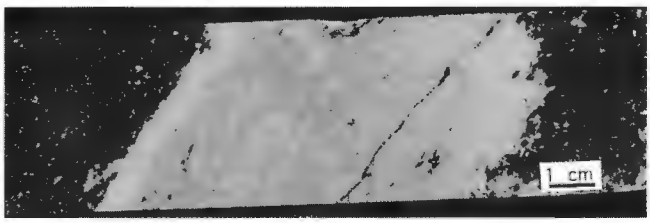

Figure 3. Rip-up clast of unconsolidated felsic volcanic ash within a feldspar-phyric flow or cryptodome. Sample taken from drill-core structurally above the Nepisiguit massive sulphide deposit.

Figure 4. Typical Spruce Lake Formation feldspar porphyry.

Rare narrow bands of tuffaceous feldspar porphyry, which are chemically and petrologically similar to the Orvan Brook porphyry, are intercalated with the alkali and tholeiitic pillow basalts of the Canoe Landing Lake Formation. Therefore, the Canoe Landing Lake Formation is a time-stratigraphic (i.e. lateral facies) equivalent to the Spruce Lake Formation and was deposited in relatively close proximity to the Spruce Lake volcanic centre. The time-equivalence is confirmed by a U-Pb zircon age of 470 +4/-2 Ma for the feldspar-phyric tuff (Sullivan and van Staal, 1993) and 470 ± 5 Ma for the Orvan Brook porphyry (R.W. Sullivan, pers. comm., 1995).

MAFIC VOLCANIC ROCKS

The mafic volcanic rocks of the Spruce Lake Formation are subordinate to the felsic volcanic rocks and generally occur as boudinaged lenses of pillow basalt and diabase within them (Fig. 9). This indicates that the bulk of volcanism in the Spruce Lake Formation took place subaqueously. These basalts and diabases were previously grouped in the Forty Mile tholeiite suite along with other basaltic rocks that are present locally in the Canoe Landing Lake and Flat Landing Brook formations, on basis of their Cr-Nb/Y distribution (Fig. 10). However, recent field studies and U-Pb age

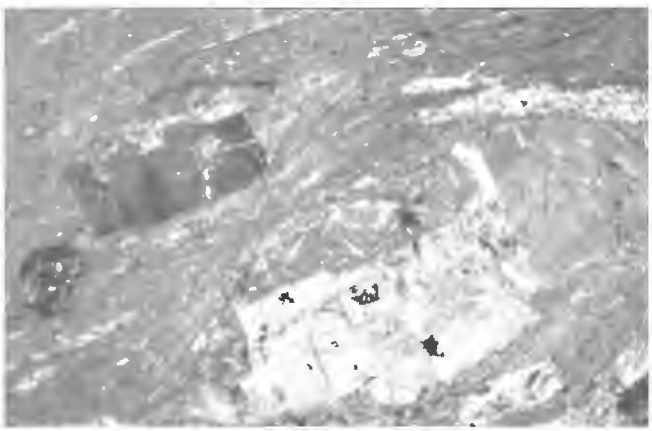

Figure 5. *Orvan Brook porphyry. Potassium feldspar phenocrysts plus occasional pseudomorphs after biotite (left centre of the photomicrograph).*

Figure 6. *Caribou Brook porphyry. Note the strongly embayed quartz phenocryst and similarities to the Orvan Brook porphyry, including the presence of psuedomorphs after biotite.*

determinations have shown that the Forty Mile tholeiites must have erupted at different time intervals in both the Spruce Lake and Flat Landing Brook formations. Preliminary investigations have shown that the tholeiites of the older Spruce Lake Formation rocks can be discriminated by their high Rb-CaO ratio (Fig. 11). The total alkalis exhibit similar relationships to Rb, implying that the difference is related to modal feldspar composition. In addition, the Forty Mile tholeiites in the Spruce Lake Formation have diopside in the CIPW norm, whereas those in the Flat Landing Brook formation have none. However, as all of the elements involved in the above discrimination are potentially extremely mobile, more data is required before these relationships can be confirmed.

SPRUCE LAKE FORMATION MASSIVE SULPHIDE DEPOSITS

There is a spatial relationship between the Orvan Brook porphyry and the massive sulphide deposits that occur within the Spruce Lake Formation (Rogers, 1994). These deposits include Caribou, McMaster, Orvan Brook, Rocky Turn, California Lake, and the Armstrong A, B, and C (Fig. 1). These deposits now occupy different structural levels, although their spatial relationship to the Orvan Brook porphyry implies that they must occur at approximately the same stratigraphic position. Barren jasper- and hematite-bearing sediments also occur within the Spruce Lake Formation, although they are not directly associated with the massive

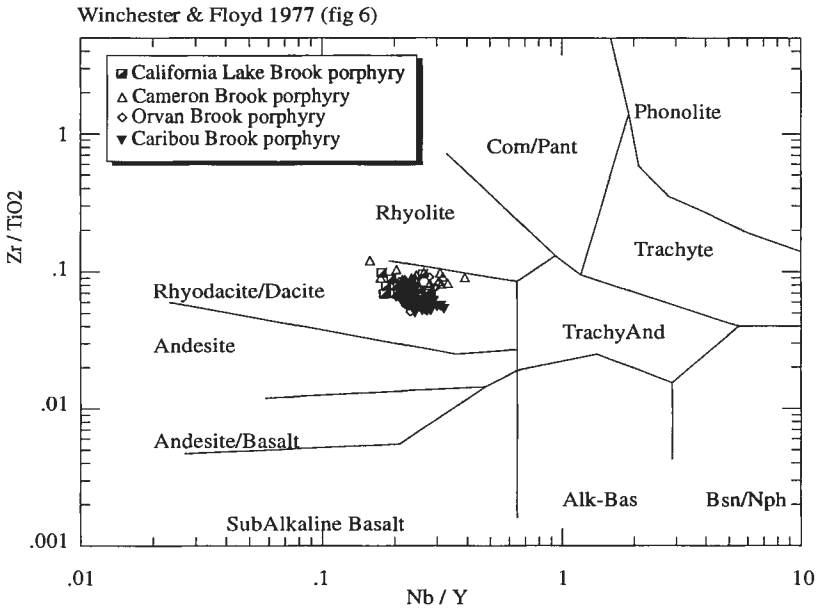

Figure 7.

Nb/Y-Zr/TiO_2 immobile element rock type discrimination plot. After Winchester and Floyd (1977).

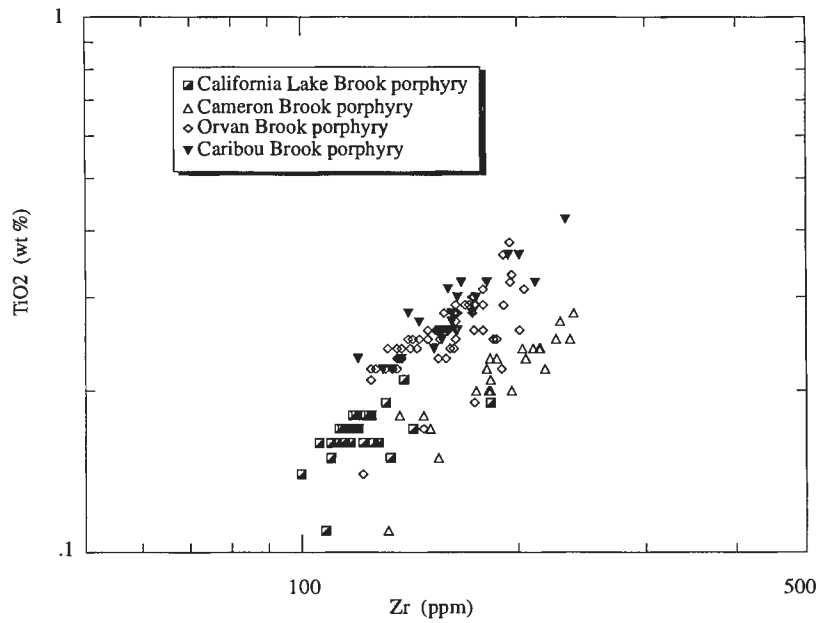

Figure 8.

Zr-TiO_2 discrimination plot for the Spruce Lake Formation.

sulphides. This is in contrast to the Brunswick-type massive sulphide deposits, which are spatially and temporally related to such sediments (van Staal et al., 1992).

Relationships at the Caribou deposit

The Caribou massive sulphide orebody consist of several en-echelon lenses which generally taper out on both ends. Several of these are connected by asymmetrical fold-like structures; Davies (1972) thought that these lenses were originally connected and were subsequently separated by attenuation of the short limbs of s-shaped isoclinal F_1 folds. Our structural investigations support his geometrical interpretations since (i) small-scale examples of such structures occur in and around the Caribou deposit; (ii) the original continuity of some en-echelon lenses can still be traced by a ghost stratigraphy of isolated very narrow sulphide bodies, which probably represent boudins; and (iii) the isoclinal to tight folds have a consistent s-shaped asymmetry (Fig. 12). However, according to our classification scheme, these folds are F_2 structures because they fold a very strong bedding parallel foliation that is also developed in the volcanic rocks.

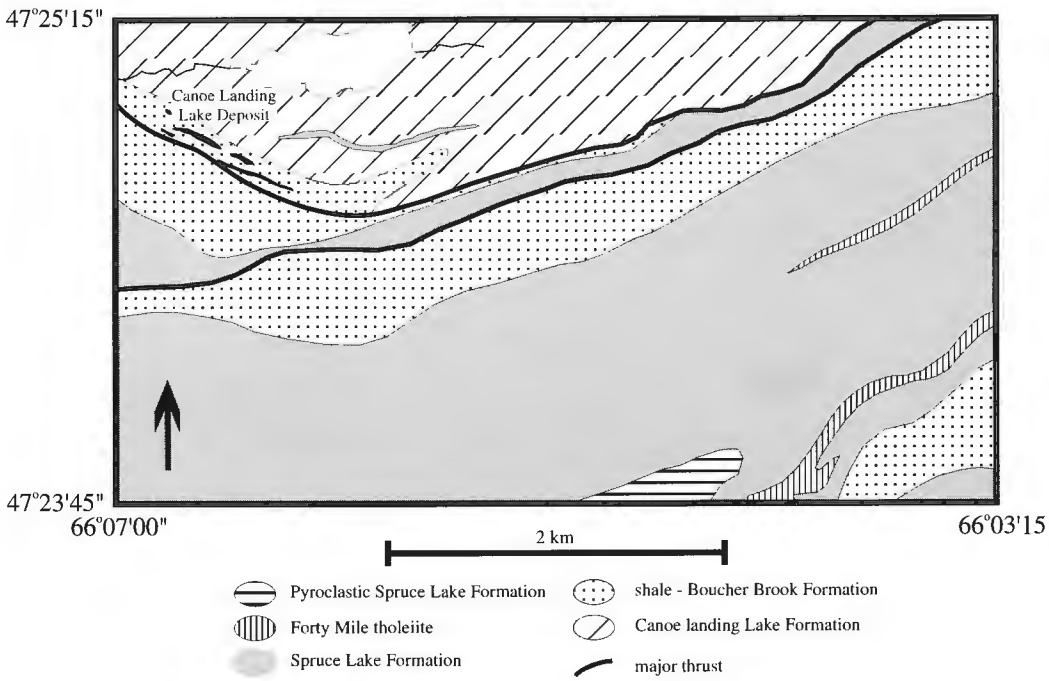

Figure 9. *Detailed geology of the Canoe Landing Lake region.*

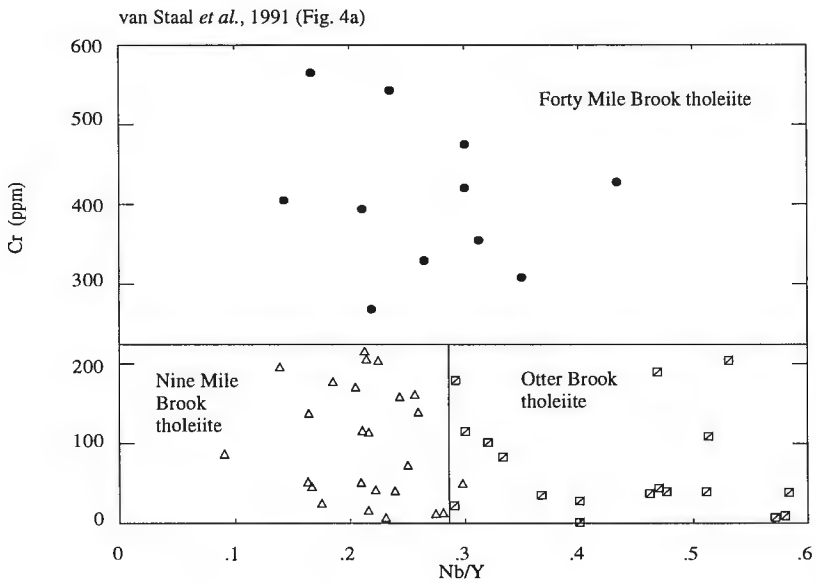

Figure 10.

Nb/Y-Cr discrimination plot for Tetagouche Group tholeiitic basalts. After van Staal et al. (1991).

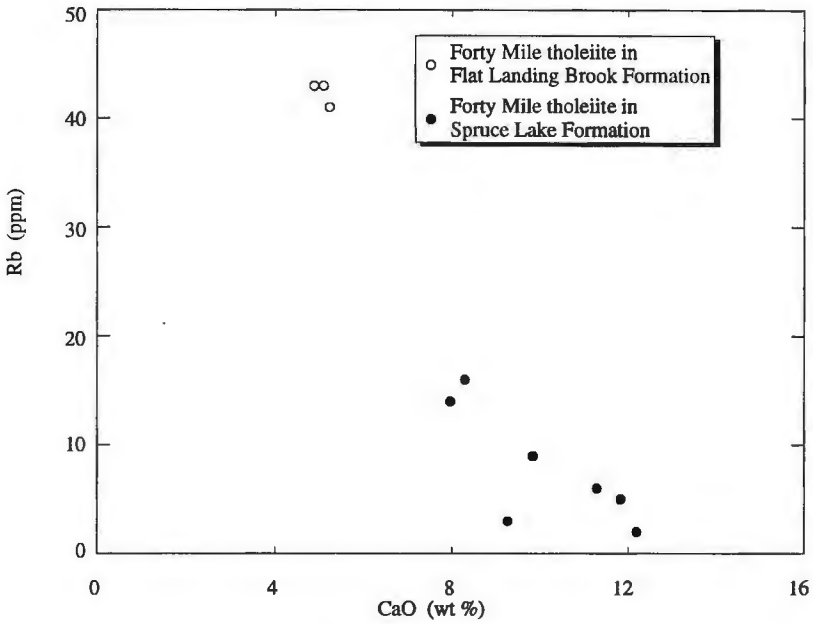

Figure 11.

CaO-Rb discrimination plot for the Forty Mile tholeiites.

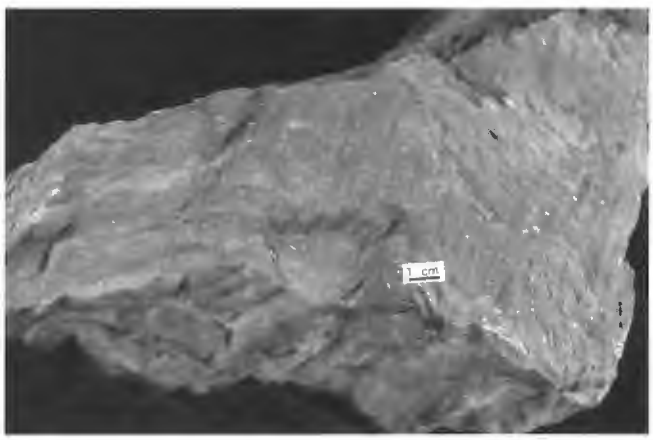

Figure 12. *S-shaped asymmetric, isoclinal F_2 in jasper bands crunulated by F_4, from near the Caribou massive sulphide deposit. Short limbs of F_2 isoclines have been attenuated such that the F_2 folds are stacked en-echelon.*

Inspection of F_1 folds described by Davies also shows that his S_1 is a crenulation cleavage of an earlier bedding-parallel foliation.

On the basis of metal zoning in the Caribou massive sulphide deposit (Cu-rich bottom and Pb-Zn-rich top), the Orvan Brook porphyry was previously interpreted to occupy the stratigraphic hanging wall to the Caribou deposit, with the footwall and immediate host rocks consisting of graphitic black and greenish-grey shales, respectively (Roscoe, 1971). The absence of significant mineralization and associated alteration in the porphyry stratigraphically above the deposit is consistent with this interpretation. The presence of Brunswick alkali basalt in the underlying (footwall) black shale demonstrates that it is, at least in part, the younger Boucher Brook Formation. As van Staal (1994) had interpreted all the black shale and host rock to be part of the same unit, it followed that the contact between the sulphides and the porphyry had to be tectonic, i.e. a ductile thrust (old over young relationship). Further work in the Caribou open pit has shown that the highest D_1 strain occurs along the F_2 folded contact between the black shales and the host rock sediments; hence we infer a thrust boundary to exist here and have included the massive sulphide deposit and host rock sediments in the Spruce Lake Formation. The recognition of tuffaceous beds, and altered and mineralized Orvan Brook porphyry in core from stratigraphically below the Caribou deposit lends credence to such an interpretation as it shows that formation of the sulphides took place during deposition of the Spruce Lake volcanic rocks. Intercalation of red hematitic shale and chert in the porphyries also shows that hydrothermal activity continued during volcanism.

Since it is likely that the sulphide deposits probably developed during periods of quiescence between the eruptions of the Orvan Brook porphyries, one might expect similar deposits to have formed in association with the other porphyry members of the Spruce Lake Formation. Hydrothermal systems were probably established in association with all of the porphyries as minor hydrothermal sediments occur throughout the formation. This suggests that the conditions necessary for massive sulphide deposition were only present for the Orvan Brook porphyry. A stratified water column in the basin has been proposed to explain the relative proportion of iron-formation to massive sulphide between the Brunswick No. 6 and 12 deposits (van Staal et al., 1992). It is reasonable to assume that similar environmental conditions would have been present for the contemporary and locally interfingering (i.e. adjacent in the basin) Spruce Lake Formation. This suggests that the Orvan Brook porphyry was formed in a part of the basin that was conducive to the preservation of massive sulphides, while the other members formed under different conditions. Therefore, it is unlikely that all the members came about as interfingering batches of magma that were erupted out of the same centre. Hence, it is proposed that the feldspar porphyries formed at several distinct volcanic centres. This

Figure 13. Strongly attenuated, shear-banded phyllonite from structurally below the Canoe Landing Lake massive sulphide deposit.

hypothesis is supported by the range of chemical compositions displayed by the porphyry members, which suggests that each of these represents a distinct fractionated series (i.e. evolved separately in, at least, some stage of their development). The current juxtaposition of the members is probably due to deformation; this is supported by the presence of high strain zones between each of the members.

Relationships at the Canoe Landing Lake deposit

The Canoe Landing Lake massive sulphide deposit occurs in sediments due south of the Canoe Landing Lake Formation alkali basalts, which are interbedded with the tuffaceous Orvan Brook porphyry (Fig. 9). Consequently, we consider it to have been formed contemporaneously with the Spruce Lake Formation massive sulphide deposits. Field relationships and radiometric age data indicate that the Canoe Landing Lake and Spruce Lake formations are lateral facies equivalents, although the former structurally overlies the latter. Furthermore, Walker and McDonald, (1995) observed that the contact between the basalts and immediately underlying sediments, which include the massive sulphides, is not marked by high D_1 strain; rather the sediments appear to face consistently towards the alkali basalts of the Canoe Landing Lake Formation. These sediments are greenish grey, pyritiferous shale and siltstone, similar to those that host the Caribou orebody and also to some of the ash beds in the Spruce Lake Formation. A high strain zone, characterized by a strongly attenuated phyllonite (Fig. 13) observed in drill-core (BM&S 212-6), marks the contact with the underlying dark grey shales of the Boucher Brook Formation. Therefore, we suggest that this phyllonite may mark the thrust that separate the panels that contain the contemporary Spruce Lake and Canoe Landing Lake formations. The presence of a thrust is also consistent with the observation that the dark grey shales are cut off towards the east (Fig. 9).

CONTINUING RESEARCH

Continued research on the Spruce Lake Formation is focusing on: (i) further investigation of the relationships between the massive sulphide deposits and the petrographically distinct (pseudomorphs after biotite) Orvan Brook porphyry member; (ii) testing the existence of the proposed subdivisions of the Forty Mile Brook tholeiites; (iii) examination of genetical relationships between the quartz-feldspar porphyries and rest of the Spruce Lake Formation; and (iv) characterization of the internal geometry of the tectonic panels that contain Spruce Lake Formation volcanic rocks.

Petrographic similarities have been noted between the Spruce Lake Formation and the higher grade Stony Brook Complex, which occurs to the southwest. Preliminary geochemical data indicates that they have similar chemical affinities, although more data is required before it can be confirmed or disproved that they are the same rocks at different metamorphic grades.

ACKNOWLEDGMENTS

We are grateful to Chris Beaumont-Smith, Les Fyffe, Wayne Goodfellow, Sue Gower, Steve McCutcheon, Jan Peter, Jim Walker, Reg Wilson, and John Winchester for sharing their ideas and data with us. Richard Lancaster is thanked for polishing and photographing our samples. We thank Jan Peter, Steve Lucas, and Wayne Goodfellow for their reviews of this paper. Neil Rogers acknowledges the support of NSERC Visiting Fellowship held at the Geological Survey of Canada. This is part of the EXTECH II research project.

REFERENCES

Davies, J.L.
1972: The geology and geochemistry of the Austin Brook area, Gloucester County, New Brunswick, with special evidence on the Austin Brook Iron Formation; PhD. thesis, Carleton University, Ottawa, Ontario, 254 p.

Fyffe, L.R.
1994: Geology of the Clearwater Stream area (NTS 21O/1b), Northumberland County, New Brunswick; in Current Research 1993, (comp., ed.) S.A.A. Merlini; New Brunswick Department of Natural Resources and Energy, Minerals and Energy Division, Miscellaneous Report 12, p. 55-64.

Langton, J.P.
1994: Tomogonops project, NTS 21 P/4 west, Gloucester County, New Brunswick; in Current Research 1993, (comp., ed.) S.A.A. Merlini; New Brunswick Department of Natural Resources and Energy, Minerals and Energy Division, Miscellaneous Report 12, p. 87-93.

Lentz, D.R. and van Staal, C.R.
1995: Predeformational origin of massive sulfide mineralization and associated footwall alteration at the Brunswick 12 Pb-Zn-Cu deposit, Bathurst, New Brunswick: evidence from the porphyry dyke; Economic Geology, v. 90, p. 453-463.

Roscoe, W.E.
1971: Geology of the Caribou deposit, Bathurst, New Brunswick, Canada; Canadian Journal of Earth Sciences, v. 8, p. 1125-1136.

Rogers, N.
1994: The geology and geochemistry of the felsic volcanic rocks of the Acadians Range Complex, Tetagouche Group, New Brunswick; PhD. thesis, Keele University, U.K., 420 p.
1995: The petrological variations of the Ordovician felsic volcanic rocks of the Tetagouche Group, New Brunswick; in Current Research 1995-E; Geological Survey of Canada, p. 279-286.

Sullivan, R.W. and van Staal, C.R.
1990: Age of a metarhyolite from the Tetagouche Group, Bathurst New Brunswick, from U-Pb isochron analyses of zircons enriched in common Pb; in Radiogenic Isotopic Studies: Report 3; Geological Survey of Canada 89-2, p. 109-117.
1993: U-Pb age of the Canoe Landing Lake Formation, Tetagouche Group, New Brunswick; in Radiogenic Age and Isotopic Studies: Report 7; Geological Survey of Canada 93-2, p. 39-43.

Tamura, Y.
1995: Liquid lines of descent of island arc magmas and genesis of rhyolites: evidence from the Shirahama Group, Japan; Journal of Petrology, v. 36, p. 417-434.

van Staal, C.R.
1994: Brunswick subduction complex in the Canadian Appalachians: record of the Late Ordovician to Late Silurian collision between Laurentia and the Gander margin of Avalon; Tectonics, v. 13, p. 946-962.

van Staal, C.R. and Fyffe, L.R.
1991: Dunnage and Gander Zones, New Brunswick: Canadian Appalachian region; New Brunswick Department of Natural Resources and Energy, Mineral Resources Branch, Geoscience Report 91-2, 39 p.

van Staal, C.R. and Williams, P.F.
1984: Structure, origin and concentration of the Brunswick No. 12 and No. 6 ore bodies; Economic Geology, v. 79, p. 1669-1692.

van Staal, C.R., Fyffe, L.R., Langton, J.P., and McCutcheon, S.R.
1992: The Ordovician Tetagouche Group, Bathurst Camp, northern New Brunswick, Canada: history, tectonic setting, and distribution of massive sulphide deposits; Exploration and Mining Geology, v. 1, p. 93-103.

van Staal, C.R., Ravenhurst, C.E., Winchester, J.A., Roddick, J.C., and Langton, J.P.
1990: Evidence for a post-Taconic blueschist suture in northern New Brunswick, Canada; Canadian Journal of Earth Sciences, v. 15, p. 207-209.

van Staal, C.R., Winchester, J.A., and Bédard, J.H.
1991: Geochemical variations in Middle Ordovician volcanic rocks of the northern Miramichi Highlands and their tectonic significance; Canadian Journal of Earth Sciences, v. 28, p. 1031-1049.

Walker, J.A. and McDonald, S.M.
1995: Preliminary investigation of the Canoe Landing Lake massive-sulphide deposit, NTS 21O/8e; in Geoscience Research 1994, (comp., ed.) J.P. Langton; New Brunswick Department of Natural Resources and Energy, Minerals and Energy Division, Miscellaneous Report 15.

Wilson, R.A.
1994: Big Bald Mountain project: geology of Mountain Brook-Stony Brook area (NTS 21O/1h), New Brunswick; in Current Research 1993, (comp., ed.) S.A.A. Merlini; New Brunswick Department of Natural Resources and Energy, Minerals and Energy Division, Miscellaneous Report 12, p. 217-223.

Winchester, J.A. and Floyd, P.A.
1977: Geochemical discrimination of different magma series and their differentiation products using immobile elements; Chemical Geology, v. 20, p. 325-343.

Geological Survey of Canada Project 940001-1A

Geology and structure in the Grandroy area south of the Brunswick No. 12 massive-sulphide deposit, Bathurst, New Brunswick[1]

David R. Lentz[2]
Mineral Resources Division

Lentz, D.R., 1996: Geology and structure in the Grandroy area south of the Brunswick No. 12 massive-sulphide deposit, Bathurst, New Brunswick; in Current Research 1996-D; Geological Survey of Canada, p. 71-80.

Abstract: The geology of the Grandroy area is similar to that around the Brunswick No. 12 massive-sulphide deposit, except for the overall smaller thickness of the Brunswick alkali basalt package. The Pabineau thrust (high-strain zone) separates the traditional Brunswick Belt, which hosts the Brunswick No. 6 and 12 deposits and the Austin Brook deposit (eastern domain), from a lithologically identical package to the southwest (western domain). The thrust occurs along the limb of a very tight to isoclinal F_2 fold but has relatively minor apparent displacement compared to D_1-related thrust faults. Within the western domain, the weakly mineralized Brunswick Horizon on the western limb of the F_2 structure is overlain by fine grained fragmental (aphyric) rhyolite and underlain by sedimentary rocks and fine- to medium-grained crystal tuffs that are variably altered. The Brunswick Horizon in the western domain hosts the Flat Landing Brook, Headway, and Pabineau deposits.

Résumé : La géologie de la région de Grandroy s'apparente à celle aux environs du gisement de Brunswick n° 12 (sulfures massifs), à l'exception de l'épaisseur globale des basaltes alcalins de Brunswick qui est plus faible. Le chevauchement de Pabineau (secteur très déformé) sépare la zone traditionnelle de Brunswick, qui renferme les gisements de Brunswick n° 6 et n° 12 et le gisement d'Austin Brook (domaine oriental), d'un complexe lithologiquement identique au sud-ouest (domaine occidental). Le chevauchement se situe en bordure du flanc d'un pli P_2 très serré à isoclinal, mais son déplacement apparent est relativement mineur comparativement aux failles de chevauchement liées à D_1. Dans le domaine occidental, l'horizon faiblement minéralisé de Brunswick sur le flanc ouest de la structure P_2 est sous-jacent à une rhyolite (aphyrique) détritique à grain fin et sus-jacent à des roches sédimentaires et des tufs à granulométrie fine à moyenne (altération variable). L'horizon de Brunswick dans le domaine occidental renferme les gisements de Flat Landing Brook, de Headway et de Pabineau.

[1] Contribution to the Canada 1994-1999 Bathurst Mining Camp, Canada-New Brunswick Exploration and Science and Technology (EXTECH II) Initiative.
[2] New Brunswick Geological Surveys Branch, Department of Natural Resources and Energy, P.O. Box 50, Bathurst, New Brunswick E2A 3Z1

INTRODUCTION

The Grandroy area occurs between the Brunswick No. 12 crown grant to the north and the FAB zone to the east along the Brunswick Belt in the vicinity of the hinge of the Pabineau Antiform (Fig. 1). There is minimal exposure and drillhole coverage in the region except for a fence of nine drillholes in the core of the Pabineau Antiform (Fig. 1), which evaluates the stratigraphy and structure in the area (Fig. 2). There is minimal exploration and drilling along the Brunswick Belt between the A-B cross section and the FAB area (Fig. 2). Until recently, only a few drillholes had intersected the Headway (-Red Lake) Horizon (see Hussey, 1992), which is probably correlative with the Brunswick Horizon. The Headway Horizon is known to host the Headway and Quebec Smelting and Refining (QSR or Pabineau) deposits (Fig. 1) to the northwest and possibly the Flat Landing Brook deposits to the south and, therefore, has considerable exploration potential.

The rocks in the Grandroy area are described in the context of the tectonostratigraphic framework of the Bathurst Camp (van Staal and Fyffe, 1991; Fig. 1). Recognition of formations as described by van Staal and Fyffe (1991) is necessary in order to correlate stratigraphy and interpret structure. Protolith names are used even though the rocks have in many cases been intensely deformed and metamorphosed to upper greenschist grade.

The Grandroy area encompasses part of the Brunswick Belt. The Brunswick Belt hosts the Brunswick No. 6 and 12 deposits, Austin Brook Fe deposit, and FAB stringer-sulphide zone that are part of the Tetagouche Group volcanic and sedimentary sequence. The Grandroy area is also transected by the Pabineau Fault, terminology used by the Brunswick Mining and Smelting geological staff. This fault is characterized as a syn- to late-F_2 high-strain zone that is localized along the limb of a very tight F_2 fold (van Staal, 1985; Lentz and Goodfellow, 1994a). Although originally mapped as a high-strain zone by van Staal (1992), it is now illustrated as a thrust by van Staal (1994) probably in recognition of the ductile strain and the reverse sense of movement. Langton and McCutcheon (1990) have mapped this structure to the south of the Nepisiguit River and refer to it as a thrust. Recently, the Pabineau thrust has been referred to as a transpressional D_2 shear zone that has vertical and horizontal movements based on lineations (deRoo and van Staal, 1994), although only vertical lineations were observed by the author along this high-strain zone.

In the FAB area, Lentz and Goodfellow (1994a) referred to the geology to the north and east of the Pabineau thrust as the eastern domain (package) and to the south and west as the western domain because, for the most part, the Brunswick Belt strikes north-south. The similarity of the geology and structural history in the eastern and western domains support a high exploration potential for the western domain. If analogous to the Brunswick Horizon in the eastern domain, the Headway Horizon should occur between the Nepisiguit Falls (felsic crystal tuff and associated sedimentary rock) and Flat Landing Brook (rhyolites and related hyalotuffaceous sedimentary rocks) formations.

Hence, this area was examined: 1) to better understand the geological and structural correlations south of Brunswick No. 12 and west of the FAB zone, 2) to determine the location and nature of the Pabineau thrust that separates the two structural domains, and 3) to describe the geological and geochemical characteristics around the Headway Horizon that is equivalent to the Brunswick Horizon in the southwestern thrust block (western domain).

PABINEAU THRUST

In the A-B cross-section (Fig. 2), the Pabineau thrust is manifested as a high-strain zone at the top of the basalt in contact with Nepisiguit Falls crystal tuffs. In the north (eastern domain), the stratigraphy is south facing, changing to north facing in the south (western domain) across this thrust (Fig. 2, A-B section) indicating that it is localized along the limb of a large-scale F_2 fold as was determined in the FAB area (Lentz and Goodfellow, 1994a). To the west, the fence of drillholes (Fig. 2, A'-B' section) indicates a profound change in structure compared to the southeast. In the eastern domain, a prominent F_2 fold is evident that folds the Brunswick Horizon. It seems this F_2 structure plunges shallowly to the north because the Brunswick alkali basalts that overlie the Flat Landing Brook rhyolite appear to core this F_2 structure to the north. The geology is complicated by the late, brittle fault, that is part of a larger set of north-south-trending brittle faults that cut the Brunswick alkali basalt package. This late fault juxtaposes the mafic rocks with Patrick Brook rocks (Fig. 2, A'-B' section). To the southwest, a complete conformable sequence occurs with the mafic rocks overlying the Flat Landing Brook or Boucher Brook sedimentary rocks (Fig. 2, A'-B' section), which represents the northeast younging limb of a slightly overturned F_2 fold. This relationship contrasts with that observed to the north and south along the belt where various parts of the upper stratigraphic section have been removed along the high-strain zone. This evidence supports minimal movement elsewhere along the thrust but also the heterogeneous strain exhibited along the limbs of the major F_2 structures. This is significant for exploration elsewhere along the inferred thrust, particularly since an iron-formation (Headway Horizon) was intersected at depth (DDH A250) between Nepisiguit Falls footwall sedimentary rocks and Flat Landing Brook/Boucher Brook sedimentary rocks along the eastern limb of the overturned F_2 anticline (western domain) (Fig. 2, A'-B' section). With this F_2 folding relationship in mind and the similarity of the eastern and western domains, the block west of the late brittle fault has been down dropped relative to the east (Fig. 2, A'-B' section). This sense of movement would have been opposite to the direction of thrusting along the Pabineau Thrust because of the overall nature of asymmetry of the westward-facing F_2 fold inferred from the thickening of units to the west (Fig. 3).

The thrust fault inferred to occur south of the Pabineau Thrust that juxtaposed Knight's Brook and Nepisiguit Falls crystal tuffs (van Staal, 1992, 1994) was not observed in the information available, therefore is not located in Figure 2.

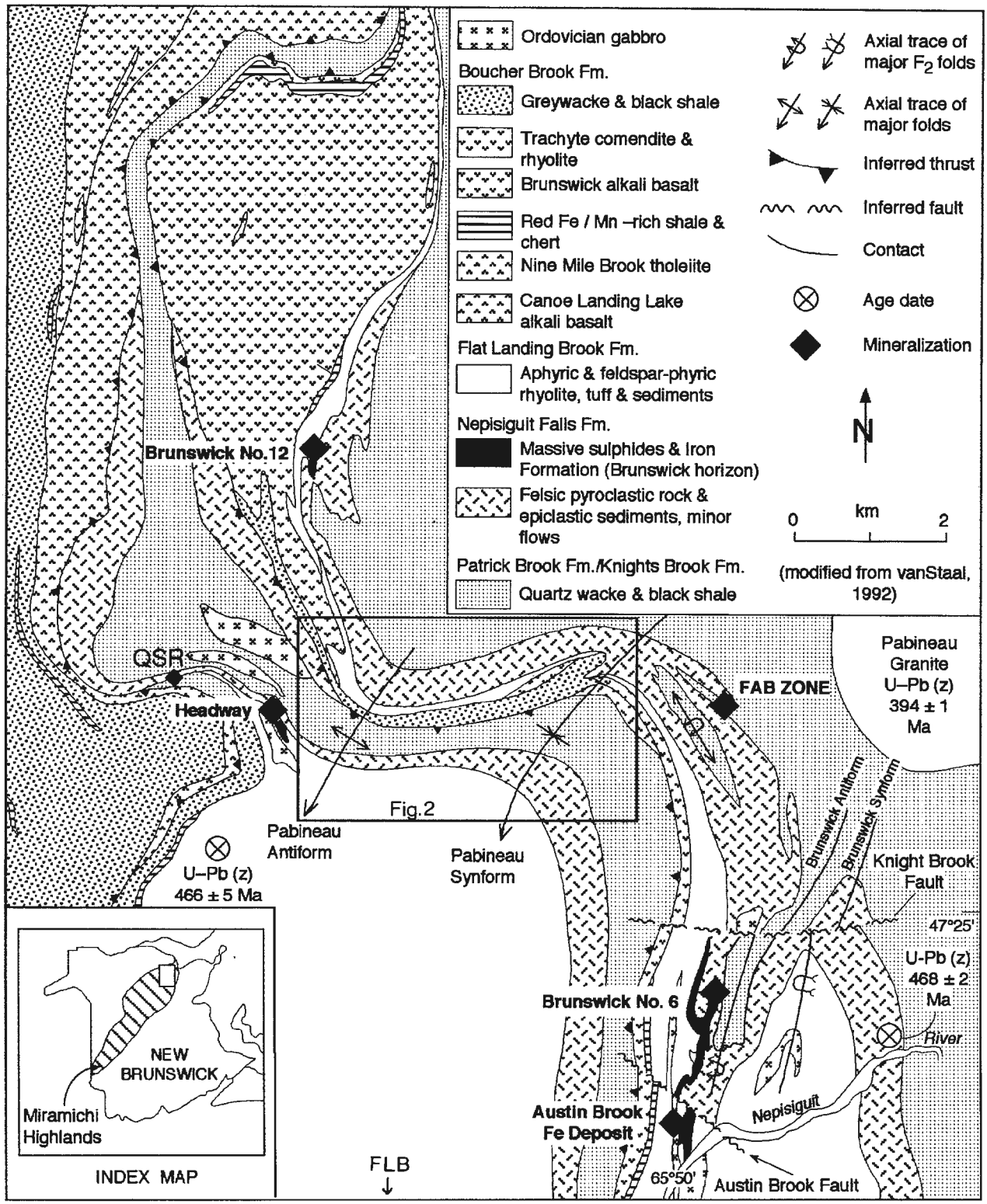

Figure 1. *Geological map of the Brunswick No. 6 and 12 areas based on recent 1:20 000 scale geological mapping (modified after van Staal, 1992). The area within the square is shown in Figure 2. FLB – Flat Landing Brook deposit is 1 km south of this location map.*

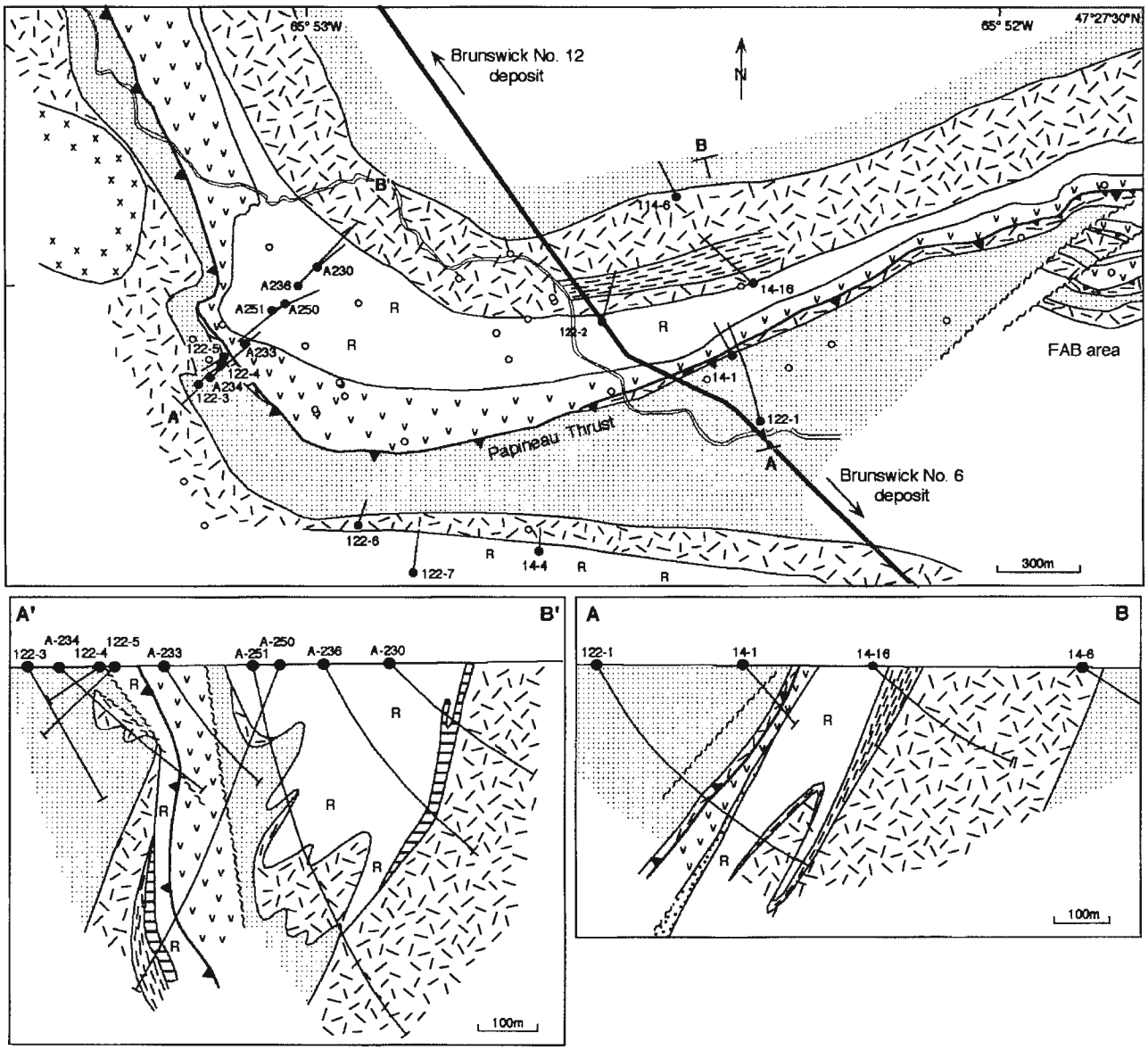

Gabbro

TETAGOUCHE GROUP

Boucher Brook Fm.- siltstone, shale and greywacke

Boucher Brook Fm.- mafic volcanic and volcaniclastic rocks

Flat Landing Brook Fm.- aphyric to feldspar phyric rhyolite, tuff, and crystal tuffite

Nepisiguit Falls Fm.- very fine-grained tuffaceous mudstones with crystal tuff layers + Brunswick Horizon

Nepisiguit Falls Fm.- fine- to coarse-grained, crystal-rich tuff±intrusive porphyry

MIRAMICHI GROUP

Patrick Brook Fm.- thinly-bedded, graphitic shale and quartz wacke

drill hole - no projection

drill hole examined in this study and drill hole number

thrust

fault

section location

road

Figure 2. Geological compilation map of the Grandroy area illustrating the series of diamond drillholes examined in this study (modified from Brunswick Mining and Smelting Limited) with A-B and A′-B′ cross-sections. All cultural features not illustrated for clarity.

EASTERN DOMAIN

The geological cross-section A-B (Fig. 2) illustrates that the geology is similar to the Brunswick and FAB areas with heterogeneous crystal tuffites (Nepisiguit Falls Formation) overlying graphitic slates and quartz wackes (Patrick Brook or Knight's Brook Formation), which are in turn overlain by rhyolitic rocks (Flat Landing Brook Formation) and fine grained sedimentary and mafic volcanic rocks of the Boucher Brook Formation. Although there are some coarse grained crystal-rich tuffs, they are texturally more heterogeneous than the massive coarse grained crystal-rich tuffs at both the Brunswick No. 6 and 12 deposits. The large thickness of fine grained, volcaniclastic sedimentary rocks within the Nepisiguit Falls crystal tuff is considered favourable as an exploration target because most sulphide accumulations along the Brunswick Belt are associated with greater than average thicknesses of sedimentary rocks in the immediate footwall suggesting a basinal control to mineralization (see Luff et al., 1993). Brunswick Horizon iron-formation is known to occur along the entire belt between Brunswick No. 12 and the FAB area as indicated by the geological compilation by van Staal (1992, 1994). The lithologies and composite S_1/S_2 foliations dip steeply south or west (strike dependant) consistent with their position on the western limb of a large F_2 fold similar to Brunswick No. 12 (van Staal, 1985). The small fold (Fig. 2, A-B section) probably represents a parasitic fold on the larger F_2 structure.

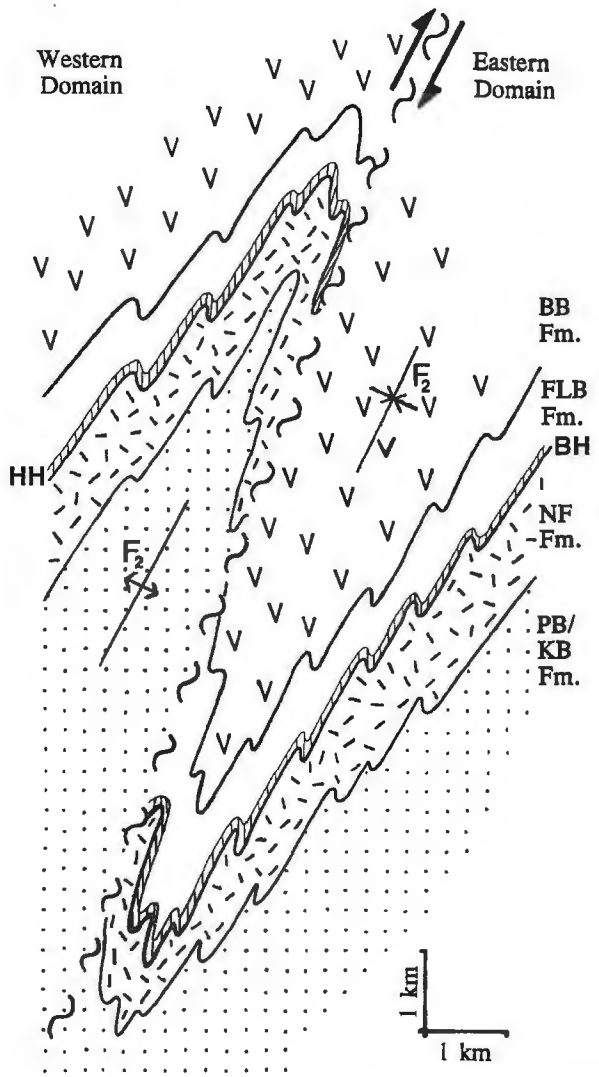

Figure 3. Schematic cross-section of the Brunswick Belt stratigraphy illustrating the various stratigraphic relationships in the eastern and western domains across the Pabineau (D_2) thrust. HH – Headway Horizon, BH – Brunswick Horizon, BB Fm. – Boucher Brook Formation, FLB Fm. – Flat Landing Brook Formation, NF Fm. – Nepisiguit Falls Formation, PB/KB Fm. – Patrick Brook/ Knight's Brook Formation.

WESTERN DOMAIN

The geology along this belt, is poorly known because of the minimal drill coverage in the immediate Grandroy area, compared to the main Brunswick Belt. The geology is based on interpretation of drillhole logs from assessment file work (see compilation by Hussey, 1992). Drillhole 122-7 (Hussey, 1992) is one of the few drillholes available that went through the Headway Horizon. This hole tested a coincident VLF and Horizontal Loop electromagnetic anomaly just to the west of drillhole 14-4, which intersected semi-massive sulphides that graded 0.69% Cu over 0.6 m in chlorite schist (Boylen, 1958).

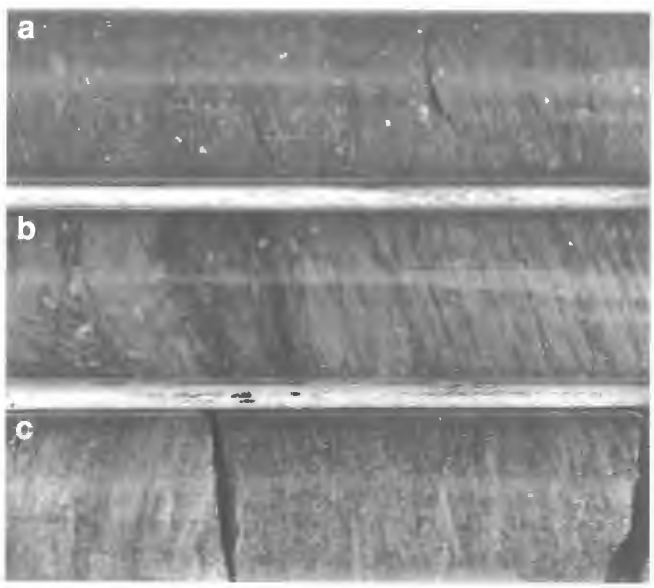

*Figure 4. Photograph of drill core (DDH 122-7) showing variably altered Flat Landing Brook hyalotuffaceous rhyolite stratigraphically above the Brunswick Horizon. **a)** grey felsic tuffaceous sedimentary rock with very small whitish rhyolite fragments (98.1 m), **b)** green-grey tuffaceous sedimentary rock with layer- and foliation-parallel chloritic alteration (105.1 m), **c)** altered, (mottled) light green tuffaceous sedimentary rock (119.2 m; LPA 331).*

Therefore, drillhole 122-7 is used to describe the various lithotypes along this part of the belt. This hole was collared in leucocratic aphyric to feldspar-phyric rhyolite (Flat Landing Brook Formation) but intersects fine grained fragmental rhyolite (Fig. 4a, b) at depth (80 to 122 m) with pseudopyroclastic textures similar to those found to the south in the Narrows area along the Nepisiguit River (Langton and McCutcheon, 1990). These fine grained fragmental rhyolites (Flat Landing Brook Formation) are commonly misinterpreted as fine-grained crystal tuffs (Nepisiguit Falls Formation) because the white rhyolite fragments resemble feldspar phenoclasts. This unit becomes increasingly altered toward the Headway Horizon contact such that the feldspars and fragments are altered to sericite and quartz (±chlorite) (Fig. 4c).

There is a very sharp contact between the altered Flat Landing Brook fragmental rhyolites and the underlying very fine grained, siliceous-pyritic sedimentary rocks (Fig. 5a). These are interpreted as intensely altered Nepisiguit Falls footwall sedimentary rocks, which are similar to silicified rocks directly beneath the Brunswick No. 12 deposit (see Lentz and Goodfellow, 1993a, b). These are probably correlative with the mineralized chloritic sedimentary rocks that host semi-massive sulphide mineralization (0.69% Cu over 0.6 m) intersected to the east (Boylen, 1958). These sedimentary rocks are underlain by sericitic and chloritic, thin-layered (graphitic) slates (Fig. 5b) that resemble sedimentary rocks of the Miramichi Group but are interlayered with more homogeneous sedimentary rocks resembling those of the Nepisiguit Falls Formation. These sedimentary rocks are underlain by variably altered fine- to medium-grained Nepisiguit Falls crystal tuff that is similar to the fine grained crystal tuffs and tuffites in the upper parts of the Nepisiguit Falls Formation (see Lentz and Goodfellow, 1992a; McCutcheon, 1992). The upper part of these tuffs is sericitized resulting in the breakdown of feldspar phenoclasts to sericite and quartz (Fig. 6a, b). These crystal tuffs are also weakly silicified locally such that recognition of the quartz phenoclasts is difficult (Fig. 6a, c).

GEOCHEMISTRY

The chemical composition of each of the rock units is presented from drillhole 122-7 (Table 1) in order to determine their relationship to the Brunswick Belt stratigraphy and characterize their alteration. The compositional data are plotted in profile (Fig. 7) to illustrate some of these trends with respect to the geology in the drillhole. Several samples of footwall "rhyolite" tuff and crystal tuff from the Flat Landing Brook deposit (Troop, 1984), as well as average data on Nepisiguit Falls crystal tuff and Flat Landing Brook rhyolite from the Brunswick Belt, are presented for comparison (Lentz and Goodfellow, 1992b; McCutcheon, 1992; Lentz and Goodfellow, 1994a, b).

Overall, the composition of the Patrick Brook sediment is similar to that in the FAB zone (Lentz and Goodfellow, 1994a) with higher Cr, TiO_2, and Sc. The Nepisiguit Falls crystal tuffs and sedimentary rocks are compositionally quite variable but within the range observed along the Brunswick Belt (see Table 1). Over a short distance (sample 334 to 335; Table 1), the Zr and TiO_2 in the crystal tuff (Fig. 7) changes dramatically, which may result from sedimentary sorting. The Y content is slightly higher in the rhyolitic rocks than in the crystal tuffs, which is consistent with the compositional

Figure 5. *Photograph of drill core (DDH 122-7) showing intensely altered footwall sedimentary rocks stratigraphically below the inferred Brunswick Horizon (Headway Horizon).* ***a)*** *very silicified sedimentary rocks with minor pyrite veins and disseminations (NF Fm.; 128.3m; LPA-332),* ***b)*** *thin-layered sericitic and chloritic footwall sedimentary rock (PB Fm.; 133.8 m; LPA-333).*

Figure 6. *Photograph of drill core (DDH 122-7) showing variably altered, Nepisiguit Falls medium grained crystal tuffs.* ***a)*** *siliceous and sericitic crystal tuff with a few relict feldspar phenoclasts (154.2 m),* ***b)*** *weakly sericitic crystal tuff (155.7 m), and* ***c)*** *silicified quartz-feldspar, crystal-rich tuff (156.4 m; LPA-335).*

Table 1. Major- and trace-element compositional data on volcanic and sedimentary rocks from the Grandroy area compared with literature data from the Flat Landing Brook deposit and Brunswick Belt, Bathurst, New Brunswick.

No.	330	331	332	333	334	335	V5	V7	V4	V3	FAB		FAB		BN6		BN6		BN12		BN12	
Ref.	1	1	1	1	1	1	2	2	2	2	3		3		4		4		5		5	
	FLBrhy	FLBsd	NFsd	PBsd	NFtf	NFtf	NFtf	NFtf	NFsd	NFsd	FLBrhy		NFtf		FLBrhy		NFtf		FLBrhy		NFtf	
m	19.5	119.2	128.3	133.8	154.2	156.4	-	-	-	-	-		-		-		-		-		-	
n	1	1	1	1	1	1	1	1	1	1	4		14		13		6		6		6	
wt.%	-	-	-	-	-	-	-	-	-	-	$\bar{x}$	1s	$\bar{x}$	1s	$\bar{x}$	1s	$\bar{x}$	1s	$\bar{x}$	1s	$\bar{x}$	1s
SiO_2	72.4	69.1	71.8	60.0	76.3	78.5	69.1	73.7	67.6	71.7	69.3	7.5	68.7	3.9	74.9	1.4	71.5	0.4	68.6	3.9	71.1	4.7
TiO_2	0.35	0.43	0.25	1.06	0.35	0.27	0.26	0.30	0.34	0.26	0.51	0.11	0.61	0.17	0.28	0.07	0.52	0.02	0.44	0.13	0.53	0.23
Al_2O_3	13.00	14.8	8.60	18.9	11.3	10.5	13.76	13.15	15.06	13.16	15.60	3.61	13.89	1.16	12.61	1.13	13.47	0.41	13.65	0.92	13.68	1.06
FeO_T	1.80	3.33	8.47	7.03	0.81	0.90	2.60	2.69	5.28	5.85	1.62	1.30	4.58	1.66	2.05	0.08	3.45	0.43	4.2	2.0	3.7	1.7
MgO	0.38	2.48	2.08	2.50	0.42	0.35	2.71	1.83	1.24	0.76	0.50	0.30	2.22	1.02	0.64	0.50	1.81	1.17	2.34	0.93	1.87	0.71
MnO	0.02	0.05	0.05	0.07	0.03	0.02	0.03	0.02	0.03	0.07	0.05	0.01	0.07	0.03	0.01	0.01	0.06	0.01	0.21	0.12	0.05	0.02
CaO	1.11	0.14	0.32	0.10	0.59	0.27	0.47	0.29	0.21	0.21	0.38	0.12	0.89	0.99	0.27	0.11	0.45	0.19	1.24	0.32	0.46	0.28
Na_2O	0.70	<0.03	<0.03	0.10	1.60	1.4	1.78	2.29	0.18	0.22	1.30	0.95	1.18	1.13	1.97	0.69	2.61	0.35	1.08	1.19	1.22	0.84
K_2O	8.59	5.10	2.51	5.18	6.74	5.82	6.55	3.11	4.84	3.20	8.40	3.34	3.65	1.39	5.73	1.74	4.11	0.15	3.88	1.84	4.69	1.03
P_2O_5	0.09	0.10	0.10	0.10	0.08	0.11	0.18	0.14	0.15	0.16	0.13	0.04	0.14	0.03	0.11	0.04	0.17	0.01	0.15	0.10	0.17	0.03
H_2O	0.8	-	-	4.2	0.5	0.6	1.28*	1.78*	3.33*	2.63*	1.2	0.9	2.6	0.8	1.2	0.5	1.4	0.1	2.5	0.5	2.3	0.7
CO_2	0.8	<0.1	0.1	< 0.1	0.5	0.1	-	-	-	-	0.2	0.1	0.7	1.2	-	-	-	-	1.4	1.1	0.5	0.9
S	0.63	1.02	4.77	0.78	0.32	0.29	0.11	0.27	1.03	0.47	0.08	0.16	0.37	0.31	0.03	0.03	-	-	0.03	0.05	0.08	0.13
SUM	100.7	96.8	99.1	100.1	99.5	99.1	98.9	99.7	99.4	98.8												
ppm																						
Ba	750	1000	230	570	1200	690	-	-	-	-	843	191	530	220	681	131	808	53	790	912	597	159
Rb	180	180	97	210	130	150	129	127	117	167	176	84	143	29	162	41	145	14	109	31	137	38
Sr	63	<20	<20	22	89	67	39	13	6	10	56	5	38	31	47	10	70	19	107	75	55	23
Zr	180	230	170	210	230	110	103	132	143	168	470	141	250	70	191	23	203	22	368	138	252	78
Y	36	28	31	30	28	20	30	29	43	44	52	16	31	7	51	7	16	2	49	8	33	4
Nb	<10	<10	13	21	<10	<10	-	-	-	-	11	5	16	5	14	3	14	5	17	7	17	3
La	50	36	23	37	31	20	-	-	-	-	50.0	19.9	37.6	10.1	35.5	10.4	38.0	3.4	44.5	12.8	37.2	11.7
Yb	4.0	3.1	2.9	3.0	3.1	1.7	-	-	-	-	5.2	1.7	2.78	0.71	4.4	-	1.6	0.2	4.97	0.83	3.12	0.35
Cu	<10	34	15	18	<10	<10	9	18	113	20	15	20	15	9	11	12	14	2	<5	-	13	7
Pb	<20	<20	23	<20	23	44	15	5	120	20	13	5	26	45	19	8	27	8	53	72	28	28
Zn	33	41	33	88	13	21	15	20	820	2000	61	44	99	145	41	10	68	10	110	23	84	32
Ni	14	11	20	49	13	10	10	12	16	11	9	5	28	17	7	8	11	1	<5	-	<5	-
Cr	12	11	15	86	15	12	-	-	-	-	5	0	29	15	19	10	16	2	<5	-	18	16
V	23	18	24	110	11	16	-	-	-	-	14	14	44	24	24	17	44	9	13	8	33	24
Sc	9.3	10	7.5	17	7.4	3.4	-	-	-	-	11	5.0	9.1	3.9	-	-	-	-	12.1	4.4	8.6	4.3

NOTES: FeO_T denotes total Fe reported as FeO; Formation Names; FLBrhy - Flat Landing Brook rhyolite, FLB sd - Flat Landing Brook sediment, NFtf - Nepisiguit Falls crystal tuff, NFsd - Nepisiguit Falls sediment. PBsd - Patrick Brook sediment. N - number of samples; $\bar{x}$ - mean; 1s - 1 standard deviation. * = LOI interpreted as H_2O. The analyses in this study (Ref. 1) were done at the Geochemical Laboratories of the Geological Survey of Canada, 601 Booth Street, Ottawa. Major-element and Ba, Nb, Rb, Sr, and Zr were determined by fused disk X-ray fluorescence spectroscopy, the remaining trace elements were analysed by Inductively Coupled Plasma - Emission Spectroscopy (ICP-ES). S, CO_2, and H_2O were determined by wet chemical methods. Reference (Ref.): 1 - this study, 2 - Troop (1984), 3 - FAB zone, Lentz and Goodfellow (1994a); 4 - Brunswick No. 6 (BN6), McCutcheon (1992) and Lentz and Goodfellow (1992b); 5 - Brunswick No. 12 (BN12), Lentz and Goodfellow (1994b).

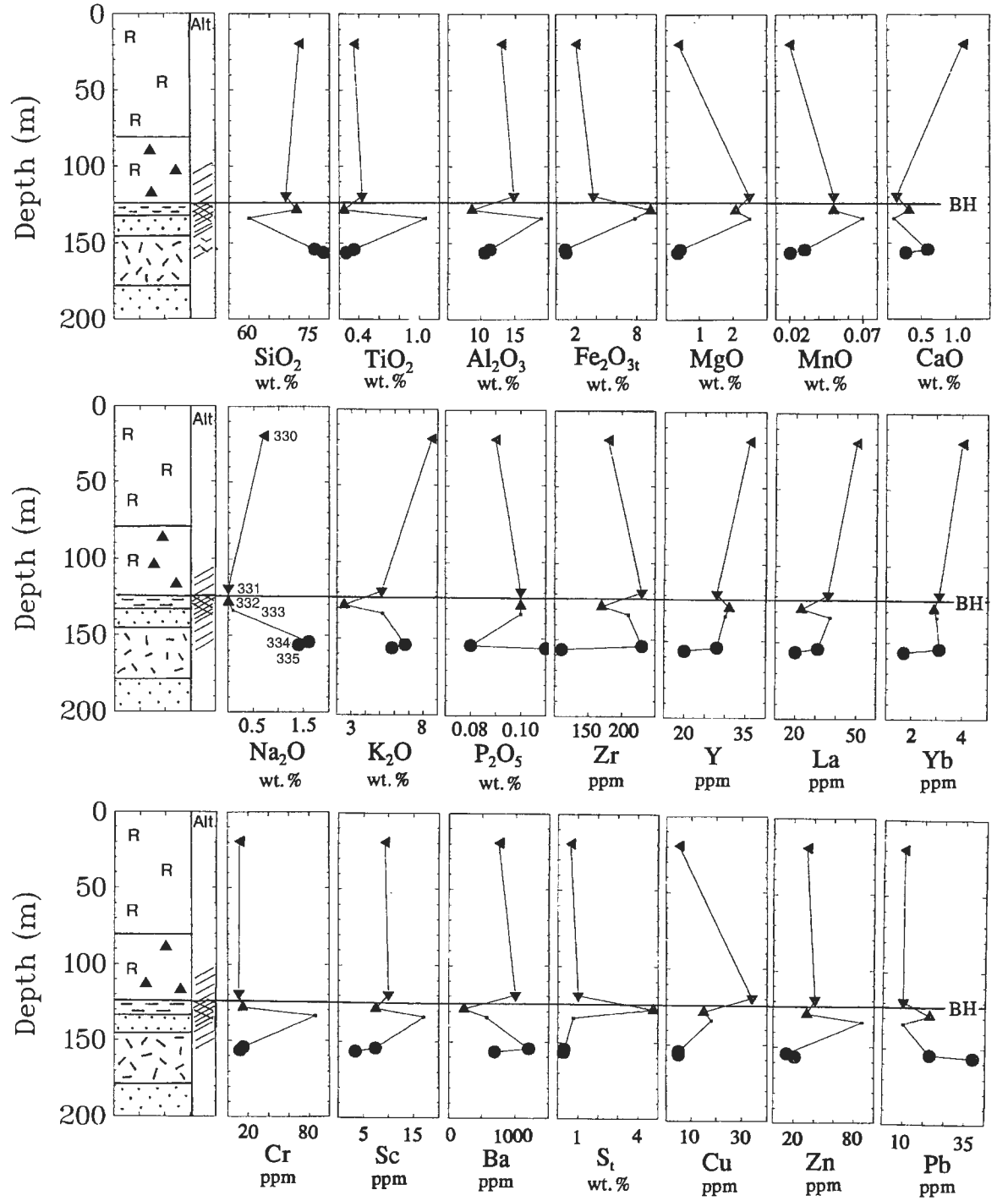

Figure 7. *Major- and trace-element compositional profiles of whole-rock compositional data (Table 1) for drillhole 122-7, Grandroy area (Fig. 2), Bathurst Camp, New Brunswick. FLB – Flat Landing Brook Formation, NF – Nepisiguit Falls Formation, PB – Patrick Brook Formation, BH – Brunswick Horizon (inferred). Alteration (Alt.) is reflected in the intensity of cross hatching.*

evolution observed along the Brunswick Belt (Lentz and Goodfellow, 1992b). The compositions of the crystal tuffs and sedimentary rocks are very similar to analogous rock types at the Flat Landing Brook deposit (Troop, 1984). In general, the Flat Landing Brook rhyolites have higher TiO_2 contents and lower Zr and Y contents than typical Flat Landing Brook rhyolites from the Brunswick Belt suggesting that these rhyolites are not fractionated to the same degree as their counterparts to the east.

For the most part, the alkali elements were mobile even in the relatively unaltered rocks. The SiO_2 contents are slightly higher than normal in the two crystal tuff samples (334 and 335) indicating they are weakly silicified. The siliceous and pyritic sedimentary rock (sample 332) has low concentrations of Al_2O_3 and possibly other immobile elements, probably related to dilution (i.e. overall mass increase), like the intensely silicified footwall rocks with stringer-sulphides at Brunswick No. 12 deposit (Lentz and Goodfellow, 1993a, b). Within the hanging wall fragmental rhyolite, MgO, Ba, S, and Cu are elevated slightly, similar to the hanging wall rocks at the Brunswick No. 12 deposit (Lentz and Goodfellow, 1994b).

DISCUSSION

Overall, the Headway Horizon seems to host several deposits in the area, although the geology is not well known. The laterally extensive nature of the exhalative sediments that characterized the Brunswick Horizon along the entire Brunswick Belt should extend to the west considering the minimal interpreted displacement along the Pabineau Thrust. The mineralization that is intersected in drillhole 122-7 occurs along the Headway Horizon, inferred to be correlative with the Brunswick Horizon. A few of the geological characteristics of the deposits along the Headway Horizon are presented below to illustrate some of these similarities in order to underline the exploration potential along the belt.

In the western domain to the north, the Headway deposit, with calculated possible reserves of 263 000 t with 1.43% Cu and 8.26% Zn+Pb (A & B blocks; McCutcheon, 1992), is inferred to be hosted in the Flat Landing Brook Formation (van Staal, 1992). The Headway deposits are bounded by dark chloritic slates hosted in felsic schists, although chloritic quartz augen schist is locally present. Lower in the footwall, basalt occurs at the contact between Patrick Brook and Flat Landing Brook formations and is referred to as Flat Landing Brook basalt but little is known about its position in the stratigraphy because it doesn't occur elsewhere along the belt. Farther to the east and south along the contact between the Nepisiguit Falls crystal tuff and Flat Landing Brook rhyolites and fragmental rhyolites (i.e., Headway Horizon) to just west of Brunswick No. 6, there are discontinuous exhalites and coincident base-metal soil geochemical anomalies that the horizon is favourable for a considerable distance the south (Don Rutledge, pers. comm.).

The Quebec Smelting and Refining (QSR or Pabineau) deposit is located along the Headway Horizon 1.5 km west-northwest of the Headway deposit (Fig. 1). It contains possible reserves of 136 000 t grading only 2.65% Zn and 0.87% Pb and is associated with Nepisiguit Falls crystal tuffs and Flat Landing Brook rhyolites (McCutcheon, 1992), although was shown to be overlain by Boucher Brook sedimentary rocks by van Staal (1992, 1994).

The Flat Landing Brook (North) deposit located 6 km due south (820 000 t at 1.71% Pb and 6.94% Zn; McCutcheon, 1992) occurs in this same belt and is exposed on the western limb of an F_2 fold that contains an inlier of Nepisiguit Falls crystal tuff. Gabbro (diorite) intrusions and late faulting complicate the local geology. These deposits (Flat Landing Brook North and South zones) are overlain by fine- to coarse-grained fragmental aphyric rhyolites similar to the Flat Landing Brook rhyolites in the Grandroy area. Interestingly, the immediate footwall rocks to the deposit were described as "rhyolite tuff" by Troop (1984) but were correlated with the silicic footwall sedimentary rocks at Brunswick No. 12. However, there is an iron-formation, termed contact banded iron-formation (Troop, 1984), located between these "rhyolite tuffs" and the Nepisiguit Falls crystal tuff. Although not mentioned, these "rhyolite tuffs" are also texturally and compositionally similar to the weakly silicified footwall sedimentary rocks immediately south of the Brunswick No. 6 deposit. The overall similarity of the iron-formation associated with the Flat Landing Brook deposit and the contact iron-formation indicates either the structure of the deposit is not fully appreciated yet or that the Flat Landing Brook deposit and associated iron-formation are hosted within the Flat Landing Brook fragmental rhyolites (i.e. further work is needed).

There is considerable exploration potential in the western domain because of the existence of significant known mineralization within the belt, and the occurrence of F_2 folds, possibly with F_1 interference patterns, that form windows of Nepisiguit Falls Formation and possibly correlative Headway Horizon in the sea of hanging wall Flat Landing Brook rhyolites.

ACKNOWLEDGMENTS

Brunswick Mining and Smelting Limited financially supported some of the investigation presented here. Discussions with Don Rutledge (former exploration geologist at Brunswick Mining and Smelting Corporation), Bill Luff (chief geologist, Brunswick Mining and Smelting Corporation), Jeff Carroll (Noranda Exploration Limited), Steve McCutcheon, Dave McDonald (Noranda Exploration Limited) and Cees van Staal helped distill some of the ideas presented. Richard Lancaster help prepare some of the figures. The manuscript was reviewed by John Langton, Steve McCutcheon, and Neil Rogers.

REFERENCES

Boylen, M.J.
1958: Assessment file, Jacquet River Mines, Project 14; New Brunswick Department of Natural Resources and Energy, Assessment File 471177.

deRoo, J.A. and van Staal, C.R.
1994: Transpression and extensional collapse: Steep belts and flat belts in the Appalachian Central Mobile Belt, northern New Brunswick, Canada; Geological Society of America Bulletin, v. 106, p. 541-552.

Hussey, J.
1992: Geotechnical report on the Grandroy Property (Project 122), Brunswick Mining and Smelting Corporation Limited, Gloucester County, north-east New Brunswick; New Brunswick Department of Natural Resources and Energy, Assessment File 474189.

Langton, J.P. and McCutcheon, S.R.
1990: Brunswick project, Gloucester County, New Brunswick; in Project Summaries for 1990, Fifteenth Annual Review of Activities, (ed.) S.A. Abbott; New Brunswick Department of Natural Resources and Energy, Mineral Resources, Information Circular 90-2, p. 121-128.

Lentz, D.R. and Goodfellow, W.D.
1992a: Re-evaluation of the petrology and depositional environment of felsic volcanic and related rocks in the vicinity of the Brunswick No. 12 massive-sulphide deposit, Bathurst Mining Camp, New Brunswick; in Current Research, Part E; Geological Survey of Canada, Paper 92-1E, p. 333-342.

1992b: Re-evaluation of the petrochemistry of felsic volcanic and volcaniclastic rocks near the Brunswick No. 6 and 12 massive-sulphide deposits, Bathurst Mining Camp, New Brunswick; in Current Research, Part E; Geological Survey of Canada, Paper 92-1E, p. 343-350.

1993a: Mineralogy and petrology of the stringer sulphide zone in the discovery hole at the Brunswick No. 12 massive-sulphide deposit, Bathurst, New Brunswick; in Current Research, Part E; Geological Survey of Canada, Paper 93-1E, p. 249-258.

1993b: Geochemistry of the stringer sulphide zone in the discovery hole at the Brunswick No. 12 massive-sulphide deposit, Bathurst, New Brunswick; in Current Research, Part E; Geological Survey of Canada, Paper 93-1E, p. 259-269.

Lentz, D.R. and Goodfellow, W.D. (cont.)
1994a: Petrology and geochemistry of altered volcanic and sedimentary rocks associated with the FAB stringer sulphide zone, Bathurst, New Brunswick; in Current Research 1994-D; Geological Survey of Canada, p. 123-133.

1994b: Character, distribution, and origin of zoned hydrothermal alteration features at the Brunswick No. 12 massive sulphide deposit, Bathurst Mining Camp, New Brunswick; in Current Research, (comp.) S.A. Abbott; New Brunswick Department of Natural Resources and Energy, Minerals Resources, Information Circular 94-1, p. 94-119.

Luff, W.M., Lentz, D.R., and van Staal, C.R.
1993: The Brunswick No. 12 and No. 6 Mines, Bathurst Camp, northern New Brunswick; in Guidebook to the Metallogeny of the Bathurst Camp, (ed.) S.R. McCutcheon and D.R. Lentz; Bathurst '93 Third Annual CIM Geological Field Conference, Trip 4, p. 75-105.

McCutcheon, S.R.
1992: Base-metal deposits of the Bathurst-Newcastle district: characteristics and depositional models; Exploration and Mining Geology, v. 1, p. 105-119.

Troop, D.G.
1984: The petrology and geochemistry of Ordovician banded iron formations and associated rocks at the Flat Landing Brook massive sulphide deposit, northern New Brunswick; MSc. thesis, University of Toronto, Toronto, Ontario, 218 p.

van Staal, C.R.
1985: The structure and metamorphism of the Brunswick Mines area, Bathurst, New Brunswick, Canada; PhD. thesis, University of New Brunswick, Fredericton, New Brunswick, 484 p.

1992: Geology and structure of the Brunswick Mines area (21P/5e, f); New Brunswick Department of Natural Resources and Energy, Mineral Resources, Open File Map 91-40f.

1994: Geology, Brunswick Mines, New Brunswick; Geological Survey of Canada Map 1836A, scale 1:20 000.

van Staal, C.R. and Fyffe, L.R.
1991: Dunnage and Gander Zones, New Brunswick: Canadian Appalachian Region; New Brunswick Department of Natural Resources and Energy, Mineral Resources, Geoscience Report 91-2, 39 p.

Geological Survey of Canada Project 940001

Geology and geochemistry of Tetagouche Group volcanic and sedimentary rocks and related debris flows north of the Brunswick No. 12 massive-sulphide deposit, Bathurst, New Brunswick[1]

David R. Lentz[2]
Mineral Resources Division

Lentz, D.R., 1996: Geology and geochemistry of Tetagouche Group volcanic and sedimentary rocks and related debris flows north of the Brunswick No. 12 massive-sulphide deposit, Bathurst, New Brunswick; in Current Research 1996-D; Geological Survey of Canada, p. 81-92.

Abstract: The geology north of the Brunswick No. 12 deposit is complicated by the occurrence of sedimentary breccias within the Tetagouche Group. The geology and structure were unravelled using the location of a stratigraphic marker (Brunswick (exhalite) Horizon) and lithotype characteristics. For the most part, the breccia fragments are matrix supported within crystal tuff and fine grained sediment. The fragments are generally composed of aphyric rhyolite, although mafic, slate, and pyritic fragments are not uncommon. Although crystal tuff occurs in the matrix, its absence as fragments in the breccia suggests that it was unconsolidated during breccia formation. This, together with the angularity and locally heterolithic composition of the fragments, as well as the depositional relationships observed, suggests a submarine debris flow origin for these breccias. Slumping of stratigraphy in the east and subsequent deposition westward into deeper parts of the back-arc basin are also present.

Résumé : La présence de brèches sédimentaires dans le Groupe de Tetagouche accroît la complexité géologique du secteur au nord du gisement de Brunswick nº 12. La géologie et le style structural y ont été décryptés sur la base de l'emplacement d'un repère (exhalite) stratigraphique (horizon de Brunswick) et les caractéristiques des lithotypes. Pour la grande partie, les brèches présentent une texture non jointive, la matrice étant constituée de tufs cristallins et de roches sédimentaires à grain fin. Les fragments sont généralement composés de rhyolite aphyrique, même si on en observe bon nombre d'autres types (fragments pyriteux, schiste ardoisier, fragments mafiques). Bien que les tufs soient présents dans la matrice, leur absence en tant que fragments dans les brèches indique qu'ils n'étaient pas consolidés durant la bréchification. Cette hypothèse, combinée à l'angularité et à la composition hétérolithique locale des fragments, mais aussi les liens établis quant à la sédimentation font en sorte que l'origine des brèches est associée à une coulée de débris sous-marine. Sont également signalées des structures de glissement observées dans la stratigraphie à l'est et une sédimentation subséquente vers l'ouest, dans les parties plus profondes du bassin d'arrière-arc.

[1] Contribution to the Canada 1994-1999 Bathurst Mining Camp, Canada-New Brunswick Exploration and Science and Technology (EXTECH II) Initiative.
[2] New Brunswick Geological Surveys Branch, Department of Natural Resources and Energy, P.O. Box 50, Bathurst, New Brunswick E2A 3Z1

INTRODUCTION

The geology and structure north of the Brunswick No. 12 massive-sulphide deposit (Fig. 1, 2) were poorly constrained until relatively recently and, although there has been considerable exploration activity in the past, much of this work was focussed mistakenly on graphitic sedimentary rocks of the Miramichi Group rather than the overlying Tetagouche Group. The Tetagouche Group in the area comprises a complex sequence of basalts, red and grey sedimentary rocks, rhyolites, and crystal tuffites, which were brecciated to variable degrees. There was renewed interest in the area in 1989 following the discovery of massive-sulphide mineralization in drillhole A248 (Fig. 2) approximately 1 km to the north of the Brunswick No. 12 deposit at a depth of 1.1 km (Hussey, 1992). Further drilling on this target outlined 1 million tonnes of 3.0% Pb, 6.2% Zn, 0.24 % Cu, and 109.6 g/t Ag (Luff, 1995). Under an option agreement with Nebex on the Theriault Gate (or Brunswick Extension "A") property, Teck Exploration Limited conducted a detailed exploration program that culminated in a drilling program (Moore, 1992a, b), but no additional mineralization of significance was found.

This investigation was undertaken to determine the origin of the breccias, to characterize the relationship between the various lithotypes and mineralization, and to make comparisons with similar rocks along the Brunswick Belt to the south, in order to help identify other exploration targets in the area.

LOCAL GEOLOGY

Introduction

The geology north of Brunswick No. 12 area is re-interpreted based on exploration-related drilling and trenching undertaken by Brunswick Mining and Smelting Limited (Brooks, 1984) and Teck Exploration Limited (Moore, 1992a, b). The geological interpretation is based on the overall known stratigraphic sequence at the Brunswick No. 12 mine in the Brunswick Belt (Luff et al., 1992; Lentz and Goodfellow, 1992a). The breccias were assigned to formations, following the nomenclature of van Staal and Fyffe (1991) for the Bathurst Camp, based on fragment types. The geology is extrapolated to surface based on the overall 70° westward-dipping axial plane of the F_2 folds (S_1/S_2 fabric; Fig. 2). The local geometry is consistent with the F_2 fold pattern similar to shallow doubly plunging F_2 folds at the Brunswick No. 12 deposit and along the Brunswick Belt (van Staal, 1985). The overall structure is that of an anticline/syncline pair, from west to east, based on the repetition of the mafic volcanic horizon and the depositional nature of the contact with the stratigraphically lower sequence. The repetitions of what is considered to be the Brunswick Horizon are due to F_2 parasitic folds within the core of the western anticline substantiated by small-scale, tight F_2 folds observed in sedimentary rocks.

A lithogeochemical survey of DDH 120-2 (Fig. 3) was undertaken by Teck Exploration Limited during the initial phase of exploration in order to help identify the various units, as well as characterize the alteration. For this reason and the fact that it transects a thick segment of the stratigraphy, it has been selected to help interpret the overall geological environment of the area and to show the significance of the breccias.

Brecciated lithotypes

This drillhole is collared in a sequence of magnetic basalts, mafic-derived sediments, and mafic-dominated fragmentals. The mafic breccias are dominantly composed of subangular to rounded, reddish to greenish mafic fragments (monolithic) hosted in a green to grey fine grained hyaloclastite matrix, although rhyolite fragments are evident locally (Fig. 4a). The mafic-dominated breccia seems to conformably overlie Boucher Brook grey siltstone (136.5 m; Fig. 4a), although the contact is strained. It is evident that the rhyolite fragment has quartz veins that are pre-brecciation (Fig. 4a). Within the felsic volcanic sequence (parts of 107.3 to 242.9 m), variably altered rhyolite fragments, and possibly sedimentary fragments, are hosted in a volcaniclastic matrix dominated by quartz-feldspar crystals (Fig. 4b) and fine grained sedimentary material. It was classified as Flat Landing Brook Formation, which is typified by rhyolites, although it locally contains sedimentary fragments and rare pyrite-rich clasts (Fig. 4c). These breccias are intercalated with massive aphyric rhyolites and hyalotuffaceous sedimentary rocks (upper part of Fig. 4c). Grading in the crystal tuffites, and to a lesser extent in the breccias, is consistent with the inferred stratigraphic position based on the structural interpretation. The contact between the felsic fragmental and the basalt, which is brecciated farther up-hole, is sharp, with very fine grained pyrite (exhalative?) at the contact (Fig. 4d).

The fine grained, light grey-green crystal-rich tuffite located in the core of the anticline (Fig. 2, cross section; below 243 m) is texturally homogeneous (lower Fig. 5a) with a few sedimentary interlayers and is similar to the fine grained crystal-rich tuff at Brunswick No. 12 (Lentz and Goodfellow, 1992a). The contact with the fragmental rhyolite (upper Fig. 5a) is commonly sharp and may locally be erosional. The volcaniclastic matrix to the overlying rhyolite and sedimentary (graphitic shale fragment) breccia is crystal-rich tuff and fine-grained tuffaceous sediments that resemble rhyolitic hyalotuffs (Fig. 5b). The Nepisiguit Falls sequence is relatively thin (6.6 m) in the eastern-most part (625.1 to 631.7 m; Fig. 2, 3) of the Tetagouche Group where mafic volcanic rocks overlie the crystal tuff. Similarly to the western-part of the sequence (upper part DDH 120-2), the mafic fragments are hosted in a crystal tuff matrix (Fig. 5c) at the base of the mafic sequence (above 82.1 m) indicating that the crystal tuffite was unconsolidated during brecciation (i.e. sedimentary). This contact seems depositional, but probably on an erosional (slump scar) surface in the crystal tuffs. The lower contact of the Nepisiguit Falls Formation with the graphitic slates of the Miramichi Group is relatively sharp, although some brecciation is evident (Fig. 5d). Generally, this Miramichi-Tetagouche contact is faulted with some gouge evident indicating that it is a late, post-S_2 feature. Within the Miramichi Group, broken formations (bottom DDH 120-1) are locally common indicative of a tectonic mélange developed locally.

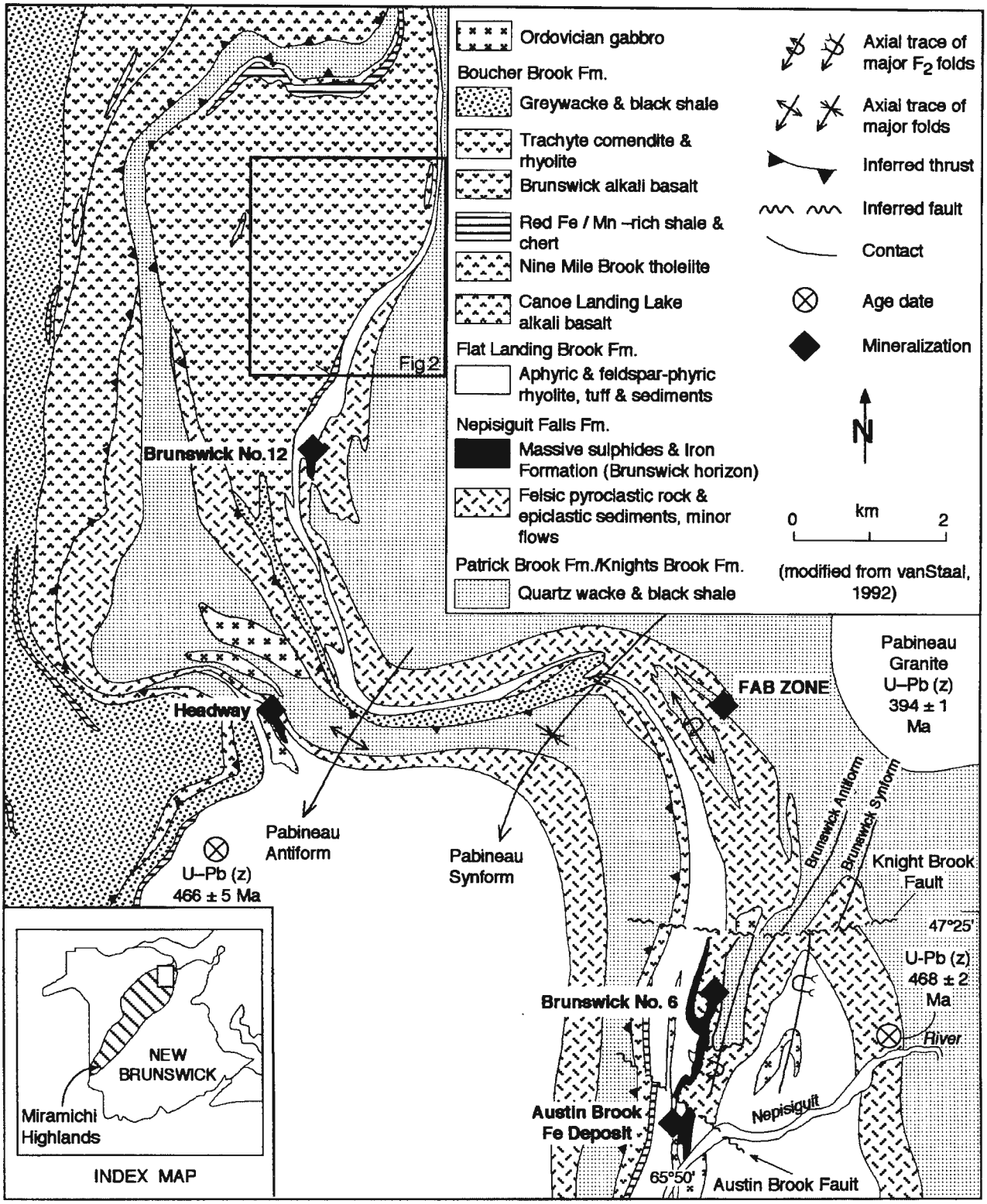

Figure 1. *Regional geology between Brunswick No. 6 and 12 deposits, Brunswick Belt (21 P/5), Bathurst, New Brunswick (modified from Lentz and Goodfellow, 1992a; van Staal, 1992). Inset shows location of Figure 2.*

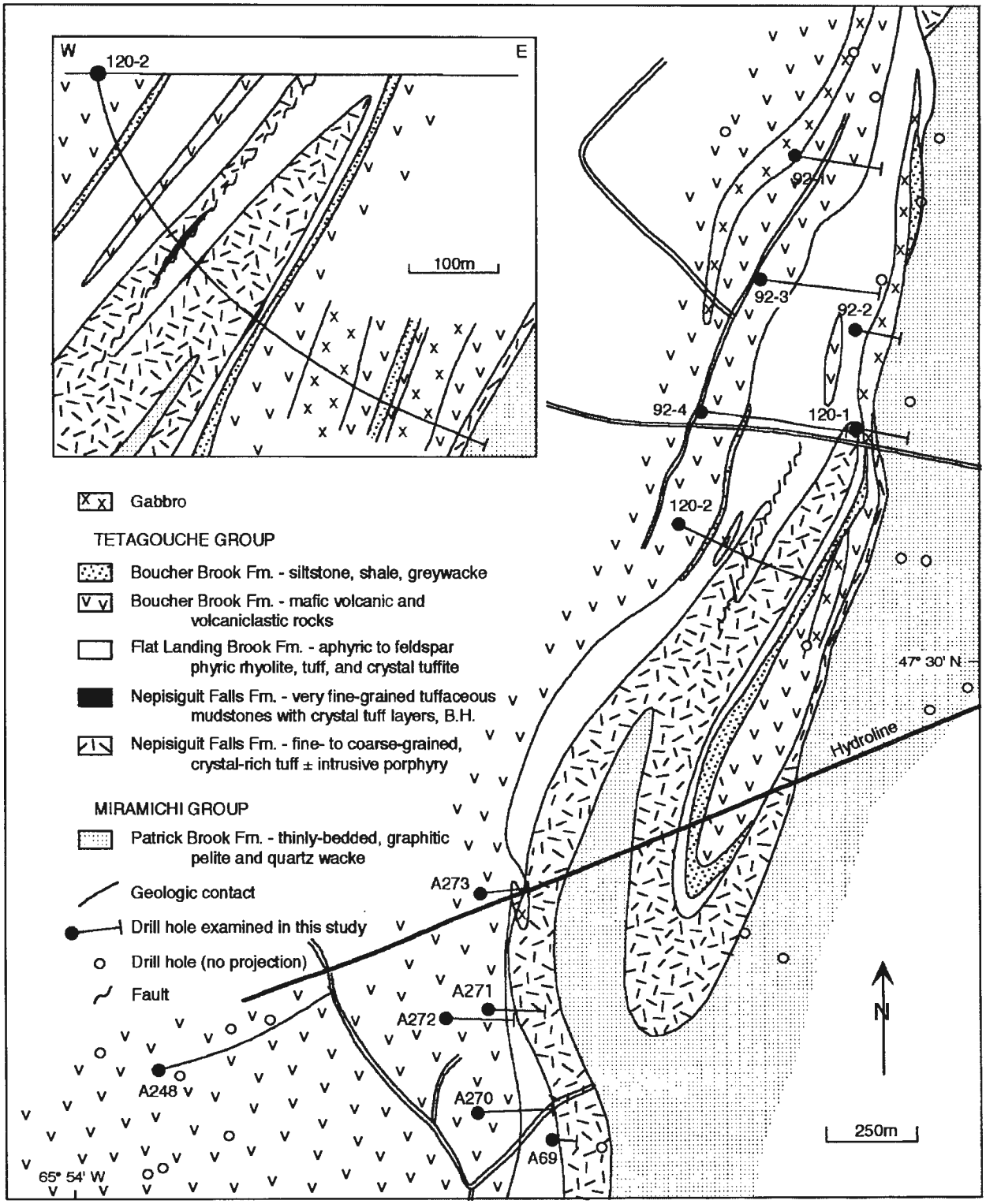

Figure 2. Local geology north of the Brunswick No. 12 deposit (modified after Moore, 1992b) showing the location of diamond-drill holes (DDH) that were examined during the course of this study. The inset cross-section of DDH 120-2 illustrates the interpreted structure of the area.

A sedimentary origin for the breccias is consistent with the angular nature of the fragments, the heterolithic nature of some of the packages, and the absence of pre-fragment folding within the fragments. Considering the nature of the heterolithic breccias, there was probably considerable mixing between the various sedimentary components including the mafic-derived sedimentary rock. Some of the sedimentary rocks, particularly those in the Miramichi Group, and the massive-sulphides were indurated as they occur as fragments locally. Usually, the fragments consist of variable altered massive basalt or rhyolite. The monolithic breccias of basalt or rhyolite hosted in a compositionally similar matrix, may represent either vent-related breccias, debris flows, or tectonic mélange, although many of the breccias are relatively unstrained. However, subaqueous debris flow origin is most consistent with the features of the heterolithic breccias.

Brunswick Horizon

The Brunswick (exhalite) Horizon, which occurs at the contact between the Nepisiguit Falls and Flat Landing Brook formations, is not readily evident in the area. Instead, high concentrations of siderite (exhalite?) and footwall alteration with disseminated pyrite were used to infer its position, as well as the differences in the footwall and hanging wall lithologies. For example, matrix-supported breccia in a fine- to medium-grained crystal matrix are characteristically intraformational below this thin siderite band (0.2 m wide at 202 m). These coarse intraformational breccias, considered to be Nepisiguit Falls Formation, grade into homogeneous fine- to medium-grained crystal tuffs toward the core of a small anticline (300 m). The intraformational breccia was intersected again down-hole overlain by thin homogeneous footwall sediment (229.3 to 237.7 m; Nepisiguit Falls Formation). This sediment has minor stringer-sulphide mineralization and has a thin zone (0.5 m) of very siderite-rich "iron-formation" above it. The overlying sequence has more breccias (238 to 243 m) and fine grained, weakly layered sedimentary rocks overlying what is considered to be Brunswick Horizon (not present). It is, therefore, interpreted as part of the hanging wall sequence and thus assigned to the Flat Landing Brook Formation. A late, chaotic quartz-rich fault zone (256 m) occurs between the rhyolitic breccias and homogeneous fine grained, weakly layered chloritic and siliceous Nepisiguit Falls Formation sedimentary rocks, i.e. at the Brunswick Horizon. On the overturned limb of the anticline, the fine grained sedimentary rocks are pyritic and siliceous (346.6 to 350.5 m), and a minor exhalite (Brunswick Horizon; 0.45 m thick @ 0.27% Zn; Brooks, 1984; Fig. 6). There is a reddish, very fine grained sedimentary rock, capping the siliceous sediments and associated veins, that is inferred to represent an oxidized equivalent of the Brunswick Horizon (labeled RMS in Fig. 6). This is overlain by weakly layered, light grey-green, fine grained tuffaceous sedimentary rocks (Fig. 6) with a minor crystal tuff component similar to Nepisiguit Falls rocks, but are probably related to the Flat Landing Brook Formation. These sediments grade up into a thinly bedded, dark grey sedimentary rock (Boucher Brook Formation) interlayered with dark green sediments of mafic affinity at the top of this sequence. These sedimentary rocks are in depositional contact (363.3 m) with the overlying thick magnetic mafic volcanic package (massive flows, tuffaceous sediments, and breccias). A thick zone of Mn-Fe sedimentary rocks occurs within the mafic volcanic rocks (520.9 to 537.4 m) that extends to the north and is intersected at the top of drillhole 120-1.

Alteration

Overall, hydrothermal alteration of the footwall rocks is weak throughout the area. Within the fine- to medium-grained crystal-rich tuffs and interlayered tuffaceous sediments, feldspar phenoclasts remain intact with minor sericitic alteration. Less than 1% of disseminated sulphides occur within these rocks. The Nepisiguit Falls sedimentary rocks that are inferred to form the footwall to the massive-sulphide deposits along the Brunswick Belt (Lentz and Goodfellow, 1992a; Luff et al., 1993) have moderate sericitic and chloritic alteration (medium-green colour) with an increasing percentage of veins (up to 15%) toward the exhalite horizon. Silicification is also

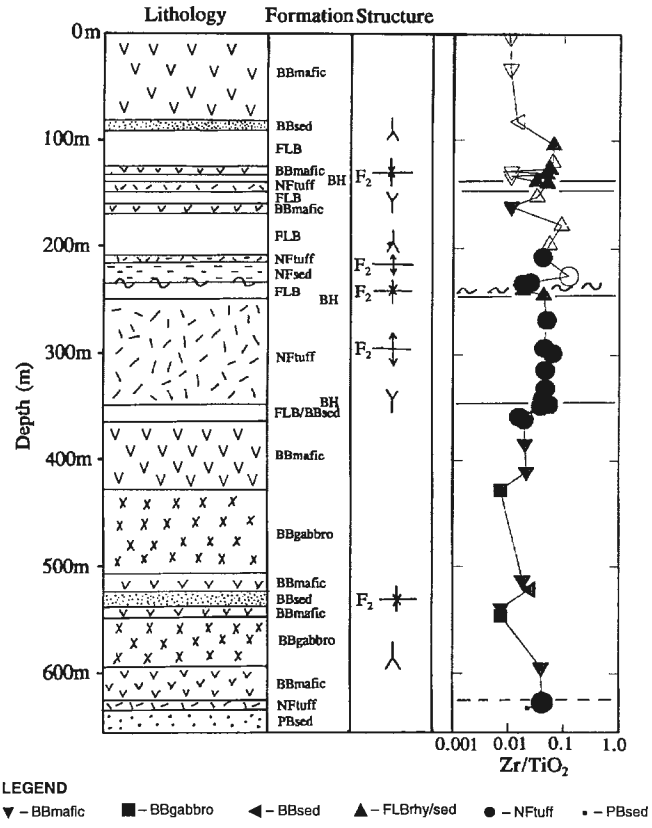

Figure 3. *Stratigraphic and structural interpretation of the rocks in DDH 120-2 using the formational nomenclature of van Staal and Fyffe (1991). BB – Boucher Brook Formation, FLB – Flat Landing Brook Formation, NF – Nepisiguit Falls Formation, PB – Patrick Brook Formation, BH – Brunswick Horizon (inferred). Closed symbols – massive or monolithic breccia, Open symbols – heterolithic breccias.*

evident, which is both vein controlled with sulphides and pervasive silicification. The rhyolite fragments in the hanging wall breccia are variably silicified, although the matrix is relatively unaltered indicating that the rhyolites were silicified before alteration.

Primary siderite disseminations and veins occur to a variable extent within all the lithologies. The most intense siderite alteration occurs within the homogeneous, medium grained, crystal-rich tuffs located above the bleached (graphitic) pelites on the eastern limb of the syncline. The siderite alteration pervades into the magnetic Fe-rich alkalic basalts. The veins are folded, probably related to the D_2 deformation, but for the most part the sideritic alteration is a post-depositional/pre-deformational feature. The siderite alteration seems to be less intense in the gabbroic intrusion and may precede its emplacement. The intense sideritic alteration within the crystal tuffs (10 to 25%) compared to the weakly sideritic tuffaceous sedimentary rocks suggests that the siderite is filling primary porosity (early paragenesis). This is also involved in the replacement of glass within the interstices, which results in a volume decrease thus producing void space in which siderite can deposit.

GEOCHEMISTRY

The drillhole section was sampled to compare the units chemostratigraphically with those elsewhere along the Brunswick Belt, as well as for lithogeochemical exploration using various

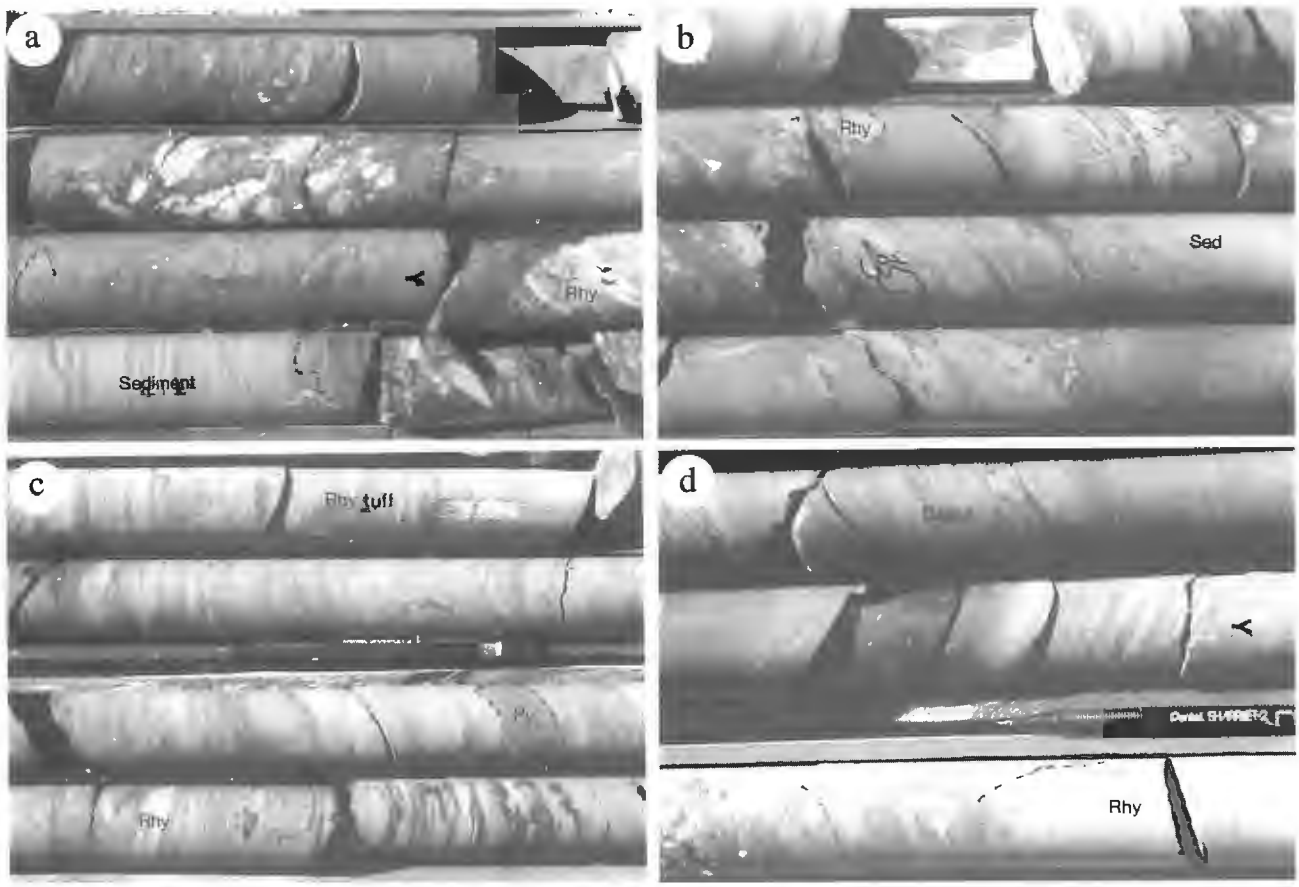

a) Reddish Boucher Brook mafic/sedimentary and Flat Landing Brook fragments hosted in dark green mafic matrix that overlies grey Boucher Brook sedimentary rock (132.3 to 138.1 m), which in turn overlies Flat Landing Brook rocks. Note the aphyric rhyolite fragment has pre-brecciation, quartz-filled fractures. Late quartz-siderite veins cut basalt.

b) Aphyric rhyolite and related sedimentary rock fragments hosted in quartz-feldspar crystal tuffite matrix (matrix hosted), Flat Landing Brook Formation (109.1 to 114.9 m).

c) Leucocratic hyalotuffaceous sedimentary rock (upper part) overlying aphyric rhyolite and pyrite breccia hosted in fine grained sedimentary and crystal tuffite matrix (lower part) with siderite and medium green chlorite alteration in fine grained sedimentary rocks at the base (140.2 to 146.3 m).

d) Pyrite-siderite (exhalite?) located at contact between dark green basalt (upper part) and aphyric rhyolite breccia in crystal tuffite matrix (lower part) (164.6 to 168.6 m).

Figure 4. *Drill core photographs illustrating macroscopic breccia features in diamond Drillhole 120-2.*

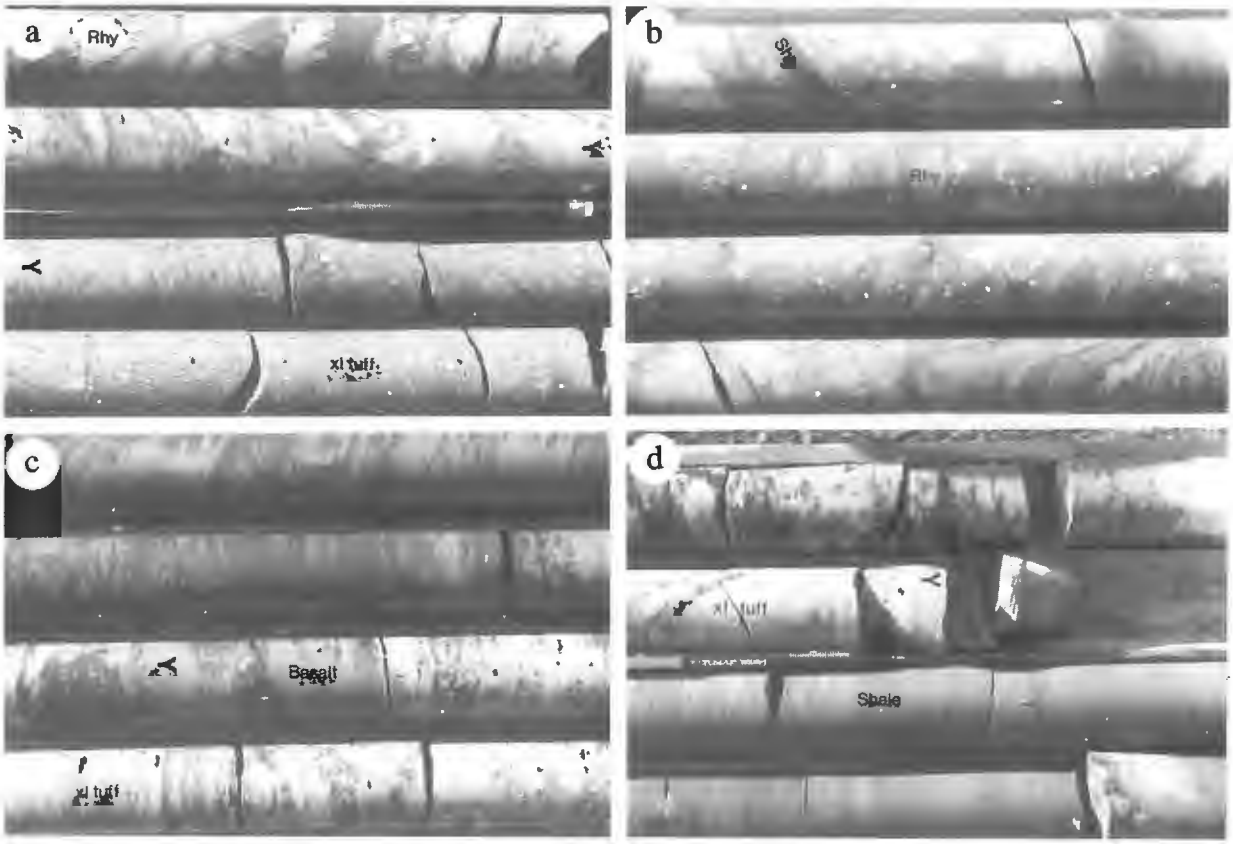

a) Aphyric rhyolite fragments hosted in a mixed fine grained tuffaceous sediment and crystal tuff matrix with considerable siderite alteration (dark brown, upper part) overlying fine grained, quartz-feldspar crystal-rich tuffite (lower part) (205.7 to 210.3 m).

b) Altered, aphyric rhyolite and graphitic slate fragments hosted in crystal tuffite matrix (283.5 to 289.3 m).

c) Dark green basalt fragments hosted in fine grained crystal tuffite near the contact Boucher Brook mafic volcanic rocks and Nepisiguit Falls crystal tuffs (622.1 to 628.2 m).

d) Fine grained crystal tuff in contact (parauthothonous?) with very fine-grained graphitic slate of the Patrick Brook Formation (Miramichi Group) (629.4 to 633.4 m).

Figure 5. *Drill core photographs illustrating macroscopic breccia features in diamond Drillhole 120-2.*

geochemical alteration features (see Moore, 1992a). Figure 3 illustrates the Zr/TiO_2 variations downhole, that directly reflect the compositional changes and supports the geological subdivisions determined. The breccias are compositionally more variable because of the mixed signatures involved (Fig. 7, 8). The major- and trace-element data are plotted in profile with the geology to highlight significant chemostratigraphic and chemical alteration features that might help in correlation (Fig. 3, 7). Selected data (Table 1) were plotted with average data from some Nepisiguit Falls crystal tuff and rhyolite (McCutcheon, 1992; Lentz and Goodfellow, 1992b), as well as the average alkali basalt composition (Fig. 8a, b) from van Staal et al. (1991).

The mafic volcanic rocks are highly alkaline, as indicated by the high Fe_2O_{3t}, TiO_2, P_2O_5, and Nb contents (Fig. 7), particularly in the mafic breccias at 130 m depth where the TiO_2 contents reach 4 wt.%, Zr approaches 500 ppm, and Nb contents are greater than 60 ppm. The eastern mafic package

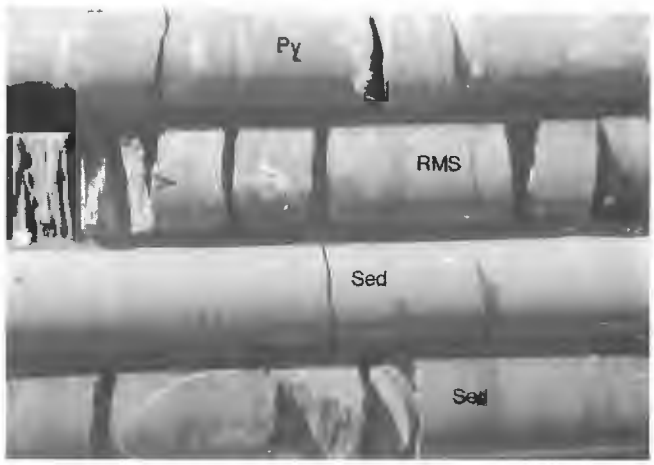

Figure 6. *Siliceous, semi-massive pyrite (Py) overlain by red (manganiferous) slate (RMS) then light to dark grey sedimentary rocks of the Boucher Brook Formation, which underlie Brunswick alkali basalts (347.5 to 353.3 m).*

Table 1. Selected major- and trace-element compositions of volcanic, subvolcanic, and sedimentary rock from the Tetagouche Group in diamond-drill hole 120-2, Brunswick Extension property, Bathurst mining camp, New Brunswick (from Moore, 1992a).

Sample	102	103	104	108	110	114	139	141	142	143	144	107	109	118	117	124	125	126	127	128	130	145
Fm.	BB	BB	BB	BB	BB	BB	BB	BB	BB	BB	BB	dike?	dike?	FLB	NF	NF	NF	NF	NF	NF	NF	NF
lith.	mv	mv	mvs	mv	mv	mv	gb	rms	mv	gb	rms	rhy	rhy	rhy	tuff	tuff	tuff	tuff	tuff	tuff	tuff	tuff
m	3.7	33.0	82.3	128.6	133.2	161.5	427.9	521.2	538.9	546.2	594.5	126.6	131.1	225.6	208.3	243.8	267.0	293.0	298.1	313.9	341.4	627.0
SiO_2 wt.%	45.2	46.9	48.4	37.6	36.4	49.9	45.9	71.4	43.3	46.4	63.2	66.2	72.9	61.6	63.9	66.4	69.9	64.1	64.2	68.5	56.7	69.3
TiO_2	3.64	3.21	1.41	4.35	4.44	2.65	1.97	0.35	2.12	2.29	0.40	0.25	0.12	0.33	0.79	0.70	0.48	0.80	0.58	0.53	0.71	0.52
Al_2O_3	13.4	13.4	9.72	14.6	15.3	11.3	14.3	6.66	12.7	14.3	9.83	16.5	14.1	16.2	13.3	15.1	14.1	15.7	15.1	13.8	13.3	13.7
Fe_2O_3	16.5	15.8	9.65	19.3	19.2	13.2	11.5	9.3	11.5	12.8	13.4	2.89	0.92	3.76	3.40	4.26	3.43	5.40	5.55	4.09	3.30	4.15
MnO	0.31	0.88	0.96	0.63	0.9	0.87	0.83	2.94	1.28	0.71	4.08	0.11	0.09	1.21	0.41	0.49	0.19	0.23	0.31	0.46	1.09	0.46
MgO	5.2	5.19	6.35	7.32	7.68	5.34	6.43	0.8	5.97	6.54	2.56	1.31	0.37	3.32	1.63	1.62	1.88	2.58	2.83	1.76	1.27	1.11
CaO	6.55	6.46	10.3	5.27	4.94	5.98	7.88	1.29	7.43	8.51	0.74	1.36	1.5	2.23	4.69	1.4	1.24	1.57	1.42	1.44	8.19	1.44
Na_2O	2.84	4.16	1.73	1.84	2.02	3.16	3.13	2.21	3.56	3.19	0.83	8.28	8.5	0.51	3.53	1.73	2.72	3.51	2.13	3.06	3.53	1.74
K_2O	1.27	0.33	0.03	0.09	0.18	0.2	0.52	0.95	0.28	0.45	1.28	0.41	0.07	4.54	1.86	3.39	2.4	2.16	2.72	2.2	2.24	3.04
P_2O_5	0.68	0.66	0.37	0.79	0.8	0.57	0.24	0.2	0.26	0.28	0.26	0.56	0.28	0.07	0.2	0.21	0.14	0.16	0.15	0.16	0.15	0.22
LOI	3.23	2.77	9.16	6.54	6.39	5.85	5.7	2.39	10.3	4.08	3.16	1.39	0.85	4.54	4.16	2.62	2.00	2.31	3.16	2.47	5.47	3.62
SUM	99.0	99.9	98.1	98.4	98.4	99.1	98.5	98.6	98.8	99.7	99.8	99.3	99.8	98.6	98.0	98.1	98.7	98.7	98.3	98.6	96.2	99.5
ppm																						
Ba	1000	343	72	83	150	299	227	514	140	337	574	259	186	1280	534	1080	957	870	996	1000	1050	948
Rb	30	28	<10	<10	22	11	36	39	11	<10	52	34	22	214	84	154	106	82	100	87	90	130
Sr	147	170	166	86	77	113	293	122	326	295	19	232	213	90	226	109	163	212	130	150	263	86
Y	36	37	<10	39	38	18	<10	20	11	26	29	<10	<10	123	39	62	50	58	65	52	37	49
Zr	372	339	196	480	485	292	142	81	159	170	160	138	57	406	323	299	235	352	359	243	299	217
Nb	54	46	34	66	64	47	24	5	27	24	24	43	20	41	18	20	21	29	48	19	25	24
Cr	32	26	24	26	25	21	51	141	32	35	41	91	90	36	75	67	53	59	51	73	67	56
Ni	24	26	36	26	29	26	37	60	29	32	73	7	5	13	16	21	13	20	16	16	19	18
Cu	32.5	27.6	79.1	31.2	38.1	25.1	31.4	58.7	32.9	30.5	155	3.6	3.3	14.5	10.5	15	10.7	19.5	13.9	15.1	10.5	10.6
Zn	174	158	748	191	205	119	94.2	65	107	118	95.1	52.8	23.6	132	77.4	72.7	68.2	112	115	77	87.6	70.1
Pb	2	2	300	4	6	1	1	8	4	2	22	4	6	30	18	20	36	14	12	20	18	6
As	6	11	51	23	22	3	17	47	3	37	120	3	3	23	6	5	7	29	9	6	2	20

NOTES: BB = Boucher Brook Formation, FLB = Flat Landing Brook Formation, NF = Nepisiguit Falls Formation, mv = mafic volcanic, gb = gabbro, rms = red manganiferous siltstone/shale, rhy = rhyolite, tuff = crystal tuffs. The samples were crushed and then pulverized in a chrome steel swing mill. The major and trace elements (Ba, Rb, Sr, Y, Zr, and Nb) were determined by X-ray fluorescence spectrometry on fused disks, loss on ignition (LOI) based on weight difference after heating to 900°C and Cr, Ni, Cu, Zn, Pb, and As by direct coupled plasma (DCP) spectrometry at X-ray Assay Labs, Don Mills, Ontario.

(363.2 to 625.1 m) has slightly higher Cr and Ni and lower TiO_2, P_2O_5, Zr, and Nb contents compared to the western mafic package and, therefore, they are not directly correlative. The basalts and associated gabbros (Fig. 8) are very Fe-rich and have an alkalic affinity like the correlative Brunswick alkali basalts and associated intrusive equivalents (see Whitehead and Goodfellow, 1978; van Staal, 1987; van Staal et al., 1991; Clarke, 1994; Lentz and van Staal, 1995; Lentz et al., 1995a) and probably reflect various degrees of chemical evolution in the back-arc rift volcanism (see van Staal et al., 1991). There are differences in the Mn contents in various parts of the Boucher Brook sequence that are probably of paleoenvironmental significance. The composition of the Mn-Fe Boucher Brook sedimentary rocks is similar to red manganiferous siltstone/slate analyzed elsewhere in the Bathurst Camp (Lentz et al., 1995b).

The felsic volcanic rocks are dominantly dacite and rhyodacite in composition (Fig. 8a, b). The lower SiO_2 compositions (Fig. 8a) of some of the Nepisiguit Falls felsic crystal tuffites is a function of the silica-leaching associated with cryptic chlorite alteration. The majority of the slightly altered felsic volcanic rocks have compositions typical of the Nepisiguit Falls and Flat Landing Brook formations (Lentz and Goodfellow, 1992b). Exceptions to these are two analyses of aphyric fragmented rhyolite dykes (samples 107 and 109; Table 1; Fig. 8), which cut the top of the Flat Landing Brook

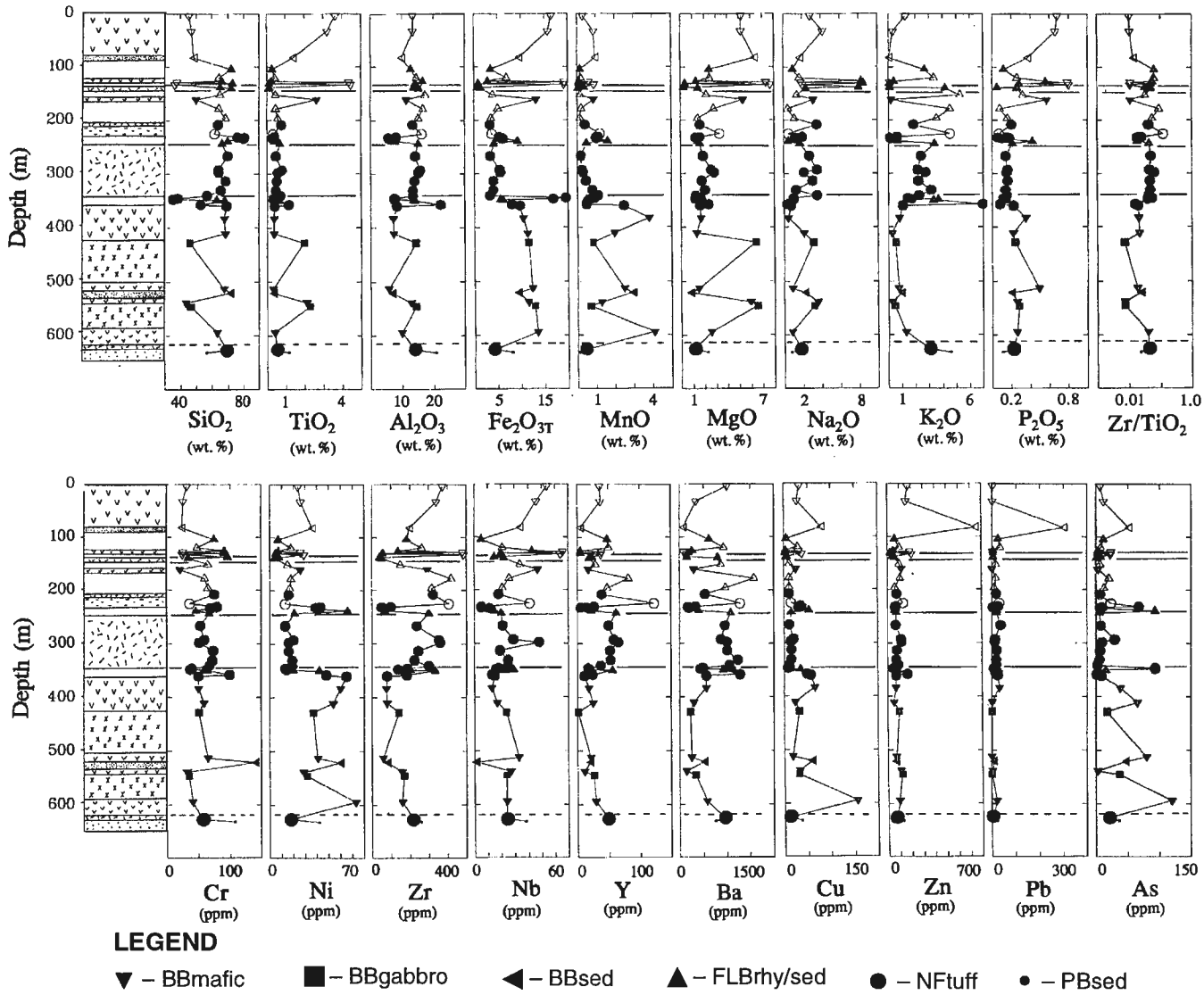

Figure 7. *Major- and trace-element compositional profiles of whole-rock compositional data (Moore, 1992a) for DDH 120-2, Brunswick Extension "A" property, Bathurst Camp, New Brunswick. BB – Boucher Brook Formation, FLB – Flat Landing Brook Formation, NF – Nepisiguit Falls Formation, PB – Patrick Brook Formation, BH – Brunswick Horizon (inferred). x – felsic rhyolite dike. Filled symbols – massive or monolithic breccia, Open symbols - heterolithic breccias.*

sequence. They have anomalously high sodium content, which could be interpreted as spilitic/keratophyric alteration, except that the surrounding rocks do not have similar sodic contents. These sodic felsic dykes also have Zr and Y contents lower than typical Flat Landing Brook rhyolite and Nepisiguit Falls crystal tuffs (Fig. 8). The low Y contents (below detection limit) result in a high Nb/Y ratio if plotted (Fig. 8b) at half detection limit (i.e. 5 ppm Y). In a trench near the collar of drillhole 120-2, an aphyric rhyolite dyke cuts basalts (Paul Moore, pers. comm.), therefore the rhyolite is younger than the Flat Landing Brook rocks and may be related to the Boucher Brook package.

Overall, there is minimal alteration in the crystal tuffites ($Na_2O>1$) with feldspar phenoclasts evident throughout (Fig. 7). Regardless of the host lithology though, the hanging wall rocks to the inferred Brunswick Horizon are high in manganese, which may be of paleoenvironmental significance. To a lesser extent, Zn, Pb, As, and Cu are anomalous around the inferred Brunswick Horizon (Fig. 7) suggesting that there is some base-metal remobilization.

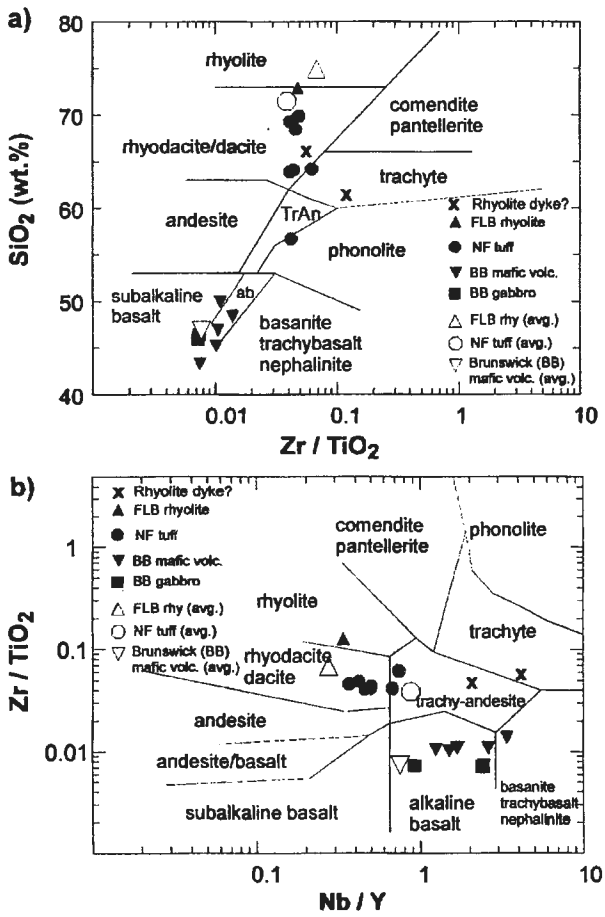

Figure 8. Comparison of geochemical composition of selected mafic and felsic rocks (Table 1; Moore, 1992a) with some analyses from the Brunswick Belt. a) SiO_2 versus Zr/TiO_2 and b) Zr/TiO_2 versus Nb/Y compositional discrimination plot (Winchester and Floyd, 1977). FLBrhy (avg.) – Flat Landing Brook rhyolite; NFtuff (avg.) – Nepisiguit Falls tuff (McCutcheon, 1992; Lentz and Goodfellow, 1992a); Brunswick mafic volcanic (avg.) (van Staal et al., 1991).

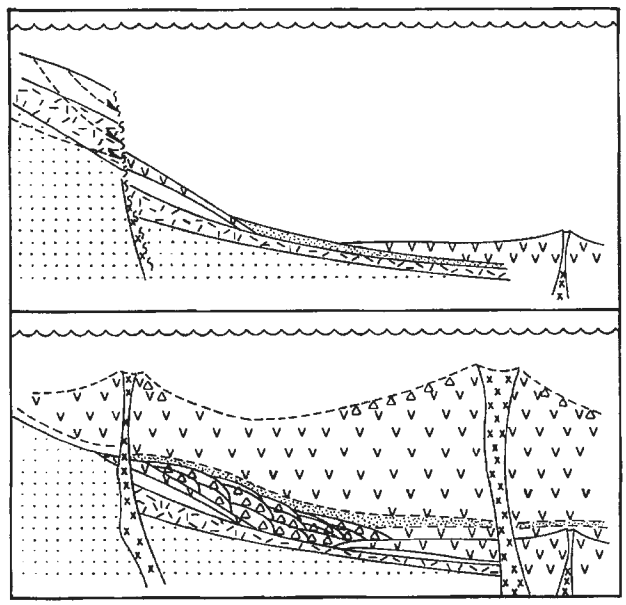

Figure 9. Schematic interpretation of the origin of these submarine debris flows north of the Brunswick No. 12 deposit and resulting stratigraphic relationships. Symbols are same as used in Figure 3. The upper part of the diagram illustrates the possible pre-slump geology of the basin, whereas the lower part of the diagram illustrates post-slump geology that was followed by the extrusion of basalts.

DISCUSSION

If the interpretation of the structural geometry and stratigraphy is correct, unfolding of the large-scale and small-scale folds would show that the upper part of the Nepisiguit Falls, the Flat Landing Brook, and Boucher Brook package are absent in the eastern-most sequence with mafic rocks directly overlying Nepisiguit Falls crystal tuff. Farther to the north, the Boucher Brook manganiferous sedimentary rocks are separated from the Miramichi Group sedimentary rocks by a gabbro dyke inferred to be a fault.

The thick sequence of hanging wall heterolithic breccias (Flat Landing Brook and Boucher Brook formations) to the west are geologically consistent with submarine, volcanic-related, debris flows (see Easton and Johns, 1986; Laznicka, 1988) similar to olistostromes originating from slumps or fault-scarps. The occurrence of mafic breccias, particularly at the base of the basalt sequence but also locally within the felsic breccias, suggests that faulting and/or seismic activity resulting from eruption of the alkalic mafic volcanic rocks may have been responsible for the slumping. A synvolcanic fault that formed or was re-initiated during mafic volcanism could have produced the topographic relief necessary to

initiate debris flows, although normal topographic relief within a caldera may have been enough also. Figure 9 schematically illustrates several possible slip lines (dashes, upper part) that would have contributed to the generation of gravity-induced debris flows. The slumps would have flowed westward into the deeper part of the basin. The various stratigraphic relationships observed in the area imply that the Boucher Brook alkaline basalts and associated sedimentary rocks were deposited after these flows (dashed, lower part; Fig. 9). If a massive-sulphide deposit formed along the eastern Brunswick Horizon (now the eastern limb of the F_2 syncline), it would be resedimented within the breccias of the hanging wall sequence to the west. However, the minimal alteration in the crystal tuffs sequence (feldspar evident, moderate Na_2O content, etc.) does not support this interpretation. Nonetheless, similar types of debris flows elsewhere along the stratigraphy may have redistributed massive-sulphide deposits analogous to the processes that formed the sulphide-rich debris flows typifying several of the Buchans massive-sulphide deposits in Newfoundland (Thurlow and Swanson, 1981, Kirkham and Thurlow, 1987).

The high Mn contents in the easternmost (lower drill intersected unit) mafic package could be a function of the intense siderite alteration, whereas the manganiferous Boucher Brook sedimentary rocks are consistent with formation in oxidized shallow water conditions (Table 1). The lower Mn contents in the western mafic sequence and the thicker breccia (debris flow) and Boucher Brook sedimentary sequence are consistent with a deeper basinal setting. The high proportion of siderite alteration and possibly siderite-rich exhalite along the western-most extent of the Brunswick Horizon is considered favourable as an exploration target because siderite saturation occurs under relatively reducing conditions. The occurrence of reddish (manganiferous) slate overlying pyritic exhalite (Fig. 6) is atypical of the Brunswick Horizon and, like the Fe-Mn Boucher Brook sedimentary rocks in the basalts, probably formed in a relatively oxygenated environment (Lentz et al., 1995b).

ACKNOWLEDGMENTS

Brunswick Mining and Smelting Limited financially supported some of the investigation presented here. Discussions with Bill Luff (chief geologist, Brunswick Mining and Smelting Limited), Gordon Clarke (formerly University of New Brunswick), Steve McCutcheon, Paul Moore (Teck Exploration Limited) and Cees van Staal helped distill some of the ideas presented. Richard Lancaster help prepare some of the figures. The manuscript was reviewed by John Langton, Steve McCutcheon, Paul Moore, and Neil Rogers.

REFERENCES

Brooks, E.A.
1984: Brunswick Mining and Smelting Limited, Assessment report on mining lease 1179, Project 120, Theriault Gate Property; New Brunswick Department of Natural Resources and Energy, Assessment File No. 473083.

Clarke, G.T.
1994: Stratigraphy and lithogeochemistry of the north end zone Zn-Pb-Cu-(Ag) deposit, Bathurst New Brunswick, Canada; M.Sc. thesis, University of New Brunswick, Fredericton, New Brunswick, 199 p.

Easton, R.M. and Johns, G.W.
1986: Volcanology and mineral exploration: the application of physical volcanology and facies studies; in Volcanology and Mineral Deposits, (ed.) J. Wood and H. Wallace, Ontario Geological Survey, Miscellaneous Paper 129, 2-40.

Hussey, J.J.
1992: Deep exploration of the "Brunswick Horizon", Bathurst District northern New Brunswick; Exploration and Mining Geology, v. 1, p. 187-195.

Kirkham, R.V. and Thurlow, J.G.
1987: Evaluation of a resurgent caldera and aspects of ore deposition and deformation at Buchans; in Buchans Geology, Newfoundland, (ed.) R.V. Kirkham; Geological Survey of Canada, Paper 86-24, p. 177-194.

Laznicka, P.
1988: Breccias and coarse fragmentites: petrology, environments, associations, ores; Developments in Economic Geology, v. 25, 831 p.

Lentz, D.R. and Goodfellow, W.D.
1992a: Re-evaluation of the petrology and depositional environment of felsic volcanic and related rocks in the vicinity of the Brunswick No. 12 massive sulphide deposit, Bathurst Mining Camp, New Brunswick; in Current Research, Part E; Geological Survey of Canada, Paper 92-1E, 333-342.
1992b: Re-evaluation of the petrochemistry of felsic volcanic and volcaniclastic rocks near the Brunswick No. 6 and 12 massive sulphide deposits, Bathurst Mining Camp, New Brunswick; in Current Research, Part E; Geological Survey of Canada, Paper 92-1E, 343-350.

Lentz, D.R., Goodfellow, W.D., and Moore, C.
1995a: The geological significance of the alkalic gabbro in the immediate hanging wall to the Brunswick No. 12 massive sulphide deposit, Bathurst, New Brunswick; in Current Research 1995-E; Geological Survey of Canada, p. 233-243.

Lentz, D.R., McCutcheon, S.R., and Walker, J.A.
1995b: Preliminary geochemical interpretation of metalliferous sedimentary rocks in the Miramichi Anticlinorium, New Brunswick; in Current Research 1994, (comp.) S.A. Merlini; New Brunswick Department of Natural Resources and Energy, Minerals and Energy Division, Miscellaneous Report 18, p. 93-113.

Lentz, D.R. and van Staal, C.R.
1995: Predeformational origin of massive sulfide mineralization and associated footwall alteration at the Brunswick No. 12, Pb-Zn-Cu deposit, Bathurst, New Brunswick: evidence from the porphyry dike; Economic Geology, v. 90, p. 453-463.

Luff, W.M.
1995: A history of mining in the Bathurst area, northern New Brunswick, Canada, Canadian Institute of Mining and Metallurgy Bulletin, v. 88, No. 994, p. 63-68.

Luff, W.M., Goodfellow, W.D., and Juras, S.J.
1992: Evidence for a feeder pipe and associated alteration at Brunswick No. 12 massive sulfide deposit; Exploration and Mining Geology, v. 1, p. 167-185.

Luff, W.M., Lentz, D.R., and van Staal, C.R.
1993: The Brunswick No. 12 and No. 6 Mines, Bathurst Camp, northern New Brunswick; in Guidebook to the Metallogeny of the Bathurst Camp, (ed.) S.R. McCutcheon and D.R. Lentz, Bathurst '93 Third Annual CIM Geological Field Conference, Trip 4, p. 75-105.

McCutcheon, S.R.
1992: Base-metal deposits of the Bathurst-Newcastle district: characteristics and depositional models; Exploration and Mining Geology, v. 1, p. 105-119.

Moore, P.J.
1992a: Assessment report on the geology, geochemistry, and geophysics of the Brunswick Extension "A" property, Gloucester County, New Brunswick; New Brunswick Department of Natural Resources and Energy, Assessment Report No. 474201.
1992b: Report of work, Brunswick Extension property, Gloucester County, New Brunswick. New Brunswick Department of Natural Resources and Energy, Assessment Report No. 474235.

Thurlow, J.G. and Swanson, E.A.
1981: Geology and ore deposits of the Buchans area, central Newfoundland; in Fifty Years of Geology and Mining, (ed.) E.A. Swanson, D.F. Strong, and J.G. Thurlow; Geological Association of Canada, Special Paper 22, p. 113-142.

van Staal, C.R. (comp.)
1985: The structure and metamorphism of the Brunswick Mines area, Bathurst, New Brunswick, Canada; Ph.D. thesis, University of New Brunswick, Fredericton, New Brunswick, 484 p.
1987: Tectonic setting of the Tetagouche Group in northern New Brunswick: implications for plate tectonic models of the northern Appalachians; Canadian Journal of Earth Sciences, v. 24, p. 1329-1351.
1992: Geology and structure of the Brunswick Mines area (21-P/5e, f); New Brunswick Department of Natural Resources and Energy, Open file Map 91-40f.

van Staal, C.R. and Fyffe, L.R.
1991: Dunnage and Gander Zones, New Brunswick: Canadian Appalachian Region; New Brunswick Department of Natural Resources and Energy, Mineral Resources, Geoscience Report 91-2, 39 p.

van Staal, C.R., Winchester, J.A., and Bedard, J.H.
1991: Geochemical variations in Middle Ordovician volcanic rocks of the northern Mirimichi Highlands and their tectonic significance; Canadian Journal of Earth Sciences, v. 28, p. 1031-1049.

Whitehead, R.E.S. and Goodfellow, W.D.
1978: Geochemistry of volcanic rocks from the Tetagouche Group, Bathurst, New Brunswick, Canada; Canadian Journal of Earth Sciences, v. 15, p. 207-219.

Winchester, J.A. and Floyd, P.A.
1977: Geochemical discrimination of different magma series and their differentiation products using immobile elements; Chemical Geology, v. 20, p. 325-343.

Geological Survey of Canada Project 940001

Unique wide-angle seismic survey samples the lithosphere beneath the Maritime Appalachians

S.A. Dehler, D.A. Forsyth[1], F. Marillier, I. Asudeh[1], I. Reid, and H.R. Jackson

GSC Atlantic, Dartmouth

Dehler, S.A., Forsyth, D.A., Marillier, F., Asudeh, I., Reid, I., and Jackson, H.R., 1996: Unique wide-angle seismic survey samples the lithosphere beneath the Maritime Appalachians; in Current Research 1996-D; Geological Survey of Canada, p. 93-99.

Abstract: The detonation of a 10 000 lb charge offshore Nova Scotia in November 1994 as part of the Canadian Patrol Frigate shock trials provided a rare opportunity to record wide-angle seismic data across the tectonic terranes beneath the Maritime provinces. Co-ordination between the Ottawa and Atlantic divisions of the GSC and the Canadian Navy resulted in the rapid planning of a 600 km-long seismic array across Nova Scotia, New Brunswick, and the Gaspésie, Quebec. Provincial departments of natural resources, universities, and GSC volunteers assisted in the deployment of 201 portable seismographs. The shot, located 300 km southeast of Halifax, was successfully recorded and the resulting record section shows clear seismic arrivals from the coast of Nova Scotia to the maximum shot-receiver offset of 900 km near Rimouski. Regional Canadian National Seismograph Network seismographs also recorded the shot. Preliminary raytrace modelling indicates a layered upper mantle structure beneath the Appalachian orogen.

Résumé : En novembre 1994, l'explosion d'une charge de 10 000 livres au large de la Nouvelle- Écosse, dans le cadre des essais aux chocs des frégates de patrouille canadiennes, a fourni une rare occasion d'enregistrer des données de sismique grand angle sur les terranes tectoniques formant les provinces de l'Atlantique. Une coordination entre, d'une part, les bureaux d'Ottawa et de l'Atlantique de la CGC et, d'autre part, la marine canadienne a permis de planifier rapidement un réseau sismique long de 600 km à travers la Nouvelle- Écosse, le Nouveau-Brunswick et la Gaspésie (Québec). Des individus des ministères provinciaux des ressources naturelles, des universités et de la CGC ont aidé au déploiement de 201 sismographes portatifs. Le tir, effectué à 300 km au sud-est de Halifax, a été enregistré avec succès et la coupe sismique obtenue montre des arrivées sismiques claires de la côte de la Nouvelle-Écosse jusqu'à la plus grande distance tir-récepteur de 900 km près de Rimouski. Les sismographes du *Canadian National Seismograph Network* installés dans la région ont aussi enregistré le tir. La modélisation préliminaire par tracé de rayons met en évidence un manteau supérieur stratifié sous l'orogène des Appalaches.

[1] Continental Geoscience Division

INTRODUCTION

The planned detonation of several large charges as part of Canadian Patrol Frigate (CPF) Shock Trial Series 825 provided a unique opportunity to record refracted seismic energy from the crust and uppermost mantle of the Appalachian orogen in Atlantic Canada. This geologically complicated region has recorded opening of the Iapetus Ocean in Late Precambrian time, terrane accretion and collision during ocean closure in the Paleozoic, and Mesozoic rifting that opened the modern Atlantic Ocean. Previous geological and geophysical observations have been used to distinguish five tectonostratigraphic zones or terranes (Meguma, Avalon, Gander, Dunnage and Humber) and three lower crustal blocks (Avalon, Central and Grenville) that generally trend east to northeast across the region (Fig. 1) (Williams, 1979; Marillier et al., 1989). Deep seismic reflection profiles across northern Maine and offshore Nova Scotia and Newfoundland have revealed significant differences in terrane structures. Information on the deep structure between these two regions is critical to understanding along-strike variations in the northern Appalachians. The seismic array was planned to extend approximately 900 km across-strike of the Appalachians from

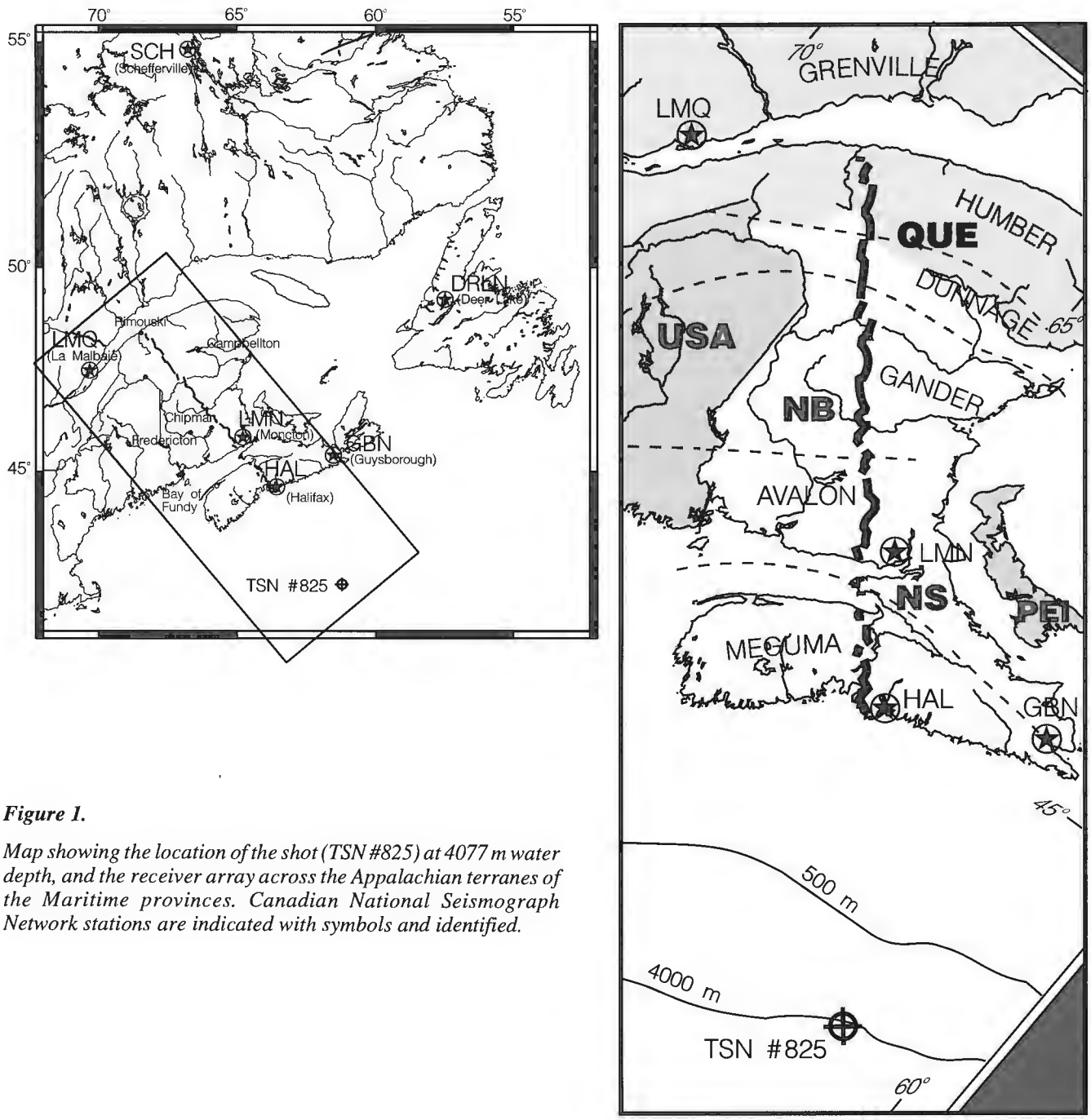

Figure 1.

Map showing the location of the shot (TSN #825) at 4077 m water depth, and the receiver array across the Appalachian terranes of the Maritime provinces. Canadian National Seismograph Network stations are indicated with symbols and identified.

the intended source location at the foot of the continental slope southeast of Halifax, Nova Scotia, to Rimouski, Quebec (Fig. 1).

FIELD PROGRAM

Data acquisition was planned and executed by a team of scientists from the Geological Survey of Canada (GSC) Atlantic and Ottawa divisions, with considerable field assistance from GSC volunteers and members of provincial natural resource departments. Receiver site surveying was conducted before and during the shock trials using GPS receivers to fix receiver locations at an accuracy of better than 100 m. The Department of National Defence (DND) was fully responsible for the planning, environmental assessment, and detonation of the charges associated with the shock trial. A system used to accurately record the ship's position and time at detonation was developed by GSC personnel and installed aboard *HMCS Halifax* (Fig. 2). The shooting schedule was worked out jointly by the GSC and the Navy shock trial team to allow programming of the many seismic receivers prior to deployment. A series of delayed recording time windows was used to compensate for the increasing shot-receiver distance along the array and thereby maximize the length of the recorded seismic signals (Fig. 3).

The 10 000 lb HBX-1 charge (ca. 15 000 lb TNT equivalent) was detonated on 18 November 1994 at approximately 42.0°N, 61.2°W, suspended at 97 m in a total water depth of 4077 m (Fig. 4). Two smaller charges detonated a few days earlier provided an opportunity to test equipment and procedures. Receivers were programmed and deployed from headquarters at the Bedford Institute of Oceanography in

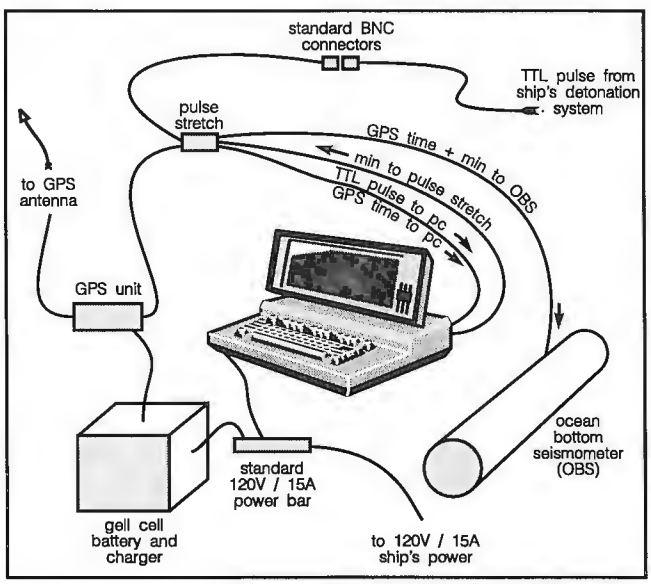

Figure 2. *GSC-Navy system interface developed to record detonation instant and position on board* HMCS Halifax. *The ocean bottom seismometer was deployed on the bridge of* HMCS Halifax.

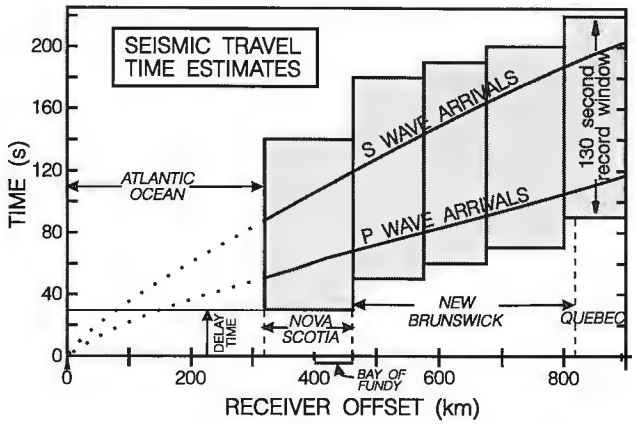

Figure 3. *Seismic traveltime estimates for P- and S-waves and recording windows delayed as shot-receiver distance increases.*

Figure 4. *Photo showing the 10 000 lb HBX-1 charge and float prior to deployment.*

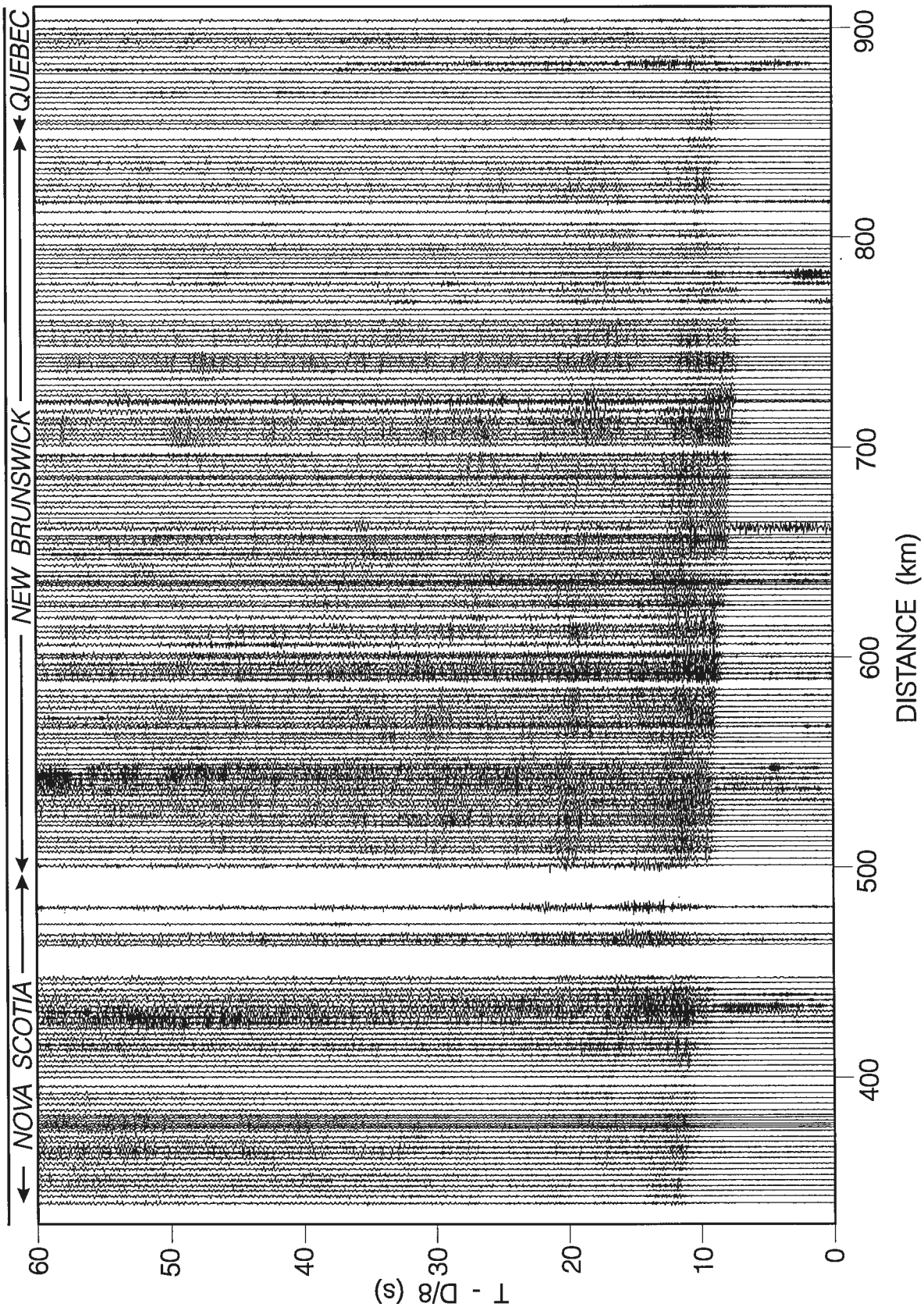

Figure 5. *Final data section of the vertical component after removal of high energy and high frequency noise, and 5-10 Hz filtering.*

Dartmouth, Nova Scotia, and from motels located in Chipman and Campbellton, New Brunswick (Fig. 1). The LithoSEIS programming and processing system (Asudeh et al., 1993) was used to program the digital Portable Recording Seismographs (PRSs) and recover the recorded information. A total of 201 instruments, including 25 3-component PRS4s, were deployed along the 565 km land segment at 2.5 km intervals to form a continuous northwest-trending profile across the Appalachians (Fig. 1).

DATA PROCESSING

Details of the processing procedure are included in Asudeh et al. (1995), and a quick overview is provided here. Each portable recording seismograph provided a 128 s long vertical component seismic record, with the PRS4s also providing data from two horizontal component sensors. The records were sorted by offset distance and reduced with a velocity of 8.0 km/s to produce seismic traces for the 0-128 s window following detonation. Processing was carried out at the GSC Ottawa seismology lab using the LithoSEIS and Landmark Insight software packages. Static shift corrections were applied to correct for drift of the portable recording seismograph internal clocks, and high frequency, high amplitude noise bursts that exceeded a derived threshold energy level were removed. These procedures considerably improved the raw data. Further enhancement was realized by applying a 5-10 Hz bandpass filter. The final record section (first 60 seconds) is shown in Figure 5.

CANADIAN NATIONAL SEISMOGRAPH NETWORK DATA

The shock trial detonation was also recorded at six stations of the Canadian National Seismograph Network (CNSN) (locations shown in Fig. 1). Seismic energy released by the detonation had an equivalent Richter magnitude of 2.7-3.1. Signals recorded at stations near the refraction array, such as Halifax (HFX) and Moncton (LMN), are very similar to the energy recorded by the portable recording seismographs. The farthest station was located in Schefferville, Quebec (SCH) at an offset distance of almost 1500 km. The signal-to-noise ratio of the seismic record is remarkably high and both primary (P) and later (X) arrivals are clearly seen (Fig. 6). Recordings of the shock trial detonation, which has a known charge size, location, and shot time, should prove extremely useful in calibrating these six seismograph stations.

PRELIMINARY INTERPRETATION

Forward raytrace modelling has been used to develop a simple crustal and upper mantle model for the refraction profile. Traveltimes and ray paths are calculated for 2-dimensional models with layered velocity structure (e.g. Reid, 1993). The velocities and model geometry are iteratively varied until the calculated arrival times agree with the observed seismic arrivals. Limited assumptions can be made about dipping layer boundaries because of the restrictions imposed by a single seismic source, but raytracing nonetheless allows us to look for variations in the thickness and velocity of lithospheric layers along the length of the profile.

A preliminary model is shown in Figure 7. The geometry shown is very simple, with a single layer representing continental and oceanic crust, and a stratified upper mantle. The crustal layer is based on results of previous seismic experiments in the area, as these data cannot constrain shallow structure. The continental crust as shown increases steadily in thickness from the continent-ocean boundary to a relatively constant thickness of 40 km beneath New Brunswick. The base of lithosphere is interpreted as lying at the relatively shallow depth of 85 km, and refractions through the lowermost lithosphere produce the strong set of first arrivals between 450 and 800 km distance. A low velocity zone (LVZ) appears to underlie the lithosphere, and velocities of 8.1 to 8.4 km/s will satisfy the arrival times. Synthetic amplitude modelling may help identify this layer.

Of particular interest in this model is the interpreted upper mantle velocity discontinuity at 60-70 km depth. This boundary, with a velocity contrast of approximately 0.4 km/s, produces a set of reflections that correspond in time with arrivals near 11.5 s at 350 km (Fig. 5, 6). An upper mantle reflection with similar depth and velocity contrast is observed under the Newfoundland Appalachians (Hughes et al., 1994; D. Chian et al., pers. comm.). The velocity discontinuity thus appears to be a regional feature, but it is unclear whether it is also a structural boundary. Several deep seismic reflection sections off Nova Scotia and Newfoundland have shown faults and other features cutting across the interpreted Moho into the upper mantle (e.g. Marillier et al., 1989; Keen et al., 1991), implying continuity between the Appalachian crustal blocks and at least the uppermost mantle. The velocity boundary may possibly be a feature of the lower lithosphere of the Appalachian terranes, or it may be a residual of the rifting process that formed the present Atlantic Ocean basin. Additional processing of the data should enhance these arrivals and permit better definition of this boundary.

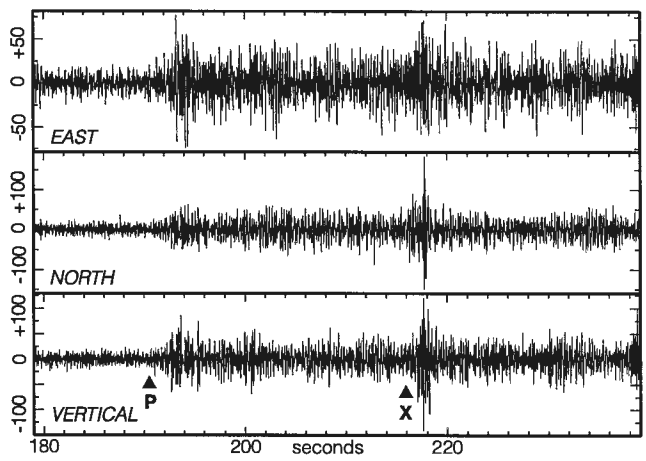

Figure 6. *Record section from CNSN station at Schefferville, Québec. Amplitude is scaled in nm/s. Time scale is referenced to shot time of 1205h ADT (16:05:00.00 UT).*

CONCLUSIONS

This study represents a very successful collaborative effort between divisions of the GSC, the Canadian Patrol Frigate Shock Trial planners and Navy personnel, and numerous others from provincial natural resource departments and universities. The collaboration has yielded a unique data set that would have been very difficult to acquire by GSC personnel alone. Energy from the shock trial detonation has passed through the upper mantle beneath the Maritime Appalachians and reached depths in excess of 100 km, well beyond the depth range of typical crustal refraction surveys. Preliminary modelling suggests that we may be able to distinguish several upper mantle velocity layers. A full-scale interpretation of these data in light of previous interpretations and future geophysical and geological observations will aid our

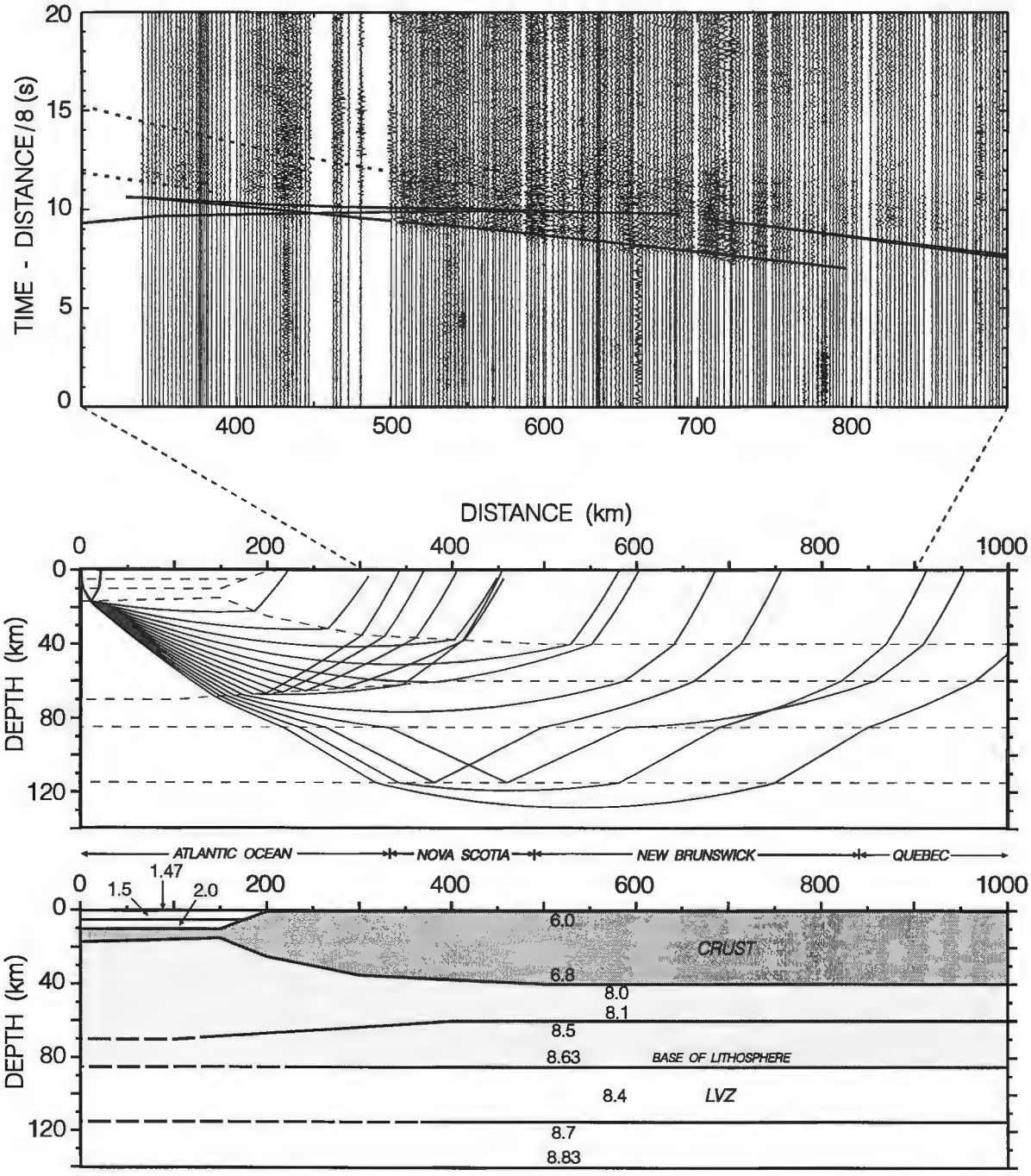

Figure 7. *Preliminary raytracing model and arrival time plot superimposed on first 20 s of recorded data. Velocities given in km/s. LVZ is low velocity zone.*

understanding of the complicated relationships between the structural terranes and the deeper parts of the lithosphere that underlie Atlantic Canada.

ACKNOWLEDGMENTS

This survey would have been impossible without the considerable field assistance provided by a team of over 30 people including GSC scientists from Dartmouth, Ottawa, and Quebec, members of the Natural Resources departments of Nova Scotia and New Brunswick and the Ministère de l'Énergie et des Ressources du Québec, and university students and others registered with the GSC Volunteers Program. The notable efforts of Cdr. D. Sweeney and crew of *HMCS Halifax*, Cdr P. Hoes at Maritime Command, Halifax, LCdr S. Garon, Lt(N) D. Spagnolo, Mr. J. Czaban, and Mr. I. Kotecki of the CPF Shock Trial Team, Lt(N) J. Ford on *HMCS Preserver* and the CPF Project Management Office, Ottawa, are gratefully acknowledged. The GSC-Navy interface system to obtain precise timing and shot positioning information was developed and deployed by D. Heffler, D. Sharon and R. Schieman. We thank Bowaters Mersey Paper Co. Ltd., Fraser Inc., and the many private citizens who graciously provided access to deploy instruments along private roads and property.

REFERENCES

Asudeh, I., Wetmiller, R., and Spencer, C.
1993: The LithoSEIS User Manual; Geological Survey of Canada Open File 2679.

Asudeh, I., Dehler, S., Forsyth, D., Jackson, R., Marillier, F., Reid, I., Cartwright, T., Heffler, D., Schieman, R., and Sharon, D.
1995: Seismic data from the Canadian Patrol Frigate Shock Trial CPF Trial Series #825; Geological Survey of Canada Open File 3110, 78 pp.

Hughes, S., Hall, J., and Luetgert, J.H.
1994: The seismic velocity structure of the Newfoundland Appalachian orogen; Journal of Geophysical Research, v. 99, p. 13,633-13,653.

Keen, C.E., MacLean, B.C., and Kay, W.A.
1991: A deep seismic reflection profile across the Nova Scotia continental margin, offshore eastern Canada; Canadian Journal of Earth Sciences, v. 28, p. 1112-1120.

Marillier, F., Keen, C.E., Stockmal, G.S., Quinlan, G., Williams, H., Colman-Sadd, S.P., and O'Brien, S.J.
1989: Crustal structure and surface zonation of the Canadian Appalachians: Implications of deep seismic data; Canadian Journal of Earth Sciences, v. 26, p. 305-321.

Reid, I.
1993: Velocity structure of reflective lower crust beneath the Grand Banks of Newfoundland; Journal of Geophysical Research, v. 98, p. 9845-9859.

Williams, H.
1979: Appalachian Orogen in Canada; Canadian Journal of Earth Sciences, v. 16, p. 792-807.

Geological Survey of Canada Project 870038

Magnetic anomalies of the Arctic and North Atlantic regions

Ron Macnab, Jacob Verhoef, Walter Roest[1], Jafar Arkani-Hamed[2], and Members of the Project Team

GSC Atlantic, Dartmouth

Macnab, R., Verhoef, J., Roest, W., Arkani-Hamed, J., and Members of the Project Team, 1996: Magnetic anomalies of the Arctic and North Atlantic regions; in Current Research 1996-D; Geological Survey of Canada, p. 101-108.

Abstract: A new database of magnetic observations has been developed as a resource for investigating continental margin development and seafloor spreading history in the Arctic and North Atlantic oceans. Containing about 40 000 000 data points, the database was constructed from numerous sets of digital profiles, grids, and maps obtained from 38 organizations in 15 countries. All data sets were carefully reviewed and processed to maximize their degree of homogeneity when merged to produce a 5 km grid. A map produced from this grid offers an unprecedented portrayal of the magnetic field over the continents and oceans of the study area, and facilitates characterizations of major tectonic elements.

Résumé : Une nouvelle base de données magnétiques a été montée dans le but d'analyser comment s'est formée la marge continentale et de reconstituer les épisodes d'expansion du plancher océanique dans l'océan Arctique et l'Atlantique Nord. La base, contenant environ 40 000 000 de points de données, a été créée à partir de nombreux ensembles numériques (profils, quadrillages et cartes) provenant de 38 organismes de 15 pays différents. Tous les ensembles de données ont été analysés et traités avec soin, afin de maximiser leur homogénéité au moment de leur fusion pour obtenir un quadrillage au mailles de 5 km de côté. Une carte, produite à partir de ce quadrillage, offre une image sans précédent du champ magnétique des continents et des océans de la région à l'étude, en plus de faciliter la caractérisation des principaux éléments tectoniques sur ce territoire.

[1] Continental Geoscience Division, Ottawa
[2] McGill University, Montreal Quebec, Canada

INTRODUCTION

A high-quality magnetic database has been developed for tectonic and mapmaking applications in a region that encompasses the Arctic and North Atlantic oceans and adjacent land areas. The database is a composite of numerous sets of magnetic observations that have been obtained in various forms from many sources, then processed and merged to create a coherent 5 km grid of magnetic anomaly values. The database will be available for public distribution in digital form in 1996, along with full documentation and regional magnetic anomaly maps.

RATIONALE FOR THE COMPILATION

The objective of the project was to develop a research tool for investigating continental margin development and seafloor spreading history in the Arctic and Atlantic oceans. A common departure point for such investigations is an examination of the crustal magnetic signatures that are imprinted in the conjugate margins of the two oceans and in the intervening seafloor. Much of the necessary magnetic information existed prior to this compilation, but it was fragmented among many locations and in a great variety of formats. Hence it was first necessary to accumulate all available sets of observations from the study region, and to merge them in a coherent fashion.

An important principle of the compilation was that it had to rely on the free exchange of information to construct a database that would eventually be released into the public domain. Many data sets were already in open circulation, and were relatively easy to obtain. Others were proprietary and could only be used on the condition that their resolution be downgraded to eliminate contents of a more detailed nature. As an incentive for making their data sets available, owners and contributors were offered access to the final grid and map products for their exclusive use at least six months before release to the general public.

THE DATABASE AND DATA HANDLING PROCEDURES

Thirty-eight organizations in 15 countries (see Table 1) contributed data in one or more forms: (1) as digital profiles representing original observations along ship tracks and aircraft flight lines; (2) as digital grids created in previous compilation projects; and (3) as paper-based contour maps and profile plots. The geographic distributions of the grid and profile data sets are shown in Figure 1, and their relative quantities are illustrated in Figure 2.

Profile data sets in digital form were reduced to anomaly values by removal of the appropriate IGRF model, and scanned with a fourth-order difference filter to detect and eliminate spiky values automatically. Initial quality assessment of shipborne data sets were produced through a statistical analysis of their crossover errors, defined as observational discrepancies at the intersections of ship tracks. Time-tagged airborne profiles were treated in a similar fashion. Observations collected during periods of high geomagnetic activity were eliminated, and corrections for ring current effects were applied. Diurnal variation corrections were applied to shipborne data, using a latitude-dependent diurnal model that was derived from an analysis of the time-varying characteristics of crossover errors. Profile crossover errors were then re-analyzed to assess the effects of corrections and to devise adjustments in order to achieve good agreement

Table 1. Sources of magnetic data.

1. Applied Geophysics Unit, University College; Galway, Ireland
2. British Geological Survey; Edinburgh, Scotland
3. British Petroleum Exploration; London, UK
4. Bullard Laboratories, Cambridge University; Cambridge, UK
5. Bundesanstalt fur Geowissenschaften und Rohstoffe; Hannover, Germany
6. Centro de Geofisica de Universidade de Lisboa; Lisbon, Portugal
7. Conoco Inc.; Ponca City OK, USA
8. Defence Research Establishment Pacific; Victoria BC, Canada
9. Department of Energy of the Republic of Ireland; Dublin, Ireland
10. Dublin Institute for Advanced Studies; Dublin, Ireland
11. Falconbridge Ltd.; Windsor NS, Canada
12. Geologian Tutkimuskeskus; Espoo, Finland
13. Geological Survey of Canada (Atlantic); Dartmouth NS, Canada
14. Geological Survey of Canada (Ottawa); Ottawa ON, Canada
15. Grant Institute of Geology, University of Edinburgh; Edinburgh, Scotland
16. Gronlands Geologiske Undersogelse; Copenhagen, Denmark
17. IFREMER Centre de Brest; Brest, France
18. Institut du physique du globe, Universite de Paris VI; Paris, France
19. Institute for Aerospace Research; Ottawa, Canada
20. Institute of Oceanographic Sciences; Wormley, UK
21. Instituto de Geologia Jaume Almera; Barcelona, Spain
22. Instituto Geografico Nacional; Madrid, Spain
23. Lamont Doherty Earth Observatory; Palisades NY, USA
24. Norges Geologiske Undersokelse; Trondheim, Norway
25. Petro-Canada Resources Limited; Calgary AB, Canada
26. Raunvisindastofnun Haskolans; Reykjavik, Iceland
27. Royal Netherlands Navy; The Hague, The Netherlands
28. SEVMORGEOLOGIA; St. Petersburg, Russia
29. Shirshov Institute of Oceanology; Moscow, Russia
30. SPbF IZMI RAN, St. Petersburg, Russia
31. Sveriges Geologiska Undersokning; Uppsala, Sweden
32. University of Liverpool; Liverpool, UK
33. US Geological Survey; Woods Hole MA, USA
34. US National Geophysical Data Center; Boulder CO, USA
35. US Naval Oceanographic Office; Stennis Space Center MS, USA
36. US Naval Research Laboratory; Washington DC, USA
37. Vening Meinesz Laboratorium; Utrecht, The Netherlands
38. VNIIOkeangeologia; St. Petersburg, Russia

between data sets. The overall improvement is illustrated in Figure 3, which compares shipborne crossover errors before and after corrections.

Gridded data sets in digital form featured a great variety of lineages and formats, and required customized procedures for their handling and processing. Essentially, each grid was converted to a standard format, inspected for errors and corrected as necessary, then re-sampled with a common origin and cell size. Wherever necessary and feasible, anomaly values were calculated with reference to the appropriate IGRF model.

Several data sets were obtained as contour maps and profile plots on paper. These were manually traced on a digitizing table, then converted into magnetic field values with positions expressed in latitude and longitude. Digitized contour data were gridded and grouped for further treatment with other digital grid sets, while digitized profile data were handled in a manner similar to the digital profile sets.

Prior to merging and adjustment, the different classes of constituent data sets were combined in separate sub-grids using a minimum curvature algorithm (Smith and Wessel, 1990) operating in a Transverse Mercator projection, with a central meridian of 50W and a grid spacing of 5 km.

Intermediate wavelength contents of the sub-grids sets were compared to satellite observations, and while the shipborne data sets were found to be in excellent agreement with satellite data (Arkani-Hamed et al., in press), the other data sets did not agree so well. Wavelengths greater than 400 km (i.e. the wavelengths present in satellite data) were therefore filtered out of all constituent data sets, which were then

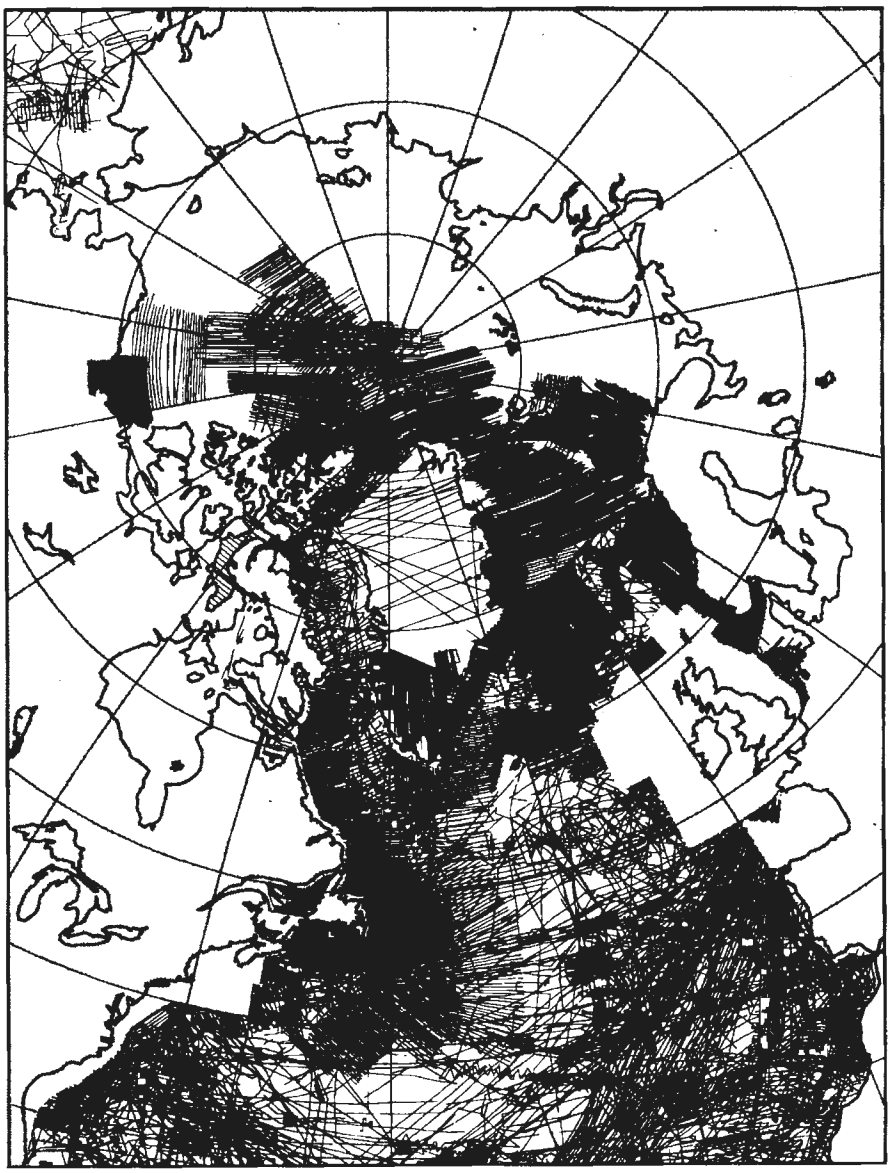

Figure 1.

Distribution of about 40 000 000 magnetic data points in the form of grids (shaded areas) and profiles of shipborne and airborne observations (lines) that were assembled at the Geological Survey of Canada (Atlantic) and combined in a coherent data base.

merged into a single grid. Various adjustment strategies were applied during this process to ensure a good match between adjacent data sets, particular care being taken to minimize contamination of the final grid through the introduction of artifacts.

REGIONAL MAP OF THE MAGNETIC FIELD

The final grid was used to produce the shaded relief map in Figure 4. Coverage is not uniform or complete throughout the map: in northern Canada and the central Atlantic, the magnetic field cannot be adequately defined because observations are sparse or nonexistent; in northwestern Europe and northern Greenland, comprehensive sets of observations are known to exist, but they were not available for incorporation in the present compilation. At the scale of reproduction, the relief map provides a regional characterization of different tectonic elements. The first-order difference between oceanic and continental regions is apparent: the magnetic field over the older continents is complex, reflecting long histories of tectonism; the magnetic field over the relatively young ocean floor is dominated by linear seafloor spreading anomalies.

The magnetic anomalies correlate directly with many structural features in the study area, as shown in Figure 5. On land, geological provinces are characterized by different magnetic signatures, reflecting their age through the degree of reworking, deformation, and metamorphic variations. The accretionary nature of many terranes and orogenic belts is easily recognized by well-defined zonations and distinctive patterns of magnetic convolutions. In North America, the Appalachian orogen displays northeast trends that reflect the convergent continental blocks and intervening oceans which formed the total orogen. Within the Grenville Front tectonic zone, the magnetic field is subdued due to tectonization and metamorphism. Distinctive magnetic anomalies are related to north-trending boundaries between the Superior, Churchill, and Nain provinces. The Makkovik Province (Labrador) and the Ketilidian mobile belt (Greenland) are separated by more recent seafloor spreading across the Labrador Sea.

In northern Russia, the magnetic field over the Uralian orogenic belt consists of numerous short-wavelength anomalies in a region along the eastern edge of the East European Craton; abrupt changes in the magnetic field coincide with

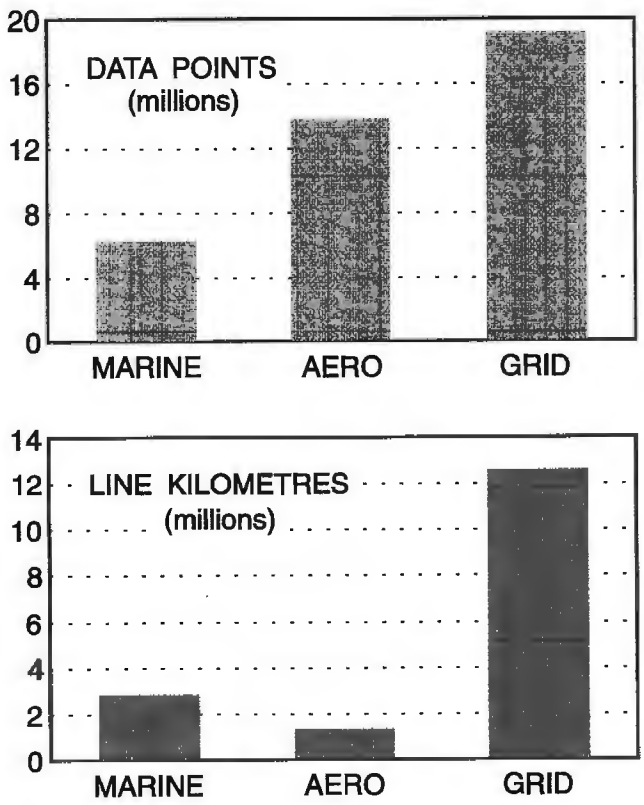

Figure 2. Histograms illustrating the relative sizes of the digital data sets that were assembled to create the database. These translate into roughly 3 000 000 line kilometres of shipborne observations (about 75 times around the earth), and 14 000 000 line kilometres of airborne profiles (more than 18 round trips to the moon). In current U.S. dollars, the replacement value of all these data sets is estimated to be $250 000 000.

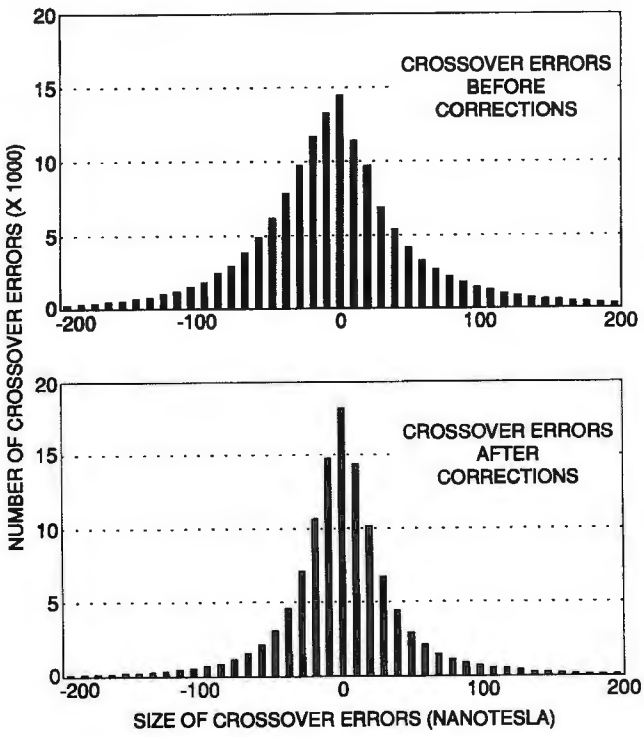

Figure 3. Shipborne profiles were subjected to extensive error checking and correction. This figure compares error distributions at track intersection points before and after corrections were applied. Before corrections, there were 147 295 crossover errors with a mean of -5 nT and a standard deviation of 61 nT. After corrections, there were 116 571 crossover errors with a mean of 0 nT and a standard deviation of 47 nT.

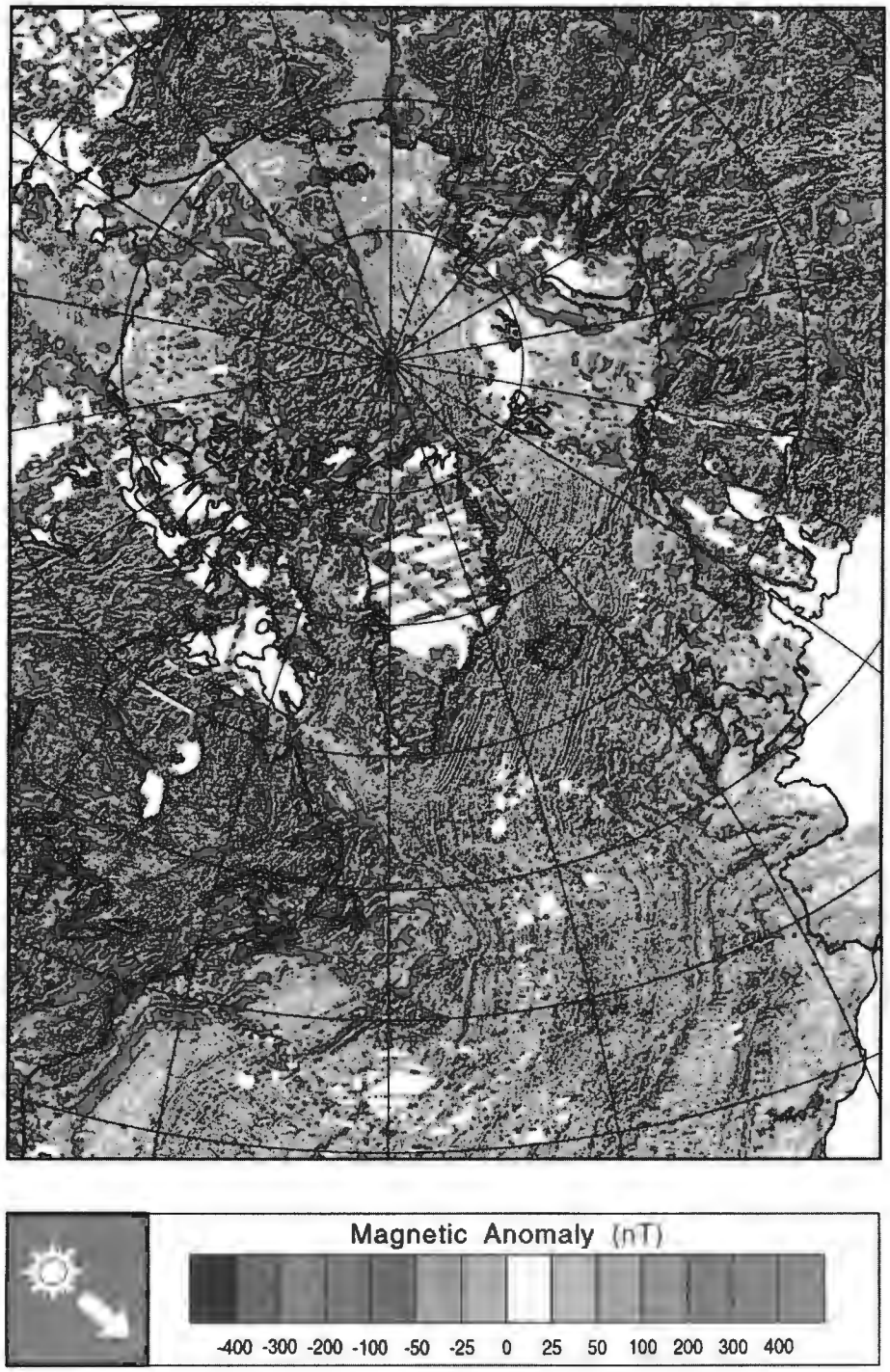

Figure 4. *Magnetic anomaly map produced at the Geological Survey of Canada (Atlantic) from an assemblage of observations that have been merged, adjusted, and gridded over a 5 km matrix. Features with wavelengths of more than 400 km have been filtered out of the final data set. The anomalies have been artificially illuminated from the upper left hand corner, which tends to emphasize features that are perpendicular or oblique to the direction of illumination. The procedure for gridding and merging the data sets included an extrapolation function for closing gaps of up to 15 km. Isolated ship tracks or aircraft flight lines therefore appear on the map as 30-km swaths, except over northern Greenland where a loose network of high-altitude airborne profiles was extrapolated to 25 km, and depicts mainly regional features. The grid and associated maps are slated for public distribution in digital form.*

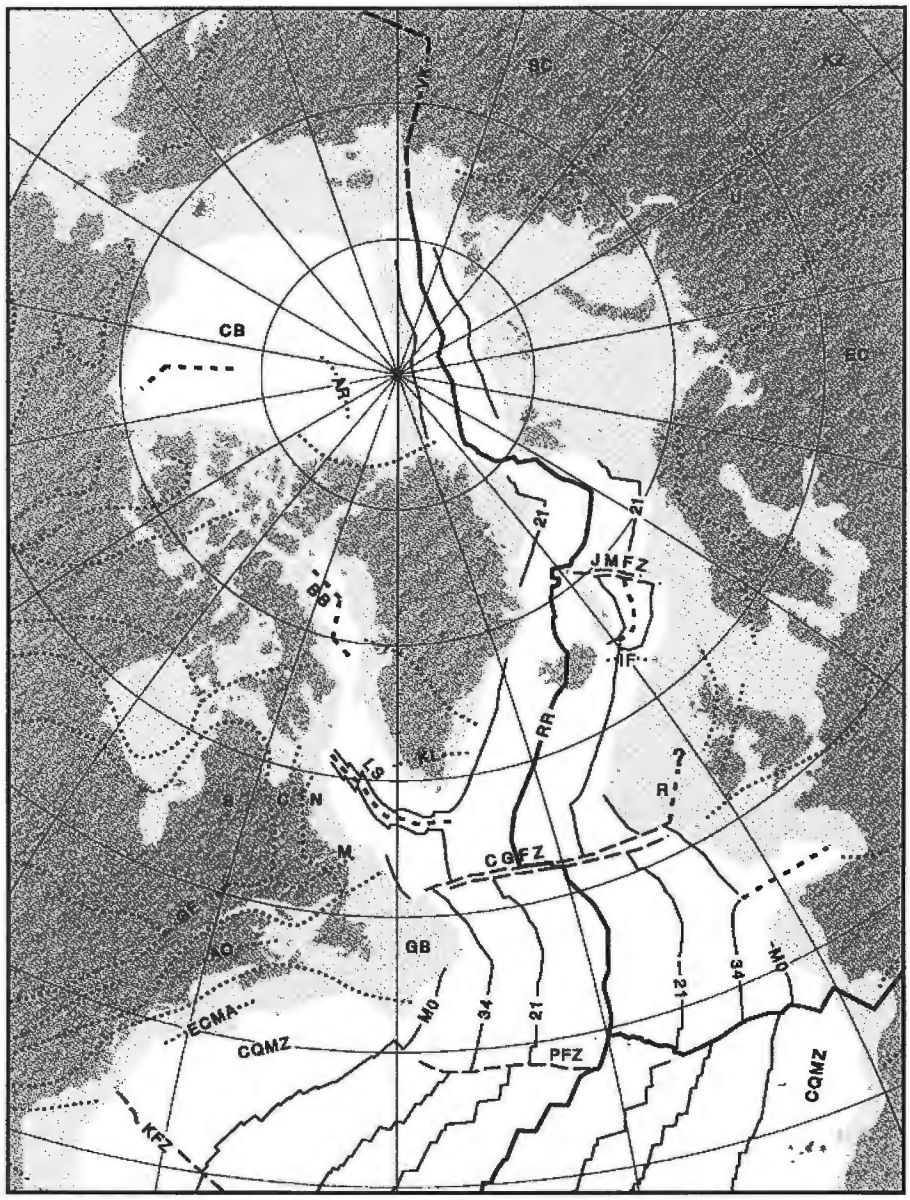

Figure 5. *Physiographic, geological, and other features of the North American Plate (left side of figure), the Eurasian Plate (central and upper right side), and the African Plate (lower right corner) – plates that are imprinted in the magnetic anomaly map of Figure 4. Thick lines are plate boundaries and/or spreading centers; thick lines with short dashes are extinct spreading centers; thin solid lines are magnetic lineations; thin dashed lines are fracture zones; thin dotted lines are major tectonic/geological boundaries or other prominent features. AO – Appalachian orogen; AR – Alpha Ridge; BB – Baffin Bay; C – Churchill Province; CB – Canada Basin; CGFZ – Charlie-Gibb Fracture Zone; CQMZ – Cretaceous Quiet Magnetic Zone; EC – East European Craton; ECMA – East Coast Magnetic Anomaly; GB – Grand Banks of Newfoundland; GF – Grenville Front; IF – Iceland-Faroe Ridge; JMFZ – Jan Mayen Fracture Zone; KFZ – Kane Fracture Zone; KL – Ketilidian mobile belt; KZ – Kazakhstan accretionary continent; LS – Labrador Sea; M – Makkovik Province; N – Nain Province; PFZ – Pico Fracture Zone; R – Rockall Plateau; RR – Reykjanes Ridge; S – Superior Province; SC – Siberian Craton; U – Uralian orogenic belt; VK – Verkhoyansk-Kolymian orogenic belt.*

two major suture zones that define the boundaries of the orogenic belt, and which remain from Late Paleozoic episodes of collision between the East European and Siberian cratons, and the Kazakhstan accretionary continent. In eastern Siberia, a broad zone of weak positive anomalies mimics the left-lateral offset of the Verkhoyansk-Kolymian orogenic belt, which formed in the early and mid-Cretaceous when numerous allochthonous terranes were amalgamated and attached to the active Eurasian margin during rapid convergence of the Izanagi-Kula and Eurasia plates (Zonenshain et al., 1991).

In the oceanic domain, the magnetic anomalies reflect first order seafloor spreading processes and are dominated by lineations and fracture zones. The classic pattern of linear anomalies along Reykjanes Ridge south of Iceland (Heirtzler et al., 1966) is a striking example. Further south, anomalies are more variable with offsets and lower amplitudes. Due to the reversal pattern of the magnetic field, oceanic fracture zones appear as a series of positive and negative discontinuities in the linear pattern of seafloor spreading anomalies. Several large offset fracture zones are visible, including the Charlie-Gibb and the Jan Mayen fracture zone pairs. Fracture zones in the Cretaceous Magnetic Quiet Zone are delineated by well-defined magnetic anomalies. In addition to these general features, the new magnetic map illustrates the complexity of seafloor spreading, as illustrated for example in ridge jumps (south of the Pico Fracture Zone), propagating rifts (the Reykjanes Ridge), major changes in seafloor spreading direction (south of the Charlie-Gibb Fracture Zone), microplate formation (Rockall Plateau), and spreading axis extinction (in the Labrador Sea). These cannot be discussed on the basis of the reduced figure, but the wealth of detail present in the database has already inspired several co-operative studies on these types of tectonic elements with original data contributors (Johnson et al., 1994; Mercuriev et al., 1994; Miles et al., in press).

In the Arctic Ocean, Figure 4 clearly illustrates the anomalous character of the seafloor magnetic anomalies in the northern and central Canada Basin. The region of the Alpha Ridge is characterized by some of the largest magnetic anomaly amplitudes observed over the deep ocean. A hot-spot model linking this region to the Iceland-Faroe Ridge, which has a similar crustal structure, has been proposed (Forsyth et al., 1986).

Seafloor spreading lineations record the separation of plates along mid-ocean ridges. The opening of the North Atlantic and Arctic oceans followed the separation of the North American, Eurasian, African, and Greenland plates, and several microplates such as Rockall Plateau, Jan Mayen, and Iberia. The results of the present compilation are not expected to drastically change recent models of first order motions of these plates, but they may help resolve uncertainties relating to the early histories of opening between the Grand Banks of Newfoundland and Iberia, and between Labrador and Greenland. The availability of magnetic data on the conjugate margins is also expected to improve our understanding of pre-rift configurations and of break-up motions. The geometry and timing of these events are key to understanding the formation of sedimentary basins that underlie the shelves, and to assessing their economic potential.

One of the least understood features in this context is the magnetic signature of the ocean-continent boundary. There is no visible, consistent signal of this important transition zone in the surface data, nor in satellite magnetic anomaly maps. Off northeastern North America, the margin is marked by a large positive anomaly, whereas the signal in the Norwegian-Greenland Sea is mixed but predominantly negative. By offering improved constraints for initial plate configurations and the timing of breakups, the new database will help explain the nature of the transition zone between continent and ocean.

CONCLUSION

The new database provides one of the most complete and coherent perspectives to date of the magnetic character of the Arctic and North Atlantic oceans, two regions that feature significant tectonic linkages and which are key to an understanding of northern hemisphere plate tectonics. By facilitating synthesis with other types of observations, the digital format of this new database promises to widen our comprehension of the processes that attended the breakup of ancient continents and the creation of intervening seafloor.

The primary product of the compilation project is a digital database in the form of a 5 km grid of magnetic anomaly values. Also available in hardcopy and computer-readable form, secondary outputs include a comprehensive project report that describes the constituent data sets and the details of their processing, ancillary grids, and colour maps at nominal scales of 1:6 million and 1:10 million for the Arctic and North Atlantic oceans, respectively. To promote their wide use and circulation, these products will be distributed in digital form; further information may be requested from the first author at macnab@agc.bio.ns.ca

ACKNOWLEDGMENTS

Members of the Project Team include: Skip Kovacs (Naval Research Laboratory, Washington D.C., U.S.A.), Serge Lévesque (now at the Atlantic Centre for Remote Sensing of the Oceans, Halifax N.S., Canada), Peter Morris (Dublin Institute for Advanced Studies, Dublin, Ireland), Gordon Oakey, Shiri Srivastava, Allen Stark (all at the Geological Survey of Canada, Dartmouth, N.S., Canada), Karl Usow, David Vardy (both at Blue Vajra Computing).

We thank many individuals affiliated with the organizations listed in Table 1, who were instrumental in transferring to us the numerous magnetic data sets that were incorporated in the final database. We appreciate also the assistance and co-operation of many other associates who gave freely of their time to discuss procedures and to review intermediate results.

REFERENCES

Arkani-Hamed. J., Verhoef, J., Roest, W.R., and Macnab, R.
in press: The intermediate wavelength magnetic anomaly maps of the North Atlantic Ocean derived from satellite and shipborne data, Geophysical Journal International.

Forsyth, D., Morel-à-l'Huissier, P., Asudeh, I., and Green, A.G.
1986: Alpha Ridge and Iceland: products of the same plume? Journal of Geodynamics, vol. 6, p. 197-214.

Heirtzler, J.R., Le Pichon, X., and Baron, J.G.
1966: Magnetic anomalies over Reykjanes Ridge, Deep Sea Research, vol. 13, p. 427-443.

Johnson, G.L., Pogrebitsky, Yu., and Macnab, R.
1994: Arctic Structural Evolution: Relationship to Paleoceanography, The Polar Oceans and their Role in Shaping the Global Environment, Geophysical Monograph Volume 85, edited by O.M. Johanssen, R.D. Muench, J.E. Overland, p. 285-294, American Geophysical Union, Washington D.C.

Mercuriev, S.A., Sotchevanova, N.A., Macnab, R., Levesque, S., and Oakey, G.
1994: Evidence for a propagating rift in Irminger Basin near Reykjanes Ridge: detailed magnetic and bathymetric investigations (abs.), EOS Transactions of the American Geophysical Union, vol. 75, no. 16, p. 131 (supp.).

Miles, P.R., Verhoef, J., and Macnab, R.
in press: Compilation of magnetic anomaly chart west of Iberia, Ocean Drilling Program Leg 149 Science Volume.

Smith, W.H.F., and Wessel, P.
1990: Gridding with continuous curvature splines in tension, Geophysics, vol. 55, p. 293-305.

Zonenshain, L.P., Verhoef, J., and Macnab, R.
1991: Magnetic Imprints of Continental Accretion in the U.S.S.R., Eos Transactions of the American Geophysical Union, vol. 72, no. 29, p. 305 and 310.

Geological Survey of Canada Project 890041

Aeromagnetic survey program of the Geological Survey of Canada, 1995-1996

R. Dumont, F. Kiss, P.E. Stone, and J. Tod
Continental Geoscience Division, Ottawa

Dumont, R., Kiss, F., Stone, P.E., and Tod, J., 1996: Aeromagnetic survey program of the Geological Survey of Canada, 1995-1996; in Current Research 1996-D; Geological Survey of Canada, p. 109-112.

Abstract: In 1995, three high-resolution, regional aeromagnetic surveys totalling 211 453 line kilometres were flown over Victoria Island, Northwest Territories, southwest Saskatchewan, and the area bordering British Columbia/Yukon Territories/Northwest Territories. All of these surveys received industry funding. Two detailed helicopter-borne electromagnetic/magnetic/gamma ray spectrometric surveys totalling 30 520 line kilometres were flown in New Brunswick and in British Columbia. These surveys were funded by the Canada-New Brunswick Cooperation Agreement on Economic Diversification and the Province of British Columbia, respectively. The program to level the Canadian aeromagnetic profile data set, for the elimination of survey boundary effects, is continuing with drape computation and levelling of surveys flown at constant altitude in Alberta and British Columbia.

Résumé : En 1995, trois levés aéromagnétiques régionaux à haute résolution couvrant 211 453 kilomètres linéaires ont été effectués au-dessus de l'île Victoria (T.N.-O.), de la partie sud-ouest de la Saskatchewan et de la région à la frontière de la Colombie-Britannique, du Yukon et des Territoires du Nord-Ouest. Ces trois levés ont été financés par l'industrie. Ont également été réalisés deux levés détaillés des propriétés électromagnétiques, magnétiques et spectrométriques (rayons gamma), à partir d'un hélicoptère qui a survolé 30 520 kilomètres linéaires au-dessus du Nouveau-Brunswick et de la Colombie-Britannique. Ces levés ont été respectivement financés par l'Entente de coopération Canada-Nouveau-Brunswick sur la diversification économique et la province de la Colombie-Britannique. L'étape suivante de ce programme, dont l'objectif est de niveler l'ensemble de données regroupant les profils aéromagnétiques du Canada de façon à éliminer les effets de frontière, consiste en un calcul suivant le relief et un nivellement des levés effectués à une altitude constante au-dessus de l'Alberta et de la Colombie-Britannique.

INTRODUCTION

The 1995-96 GSC aeromagnetic survey program included three regional aeromagnetic projects in British Columbia/ Yukon/Northwest Territories, Saskatchewan, and Victoria Island, Northwest Territories. Two detailed surveys were undertaken in New Brunswick and in British Columbia. Survey activity for 1995 is shown in Figure 1 and summarized in Table 1.

BRITISH COLUMBIA/YUKON/ NORTHWEST TERRITORIES

An aeromagnetic survey totalling 108 153 line kilometres was initiated under a consortium of three oil companies and the Geological Survey of Canada on a cost shared basis (Fig. 1, Table 1). Data within British Columbia will be released to the public in 1996, while the release of Yukon and Northwest Territories data will be made public in 1999. These data will support detailed geological mapping and future mineral exploration programs.

A helicopter-borne electromagnetic/magnetic/VLF-EM/radiometric survey totalling 8285 line kilometres of the Purcell supergroup rocks in the Kimberley area, is to be completed and compiled for publication in 1996. Funding for this survey was provided by the Province of British Columbia. The survey objectives are to search for new deposits similar to the Sullivan ore body, assist in the search for other types of mineralization, and to map basement structure relevant to base metal exploration.

Draping (computing magnetic data to a draped surface) of the constant altitude surveys over the Rocky Mountains was tested and a reference grid is being generated, in order to level the profile data to a common datum.

SASKATCHEWAN

This is the sixth phase of a multi-year program to complete the regional aeromagnetic coverage of southern Saskatchewan (Fig. 1, Table 1). The current program, comprising 49 950 line kilometres, is being funded by the Geological Survey of Canada (GSC-Ottawa and GSC-Calgary), Lithoprobe, Saskatchewan Energy and Mines (SEM), and two industry partners. Survey results will be useful for hydrocarbon and kimberlite exploration, as well as for detailed mapping of the sub-Phanerozoic basement. Consortium members receive one year exclusive use of the data, prior to release to the public.

NEW BRUNSWICK

A helicopter-borne/electromagnetic/magnetic/VLF-EM/ radiometric survey of 22 235 line kilometres covering the entire Bathurst mining camp in New Brunswick has been undertaken for completion and publication in 1996 (Fig. 1, Table 1). Funding for this survey was provided by the Canada-New Brunswick Cooperation Agreement on Economic Diversification. Survey objectives are to assist the EXTECH-II project in mapping bedrock and surficial geology, locating structures and conductors, and outlining zones of hydrothermal alteration which should lead to identification of new targets for base metal exploration.

Table 1. Aeromagnetic survey activity in 1995-96.

SURVEY	TYPE	LINE KM	LINE SPACING	ALTITUDE	YEAR OF PUBLICATION
British Columbia Yukon Northwest Territories	Aeromagnetic Total Field	51,244 31,463 13,640 11,806	800 m 800 m 800 m 800 m	305 m MTC 2,000 m ASL 1,525 m ASL 850 m ASL	1996 1999 1999 1999
Saskatchewan Phase VI 1995 (Maple Creek)	Aeromagnetic Total Field	49,950	800 m	150 m MTC	1997
Victoria Island, N.W.T. 1995	Aeromagnetic Total Field	40,300 21,000	800 m 400 m	200 m MTC	1998
British Columbia 1995-96 (Kimberley)	Aeromagnetic Frequency Domain EM Radiometric	8,285	400 m	60 m MTC	1996
New Brunswick 1995-96 (Bathurst area)	Aeromagnetic Frequency Domain EM Radiometric	22,235	200 m	60 m MTC	1996

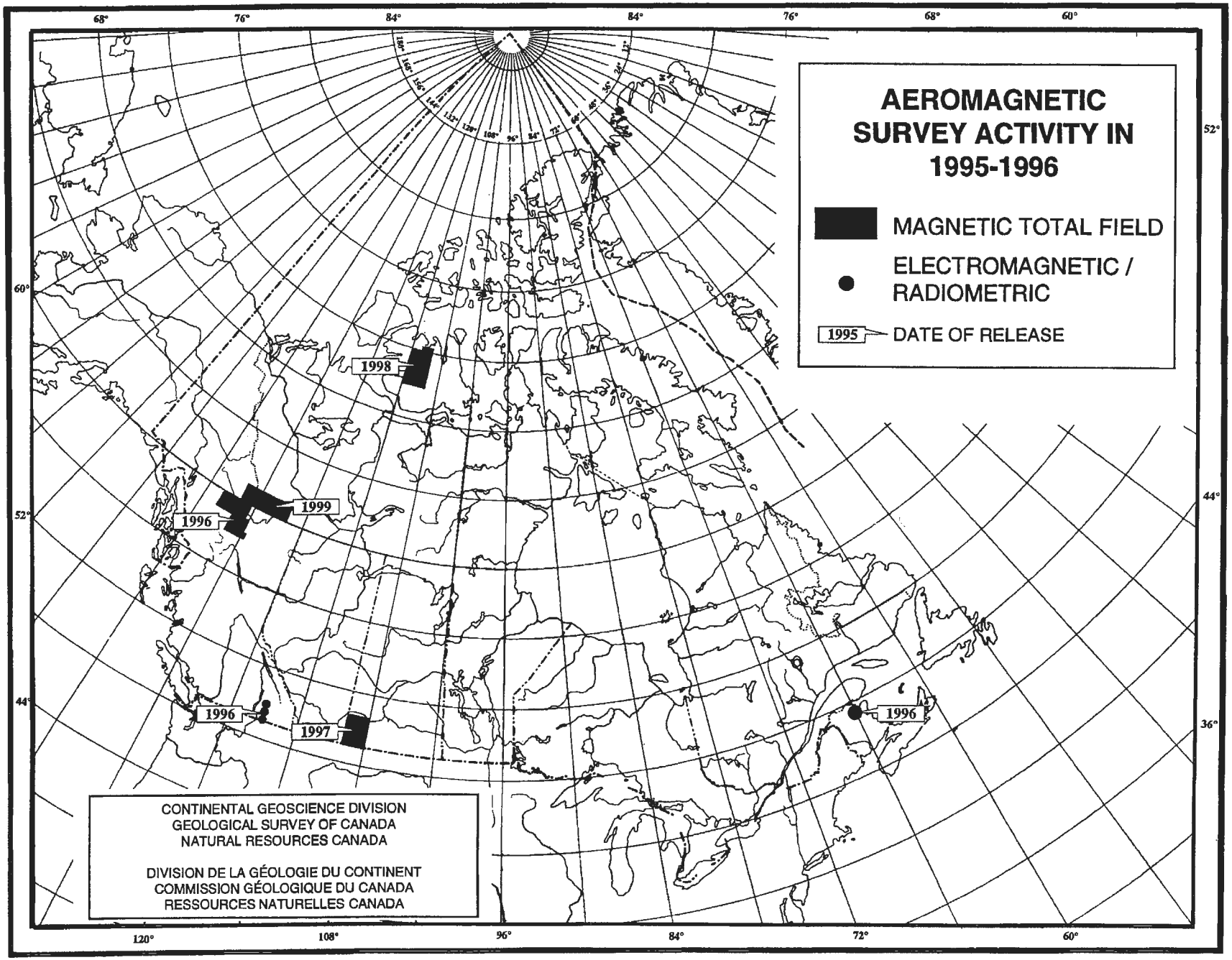

Figure 1. Aeromagnetic survey activity in 1995-1996.

NOVA SCOTIA

Compilation of the helicopter-borne magnetic gradiometer survey flown in western Cape Breton, Nova Scotia has been completed. The digital data and printed colour maps were published in 1995. Funding for this survey was provided by the Canada-Nova Scotia Cooperation Agreement on Mineral Development.

VICTORIA ISLAND, NORTHWEST TERRITORIES

A total field survey totalling 61 300 line kilometres was flown over the central part of Victoria Island in the summer of 1995 (Fig. 1, Table 1). These data will support detailed geological mapping, base metal, and kimberlite exploration programs. Two industry partners participated in a cost-sharing agreement with GSC to survey this area. The survey data is to be merged with industry data and subsequently released to the public in 1998.

Geological Survey of Canada Projects 900033, 910029, 920024, 930002, 940001, 940015, 950028

National Gravity Program of the Geodetic Survey of Canada, 1995-1996

R.A. Gibb[1] and D.B. Hearty[1]

Gibb, R.A. and Hearty, D.B., 1996: National Gravity Program of the Geodetic Survey of Canada, 1995-1996; in Current Research 1996-D; Geological Survey of Canada, p. 113-116.

Abstract: The National Gravity Program (NGP) was transferred on July 12, 1995 (with an effective date of April 1, 1995) from the Geological Survey of Canada to Geomatics Canada. During the year seven gravity surveys were completed under the National Gravity Program; two were reconnaissance surveys, one located in parts of Ellesmere and Axel Heiberg islands and in Nares Strait and the other in Victoria Strait; five were detailed surveys of geological targets including the Oak Ridges Moraine, Ontario; the Bathurst mining camp, New Brunswick; the Cumberland Basin, Nova Scotia; a transect of the Trans-Hudson Orogen in Manitoba/Saskatchewan; and an on-ice survey of the southeastern part of Great Slave Lake, Northwest Territories. A total of 5427 new gravity stations was collected during these surveys. These new data will be added to the National Gravity Database. The NGP participated in international comparisons of absolute gravimeters at the Canadian Absolute Gravity Site (CAGS) in January, 1995 and at Boulder, Colorado in July, 1995.

Résumé : Le 12 juillet 1995 (en vigueur au 1er avril 1995), le Programme national de gravimétrie (PNG) était transféré de la Commission géologique du Canada à Géomatique Canada. Au cours de l'année, sept levés gravimétriques ont été effectués dans le cadre de ce programme; ce sont les suivants : deux levés de reconnaissance, l'un dans certaines parties des îles d'Ellesmere et Axel Heiberg et dans le détroit de Nares et l'autre dans le détroit de Victoria; cinq levés détaillés de cibles géologiques, dont la moraine d'Oak Ridges (Ontario), le camp minier de Bathurst (N.-B.), le bassin de Cumberland (N.-É.), l'orogène trans-hudsonien (Manitoba et Saskatchewan, transect) et la partie sud-est du Grand lac des Esclaves (T.N.-O., levé sur glace). Les données ont été recueillies à partir d'un total de 5 427 nouvelles stations gravimétriques et seront ajoutées à la Base nationale de données gravimétriques. Les scientifiques travaillant au PNG ont participé à des comparaisons internationales de gravimètres absolus au Site de gravitmétrie absolue canadien, en janvier 1995, et à Boulder (Colorado), en juillet 1995.

[1] Geodetic Survey Division, Geomatics Canada, 615 Booth St., Ottawa, Ontario K1A 0E9

INTRODUCTION

On July 12, 1995, the national gravity program (NGP) was transferred from the GSC to Geomatics Canada (with an effective date of April 1, 1995). The transfer brings together the expertise required for improved methods of geoid determination and permits integration of the Canadian Gravity Standardization Net with the Canadian Active Control System and horizontal and vertical geodetic networks to form a new Canadian Spatial Reference Frame. Components of the NGP transferred to Geomatics Canada include: the Gravity Mapping Program, gravity standards, gravimetry and instrumentation, and the National Gravity Database. Geological target gravity surveys will be implemented by Geodetic Survey for GSC but geological interpretation of gravity anomalies will remain the responsibility of the GSC. GSC will also remain responsible for absolute gravity measurements that are part of its earthquake hazard program. Geodetic Survey will be responsible for absolute gravity measurements required for the Canadian Spatial Reference Frame and for providing absolute gravity measurements on a commercial basis to clients in Canada and abroad.

In 1995-1996, the national gravity mapping program comprised two reconnaissance surveys and detailed surveys over five geological targets. Details of these surveys and one network inspection survey to support the Canadian Gravity Standardization Net are given below. Two international intercomparisons of absolute gravimeters performed in 1995 are also described.

ELLESMERE ISLAND, AXEL HEIBERG ISLAND, NARES STRAIT SURVEY

One of the last major voids in the systematic regional gravity coverage of Canada has been filled with the establishment of 1349 new gravity stations in the period May-July 1995, on Ellesmere Island and Axel Heiberg Island and 194 stations on the ice of Nares Strait in the Canadian Arctic. A multi-agency international project was sponsored by the Mapping and Charting Subcommittee of the Canada-United States Military Cooperation Committee and was funded largely by the United States Defence Mapping Agency and the Mapping and Charting Establishment (MCE), Department of National Defence, with contributions from the National Gravity Program, Geomatics Canada (formerly with GSC), the Canadian Hydrographic Service, and the Polar Continental Shelf Project, GSC. Mapping and Charting Establishment co-ordinated the project and carried out the gravity observations and, with surveyors from the National Survey and Cadastre of Denmark (KMS), it established a precise GPS network to monitor future vertical and/or horizontal movements across Nares Strait. National Survey and Cadastre of Denmark also completed a gravity survey of parts of Greenland adjacent to Nares Strait during the same time period. The gravity data collected under this project will meet the demands of the North American Defence Plan, will contribute to an improved geoid for Canada, and will augment the National Gravity Database. The gravity data will also be used to help resolve longstanding controversial questions of plate tectonic reconstruction and geological processes in this area of possibly major transform faulting.

VICTORIA STRAIT SURVEY

An on-ice gravity survey of Victoria Strait, from the northern tip of King William Island to the southern end of Jenny Lind Island in Queen Maud Gulf, was completed in the period February 14 to April 16, 1995. The survey, which produced 425 new gravity stations at 6 km spacing, formed part of a long-term program of combined bathymetry/gravity surveys of the Canadian Arctic channels carried out in co-operation with the Canadian Hydrographic Service (Central Region) and GSC's Polar Continental Shelf Project on an annual basis.

OAK RIDGES MORAINE SURVEY

The gravity survey of the Oak Ridges Moraine, Ontario, which commenced in 1994-1995, was extended during the year to supplement last year's total of 1400 stations. By August, 1442 new gravity stations had been collected at 500 to 1000 m intervals along east-west and north-south roads in the Bolton, Alliston, Newmarket, Markham, Scugog, and Oshawa 1:50 000 NTS map areas. Gravity measurements have been made using either a Scintrex CG-3 AUTOGRAV or a LaCoste and Romberg gravimeter, horizontal positions have been scaled from 1:50 000 maps and vertical positioning has been derived from altimeter observations tied to available provincial and federal benchmarks. Data collection will continue until the end of October on the Rice Lake, Port Hope, and Trenton map areas with an anticipated total production of between 2000 and 2500 stations for the eight and one half map areas. Final modelling and interpretation of the gravity anomalies will commence at the end of December when the data processing has been completed.

The objective of this survey, sponsored and funded by GSC's Terrain Sciences Division as part of the Oak Ridges Hydrogeology Project, is to evaluate the feasibility of using gravity for mapping the bedrock surface beneath the moraine in a cost-effective way.

BATHURST MINING CAMP SURVEY

At the request of the Continental Geoscience Division, GSC, detailed gravity measurements were made over two potential ore-zones in the Bathurst mining camp, New Brunswick, in support of GSC's multidisciplinary Extech II project. Between July 5 and August 12, 1995, 353 stations were observed at 15 m intervals along seven cut-lines averaging 600 m in length in the Willett property and 271 stations were observed at 25 m intervals along six cut-lines averaging 1 km in length in the Canoe Landing Lake area. In addition, 80 fill-in regional stations were observed at the Willett, Canoe Landing Lake, Half Mile Lake, and Key Anacon properties. The majority of gravity measurements were made with a

Scintrex CG-3 AUTOGRAV gravimeter using locally established control, tied to the Canadian Gravity Standardization Net. Horizontal and vertical positioning for stations along cut lines were supplied by private contractor, while positioning for the regional stations was determined from differential GPS using TurboRogue SNR-8000 model receivers. Terrain corrections out to a radius of 53.24 m were computed for selected stations in the Willett property.

CUMBERLAND BASIN SURVEY

A detailed gravity survey was conducted in the Cobequid Mountains area of Nova Scotia between October 8 and October 15, 1995 in response to a request from GSC Atlantic in Dartmouth. Gravity and GPS observations were made at 464 points at 200 m intervals along eight profile lines varying from 5 to 24 km in length. Gravity measurements were made using a Scintrex CG-3 AUTOGRAV gravimeter at all stations. Every tenth station was repeated for quality control. Horizontal and vertical positioning were derived from differential GPS measurements using two TurboRogue SNR-8000 receivers in rapid-static mode. Baseline lengths between the base and mobile receiver were less than 30 km for seven profiles and approximately 50 km for one line 9 km long. Expected accuracy is ±25 cm for the horizontal and vertical positioning after final data processing has been completed and ±0.03 mGal for the Bouguer anomalies.

The gravity data will be used to model faults, to differentiate geological units at depth, and to correlate gravity and geological data with seismic data along the profiles. The new data over the Cobequid Highlands will be combined with existing gravity data from the Nova Scotia Research Foundation to model the Cumberland Basin which lies to the east of the survey area.

TRANS-HUDSON OROGEN TRANSECT

A detailed gravity survey along seismic lines in northern Manitoba and Saskatchewan was completed between September 8 and 24, 1995. A total of 700 new gravity stations was established at a maximum spacing of 2 km. The survey was funded by GSC as a contribution to Lithoprobe. The data will contribute to geological interpretations of crustal structure across a transect of the Trans-Hudson Orogen using integrated geophysical data sets (seismic, magnetotelluric, magnetic, and gravity).

GREAT SLAVE LAKE SURVEY

In March 1995, 117 new gravity measurements were observed by the Pacific Geoscience Centre at an average spacing of 8.5 km on the ice of western Great Slave Lake. The measurements were acquired using a LaCoste and Romberg gravimeter, which was operated in damped mode to compensate for oscillations of the lake ice. Station co-ordinates were computed using differential GPS. Water depths were measured using an Edo 9040 acoustic sounder at each gravity station, and water level gauge measurements, tied to local benchmark networks, were used to determine station elevations. Simple Bouguer anomalies, considered to be accurate to ±0.4 mGal, have been computed for all stations. This survey will contribute to the Slave-Northern Cordillera Lithospheric Evolution Transect (SNORCLE).

CANADIAN GRAVITY STANDARDIZATION NET

Approximately 39 of the more than 1550 active reference sites of the Canadian Gravity Standardization Net (CGSN) were inspected as part of the annual inspection program to maintain the integrity of this network, which provides datum for all relative gravity surveys completed under the National Gravity Program and for surveys carried out by geophysical exploration companies. Stations in Ontario south of latitude 43°40′ and between longitudes 79°20′ and 83°02′ were inspected. New stations were established to replace destroyed stations and additional ties (124) were made between existing stations in the area to improve the accuracy of the network. Inspected sites were categorized and photographed according to national standards, descriptions were recompiled, and corresponding databases were updated. In addition, several control stations were inspected on an opportunity basis in areas where surveys were being conducted or while en route to survey areas. A total of 98 station descriptions was recompiled and preliminary copies are available on demand.

Scale factors were updated for two LaCoste and Romberg gravity meters based on observations over the Ottawa-Inuvik long range calibration line. The data were also analyzed to provide an evaluation of the performance of the meters over the gravity range in which they are normally deployed.

ABSOLUTE GRAVITY

In January, a comparison of NOAA and GSC absolute gravimeters was made at the Canadian Absolute Gravity Site, Gatineau. Two JILA-type and two FG5-type instruments were compared. Systematic differences between the two types of instrument were identified, revealing a problem with the FG5 instruments that was later resolved.

The absolute gravity team also participated in the first North American comparison of absolute gravimeters hosted by NOAA at their Table Mountain Gravity Observatory in Boulder, Colorado. In the period June 26 to July 14, eight instruments from NOAA, IFAG, Scripps, Japan, and JILA-2 from Geomatics Canada and FG5-106 from GSC were compared. The team also participated in an IUGG workshop where the results of the previous intercomparison held at BIPM, Paris in 1994 were finalized. It was concluded that all FG5 measurements required a reduction of 14 microgals, due to the discovery of a systematic instrumental error in these instruments. The next comparison will be held at BIMP, Paris in 1997.

CANADIAN SUPERCONDUCTING GRAVIMETER INSTALLATION

The support of the Canadian Superconducting Gravimeter Installation (CSGI) continued. In June, the gravity standards team participated actively in the reinstallation of GWR-12 at the Canadian Gravity Absolute Site (CAGS). Regular maintenance and operation of the Canadian Superconducting Gravimeter Installation was assumed this year by the Standards Group (previously with the Gravity and Geodynamics Section, GSC) to ensure uninterruptable records of gravity and weather data for the next six years, as a contribution to the Global Geodynamics Program (GGP). The team is in close collaboration with the consortium of Canadian universities, which owns the gravimeter, in order to raise and ensure long term funding for Canadian Superconducting Gravimeter Installation and thus meet the obligations to the Global Geodynamics Program.

GRAVITY SYSTEMS DEVELOPMENT

With funding support from GSC's Industrial Partners Program (IPP), the development of new airborne gravity technology continued this year as a co-operative effort of private industry, universities, and government agencies. The Standards Group is developing software for precise kinematic GPS positioning of the aircraft and provides the project with the use of GPS receivers. Also under the GSC's IPP, an agreement was signed by Scintrex Ltd., GSC, and Geomatics Canada to develop Heligrav, a system that will allow the use of a helicopter and a self-levelling, remotely operated gravimeter for cost-effective regional gravity surveys.

MARINE TIDE MODELLING

In the forefront of theoretical modelling and software development, a new version of the LOADSDP program (v. 4.0) was completed. LOADSDP (v. 4.0) enforces mass conservation in the regional/local marine tide models for the calculation of ocean tide load effects. Work, in collaboration with GSC, on the development of regional marine tide models (Hudson Bay, Canadian east and west coasts) is in its final stages. These models ensure a more accurate evaluation of the load effects necessary to support the analysis of gravity records with high accuracy, such as those obtained by GWR-12 and absolute meters. Calculations of the ocean tide load effect (global and local effects) were carried out on behalf of NOAA for several VLBI and GPS stations across North America. New statistical methods were developed for the detection of significant peaks in the least-squares spectrum when the covariance matrix of the input time series is unknown to a scale factor. This development was followed by appropriate updates of LSSA software.

Geodetic Survey of Canada Projects 930029, 930030, 930031, 930032

Resolution of the mineralogy of coal samples

Marcel Labonté
GSC Calgary, Calgary

Labonté, M., 1996: Resolution of the mineralogy of coal samples; in Current Research 1996-D; Geological Survey of Canada, p. 117-123.

Abstract: A two-part system to describe the mineralogy of the mineral part of coal samples has been developed. One part consists of a procedure which uses normative minerals to match the real ones determined by X-ray diffraction, and whose detailed chemistry sum up to the observed oxides measured by X-ray fluorescence. The other part uses linear programming, with more realistic mineral compositions, to achieve a realistic description of the minerals present in the coals. Despite differences, these two methods achieve a similar results in the end and complement each other.

Résumé : Un système a été mis au point dans le but de déterminer la composition de la partie minérale d'échantillons de charbon. Il est basé sur deux méthodes. La première consiste en une procédure qui fait le parallèle entre, d'une part, des minéraux normatifs et, d'autre part, ceux qui composent vraiment le charbon et qui ont été identifiés par diffraction des rayons X. La seconde fait appel à la programmation linéaire et permet d'obtenir des compositions minérales plus réalistes. Les résultats sont à peu près semblables pour ces deux méthodes qui se complètent.

INTRODUCTION

The mineralogy of ashed coal samples has been resolved by using a double approach of the sedimentary geological norm calculation (SEDNORM) and linear programming geological norm calculation (LPNORM) with the oxide percentages given by the X-ray fluorescence method and also with the qualitative crystalline mineral phase identification provided by the X-ray diffraction method.

When coal samples are ashed, the only data available on the volatiles is the loss on ignition value. The advantage of the SEDNORM program is that it can provide a CO_2 percentage value estimate and also a water percentage estimate because of the norm calculation procedure (for example see Barth, 1959). Because the norm procedure is a fixed procedure as explained by the flowchart of Cohen and Ward (1991), the SEDNORM program has "built in" inflexibilities which can be otherwise used to estimate volatile components of the mineral phases.

On the other hand, the LPNORM program, which has greater flexibility but requires the CO_2 percentage value as input, depends upon the use of the proper mineral chemical formulas in order to produce good results. Further, the use of end-members for certain clay varieties as shown by de Caritat et al. (1994), can simplify the use of LPNORM. He also suggested that if a selection of mineral formulas were precoded in a dictionary, and a program was made to "prepare" the files necessary for LPNORM, it would greatly facilitate the use of LPNORM. Consequently, the program PREPARE, described below, serving as input file creator for both SEDNORM and LPNORM programs, was made and adapted to read "coma separated variable" files such as those created by spreadsheet programs like EXCEL or the PARADOX database system.

The use of the norm concept

The concept of "normative analysis" needs to be covered. This is best done by consulting manuals like Barth (1959), or other more recent ones. An article like the one of Kelsey (1965) covers what is called the calculation of the "CIPW" norm, which is meant to allow comparisons between different rocks of igneous nature. Cohen and Ward (1991) extended this concept of norm into the domain of sedimentary rocks. However, since there is less homogeneity in sedimentary rocks than in igneous rocks, a method of using the normative analysis procedure for sedimentary rocks involved the need to remove or introduce what is called normative minerals to achieve a reasonable fit, this amounts to using normative minerals similar to the ones present in the rock being analyzed. Linear programming allows the refinement of these decisions and the calculation of better mineral percentages but its use in coal sample analysis is complicated by the ashing processes because there is some confusion in the partition of the volatiles. Using chemical and physical methods, many authors (Pollack, 1979; Pike et al., 1989; Finkelman et al., 1990) explored, to some extent, the difficulties of coal chemistry, especially the effects of different ashing temperatures.

How linear programming works

The concept of linear programming is used more in the domain of operations research, and usually leads to the optimal use of resources in commercial situations. A good practical example of the use of linear programming can be found in the user's manual of a spread sheet system like Quattro Pro (1991), where a simple commercial allocation problem is presented and solved. Linear programming involves obtaining the maximum value for a multivariate linear polynomial (a target polynomial), given that the value of each variable used in this polynomial must satisfy some constraints. The set containing the target polynomial to be maximized (or minimized) and the constraints to be respected constitute the linear programming problem. In geology, the target polynomial is not as important in operations research because each mineral is equally important. However, formulating the constraints which are expressed as a set of inequations constitute the main part of the work involved. De Caritat et al. (1994) gave a good example of how to formulate these constraints by using the chemical formulas of the oxide concentrations measured and also the chemical formulas of the supposed minerals.

Comparisons of SEDNORM and LPNORM programs

The simultaneous usage of these two programs has been made easier by organizing the input file to serve for both of these programs. On the whole, if the inflexible approach of SEDNORM is taken into account, both programs appear to produce similar results. However, if the mineral phases are better resolved, as would be the case if no organic part were present, then it is very likely that only LPNORM would be usable.

The PREPARE program

A program for constructing input files for both the SEDNORM and the LPNORM programs has been coded. The PREPARE program can be used to enter the oxide and default mineral phases as a first step, and store this information into a file. The SEDNORM program of Cohen and Ward (1991), can be used to read this data file directly and produce its output in the "SEDNORM.OUT" file, which can be printed after the run. Then it can also be used to prepare the specific files "OXLIST.DAT" and "MINLIST.DAT" required for each case by the LPNORM program.

As mentioned earlier, the PREPARE program can be used to:

1. Enter a new set of data coming from the instrumentation, namely: X-ray diffraction, X-ray fluorescence, and possibly Differential Thermal Analysis. When this is done, the user should take notice of all the mineral phases that are common to all the samples, and assign common phases in the LPNORM part of the data entry. The result of this data entry is stored into a file which can be used by the second part of the PREPARE program, which is shown below.
2. The user can then use the data stored in the step above and prepare the files to submit each sample, one sample at a time, to the LPNORM program. Upon preparing the files

"OXLIST.DAT" and "MINLIST.DAT" by using the "process this case" option, the user can include some of the mineral phases unique to each sample.

Upon completion of the second step, the file containing all of the data has been copied to a new file "file.new", that is, a suffix ".new" is added to the old name. This new file contains all the changes made to each sample case. By deleting the original file and renaming "file.new" as "file", all the updates are kept. The LPNORM executable program has been loaded with the SEDNORM account and it can be done immediately. Usually a few runs will be necessary in order to have the unexplained oxides minimized.

Mineral phases that can be used

Appendix 1 contains the possible phases that can be utilized for the LPNORM program at the date of writing. The user selects the desired mineral phases by entering the record number at the beginning of each record in Appendix 1. The choice of the proper mineral phases is critical for each problem because linear programming operates with a convex hull approach in "n" dimensions, or a "solution space representation" in the terminology of Wagner (1969), and the possible solutions are usually at apexes of these hulls. It is the stoichiometry of each mineral phase which determines the position of these boundaries. If for a given sample, the mineral phase is not present in "SEDNORM.BAG", then it should be added to the list and used. Another approach used by de Caritat et al. (1994) is to include the end members of a mineral series like the plagioclases, because the members of this series form a complete series of mixed crystals (Barth, 1959). Conceptually, linear programming can be described to operate by finding the highest value of a function whose domain is a "fenced" area, when two dimensions are used. It is the constraints which define the "fences". Thus if a mineral phase happens to define a fence that does not create a reachable limit, because another mineral phase introduces a more restrictive limit, then such a mineral phase will not be given any value (Wagner, 1969). This is a recognition that a linear programming approach is not sufficient, and nonlinear programming, or perhaps a more generalized optimization approach, is really needed as noted by Engler and Iyengar (1987). Laird and Dowdy (1994) have presented a good review of all the analytical and instrumental techniques and also the data-processing methods that can be used to quantify the chemical characteristics of clays.

An example of the use of the LPNORM program

The type of files needed by the LPNORM program are shown in Appendix 2. Two files serve as input files to the LPNORM program: namely, "MINLIST.DAT" and "OXLIST.DAT". This appendix shows first these two files and then also the "LPNORM.OUT" file which results from the choice of "minimize the slack variables" that is shown in the document of de Caritat et al. (1994). The sample processed here is a coal sample labelled "goqs36c". The mineral part in this sample sums up to 5.82%, the rest is in the form of organics. The usage of CaO as an assigned mineral phase is an alternative to the use of $CaCO_3$, because the CO_2 is evidently very small and has not been determined in this case. A "finite solution" to the linear programming problem is shown and two sets of percentages are given: one for redistributing the percentages of the mineral phases inside the 5.82%, and adjacent to it, the same proportional values but in percentage magnitudes that total about 100%. The last table shows how well the fitting to the given oxide percentages has been done. Appendix 3 shows the same data processed with the SEDNORM program.

CONCLUSION

Although there are some limitations to the applications of the linear programming approach to solve the mineralogy of coal samples, with some practice a reasonable fit can be achieved in a short time.

ACKNOWLEDGMENTS

This work was done as a part of the survey of the trace elements in coal power plants in the Geolgical Survey of Canada Project 930009.

REFERENCES

Barth, T.F.W.
1959: Theoretical Petrology; John Wiley & Sons, second printing, 387 p.
Cohen, D. and Ward, C.R.
1991: SEDNORM – A program to calculate a normative mineralogy for sedimentary rocks based on chemical analyses; Computers and Geosciences v. 17, no. 9, p. 1235-1253.
de Caritat, P., Bloch, J., and Hutcheon, I.
1994: LPNORM: A linear programming normative analysis code; Computers and Geosciences, v. 20, no. 3, p. 313-347.
Engler, P. and Iyengar, S.S.
1987: Analysis of mineral samples using a combined instrument (XRD, TGA, ICP) procedures for phase quantification; Amerian Mineralogy, v. 72, p. 832-838.
Finkelman, R.B., Palmer, C.A., Krasnow, M.R., Aruscavage, P.J., Sellers, G.A., and Dulong, F.T.
1990: Combustion and leaching behaviour of elements in the argonne premium coal samples; Energy and Fuels, v. 4, p. 755-766.
Kelsey, C.H.
1965: Calculation of the CIPW norm; Mineralogical Magazine, v. 34, p. 276-382.
Laird, D.A. and Dowdy, R.H.
1994: Simultaneous mineralogical quantification and chemical characterization of soil clays; Clay and Clay Minerals, v. 42, no. 6, p. 747-754.
Pike, S., Dewison, M.G., and Spears, D.A.
1989: Sources of error in low temperature plasma ashing procedures for quantitative mineral analysis of coal ash; Fuel, v. 68, p. 664-668.
Pollack, S.S.
1979: Estimating mineral matter in coal from its major inorganic elements; Fuel, v. 58, p. 76-78.
Quattro Pro
1991: User's Guide; Borland International, Version 3.0.
Wagner, H.M.
1969: Principles of operation research, with applications to managerial decisions; Prentice-Hall, Englewoods, New Jersey, U.S.A. 937 p.

Geological Survey of Canada Project 930009

Appendix 1

The different phases and their stoïchiometries used in the PREPARE program, in the "SEDNORM.BAG" file:

No.Name.....Elements+Stoichiometry.....

1- Quartz	Si 1.00	O 2.00						
2- Kaolinite	Al 2.00	Si 2.00	O 5.00	OH 4.00				
3- Ill1_K	K 2.00	Al 6.00	O 20.00	OH 4.00				
4- Ill2_Na	Na 2.00	Al 6.00	O 20.00	OH 4.00				
5- Illite K 0.76	Fe 0.31	Mg 0.28	Al 1.97	Si 3.46	O 10.00	OH 2.00		
6- Muscovite1	K 1.00	Al 3.00	Si 3.00	O 10.00	OH 2.00			
7- Muscovite2	K 0.75	Al 3.00	Si 3.00	O 10.00	OH 2.00			
8- Biotite_Fe	K 1.00	Fe 3.00	Al 1.00	Si 3.00	O 10.00	OH 2.00		
9- Biotite_Mg	K 1.00	Mg 3.00	Al 1.00	Si 3.00	O 10.00	OH 2.00		
10-Mont_Ca	Ca 2.00	Al 2.00	Mg 2.00	Si 4.00	O 10.00	OH 2.00		
11-Mont_Na	Na 2.00	Al 2.00	Mg 2.00	Si 4.00	O 10.00	OH 2.00		
12-Smectite	Na 1.00	Ca 1.0	Mg 0.50	Fe 0.50	Al 3.00	Si 8.00	O 20.00	OH 4.00
13-Chlor_Fe	Mg 5.00	Fe 1.00	Al 1.00	Si 3.00	O 10.00	OH 8.00		
14-Chlor_Mg	Mg 5.00	Al 2.00	Si 3.00	O 10.00	OH 8.00			
15-Chlorite	Fe 3.00	Mg 2.00	Al 2.00	Si 3.00	O 10.00	OH 8.00		
16-Albite	Na 1.00	Al 1.00	Si 3.00	O 8.00				
17-Anorthite	Ca 1.00	Al 2.00	Si 2.00	O 8.00				
18-Microline	K 1.00	Al 1.00	Si 3.00	O 8.00				
19-Plagioclas	Ca 0.50	Na 0.50	Al 1.50	Si 2.50	O 8.00			
20-Calcite	Ca 1.00	C 1.00	O 3.00					
21-Dolomite	Ca 0.50	Mg 0.50	C 1.00	O 3.00				
22-Siderite	Fe 1.00	C 1.00	O 3.00					
23-Magnesite	Mg 1.00	C 1.00	O 3.00					
24-Pyrite	Fe 1.00	S 2.00						
25-Apatite	Ca 5.00	P 3.00	O 12.00	OH 1.00				
26-Hematite	Fe 2.00	O 3.00						
27-CaO Ca 1.00	O 1.00							
28-K2O K 2.00	O 1.00							
29-MgO	Mg 1.00	O 1.00						
30-Gibbsite	Al 1.00	OH 3.00						
31-Gypsum	Ca 1.00	S 1.00	O 4.00					
32-Anhydrite	Ca 1.00	S 1.00	O 4.00					
33-Anatase	Ti 1.00	O 1.00						
34-Zeolite_C	Na 2.30	K 1.70	Ca 0.50	Mg 0.20	Al 6.20	Si30.00	O 72.00	
35-Jarosite	K 1.00	Fe 3.00	S 2.00	O 8.00	OH 6.00			
36-Na2O	Na 2.00	O 1.00						

This list represents the possible entries that can be included in the "MINLIST.DAT" file which serves as input to the LPNORM program.

Appendix 2

The "MINLIST.DAT" file example:
goqs36c

quartz		Si 1.00	O 2.00		
kaolinite	Al 2.00	Si 2.00	O 5.00	OH 4.00	
Pyrite		Fe 1.00	S 2.00		
Jarosite	K 1.00	Fe 3.00	S 2.00	O 8.00	OH 6.00
Anatase	Ti 1.00	O 1.00			
CaO		Ca 1.00	O 1.00		
Apatite	Ca 5.00	P 3.00	O 12.00	OH 1.00	
K2O		K 2.00	O 1.00		
Na2O		Na 2.00	O 1.00		
Hematit	Fe 2.00	O 3.00			

End.

The "OXLIST.DAT" file example:

SiO2	Al2O3	Fe2O3	MgO	Na2O	CaO	K2O	TiO2	P2O5	MnO	inCO2	S
goqs36c											
1.63	.78	2.09	.03	.12	.21	.05	.05	.02	.00	.00	.84

End.

The "LPNORM.OUT" output file example:

```
==========================================================================
Program LPNORM - University of Calgary - Copyright 1992,1993
Patrice de Caritat
[Ref: de Caritat, Bloch and Hutcheon, Computers & Geosciences,1994]
==========================================================================
*** Computing mineral data
# MINERAL                                MOL.WT.    #EL.      *CH.BAL.
--------------------------------------------------------------------------

 1:quartz ..................................  60.08      2         .0000
    Si 1.00 O 2.00
 2:kaolinite ...............................  258.16     4         .0000
    Al 2.00 Si 2.00 O 5.00 OH 4.00
 3:Pyrite ..................................  119.97     2         .0000
    Fe 1.00 S 2.00
 4:Jarosite ................................  500.80     5       -17.0000
    K 1.00 Fe 3.00 S 2.00 O 8.00 OH 6.00
 5:Anatase .................................  63.90      2        2.0000
    Ti 1.00 O 1.00
 6:CaO .....................................  56.08      2         .0000
    Ca 1.00 O 1.00
 7:Apatite .................................  502.32     4         .0000
    Ca 5.00 P 3.00 O 12.00 OH 1.00
 8:K2O .....................................   94.20     2         .0000
    K 2.00 O 1.00
 9:Na2O ....................................  61.98      2         .0000
    Na 2.00 O 1.00
10:Hematite ................................  159.69     2        -2.0000
    Fe 2.00 O 3.00
```

Appendix 2 (cont.)

(*CH.BAL. based on following valences: -2:O -1:F,S,Cl,OH +1:H,Na,K
+2:Mg,Ca,Mn,Fe,Ba +3:Al +4:C,Si,Ti +5:N,P)

MINERALS quartz kaolinite Pyrite Jarosite Anatase
CaO Apatite K2O Na2O Hematite

SAMPLE goqs36c

SiO2	Al2O3	Fe2O3	MgO	Na2O	CaO	K2O	TiO2	P2O5	MnO	inCO2	S	SUM
1.63	0 .78	2.09	0.03	0.12	0.21	0.05	0.05	0.02	0.00	0.00	0.84	5.82

*** Obj.fct.: minimize slack variables AND maximize mineral abundances
*** A finite solution was found for sample goqs36c

1 (.71) wt% quartz	11.93
2 (1.97) wt% kaolinite	33.15
1 (.87) wt% Hematite	14.68
0 (.12) wt% Na2O	2.01
0 (.18) wt% CaO	3.08
1 (.53) wt% Jarosite	8.92
0 (.04) wt% Anatase	.67
0 (.05) wt% Apatite	.79
1 (1.44) wt% Pyrite	24.24
6 (5.93) wt% total	99.50
5.90 wt% objective function	

VERIFY OUTPUT

Si:	1.63 wt% used of the initial	1.63 wt%	(diff.= .00wt%)
Al:	.78 wt% used of the initial	0.78 wt%	(diff.= .00wt%)
Fe:	2.09 wt% used of the initial	2.09 wt%	(diff.= .00wt%)
Mg:	.00 wt% used of the initial	0.03 wt%	(diff.= .03wt%)
Na:	.12 wt% used of the initial	0.12 wt%	(diff.= .00wt%)
Ca:	.21 wt% used of the initial	0.21 wt%	(diff.= .00wt%)
K :	.05 wt% used of the initial	0.05 wt%	(diff.= .00wt%)
Ti:	.05 wt% used of the initial	0.05 wt%	(diff.= .00wt%)
P :	.02 wt% used of the initial	.02 wt%	(diff.= .00wt%)
Mn:	.00 wt% used of the initial	.00 wt%	(diff.= .00wt%)
C :	.00 wt% used of the initial	0.00 wt%	(diff.= .00wt%)
S :	.84 wt% used of the initial	.84 wt%	(diff.= .00wt%)
		total diff.= .03wt%	

Appendix 3

The same data processed by the "SEDNORM" program.
Input file: By Hand... 1 samples
****
Sample: goqs36c
Anal values (Wt%) for oxide:

Mineral	Si	Ti	Al	Fe	Mn	Mg	Ca	Na	K	P	H	C	S	Cl
Formed	1.6	.1	.8	2.1	.0	.0	.2	.1	.1	.0	.0	.0	2.1	.0
Apat	1.6	.1	.8	2.1	.0	.0	.2	.1	.1	.0	.0	.0	2.1	.0
Pyr	1.6	.1	.8	1.5	.0	.0	.2	.1	.1	.0	.0	.0	.0	.0
Calc	1.6	.1	.8	1.5	.0	.0	.0	.1	.1	.0	.0	.0	.0	.0
Magn	1.6	.1	.8	1.5	.0	.0	.0	.1	.1	.0	.0	.0	.0	.0
Musc	1.6	.1	.8	1.5	.0	.0	.0	.1	.1	.0	.0	.0	.0	.0
Hal	.7	.1	.0	1.5	.0	.0	.0	.0	.1	.0	-.3	.0	.0	.0
Hm	.7	.0	.0	.0	.0	.0	.0	.0	.1	.0	.0	.0	.0	.0
Qtz	.0	.0	.0	.0	.0	.0	.0	.0	.1	.0	.0	.0	.0	.0

Normative mineral composition:

Mineral	Percent by mass	by volume	orig mass%
Quartz	9.3	12.5	.7
Kaolinite	25.8	34.7	1.8
Calcite	4.3	5.7	.3
Magnesite	.8	1.2	.1
Hematite	19.5	13.4	1.4
Halite	4.0	6.5	.3
Pyrite	35.3	25.1	2.5
	98.96	99.00	7.01

Sum of oxides was; 7.08

H2O Added in calculation: .3 %
CO2 Added in calculation: .2 %
Cl Added in calculation: .2 %
Excess of:K .1 % as oxide.
Options selected were:

1 Exclude: Illite & Muscovite;
2 Exclude; Feldspar
4 ; S as Sulphide (Pyrite)
5 Exclude "Smectite"
10 ;CO2 data non-available, all Ca+Mg to carbonates
11 ; H2O Partially variable

Development of pulseEKKO borehole radar

Eric Gilson[1], Jean Pilon, David Redman[2], Peter Annan[3], and Dave Leggatt[3]

Terrain Science Division, Ottawa

Gilson, E., Pilon, J., Redman, D., Annan, P., and Leggatt, D., 1996: Development of pulseEKKO borehole radar; in Current Research 1996-D; Geological Survey of Canada, p. 125-131.

Abstract: This paper presents a progress report on a project undertaken in September 1994 to develop low cost borehole antennas for the pulseEKKO ground penetrating radar family. Survey methodology, data acquisition procedures, and interpretation are described for applications of these borehole antennas in near surface environments (≤30 m). An application of these antennas at boreholes installed at the Woolwich landfill site is also presented. These data show the ability to determine moisture content variations within the unsaturated and saturated zone, and to outline a contaminated zone of high conductivity.

Résumé : Le présent article constitue un rapport d'étape sur un projet entrepris en septembre 1994 visant la mise au point d'antennes à bon marché de géoradars pour trous de forage (géoradars pulseEKKO). La description des techniques de levé, des procédures d'acquisition des données et des méthodes d'interprétation s'applique à l'utilisation de ces antennes dans le cas de trous de forage peu profond (≤30 m). Les résultats d'un levé effectué au site d'enfouissement de Woolwich sont également présentés. Les données montrent la capacité de l'appareil, d'une part, à déterminer les variations du taux d'humidité des sols à l'intérieur des zones saturées et non saturées et, d'autre part, à détecter une zone contaminée à forte conductivité.

[1] Department of Earth Sciences, University of Waterloo, Waterloo, Ontario N2L 3G1
[2] Waterloo Centre for Groundwater Research, University of Waterloo, Waterloo, Ontario N2L 3G1
[3] Sensors and Software Inc., 1091 Brevik Place, Mississauga, Ontario L4W 3R7

INTRODUCTION

In September 1994, an Industrial Partner Program (IPP) agreement (No. 94-041) was signed by the Geological Survey of Canada (GSC) and Sensors and Software Inc. (SSI) to develop and test, over a two year period, low cost borehole radar (BHR) transducers and the associated support software. These transducers were developed for the pulseEKKO ground penetrating radar (GPR) systems to provide a unique geophysical tool and technology for Canadian industry. Borehole GPR developments are not new to the GSC, original efforts commenced in the 1970s and are described by Davis and Annan (1986).

To achieve this end, the project was divided into two components: 1) The development of the appropriate instrumentation and basic software (SSI); and 2) the testing of the instrumentation in the field with applications to specific hydrogeological problems, and development of interpretation software (GSC/University of Waterloo (UW) under contract No. 23397-4-0710-01-SS). These two aspects of the project are being performed concurrently as the various prototype hardware becomes available. We are currently working with the third generation of borehole antennae. During the course of this ongoing project, GSC/UW selected, prepared and logged a variety of appropriate test sites using the prototype hardware and software. The purpose of this work is to: 1) verify the stability and repeatability of the measurements in a variety of geological settings and environmental conditions; 2) perform surveys using different types of antennae and borehole configurations; 3) test, evaluate, and develop data processing software; and 4) develop case histories relevant to geological, hydrogeological, geotechnical, and environmental problems.

During the first stage of this project, borehole radar test sites were established at CFB Borden, the Bauer Warehouse and the B parking lot at the University of Waterloo and at the Woolwich landfill site located 5 km north of Elmira, Ontario. The results of the tests performed at these sites are discussed in this report.

SURVEY METHODOLOGY

Borehole radar techniques can be grouped into two separate types (Table 1, Fig. 1). The first type is called Crosshole Radar Profiling (CRP) in which the transmitter and receiving antennas are in separate boreholes and data are collected with the antennas at various vertical offsets. The second type is Vertical Radar Profiling (VRP) which is comparable to Vertical Seismic Profiling.

In crosshole radar profiling, there are three possible data acquisition modes. In the first acquisition mode, the transmitter and receiving antennas have a fixed vertical offset (Fig. 1a); this is called a Common Offset Gather (COG). In the second, the two antennas are fixed so that there is no vertical offset (Fig. 1b); this is called a Zero Offset Gather (ZOG). In the third mode, one antenna remains at a fixed depth while the second is moved incrementally in the second borehole; this is referred to as a Multiple Offset Gather (MOG) (Fig. 1c). A series of multiple offset gathers are used to acquire the multiple raypaths required for tomographic imaging (Fig. 1d).

Vertical radar profiling is normally used to collect surface to borehole data when it is not possible to perform crosshole surveys. In the vertical radar profiling mode, one antenna (usually the receiver for noise considerations) is lowered incrementally downhole while the second antenna remains on the surface at a fixed distance from the borehole (Fig. 1e). This surface antenna may be a borehole antenna lying on the ground or a regular ground penetrating radar surface antenna oriented radially from the borehole. This type of survey is normally performed when there is only a single borehole

Table 1. Summary of terms used for describing various borehole radar antenna configurations.

Term	Abbreviation	Brief Description
Crosshole Radar Profiling	CRP	Antennas are in separate boreholes. This is the general term.
Vertical Radar Profiling	VRP	Similar to Vertical Seismic Profiling. One antenna remains on surface while the second antenna is in the borehole.
Common Offset Gather	COG	Data set collected in the crosshole radar profiling mode where the vertical offset between antennae are fixed.
Zero Offset Gather	ZOG	Data set collected in the crosshole radar profiling mode where there is no vertical offset between antennae
Multiple Offset Gather	MOG	A type of crosshole radar profiling where one antenna remains at a fixed depth while the second is moved incrementally downhole.

available. With this profiling technique, by moving the surface and borehole antennae, additional raypaths for tomographic modelling can also be acquired (Fig. 1e).

MEASUREMENT TECHNIQUES

The ground penetrating radar system used in this project was a pulseEKKO IV with the following acquisition parameters:

1. Pulser voltage – 400 V;
2. Antenna frequency – 100 MHz;
3. Sampling interval – 800 ps; and
4. Number of stacks – 64.

To determine accurate travel times between the transmitter and receiver antenna, it is important to know the precise time (time-zero) when the transmitter fires. Previously, the procedure used to collect data in this project was to place the two antennas 1 m apart on the surface and collect four traces. Recent studies indicate that the pulse shape is not consistent when the antennas are within 1 m, resulting in inconsistent arrival times for the direct air wave. Current procedure is to collect a set of traces for offsets from 2 to 10 m in air. Using the intercept from a best line fit for these arrival times allows us to define time-zero.

After the time-zero data were collected, the antennas were immediately moved and placed in their respective boreholes and a data set was collected for the desired antenna set of transmitter and receiver locations.

RESULTS AND INTERPRETATION

Figure 2 presents a Multiple Offset Gather collected with the second generation of borehole antennas, in boreholes 3.7 m apart at the B parking lot site at the University of Waterloo. In this gather, the receiver was located at a depth of 6 m and the transmitter was lowered by 0.25 m increments from 0 to 20 m. This multiple offset gather has been processed with a constant gain of 1000 to enhance the pre-time-zero events. Traces shown for depths less than 0 m are the traces collected for time-zero analysis.

In this discussion of the events (Fig. 2), zero on the time scale corresponds to the arrival time of a pulse received from the transmitter electronics when the transmitter and receiver electronics have a 0 m separation. This event cannot be recorded at zero separation because of potential damage to the electronics. The borehole radar antennas are connected to the electronics by 30 m long cables. Therefore, the analysis of the gather must take into account travel time on the cables. Time domain reflectrometry (TDR) was used to determine these travel times. The travel times measured on the two cables were 119.5 ns and 127.5 ns. Since a pulse requires 247 ns to travel the length of two antenna cables plus an extra 3 ns to travel across the 1 m air gap, time-zero as commonly defined would be 250 ns. Using the measured travel times on the antenna cables, and assuming a uniform subsurface velocity (0.065 m/ns), simple raypath modelling has been used to compute event arrival times that are consistent with the events observed in Figure 2. The raypaths for each of the modelled events are described below and the modeled arrival times are presented in Figure 3.

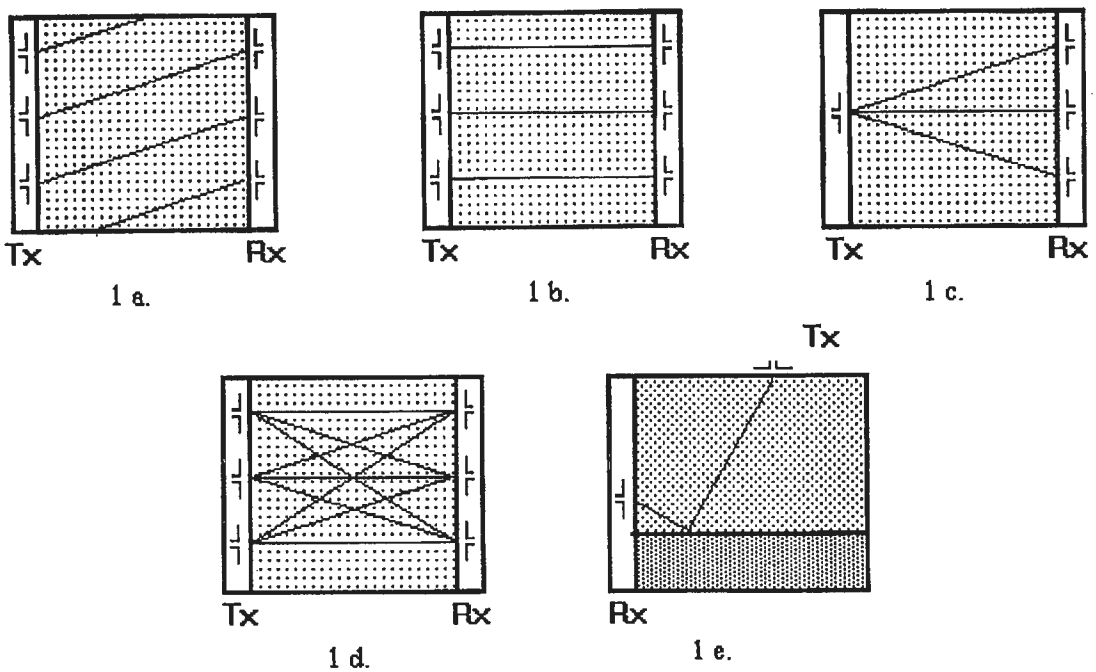

*Figure 1. Borehole radar antenna configurations: **1a)** Common Offset Profiling (CRP); **1b)** Zero Offset Gather (ZOG); **1c)** Multiple Offset Gather (MOG); **1d)** Several MOGs yield raypaths used for tomographic imaging; and **1e)** Vertical Radar Profiling (VRP).*

Event 1 is a linear event, constant in time occurring at 24 ns. This event is caused by the leakage of energy from the impedance mismatch at the transmitter electronics/antenna cable connector. This energy travels directly from the transmitter electronics to the receiver electronics in air. As both the point of emission and the receiving point are stationary, the event is constant in time. The arrival time is consistent with an event that travels in air between the transmitter and receiver electronics.

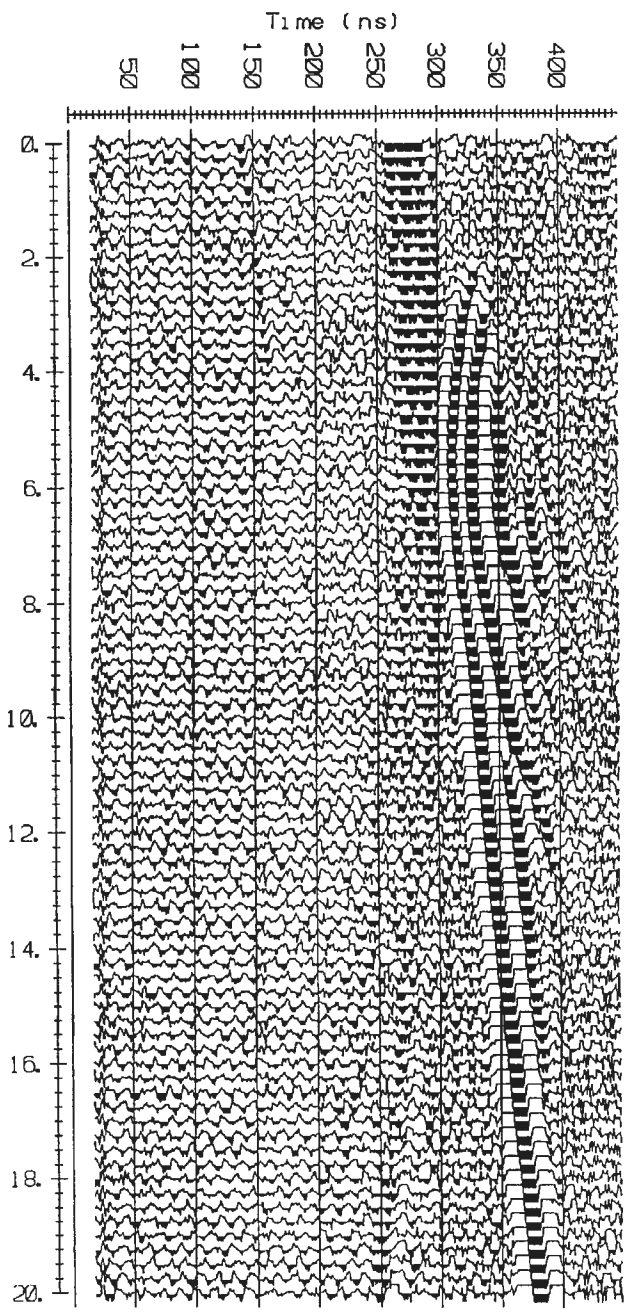

Figure 2. *Multiple offset gather (MOG) acquired with the second generation borehole radar antennas.*

Event 2 is also a linear event which starts on the gather at 137 ns at 0 m depth and moves out in time with a velocity of 0.16 m/ns. The path of this signal is not completely understood, although it is likely that it travels down the transmitter cable, reflects at the antenna, then travels back along the cable to the ground surface and radiates towards the receiver electronics. The first observed arrival time for this event matches the time required to travel the length of the transmitter cable (119.5 ns) plus the time to travel from the borehole containing the transmitter to the receiver electronics through air (17.5).

Event 3 is the direct arrival between the transmitter and the receiver antennas. This arrival occurs between depths of 2.25 and 9.25 m. Note that the apex of the curve occurs at 307 ns at a depth of 6 m. This arrival time corresponds to a velocity of 0.065 m/ns, which is typical for water saturated sediments found in the area. A comparison of observed data and simple modeling supports this conclusion. The event was modeled using:

$$time = \sqrt{x^2 + h^2} \; / \; velocity + 250$$

where x is the distance between boreholes, h is the vertical offset between antennas. The value of 250 is added to account for travel time through the antenna cables.

Event 4 is another linear event beginning at 323 ns at 9.25 m depth and continuing to 375 ns at 20 m depth. The velocity calculated from the slope of the event is 0.21 m/ns. This is energy which travels up the cable after the initial emission from the transmitter antenna. As it travel upwards, it is radiating energy into the ground at the critical refraction angle. As the contrast in velocities between the borehole environment and the ground is very large (0.21 to 0.065 m/ns), the critical angle is small (≈18°). The travel time includes the time required by the energy to travel the distance from the transmitter antenna up the cable to a depth of 6 m and across to the receiver antenna. This event only occurs when the moving antenna is below the depth of the fixed antenna While not evident in the figure because of the high constant gain applied, the signal becomes weaker as the transmitter antenna is lowered.

Event 5 is a weak, barely coherent event, beginning at a depth of 6 m and arriving earlier in time as the depth of the transmitter antenna increases. This event is caused by energy that leaks from the transmitter electronics/cable connector, and travels along the antenna cable. This energy radiates in a manner similar to event 4. Because this energy radiates from a fixed depth related to the critical angle and the depth of the fixed antenna, as the transmitter antenna is lowered, the path length along the cable is shortened resulting in less attenuation along the cable to that depth and hence a stronger signal.

Event 6 appears as a band of noise extending from 0 to 8 m depth and ranging from 250 to 300 ns. The raw, unfiltered gather of the data shown in Figure 2 has a low frequency oscillation with a period of 250 ns which produces the observed noise band. It is not clear what the cause of this signal is, however, it not present in the third generation of borehole radar antennas.

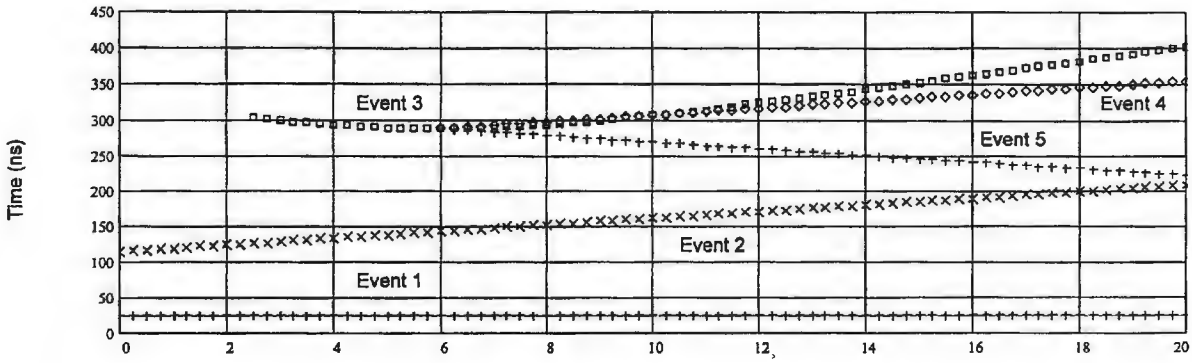

Figure 3. *Results of raypath modelling.*

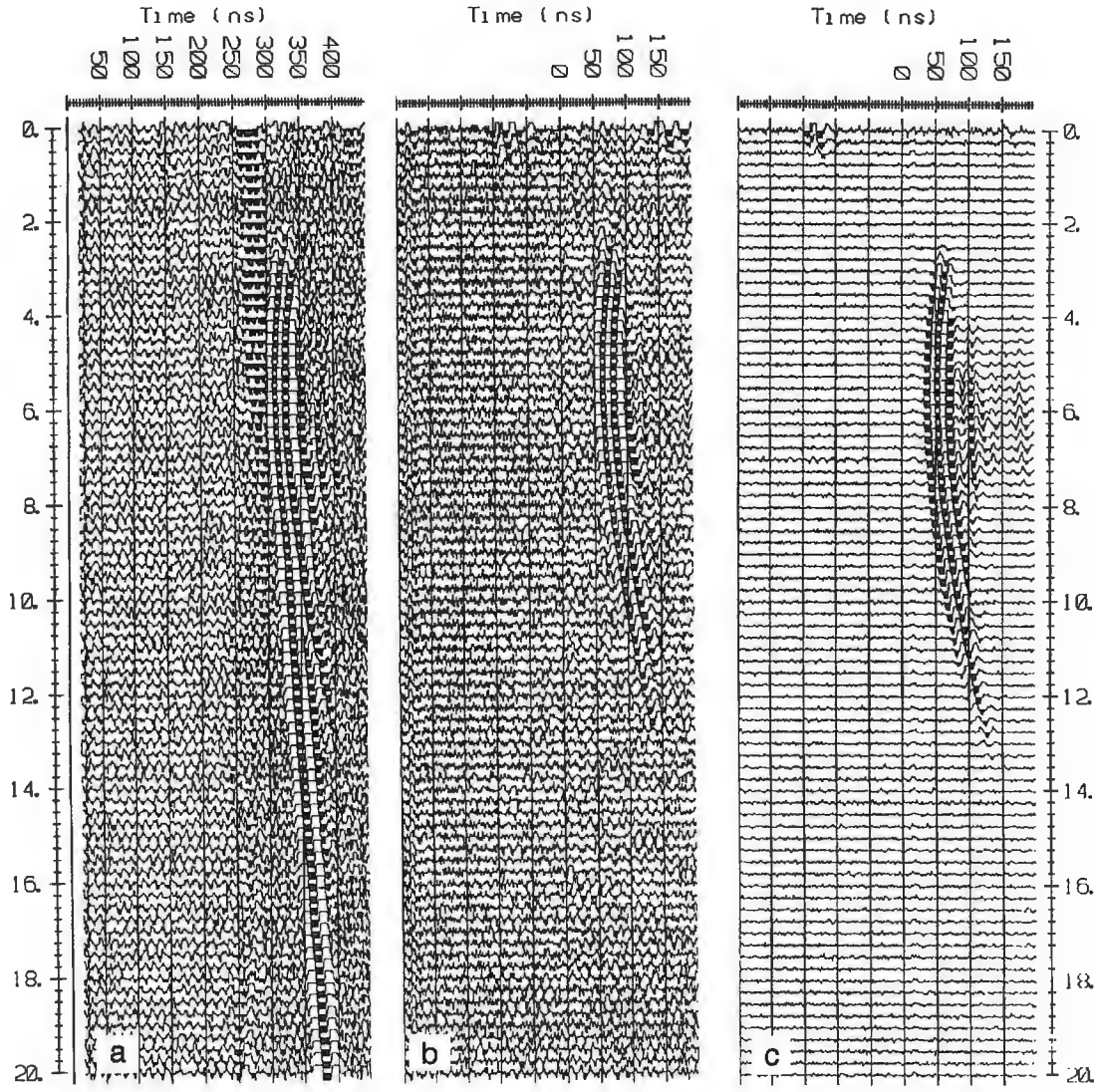

Figure 4. *Evolution of borehole radar antenna design:* ***a)*** *Multiple offset gather acquired with two second generation borehole radar antenna;* ***b)*** *Multiple offset gather acquired with one second and one third generation borehole radar antenna; and* ***c)*** *Multiple offset gather acquired with two third generation borehole radar antenna.*

The significant coherent events observed on this gather agree well with events calculated using raypath modelling. The calculated model response agrees well with the field data. The analysis of this multiple offset gather shows that the identification of the all significant events on a borehole radar gather is now possible and we now have a fair understanding of the cause of each event. Refraction arrivals from the air/ground interface and from strong dielectric contrasts such as the water table can be seen on other multiple offset gathers.

DATA IMPROVEMENT OVER A SUCCESSION OF TWO ANTENNA DESIGNS

Figure 4 presents three multiple offset gathers collected at the B Parking Lot site at the University of Waterloo using the same survey acquisition parameters over a succession of two antenna designs. All three are displayed with the same gains and filter settings. The first (Fig. 4a) was collected with the second generation antenna. Note the importance of the hardware-induced artifacts, and the amount of background noise evident on the gather, as discussed in the previous section.

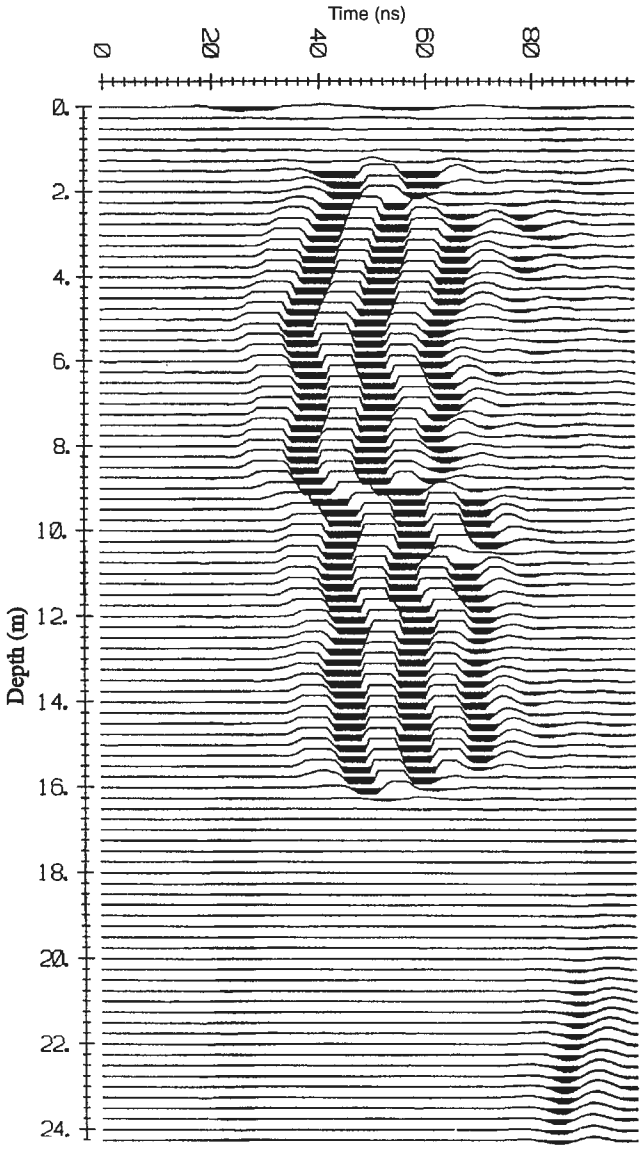

Figure 5. Zero offset gather (ZOG) acquired at the landfill site.

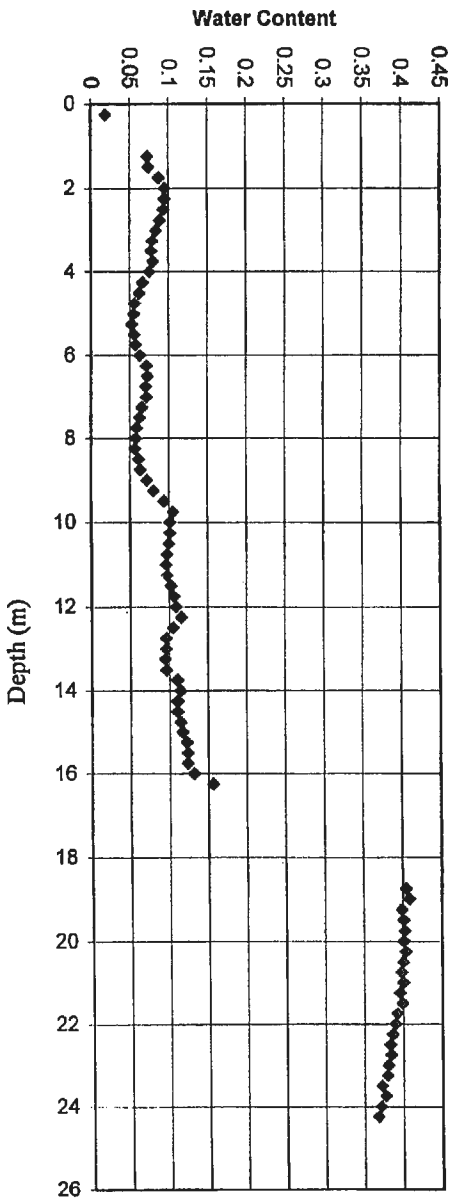

Figure 6. Water content by volume derived from the velocities determined from the direct arrival events for the zero offset gather.

The second multiple offset gather (Fig. 4b) was gathered with one second generation antenna and one third generation antenna. The spurious events caused by the second generation antenna design have disappeared. Event 1 is still visible because it is due to the mismatched impedance at the junction boxes and not the antenna design.

The third multiple offset gather (Fig. 4c) was collected with both third generation antennas. This design is virtually free of hardware-induced artifacts. Note particularly the marked improvement in the signal- to-noise ratio. The only event remaining, of those presented in Figure 3, is the direct arrival event (event 3).

With this comparison between the old and new designs, it is clear that there has been significant progress in antenna design.

ZERO OFFSET GATHER AND WATER CONTENT

Figure 5 is a zero offset gather collected at the Woolwich Landfill Site with the third generation antennas. This landfill site consists of approximately 30 m of relatively homogeneous glaciolacustrine sand with the water table at 16.25 m. The upper 3.75 m (from 16 to 19.75 m) of the saturated zone is highly contaminated and in it the direct arrival event is attenuated below the system noise level by the highly conductive groundwater. This event does reappear lower in the record, at depths of greater than 20 m, indicating that the degree of contamination in this zone is lower. Direct arrival times from the zero offset gather were used to determine the EM wave velocities of the subsurface. These velocities were then converted into water content (Fig. 6) using an empirical relationship between water content and dielectric permittivity (Topp et al., 1980). The values obtained are typical of glaciolacustrine sands, and the observations correlated very well with EM-39 conductivity logs collected in the same boreholes.

CONCLUSION

This progress report on the IPP agreement to develop a commercially viable low cost borehole antenna system for the pulseEKKO ground penetrating radar family demonstrates that this project which terminates in March 1996 is well underway. We have developed a suite of survey modes, improved survey methodology, and developed interpretation software that allow a precise analysis of the data obtained at the various field sites. Finally, hardware development has progressed sufficiently for us to have confidence that the initial objectives will be successfully met by project completion. Further research needs to be carried out particularly on the determination of which survey mode is most appropriate to the successful resolution of a specific environmental problem such as a contamination plume, or a specific geotechnical problem such as rock fracture, or for a geological application such as unconsolidated material layering. These issues will be addressed in later phases of the project.

ACKNOWLEDGMENTS

The authors wish to acknowledge the help of Richard Laframboise with the preparation of the digital figures for this paper.

REFERENCES

Davis, J.L. and Annan, A.P.
1986: Borehole radar soundings in CR-6, CR-7, and CR-8 at Chalk River, Ontario; Atomic Energy of Canada Limited, TR-401, 64 p.
Topp, G.C., Davis, J.L, and Annan, A.P.
1980: Electromagnetic Determination of Soil Water Content: Measurements in Coaxial Transmission Lines, Water Resources Research, Vol. 16, No. 3, pages 574-582, June 1980.

Geological Survey of Canada Project 920039WP

Modelling of metal concentrations in rift-related basaltic magmas: the Melt Generation Project

Marie-Claude Williamson
GSC Atlantic, Dartmouth

Williamson, M.-C., 1996: Modelling of metal concentrations in rift-related basaltic magmas: the Melt Generation Project; in Current Research 1996-D; Geological Survey of Canada, p. 133-138.

Abstract: Previous studies of the rifted margin offshore eastern Canada showed that the volume and rare-earth element concentrations of mantle-derived basaltic melts are sensitive to the physical and thermal state of the lithosphere at the time of rifting. The objectives of the Melt Generation Project (MGP) are: (1) to expand the current model to include metals of economic interest, and (2) test the model predictions with data from onshore rifts that also constitute mineral exploration targets. The rationale for creating the project stems from a need to improve the sensitivity of the geochemical model for mantle temperatures and lithospheric stretching factors typical of anomalously hot rift systems. As well as providing a scientific and business link with the mineral sector, the Melt Generation Project will increase our presently limited understanding of the large-scale mantle processes that can lead to the genesis of Ni-Cu sulphide deposits in rift zones.

Résumé : Des études antérieures sur la marge de divergence au large de l'est du Canada ont montré que le volume des magmas basaltiques dérivés du manteau et leur concentration en éléments des terres rares varient selon l'état physique et thermique de la lithosphère à l'époque du rifting. Les objectifs du Projet sur la genèse des magmas sont les suivants : 1) améliorer le modèle actuel pour y intégrer les métaux offrant un intérêt économique et 2) vérifier les prévisions du modèle avec des données sur d'autres rifts continentaux qui constituent également des cibles d'exploration minérale. Le projet tire sa raison d'être de la nécessité d'améliorer le modèle géochimique, pour qu'il tienne mieux compte des températures du manteau et des facteurs d'étirement de la lithosphère représentatifs des systèmes de rifting anomalement chauds. En plus d'établir un lien avec le secteur minéral, le Projet sur la genèse des magmas permettra d'approfondir les connaissances sur les processus mantelliques à grande échelle qui peuvent être à l'origine de gisements sulfurés minéralisés en Ni-Cu dans les zones de rift.

THE MELT GENERATION PROJECT

The GSC Atlantic's Melt Generation Project was started in January 1995 with the following objectives: (1) to develop a numerical model that simulates the behaviour of metals during mantle melting; (2) to determine the sensitivity of the model to changing input parameters, so that realistic objectives can be set when comparing the model predictions with observations from natural igneous systems; (3) to test the model by comparing the predictions with stratigraphic and geochemical data from onshore rifts.

Several observations led to the initiation of this project. The sensitivity studies and applications of the melting model to offshore rift basins suggest that it is capable of simulating a realistic range of physical and chemical conditions in rifted lithosphere (Keen et al., 1994). Rare-earth elements (REE) behave coherently during the melting process and thus constitute excellent indicators of the deformation style, mantle source, and melting history at the time of rifting (Williamson et al., 1994; 1995). An exceptional case is the reduced sensitivity of REE at the high asthenospheric mantle temperatures and large degrees of lithospheric stretching that are typical of some rifts associated with hot spots. One way to improve the quality of model predictions is to expand the geochemical model by including other groups of geochemically coherent trace elements, such as Ni, Cu, Au, and the platinum group elements (PGEs). This observation, and the current interest in PGE-bearing, Ni-Cu sulphide deposits associated with continental rifting and plume-type sources (e.g. Ryan et al., 1995), provide the impetus behind the Melt Generation Project.

Another major question framing the project concerns the role of geodynamic processes in controlling the initial concentrations of Ni, Cu, and the noble metals in rift-related basaltic magmas (e.g. hosting the Class II deposits of Naldrett, 1981). Basaltic rocks in general are not particularly rich in these elements. To constitute an economic deposit, the initial platinum concentrations in basaltic magmas (~30 ppb) must be increased by at least two orders of magnitude, or 70 times the mantle values (Fig. 1). The possible causes for higher concentrations of noble metals in some types of igneous rocks are still debated. Several authors have suggested a link with deep, "plume-type" mantle sources (e.g. Fryer and Greenough, 1992; Emslie et al., 1994) but enrichment processes at upper mantle depths cannot be discounted (e.g. Lorand et al., 1993).

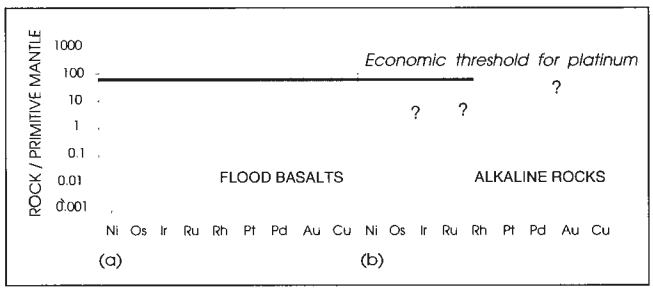

Figure 1. *Mantle-normalized diagrams for Ni, Cu, Au, and the platinum-group elements showing the range of concentrations in tholeiitic flood basalts and alkaline rocks (after Barnes et al., 1988).*

The Melt Generation Project allows the investigation of the conditions in rifted lithosphere and the dynamic processes that might favour the enrichment of Ni, Cu, and the noble metals in both tholeiitic and alkaline magmas (Fig. 1). Where case studies are concerned, the adopted methodology follows the pattern illustrated in Figure 2: the rifting models are continuously improved by the results of case studies, selected through co-operation with experts from universities and other divisions within the Geological Survey of Canada; and through research agreements with mining companies.

This paper describes some of the preliminary applications of the model to oceanic and continental rifts, that led to the initiation of the Melt Generation Project.

BACKGROUND

A geodynamic model based on studies of rift basins located on the continental margin offshore eastern Canada allows the prediction of the volume and rare earth element (REE) concentrations of basaltic melts emplaced during rifting. As described in previous publications (e.g. Keen et al., 1994; Williamson et al., 1995) we assume a two-layered lithosphere (crust and upper mantle) and include the history of rifting over time as part of the model parameterization. Figure 3 illustrates

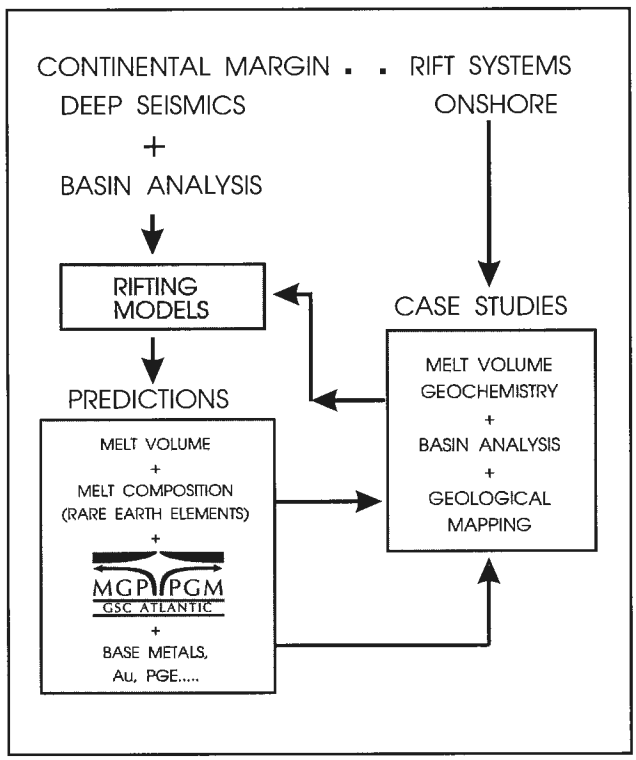

Figure 2. *Flow diagram illustrating the position of the Melt Generation Project in current research on crustal processes at GSC Atlantic.*

the modelling approach. Calculations of the volume and REE concentrations of basaltic melts proceed from a set of initial assumptions that include the physical and thermal state of the lithosphere at the time of rifting, the composition of the mantle source, and the style of melting. The amount of lithospheric and crustal extension during rifting (factors δ and ß, respectively) is required as input for the melting and geochemical calculations. These values are normally estimated from subsidence and crustal thinning in our offshore basins. Melting proceeds by adiabatic decompression of mantle material as it rises during the rifting process (McKenzie and Bickle, 1988). Episodic rifting is modelled as a series of "instantaneous" stretching events.

The main conclusion from our previous studies is that the calculated melt thickness and REE concentrations are most sensitive to variations in the basal mantle temperature (Tm), magnitude of subcrustal stretching (δ), and rifting history. Multiple stretching events can delay and reduce melt production (Keen et al., 1994). Given moderate basal temperatures (Tm ~1450°C) and large amounts of stretching in the upper mantle, the model is capable of generating alkaline melts and predicts the transition from alkaline to tholeiitic magmatism observed in many continental rifts (Williamson et al., 1995).

MODEL APPLICATIONS TO OCEANIC RIFTS

To date, we have focused attention on the genesis of relatively small volumes (1-5 km equivalent basalt thickness) of melt generated in "cool" rift systems (e.g. nonvolcanic margins) characterized by normal to moderately high temperatures in the asthenospheric mantle (1350-1450°C). Variations in the thickness and composition of mid-ocean ridge basalts (MORB) generated by the melting of mantle at 'normal' temperatures (1300-1350°C) are well documented in the literature and have provided a standard of reference for these models. In contrast, rifts developed above anomalously hot regions in the mantle are characterized by the presence of large volumes of tholeiitic magma generated and emplaced during a protracted rifting history (e.g. volcanic margins and flood basalt provinces; White and McKenzie, 1989). The melting model described above predicts that the thickness of basaltic melt generated under conditions of infinite stretching (ß = δ = ∞; e.g. at ridge crests) will increase by an order of magnitude for temperatures that are characteristic of plume-type mantle (Tm = 1550-1600°C). In contrast, the corresponding change in the predicted REE concentrations is small (Fig. 4).

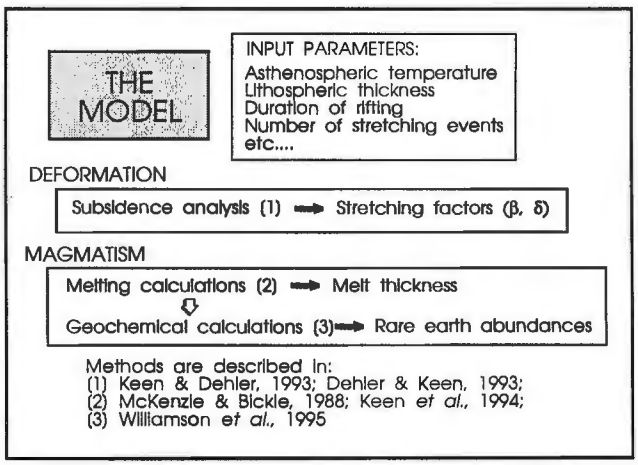

Figure 3. *Modelling approach used to calculate the volume and rare-earth element concentrations of basaltic melts. The symbols ß and δ describe the amount of stretching in the crust and upper mantle, respectively (modified from Williamson et al., 1994).*

Another limitation of the present model concerns the assumption of a single mantle source of asthenospheric origin in the geochemical calculations. In Figure 4, the depleted source (DM) corresponds to oceanic upper mantle responsible for the generation of MORB; and the enriched source (EM) corresponds to the deep, plume-type mantle that rises at hot spots. To calculate the concentrations of REE, we use the concept of a melt column where the composition of each per cent melt increment is calculated sequentially, assuming either depleted or enriched mantle compositions. Each melt increment is then extracted and accumulated in a reservoir ('pooled melt'). There is now good evidence that in the oceanic domain, the melting processes occurring at hot spots are more complex. Figure 5 shows selected REE patterns for primitive basaltic and picritic melts from Iceland. The data suggest that melting and mixing of both depleted and enriched sources occur when hot, plume-type mantle intersects the oceanic lithosphere at ridge crests.

There is a clear advantage in our modelling studies in relying on the simplest possible melting and geochemical calculations, to restrict the number of starting assumptions. This precludes the use of the Iceland analogue as a standard of reference in our models of rifting associated with hot spot activity.

MODEL APPLICATIONS TO CONTINENTAL RIFTS

Unlike their oceanic counterparts, continental rifts show a variety of magma types and a complex association between igneous and tectonic activity over time. Once the effects of secondary alteration, crustal contamination, and magma chamber processes are accounted for, the composition of rift-related basaltic magmas can be used to constrain the nature of the source and of the rifting process. Despite the added influence of continental crust, information on the nature of the enriched (EM) mantle source component (deep, asthenospheric "plume" mantle or subcontinental lithospheric mantle) may be preserved without the added complexity of mixing with a depleted (DM) mantle source. The Midcontinent Rift System, in the Lake Superior region of Canada and the United States, is a case in point.

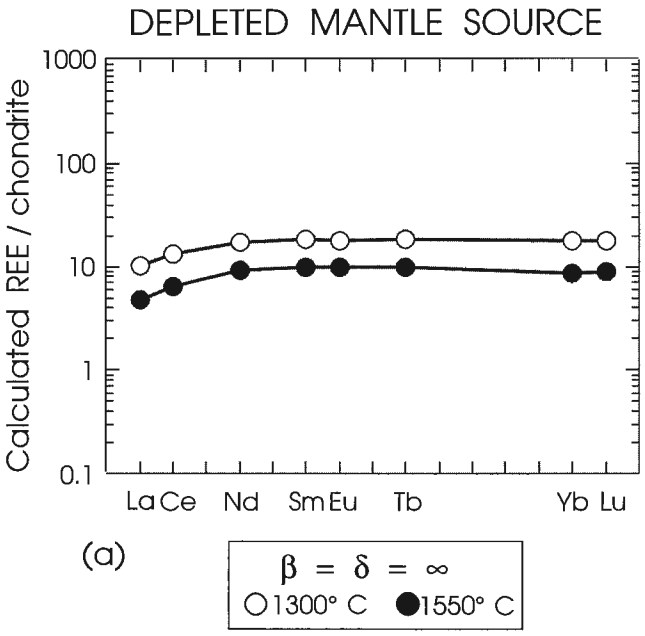

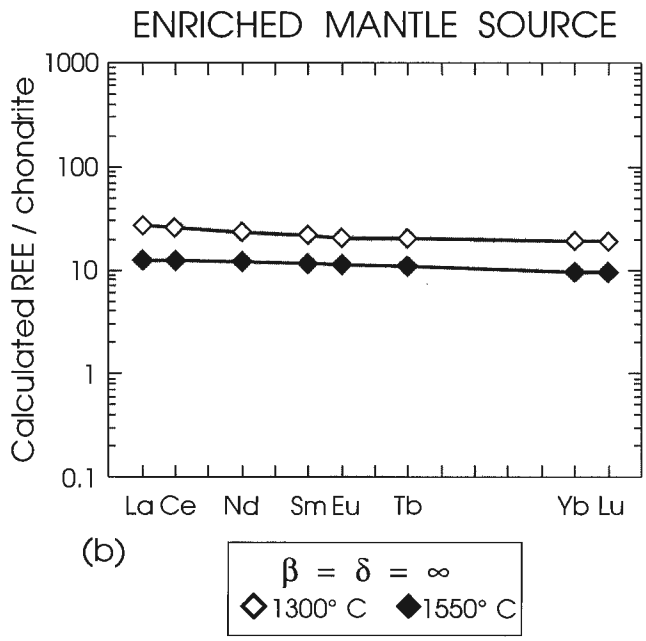

Figure 4. *Chondrite normalized rare-earth patterns of pooled melts calculated by assuming sequential melting of* ***(a)*** *depleted and* ***(b)*** *enriched mantle sources, during infinite stretching of the crust and upper mantle. Under these conditions, the large increase in the predicted rare-earth abundances of melts show little sensitivity to the increase in mantle temperature.*

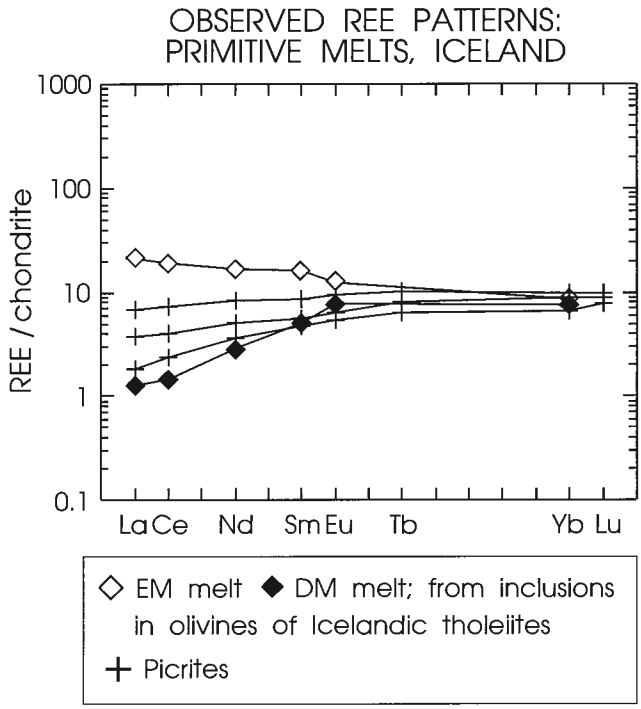

Figure 5. *Examples of rare-earth patterns of picritic melts and inclusions of primitive melt in tholeiites generated at the Iceland hot spot. The combined data from melt inclusions and picritic magmas illustrate the presence and mixing of two sources: (shallow) 'depleted' oceanic upper mantle and (deep) 'enriched' plume-type mantle. Data sources: Hemond et al. (1993); Gurenko and Chaussidon (1995).*

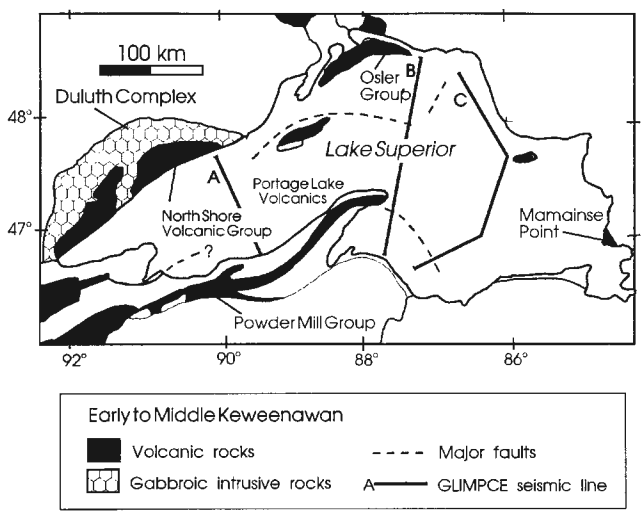

Figure 6. *Map of the Lake Superior region showing the distribution and nomenclature of Keweenawan volcanic and intrusive rocks in the Midcontinent Rift System. Lines A-C correspond to GLIMPCE seismic profiles across the rift (modified after Hutchinson et al., 1990).*

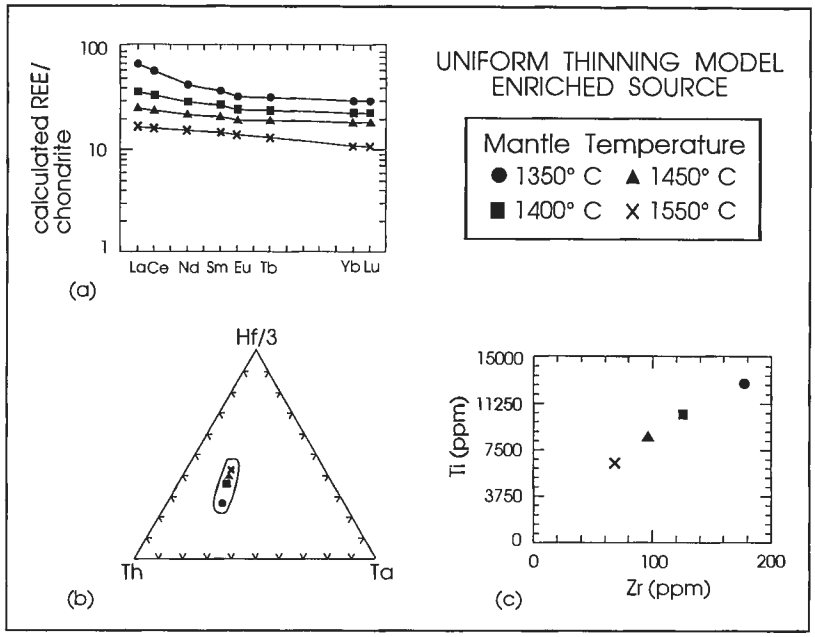

Figure 7.

Predicted variations of rare-earth element and some high-field strength element concentrations with increasing mantle temperature, calculated for basaltic melts generated during rifting in the Midcontinent Rift System. The model assumes a single, instantaneous stretching event, with the following input parameters (from Hutchinson et al., 1990): initial crustal thickness, 40 km; initial lithospheric thickness, 120 km; $\beta = \delta = 3$.

Hutchinson et al. (1990) have attributed the large volume of tholeiitic magma generated in the Midcontinent Rift System to decompression melting of an upwelling mantle plume in a region of thinned continental lithosphere (Fig. 6; 15-20 km over 7 Ma). These authors suggest that uniform stretching of the lithosphere by a factor of 3-4, and a mantle potential temperature in the range 1500-1570°C are consistent with gravity models and subsidence analyses for the Midcontinent Rift System. This model is supported by geochemical data indicative of a plume-type source (Nicholson and Shirey, 1990).

The model of Hutchinson et al. (1990) allows us to make two additional observations concerning the melting model. First, we compared the rare-earth patterns predicted by assuming uniform and two-layer stretching of the lithosphere (not shown here) and concluded that, for mantle temperatures exceeding about 1500°C, both types of models produce very similar rare-earth patterns. We then chose the uniform stretching model to predict the variations displayed by other trace elements, including Ti, Ta, Hf, Th, and Zr (Fig. 7). Our conclusion is that the model can be improved by including a number of other trace elements that remain geochemically coherent during the partial melting process and are sensitive to variations in mantle temperature. The noble metals (Au, PGEs) constitute such a group, as documented in previous studies on the behaviour of these metals in basaltic melts emplaced in rifts (Barnes et al., 1988; Fryer and Greenough, 1992; Lorand et al., 1993). Together with rare-earth and high-field strength elements, these metals are powerful indicators of the fractionation and contamination processes that contribute to the genesis of Ni-Cu sulphide deposits hosted in mafic and ultramafic rocks. Finally, it appears possible to use the data from a well-documented onshore rift, such as the Midcontinent Rift System, to construct a reference model for our studies of continental rifting above anomalously hot regions in the mantle.

SUMMARY

From earlier studies, Keen et al. (1994) and Williamson et al. (1995) have shown that the rare-earth element contents of mantle-derived melts are sensitive to the physical and thermal state of the lithosphere at the time of rifting. The objectives of the GSC Atlantic's Melt Generation Project (MGP) are: (1) to extend the model to include metals of economic interest, in particular Ni, Cu, Au, and the platinum-group elements (PGEs); and (2) test the model predictions with data from onshore rifts. Through scientific and business links with experts from other divisions within the GSC, universities, and the mineral industry, the project will lead to a better understanding of the dynamic processes and conditions in rifted lithosphere that favour the generation of 'fertile' magmatic systems. This will form the basis of applications to volcanic-hosted massive sulphide deposits (VHMS) and exploration targets associated with continental rifting.

ACKNOWLEDGMENTS

The numerical approach described in this paper is the result of team research undertaken at GSC Atlantic with Charlotte Keen, Sonya Dehler, and Robert Courtney. The author wishes to thank Jacob Verhoef, Charlotte Keen, Jim Franklin, Eckart Buhlmann, Jean Bédard, and Bernd Milkereit for their encouragement and advice during the early stages of the project. Sonya Dehler and Mark Williamson provided helpful comments on the manuscript. The idea for the Melt Generation Project was born following many fruitful discussions with Canadian and French colleagues present at the 1993 IAGOD conference on "Mineralization in Mafic and Ultramafic Rocks", held in Orléans, France.

REFERENCES

Barnes, S-J., Boyd, R. Korneliussen, A., Nilsson, L-P., Often, M., Pedersen, R.B., and Robins, B.
1988: The use of mantle normalization and metal ratios in discriminating between the effects of partial melting, crystal fractionation and sulphide segregation on platinum-group elements, gold, nickel and copper: examples from Norway; in GeoPlatinum '87; (ed.) H.M. Prichard, P.J. Potts, J.F.W. Bowles, and S.J. Cribb; Elsevier, p. 113-143.

Dehler, S.A. and Keen, C.E.
1993: Effects of rifting and subsidence on thermal evolution of sediments in Canada's east coast basins; Canadian Journal of Earth Sciences, v. 30, p. 1782-1798.

Emslie, R.F., Hamilton, M.A.,and Thériault, R.J.
1994: Petrogenesis of a Mid-Proterozoic anorthosite-mangerite-charnockite-granite (AMCG) complex: isotopic and chemical evidence from the Nain Plutonic Suite; Journal of Geology, v. 102, p. 539-558.

Fryer, B.J. and Greenough, J.D.
1992: Evidence for mantle heterogeneity from platinum-group-element abundances in Indian Ocean basalts; Canadian Journal of Earth Sciences, v. 29, p. 2329-2340.

Gurenko, A.A. and Chaussidon, M.
1995: Enriched and depleted primitive melts included in olivine from Icelandic tholeiites: origin by continuous melting of a single mantle column; Geochimica et Cosmochimica Acta, v. 59, p. 2905-2917.

Hemond, C., Arndt, N.T., Lichtenstein, U., and Hofmann, A.W.
1993: The heterogeneous Iceland plume: Nd-Sr-O isotopes and trace element constraints; Journal of Geophysical Research, v. 98, p. 15833-15850.

Hutchinson, D.R., White, R.S., Cannon, W.F., and Schulz, K.J.
1990: Keweenaw hot spot: evidence for a 1.1 Ga mantle plume beneath the Midcontinent Rift system; Journal of Geophysical Research, v. 95, p. 10869-10884.

Keen, C.E. and Dehler, S.A.
1993: Stretching and subsidence: rifting of conjugate margins in the North Atlantic region; Tectonics, v. 12, p. 1209-1229.

Keen, C.E., Courtney, R.C., Dehler, S.A., and Williamson, M-C.
1994: Decompression melting at rifted margins: comparison of model predictions with the distribution of igneous rocks on the eastern Canadian margin; Earth and Planetary Science Letters, v. 121, p. 403-416.

Lorand, J.P., Keays, R.R., and Bodinier, J.L.
1993: Copper and noble metal enrichments across the lithosphere-asthenosphere boundary of mantle diapirs: evidence from the Lanzo lherzolite massif; Journal of Petrology, v. 34, p. 1111-1140.

McKenzie, D. and Bickle, M.J.
1988: The volume and composition of melt generated by extension of the lithosphere; Journal of Petrology, v. 29, p. 625-679.

Naldrett, A.J.
1981: Platinum-group element deposits; Canadian Institute of Mining and Metallurgy, Special Issue, no. 23, p. 197-231.

Nicholson, S.W. and Shirey, S.B.
1990: Midcontinent Rift volcanism in the Lake Superior region: Sr, Nd, and Pb isotopic evidence for a mantle plume origin; Journal of Geophysical Research, v. 95, p. 10851-10868.

Ryan, B., Wardle, R., Gower, C., and Nunn, G.
1995: Nickel-copper-sulphide mineralization in Labrador: the Voisey Bay discovery and its exploration implications; in Current Research, Newfoundland Department of Natural Resources, Geological Survey, Report 95-1, p. 177-204.

White, R.S. and McKenzie, D.
1989: Magmatism at rift zones: the generation of volcanic continental margins and flood basalts; Journal of Geophysical Research, v. 94, p. 7685-7730.

Williamson, M-C., Courtney, R.C., Keen, C.E., and Dehler, S.A.
1994: Relationship between crustal deformation and magmatism in rift zones: modelling approach and applications to the eastern Canadian margin; in Current Research 1994-E; Geological Survey of Canada, p. 251-258.
1995: The volume and rare earth concentrations of magmas generated during finite stretching of the lithosphere; Journal of Petrology, v. 36, p. 1433-1454.

Geological Survey of Canada Project 800034

Petrophysical testing of limestone samples from former Yugoslavia

T.J. Katsube, G.M. LeCheminant, J.B. Percival, N. Scromeda, D. Walker, and Y. Das[1]

Mineral Resources Division, Ottawa

Katsube, T.J., LeCheminant, G.M., Percival, J.B., Scromeda, N., Walker, D., and Das, Y., 1996: Petrophysical testing of limestone samples from former Yugoslavia; in Current Research 1996-D; Geological Survey of Canada, p. 139-146.

Abstract: A comprehensive data set consisting of petrophysical, mineralogical, chemical, and scanning electron microscope analysis were obtained for three limestone samples from former Yugoslavia, representing different textures (tight to porous). These analyses were for a study carried out in support of land-mine detection activities by military engineers of the Canadian Peacekeeping forces.

Results indicate that a strikingly good relationship exists between pore-size distribution and scanning electron microscope (SEM) analysis for two samples, with both analysis supporting extremely small pores (6-25 nm) for the tight and low porosity (2-3%) limestone, and large pores (1-60 μm) for the higher porosity (13-15%) sample. The third sample shows a discrepancy between the porosities determined by water immersion (23%) and mercury porosimetry (13%). The pore-size distribution, SEM images, and visual examination suggest that this is due to large vugular pores (2-4 mm) interconnected by extremely small pores (6-25 nm), resulting in incomplete saturation by mercury under conventional measuring conditions.

Résumé : Diverses analyses (pétrophysiques, minéralogiques, chimiques et au microscope électronique à balayage) ont permis de monter un ensemble de données complet sur trois échantillons de calcaire (peu perméable à poreux) provenant de l'ex-Yougoslavie. Elles visaient à appuyer les opérations de détection de mines terrestres par les forces canadiennes de maintien de la paix.

Il existe un parallèle étonnamment bon entre les résultats quant à la distribution du diamètre des pores et ceux de l'analyse par microscope électronique à balayage (MEB) de deux échantillons. Dans les deux cas, les pores très petits (6-25 nm) sont associés au calcaire peu perméable à porosité faible (2-3 %) et les pores de grande taille (1-60 μm), à l'échantillon à porosité plus élevée (13-15 %). Le troisième échantillon montre un écart entre les porosités déterminées par immersion dans l'eau (23 %) et par porosimétrie au mercure (13 %). La distribution du diamètre des pores, les images obtenues de l'analyse au MEB et l'examen visuel suggèrent que cet écart est attribuable à des pores vacuolaires de grande taille (2-4 mm) reliés entre eux par des pores de très petite taille (6-25 nm), d'où une saturation incomplète en mercure dans les conditions de mesure classiques.

[1] Defence Research Establishment Suffield (DRES), P.O. Box 4000, Medicine Hat, Alberta, Canada T1A 8K6

INTRODUCTION

A comprehensive set of tests and analysis consisting of petrophysics, mineralogy, chemistry, and scanning electron microscopy were performed on a suite of limestone samples from former Yugoslavia. These tests and analysis were carried out, as part of a study (DRES, 1995) designed to determine the characteristics of some Croatian soil that were causing interference in the operation of land mine-detectors in the area of Benkovac (Croatia), in response to a request received from Defence Research Establishment Suffield (DRES) to assist the operations of Military engineers of the Canadian Peacekeeping force stationed in Croatia.

The petrophysical tests include effective porosity (ϕ_E), bulk electrical resistivity (ρ_r), formation factor (F), and pore-size (d) distribution determinations. Three samples representing texturally distinct rock types of limestone found in these soils were selected for this test. They represent tight microcrystalline limestone (micrite); porous, medium grained, buff allochemical limestone; and porous, slightly bedded microcrystalline limestone (micrite). This is a comprehensive set of data consisting of a wide variety of measurements and analysis on identical samples, a set that is difficult to find. The purpose of this paper is to document these results for future petrophysical analysis and pore structure modelling that could contribute to the understanding of mechanisms related to the subsurface transport of fluids (hydrocarbons and ground water), chemical species (contaminants), and electrical currents (geophysics). Results on the cause of the land mine-detection interference (DRES, 1995) is not the main subject of this paper.

METHOD OF INVESTIGATION

Samples and sample preparation

The three samples have been labelled YG-1-1 for the microcrystalline limestone (micrite); YG-1-2 for the medium grained, buff allochemical limestone; and YG-2-1 for the slightly bedded, microcrystalline limestone (micrite). These samples are limestone fragments of about 5-20 cm across that were found in the soil. Several specimens were taken from each of these samples for chemical determination of major and trace elements, for mineralogical characterization by X-ray diffraction (XRD), for scanning electron microscopy (SEM), and for the petrophysical tests. Rectangular specimens have been cut from the limestone samples with dimensions of (1.1-2.1)x(1.7-2.3) cm for the cross-section, and 0.7-1.4 cm in thickness (see Table 2, below) for electrical formation factor measurements. Two irregular-shaped chips from each sample were prepared for effective porosity and pore-size distribution determinations.

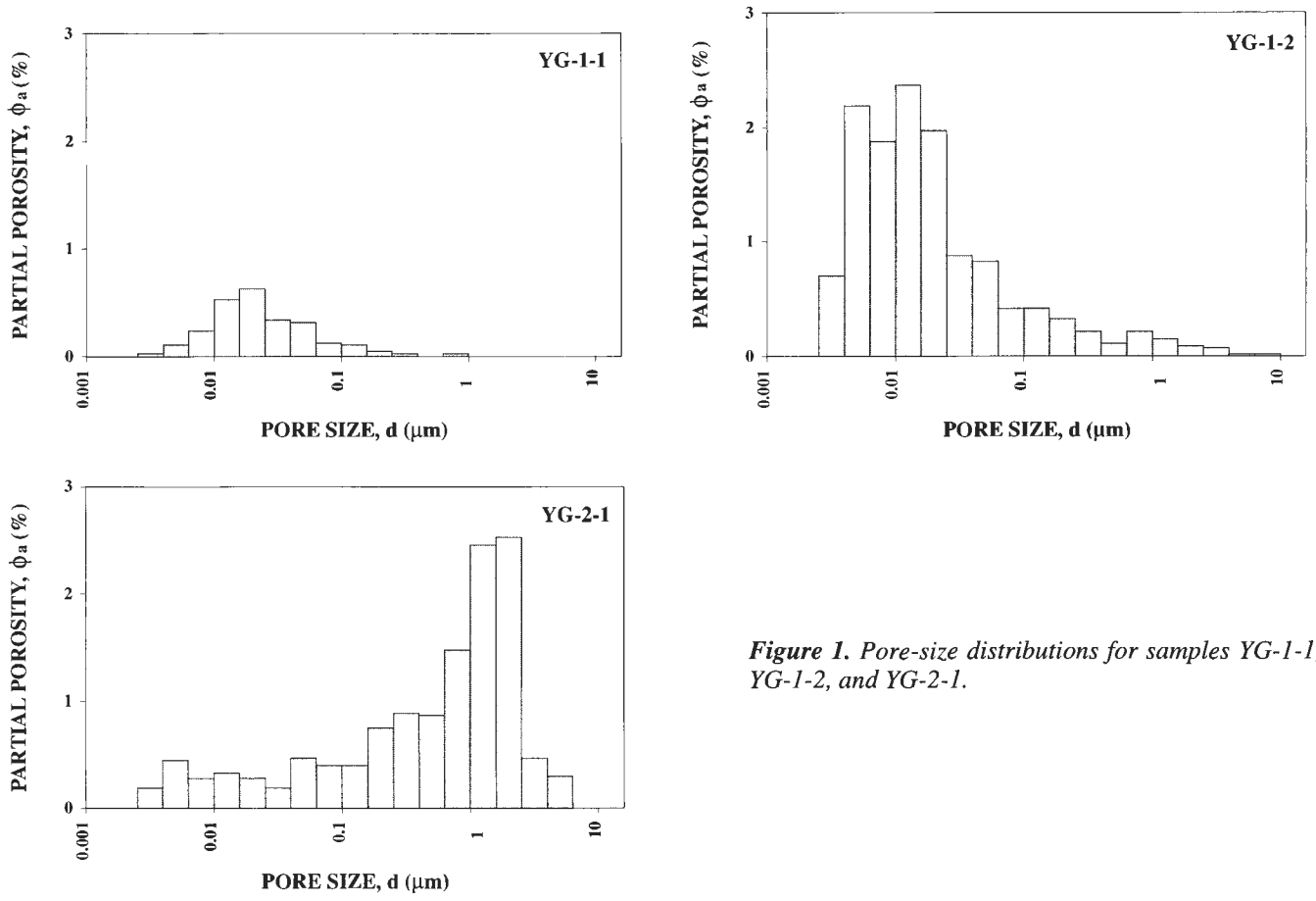

Figure 1. Pore-size distributions for samples YG-1-1, YG-1-2, and YG-2-1.

Sample description (LeCheminant and Percival, 1995)

Sample YG-1-1:

Micrite. Large fragments of light buff to tan, fine grained or microcrystalline (<0.05 mm) limestone containing minor amounts of evenly distributed, nonmagnetic, dark brown accessory minerals and several, randomly-distributed, small, feathery, black manganese stains. Visual examination indicates that porosity is very low. This limestone exhibits both rounded and angular surfaces that show a thin, lighter coloured weathering rind, and has soil and root fragments packed into fractures.

Sample YG-1-2:

Medium grained, buff allochemical limestone with clasts of fine grained to aphanic limestone (similar to YG-1-1), or rounded pink and buff calcite grains set in a microcrystalline matrix. Visual porosity is moderate to high, with many dissolved clasts (2-4 mm), with some interconnected macroporosity. There is a high proportion of allochemical clasts giving a framework supported rock infilled by an aphanic calcareous matrix.

Sample YG-2-1:

Micrite. Very fine grained, slightly bedded microcrystalline limestone. Bedding on the scale of 1 cm is seen as a narrow layer of reddish alteration outlining a bedding plane. This sample is very similar to YG-1-1, with very fine grained, dark brown accessory minerals disseminated throughout the buff-brown limestone. A very thin, lighter, alteration surface is developed.

Mineralogical analysis

The mineral constituents in each sample were identified (Percival and Delabio, 1995) by X-ray diffraction (XRD) using a Phillips PW1710 automated powder diffractometer equipped with a graphite monochromater, using Cu Kα and Co Kα radiation at 50/40 kV and 30 mA. Representative samples of each limestone type were washed in distilled water and immersed in an ultrasonic bath to remove clinging soil particles. Approximately 50 g of sample was crushed using a Bico ceramic disc mill to provide a powdered sample for XRD analysis.

Chemical analysis

A specimen of each limestone sample was cleaned in distilled water and an ultrasonic bath to remove surface soil material (ACL, 1995). The specimens were then pulverized using a ceramic Bico disc mill and ceramic ball milling to 0.12 mm and oven-dried (105-110°C) for chemical analysis. The specimens were analyzed for total C, carbonate C, S, H_2O, and Loss on Ignition (LOI) using Leco analyzers. Major elements were determined by X-ray fluorescence, and trace elements by ICP-OES, following dissolution with an acid mixture.

Petrophysical tests

The effective porosity (ϕ_E) was determined by the immersion technique, which compares the weights of the water-saturated and oven-dried (at 105°C) specimens (Katsube and Scromeda, 1995), by methods described in the literature (e.g., Scromeda and Katsube, 1993, 1994; API, 1960). The electrical resistivity (ρ_r) of the rectangular limestone specimens was measured using the two-electrode system over frequencies of 1-10^6 Hz, as also described in the literature (e.g., Katsube and Walsh, 1987; Katsube and Salisbury, 1991; Katsube et al, 1992). The formation factor (F) was determined by use of the usual procedure, using the five different NaCl concentrations of 0.02 to 0.5 N, as described in the literature (e.g., Katsube and Scromeda, 1993; Katsube et al., 1995). Specimens used for mercury intrusion porosimetry were initially oven dried for 24 hours at a temperature of 105°C, while under vacuum. This was followed by a cooling, in a desiccator, prior to the measurement. The pore-size distribution of the samples was then determined by mercury intrusion porosimetry, following the procedures described in previous publications (e.g. Katsube and Walsh, 1987; Katsube and Issler, 1993), using an equilibration time of 45 seconds for each of the high pressure steps, and 10 seconds for the low pressure (<0.7 MPa) steps. The measured pore-size distributions are plotted in a standard format by grouping the data into different size classes (e.g., Katsube and Issler, 1993; Katsube and Williamson, 1994).

Scanning Electron Microscope (SEM) analysis

Surfaces of the limestone specimens were examined (Walker et al., 1995), in order to determine the microscopic textures. First the specimens were mounted with epoxy on 1" aluminium pin mounts. Then, they were coated with a thin film of carbon using an Edwards E306A high vacuum evaporator. Examination was carried out using a Cambridge/Leica S-360 scanning electron microscope and a Link/Oxford eX-II energy dispersive X-ray spectrometer. The SEM was operated under the conditions of an accelerating voltage of 20 kv, a probe current of 10.5 nA, and a working distance of 25 mm.

EXPERIMENTAL RESULTS

Results of the mineralogical and chemical analysis for the three limestone samples are listed in Table 1 (Percival and Delabio, 1995; ACL, 1995). Both major and trace element contents are listed in the table. The mineralogy determined by XRD indicates the almost pure calcite composition of the very fine grained micritic limestone sample YG-1-1. This sample has a very low allochemical quartz component, which shows up as very low SiO_2 levels. The other micrite sample, YG-2-1, which has a slight bedding and is slightly more granular, has nearly 42% SiO_2 by weight.

Results of the effective porosity (ϕ_E), electrical resistivity (ρ_r), formation factor (F), and pore-size (d) distribution determinations for these limestones are listed in Tables 3, 4, 5, and 6 (Katsube and Scromeda, 1995), respectively. The electrical resistivity (ρ_r) and formation factor (F), for two of the samples, were measured in three directions: α, β, and γ,

Table 1. Mineralogical and chemical composition of the limestone samples from former Yugoslavia (Percival and Delabio, 1995; ACL, 1995).

Samples	YG-1-1	YG-1-2	YG-2-1
Minerals	Calcite	Calcite + Quartz	Calcite + Quartz
SiO_2 (%)	3.70	11.0	41.9
TiO_2	0.04	0.12	0.32
Al_2O_3	0.90	2.30	2.70
Fe_2O_3t	0.20	1.00	0.50
Fe_2O_3	<0.2	0.6	0.4
FeO	<0.2	0.4	<0.2
MnO	<0.01	0.06	0.04
MgO	0.86	0.99	0.49
CaO	49.7	45.4	28.5
Na_2O	0.10	<0.03	0.40
K_2O	0.12	0.10	0.62
H_2O	0.8	4.9	0.7
CO_2	40.5	28.0	23.0
C	<0.2	<0.2	<0.2
P_2O_5	0.05	0.05	0.07
St	0.03	0.35	<0.02
Ba (ppm)	90	170	180
Be	<0.5	<0.5	1.4
Co	<5	<5	<5
Cr	23	43	130
Cu	<10	<10	<10
La	<10	<10	10
Nb	<10	<10	11
Ni	<10	23	<10
Rb	21	19	34
Sc	0.9	2.7	2.1
Sr	630	410	340
V	9	25	11
Y	<5	8	11
Yb	<0.5	0.6	1.0
Zn	<5	<5	<5
Zr	16	34	250
Total	97.1	94.3	99.3

Table 2. Dimensions of specimens cut out from rock samples for electrical measurements (Katsube and Scromeda, 1995).

Sample	a_1 (cm)	a_2 (cm)	ℓ (cm)	W (g)	K_G (10^{-2}m)	δ_E (g/mL)
YG-1-1α	1.621	1.757	1.410	10.8131	2.02	2.69
-1β	1.410	1.757	1.621	10.8131	1.53	2.69
-1γ	1.410	1.621	1.757	10.8131	1.30	2.69
YG-1-2a	2.060	2.132	0.731	7.1512	6.01	2.23
-2b	2.100	2.268	0.832	9.1247	5.73	2.30
YG-2-1α	1.792	1.902	1.140	9.5254	2.99	2.45
-1β	1.140	1.902	1.792	9.5254	1.21	2.45
-1γ	1.140	1.792	1.902	9.5254	1.07	2.45

a_1, a_2 = Length of the two sides of the rectangular specimen.
ℓ = Thickness of specimen.
W = Weight of specimen under room dry conditions.
K_G = Geometric factor.
δ_E = Bulk density (Equation x).
a, b = Specimen number.
α, β, γ = The three directions of the specimen.

Table 3. Results of the effective porosity measurements (Katsube and Scromeda, 1995).

Sample	δ_E (g/mL)	W_W (g)	W_D (g)	S_{ir} (%)	ϕ_E (%)
YG-1-1	2.69	6.4192	6.3456	15.6	3.1
YG-1-2	2.23	6.8370	6.1988	53.3	23.0
YG-2-1	2.45	7.3718	6.9402	2.0	15.2

W_w = wet weight
W_D = dry weight
S_{ir} = irreducible water saturation
δ_E = bulk density (Equation 2)
ϕ_E = effective porosity

Table 4. Results of electrical resistivity measurements (Katsube and Scromeda, 1995).

Sample	ρ_r, (10^3 Ωm) Mes. #1	Mes. #2	Mean
YG-1 -1α	490	460	475
-1β	460	480	470
-1γ	500	500	500
YG-1 -2a	130	130	130
-2b	150	150	150
YG-2 -1α	360	350	355
-1β	320	360	340
-1γ	280	310	295

ρ_r = Bulk Electrical Resistivity.
Mes. (#1) = Measurement after 24 hours of saturation.
Mes. (#2) = Measurement after 48 hours of saturation.

Table 5. Formation-factor, surface resistivity, and bulk resistivities for different NaCl solutions for the limestone samples.

Sample	ρ_m ($x10^3$ Ω-m)					F ±%	ρ_c ±%
ρ_w (Ω-m)	0.26± 0.001	0.55± 0.002	1.09± 0.003	1.97± 0.005	5.27± 0.03	($x10^2$)	($x10^3$) (Ω-m)
NaCl (N)	0.5	0.2	0.1	0.05	0.02		
YG-1-1α	0.25	0.30	0.33	0.36	0.57	18.6 ±14	0.46 ±5
YG-1-1β	0.25	0.31	0.33	0.37	0.55	18.5 ±10	0.46 ±4
YG-1-1γ	0.26	0.33	0.37	0.41	0.61	18.2 ± 7	0.52 ±3
YG-1-2a	0.074	0.096	0.12	0.13	0.21	4.50± 5	0.175±3
YG-1-2b	0.063	0.094	0.12	0.14	0.20	3.53± 1	0.189±1
YG-2-1α	0.008	0.017	0.029	0.050	0.081	0.32± 0	0.196±1
YG-2-1β	0.009	0.019	0.031	0.053	0.087	0.44± 0	0.177±1
YG-2-1γ	0.011	0.019	0.026	0.044	0.080	0.48± 1	0.076±2

ρ_w = pore fluid resistivity
ρ_m = bulk resistivity of the rock for solutions of different salinities
F = formation-factor
ρ_c = surface resistivity

Figure 2.

Scanning electron microscope (SEM) photomicrograph displaying a secondary electron image (x80) for sample YG-1-1. The scale bar is 500 µm (Walker et al., 1995).

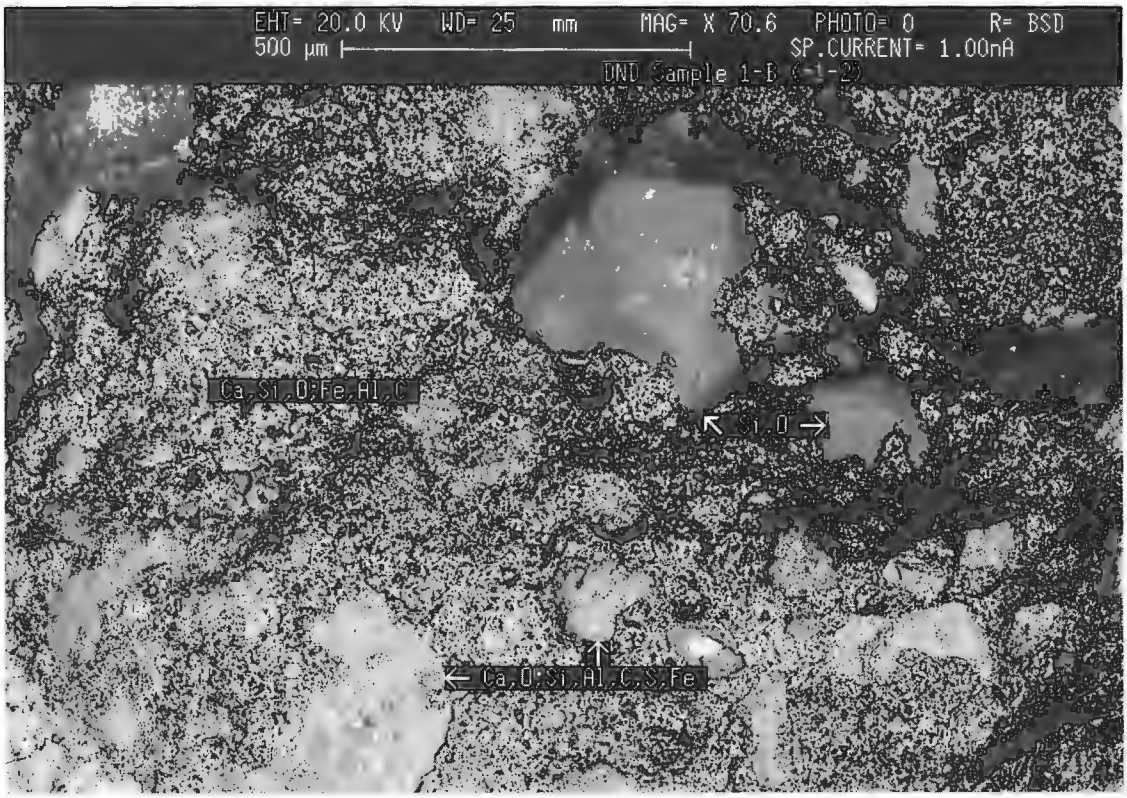

Figure 3. *SEM photomicrograph illustrating backscatter electron image (x70) of the surface of sample YG-1-2. The scale bar is 500 µm (Walker et al., 1995).*

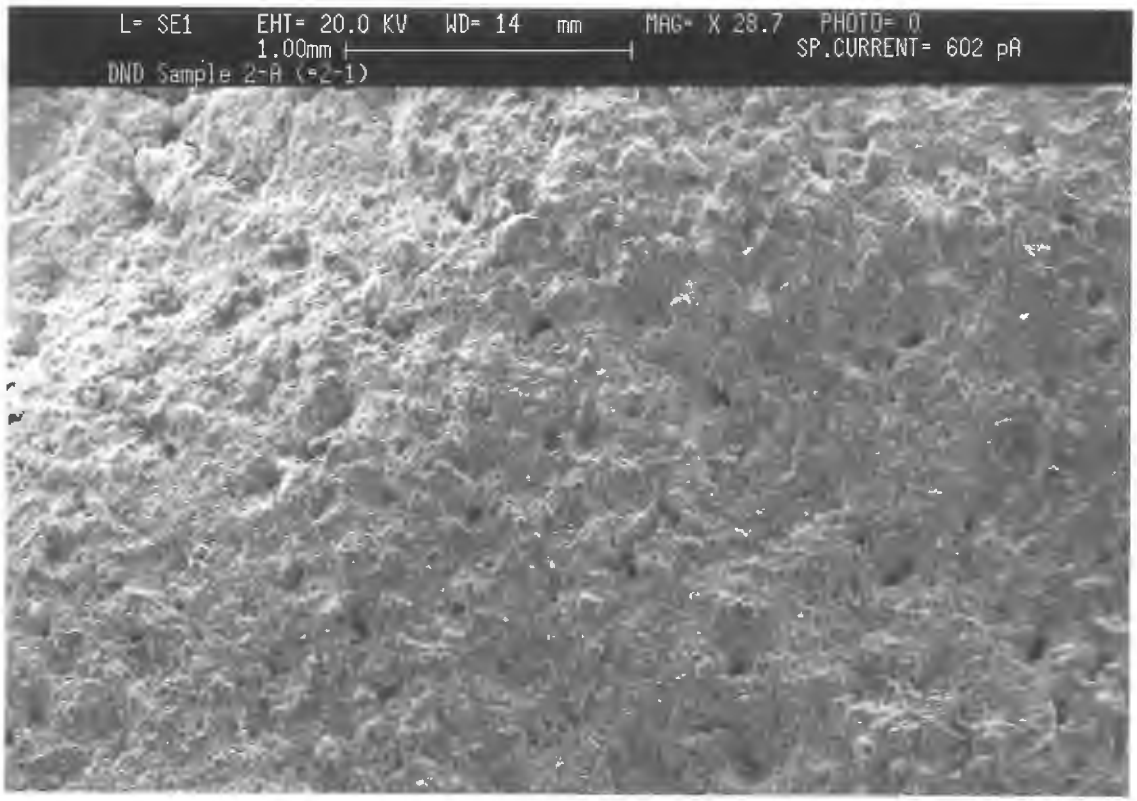

Figure 4. *SEM photomicrograph illustrating secondary electron image (x40) of sample YG-2-1, shows that this sample is highly porous with pore diameters in the order of 60 μm. The scale bar is 1 mm (Walker et al., 1995).*

as indicated in Tables 4 and 5. Results of the bulk density (δ_E) determination by the calliper method are listed in Table 2. This determination constitutes part of the effective porosity (ϕ_E) determination process (e.g., API, 1960; Scromeda and Katsube, 1993, 1994). Histograms of the pore-size (d) distribution are displayed in Figure 1.

The effective porosities (ϕ_E) are in the range of 3.1-23.0% (Table 3), the maximum being slightly higher than the commonly accepted range of values (2-15%, Daly, et al., 1966) for these type of rocks. The electrical resistivities (ρ_r) are in the range of 130-500 Ωm (Table 4), with little directional effects. These are in the lower end of the resistivity values commonly accepted (50-10^5 Ωm, Keller, 1966) for these type of rocks. The formation factor (F) values are in the range of 32-1900 (Table 5) with some directional effect for one sample (YG-2-1). The higher end of these values are about 10 times that of the commonly accepted range values (12-180, Keller, 1966), for these type of rocks. Although the effective porosities (ϕ_E, ϕ_{Hgl}) of samples YG-1-1 (ϕ_E = 3.1%, ϕ_{Hgl} = 2.5%) and YG-1-2 (ϕ_E = 23%, ϕ_{Hgl} = 13%) differ considerably, both of their pore-size distributions (d) resemble those of tight shales (Katsube and Williamson, 1994, 1995), with pore-size modes in the range of 6-25 nm (Fig. 1). Sample YG-2-1 (ϕ_E = 15%, ϕ_{Hgl} = 13%) displays a pore-size distributions (d) that differs considerably from the other two, with a pore-size mode in the range of 1-2.5 μm (Fig. 1). This pore-size distribution somewhat resembles that of a crystalline rock (Katsube and Hume, 1987), although its effective porosity value (ϕ_E) is considerably larger than that for such a rock type.

Scanning electron microscope (SEM) images are displayed in Figures 2-4 (Walker et al., 1995). Figure 2, which displays a secondary electron image (x80) for sample YG-1-1, shows the nonporous texture of this limestone. The "bright" or heavy-element-bearing minerals identified in this limestone sample are zircon, chrome-bearing spinel, monazite, ilmenite, zenotime, iron oxide (magnetite or hematite), a Cu-Zn alloy, and possibly some amphibole. The matrix is calcite which is nearly pure $CaCO_3$. Figure 3, which displays a backscatter electron image (x70) of the surface of sample YG-1-2, shows large subangular grains of quartz (300 μm) in a very fine grained matrix of calcite, quartz, and some iron-bearing minerals. The accessory minerals are iron oxides (magnetite or hematite) and very minor Ca-Al silicate. Figure 4, which displays a secondary electron image of sample YG-2-1, shows that this sample is highly porous with pore diameters in the order of 60 μm. This micrite sample has a greater quartz content, compared to the other micrite sample (YG-1-1).

DISCUSSIONS AND CONCLUSIONS

A preliminary interpretation of the results indicate that there exists a strikingly good relationship between the results of the pore-size distribution (d) and the scanning electron

Table 6. Pore-size distribution data for different pore-size ranges, d, obtained by mercury porosimetry for limestone samples.

d_a(nm)	YG-1-1	YG-1-2	YG-2-1
		ϕ_a (%)	
3.2	0.03	0.70	0.19
5.0	0.11	2.19	0.45
7.9	0.24	1.88	0.28
12.6	0.53	2.37	0.33
20.0	0.63	1.97	0.28
31.6	0.34	0.88	0.19
50.1	0.32	0.83	0.47
79.4	0.13	0.42	0.40
126	0.11	0.42	0.40
200	0.05	0.33	0.75
316	0.03	0.22	0.89
501	0.00	0.11	0.87
794	0.03	0.22	1.48
1259	0.00	0.15	2.46
1995	0.00	0.09	2.53
3162	0.00	0.07	0.47
5012	0.00	0.02	0.30
7943	0.00	0.02	0.00
ϕ_{Hg1}	2.52	12.9	12.7
ϕ_{Hg2}	2.70	13.4	13.8
d_{hg}	36.8	24.3	569
δ_{BD}	2.63	2.19	2.35
δ_{SD}	2.70	2.53	2.72
A	2.02	20.1	3.97
ϕ_s	2.02	7.55	7.82
ϕ_{rr}	0.802	0.585	0.616

d_a = Geometric mean pore-sizes for the different pore-size ranges (nm).
d_{hg} = Geometric mean of the entire pore-size distribution (nm).
ϕ_a = Partial porosity (%).
ϕ_{Hg1} = Total porosity measured by mercury porosimetry for pore-sizes up to 10 μm (%).
ϕ_{Hg2} = Total porosity measured by mercury porosimetry for pore-sizes up to 250 μm (%).
δ_{BD} = Bulk density (g/mL).
δ_{SD} = Skeletal density (g/mL).
A = Surface area (m^2/g).
ϕ_s = Residual or storage porosity (%).
ϕ_{rr} = ϕ_s/ϕ_{Hg1}.

microscope (SEM) analysis, for samples YG-1-1 and YG-2-1. Based on previous work (e.g., Katsube and Williamson, 1994), the pore-size distribution (d) for sample YG-1-1 suggests that it has texture resembling that of a tight rock with extremely small pores. This fact is confirmed by the SEM analysis (Fig. 2). The pore-size distribution (d) for sample YG-2-1 suggests that it is very porous with large pores, a fact also confirmed by the SEM analysis (Fig. 4). That is, both methods of analyses suggest smaller pores for sample YG-1-1 and larger pores for sample YG-2-1, although the actual pore-size values suggested by each method may differ as discussed later for sample YG-2-1. The low effective porosity (ϕ_E), high electrical resistivity (ρ_r), and formation factor (F) values for sample YG-1-1, and the high effective porosity (ϕ_E), low electrical resistivity (ρ_r), and formation factor (F) values for sample YG-2-1 also support this finding.

If it is assumed that the large pores observed in the SEM images for sample YG-2-1 (Fig. 4) represent interconnected pores, then there is a discrepancy between the diameters of the interconnected pores, with the pore-size distribution suggesting 1-2.5 μm and the SEM indicating 60 μm. Probably, the mean diameter of these pores are in the order of 60 μm, as indicated by the SEM, but the mean pore throats are in the range of 1-2.5 μm, as indicated by the pore-size distribution.

There is a discrepancy between the porosities determined by the immersion technique and that determined by mercury porosimetry for sample YG-1-2, that is ϕ_E = 23% and ϕ_{Hg1} = 13%. One explanation is that the former technique is sensitive to the large pores representing dissolved clasts with dimensions in the order of 2-4 mm (visually determined), whereas pores above 250 μm would be ignored in the analysis of the mercury porosimetry data. However, the pore-size distribution of this sample indicates that the pores of the interconnecting pore network are extremely small (6-25 nm), as indicated in Figure 1. This implies that large vugular pores (2-4 mm) that are not connected to the specimen surface could be interconnected by the network of these extremely small pores. This could result in incomplete saturation of the large vugular pores by mercury, under the conventional measuring conditions. This is probably a more likely explanation of the porosity discrepancy. The extremely small pores of the interconnecting pore network of this sample, combined with its high ϕ_E, low ρ_r (130-150 Ωm) but moderate F values, suggests (Katsube et al., 1990) that it has a high density of interconnecting pores, and that it is likely that they have a significant lining of alteration products, such as clays.

ACKNOWLEDGMENTS

The main part of this work has been financially supported by the Defence Research Establishment Suffield (DRES). The authors express their appreciation to D.C. Harris (Geological Survey of Canada, Ottawa) for critically reviewing this paper.

REFERENCES

Analytical Chemistry Laboratory (ACL)
1995: Mineralogical analysis of bulk soil samples from former Yugoslavia; in Appendix C of Report titled "Petrophysical testing of soil samples from former Yugoslavia" (PI: T.J. Katsube and G.M. LeCheminant) Defence Research Establishment Suffield (DRES), May 26, 1995, 40 p., Appendix p. 6-7d. Copies available from DRES (Report No. P-VD-AR4.R1).

API (American Petroleum Institute)
1960: Recommended practices for core-analysis procedure: API Recommended Practice 40 (RP 40) First Edition, American Petroleum Institute, Washington, D.C., p. 55.

Daly, R.A., Manger, E.G., and Clark, S.P.,Jr.
1966: Density of rocks; in Handbook of Physical Constants, Sec. 4 (p. 23), The Geological Society of America, Inc. Memoir 97, 19-26.

DRES (Katsube, T.J., LeCheminant, G.M., and Percival, J.B.)
1995: Petrophysical testing of soil samples from former Yugoslavia; Report (PI: T.J. Katsube and G.M. LeCheminant) Defence Research Establishment Suffield (DRES), May 26, 1995, 40 p. Copies available from DRES (Report No. P-VD-AR4.R1).

Folk, R.L.
1968: Petrology of Sedimentary Rocks; University of Texas, Hemphill's, 170 p.

Katsube, T.J. and Hume, J.P.
1987: Pore structure characteristics of granitic rock samples from Whiteshell Research Area; in Geotechnical Studies at Whiteshell Research Area (RA-3), CANMET, Report MRL 87-52, p. 111-158.
Katsube, T.J. and Issler, D.R.
1993: Pore-size distribution of shales from the Beaufort-MacKenzie Basin, northern Canada; in Current Research, Part E; Geological Survey of Canada, Paper 93-1E, p. 123-132.
Katsube, T.J. and Salisbury, M.
1991: Petrophysical characteristics of surface core samples from the Sudbury structure; in Current Research, Part E; Geological Survey of Canada, Paper 91-E, p. 265-271.
Katsube, T.J. and Scromeda, N.
1993: Formation factor determination procedure for shale sample V-3; in Current Research, Part E; Geological Survey of Canada, Paper 93-1E, p. 321-330.
1995: Electrical resistivity and porosity of bulk soil samples from former Yugoslavia: Appendix F of Report titled "Petrophysical testing of soil samples from former Yugoslavia (DRES, 1995)": (PI: T.J. Katsube and G.M. LeCheminant) submitted to Defence Research Establishment Suffield (DRES), May 26, 1995, 40 p., Appendix p. 13-18. Copies available from DRES (Report No. P-VD-AR4.R1).
Katsube, T.J. and Walsh, J.B.
1987: Effective aperture for fluid flow in microcracks; International Journal of Rock Mechanics and Mining Sciences, Geomechanical Abstract, v. 24, p. 175-183.
Katsube, T.J. and Williamson, M.A.
1994: Effects of diagenesis on shale nano-pore structure and implications for sealing capacity; Clay Minerals, v. 29, p. 451-461.
1995: Critical depth of burial of subsiding shales and its effect on abnormal pressure development; Proceedings of the Oil and Gas Forum '95 ("Energy from Sediments"), Geological Survey of Canada Open File 3058, p. 283-286.
Katsube, T.J., Murphy, T.B., Best, M.E., and Mudford, B.S.
1990: Pore structure characteristics of low permeability shales from deep formations; in Proceedings of the 1990 SCA (Society of Core Analysts) 4th Annual Technical Conference, August, 1990, Dallas, Texas, SCA-9010, p. 1-21.
Katsube, T.J., Scromeda, N., Mareschal, M., and Bailey, R.C.
1992: Electrical resistivity and porosity of crystalline rock samples from the Kapuskasing Structural Zone, Ontario: in Current Research, Part E; Geological Survey of Canada, Paper 92-1E, p. 225-236.
Katsube, T.J., Scromeda, N., and Williamson, M.A.
1995: Improving measurement accuracy of formation resistivity factor measurements for tight shales from the Scotian Shelf; in Current Research 1995-D, Geological Survey of Canada, p. 65-71.
Keller, G.V.
1966: Electrical properties of rocks and minerals; in Handbook of Physical Constants, (ed.) S.P. Clark, Jr.; Geological Society of America, Memoir 97, p. 553-577.
LeCheminant, G.M. and Percival, J.B.
1995: Macroscopic description testing of soil samples from former Yugoslavia; in Appendix A of Report titled "Petrophysical testing of soil samples from former Yugoslavia (DRES, 1995)" (PI: T.J. Katsube and G.M. LeCheminant) submitted to Defence Research Establishment Suffield (DRES), May 26, 1995, 40 p., Appendix p. 1-3. Copies available from DRES (Report No. P-VD-AR4.R1).
Percival, J.B. and Delabio, R.N.
1995: Mineralogical analysis of bulk soil samples from former Yugoslavia; in Appendix B of Report titled "Petrophysical testing of soil samples from former Yugoslavia (DRES, 1995)" (PI: T.J. Katsube and G.M. LeCheminant) submitted to Defence Research Establishment Suffield (DRES), May 26, 1995, 40 p., Appendix p. 4-5. Copies available from DRES (Report No. P-VD-AR4.R1).
Scromeda, N. and Katsube, T.J.
1993: Effect of vacuum-drying and temperature on effective porosity determination for tight rocks; in Current Research, Part E; Geological Survey of Canada, Paper 93-1E, p. 313-319.
1994: Effect of temperature on drying procedures used in porosity measurements of tight rocks; in Current Research 1994-E; Geological Survey of Canada, p. 283-289.
Walker, D., LeCheminant, G.M., and Percival, J.B.
1995: Scanning electron microscope (SEM) examination of texture and mineralogy for bulk soil samples from former Yugoslavia; in Appendix D of Report titled "Petrophysical testing of soil samples from former Yugoslavia (DRES, 1995" (PI: T.J. Katsube and G.M. LeCheminant) submitted to Defence Research Establishment Suffield (DRES), May 26, 1995, 40 p., Appendix p. 8-9. Copies available from DRES (Report No. P-VD-AR4.R1).

Geological Survey of Canada Project 870057

AUTHOR INDEX

NOTE TO CONTRIBUTORS

Submissions to the Discussion section of Current Research are welcome from both the staff of the Geological Survey of Canada and from the public. Discussions are limited to 6 double-spaced typewritten pages (about 1500 words) and are subject to review by the Chief Scientific Editor. Discussions are restricted to the scientific content of Geological Survey reports. General discussions concerning sector or government policy will not be accepted. All manuscripts must be computer word-processed on an IBM compatible system and must be submitted with a diskette using WordPerfect. Illustrations will be accepted only if, in the opinion of the editor, they are considered essential. In any case no redrafting will be undertaken and reproducible copy must accompany the original submissions. Discussion is limited to recent reports (not more than 2 years old) and may be in either English or French. Every effort is made to include both Discussion and Reply in the same issue. Current Research is published in January and July. Submissions should be sent to the Chief Scientific Editor, Geological Survey of Canada, 601 Booth Street, Ottawa K1A 0E8 Canada.

AVIS AUX AUTEURS D'ARTICLES

Nous encourageons tant le personnel de la Commission géologique que le grand public à nous faire parvenir des articles destinés à la section discussion de la publication Recherches en cours. Le texte doit comprendre au plus six pages dactylographiées à double interligne (environ 1500 mots), texte qui peut faire l'objet d'un réexamen par le rédacteur scientifique en chef. Les discussions doivent se limiter au contenu scientifique des rapports de la Commission géologique. Les discussions générales sur le Secteur ou les politiques gouvernementales ne seront pas acceptées. Le texte doit être soumis à un traitement de texte informatisé par un système IBM compatible et enregistré sur disquette WordPerfect. Les illustrations ne seront acceptées que dans la mesure où, selon l'opinion du rédacteur, elles seront considérées comme essentielles. Aucune retouche ne sera faite au texte et dans tous les cas, une copie qui puisse être reproduite doit accompagner le texte original. Les discussions en français ou en anglais doivent se limiter aux rapports récents (au plus de 2 ans). On s'efforcera de faire coïncider les articles destinés aux rubriques discussions et réponses dans le même numéro. La publication Recherches en cours paraît en janvier et en juillet. Les articles doivent être envoyés au rédacteur en chef scientifique, Commission géologique du Canada, 601, rue Booth, Ottawa K1A 0E8 Canada.